Use of Optimized Aggregate Gradations and Dust-of-Fracture Mineral Filler for Concrete Applications

by

Christopher T. Harrigan

A thesis submitted to the Graduate Faculty of
Auburn University
in partial fulfillment of the
requirements for the Degree of
Master of Science

Auburn, Alabama
December 12, 2015

Keywords: Shilstone Method, Proportioning, Percent Retained Chart, Manufactured Fine Aggregate, Microfines, Workability

Approved by

Anton K. Schindler, Chair, Professor and Director of Highway Research Center
Robert W. Barnes, Associate Professor of Civil Engineering
James S. Davidson, Professor of Civil Engineering

ABSTRACT

Many proportioning methods exist to help the designer achieve a well-graded, or optimized aggregate gradation in the concrete industry, but not all are effective. The Shilstone Method and percent retained chart have been shown in previous research to enhance the fresh and hardened states of concrete, while also yielding more economical results. These proportioning methods were studied during this research, and found to improve the workability of concrete.

In addition, the diminishing supply of natural fine aggregate throughout the country has given rise to the use of manufactured fine aggregate in its place. However, this material has been thought to cause adverse effects on concrete performance, resulting in standard specifications limiting its use and the build-up of dust-of-fracture mineral filler in aggregate quarries. The parent aggregate used to produce the manufactured fine aggregate during this research was dolomitic limestone. This research has found this material to be non-detrimental to the concrete performance with the use of water-reducing admixtures.

ACKNOWLEDGEMENTS

The successful completion of this research and my time here at Auburn University would not have been possible without the helpful guidance I received along the way. I would like to first thank my advisor, Dr. Anton Schindler. It has been an honor and privilege working with someone with as much knowledge and respect in the concrete industry. I owe my success to his continued assistance. In addition, I would like to thank the other committee members of this research project. Dr. Barnes and Dr. Davidson have given valuable input on the final work of this project, and have been exceptional teachers in the classroom.

This project would not have been possible without the generous donation from Rick Phillips at Vulcan Materials Company. The manufactured sand and microfines used during this project was donated from Vulcan. In addition, Mr. Phillips took the time to have a conference call with Dr. Schindler and me at the beginning of this project, providing us with valuable information to review. I also received assistance from Billy Wilson and Andy Weldon, the Structures and Aerospace laboratory technicians here at Auburn University. Their guidance with the development of the experimental work was crucial. Mr. Wilson also went out of his way in helping me with whatever I needed throughout my graduate career. All his advice was much appreciated, even coming from a Red Sox fan, my baseball teams arch-rival.

I would also like to thank all of the graduate students, laboratory help, and friends who had a part in assisting me throughout the last two years. The continual guidance that I received from Aaron Grubbs, Adam Carroll, Dave Mante, and Dr. Taylor Rawlinson was invaluable. I am positive my graduate student experience would not have been possible and have been very different without their friendship and help. In addition, the physical labor of this research work would not have been possible without the help of Eric Gross, Michael Harris, and Justin McLaughlin. Lastly, I would like to thank my parents for their love and support throughout my life. I would not be in the position I am today without them, and I hope to make them proud.

TABLE OF CONTENTS

LIST OF TABLES

LIST OF FIGURES

CHAPTER 1

INTRODUCTION

1.1 BACKGROUND

The world's most widely used construction material is concrete, commonly made by mixing portland cement with fine aggregate, coarse aggregate, and water. It is estimated that the present consumption of concrete in the world is of the order of 33 billion metric tons every year (Mehta and Monteiro 2014). Each constituent influences the characteristics of the concrete and its composition and quantity must be controlled if the end product is to be within acceptable limits of workability and performance. Typically, the aggregate portion of the concrete will occupy 80 percent of the total volume of the final mixture. A typical value of the cement for the same volume of concrete is 60 percent of the cost of all the raw materials (Fowler and Ahn 2001). The paste (cement and sand) is the part of the concrete that produces durability problems, but is the element that fills aggregate voids and provides workability to the mixture. The workability of concrete changes significantly with aggregate grading. Poorly graded and poorly shaped aggregates have increased void contents and require more paste to achieve the same workability as a well-graded aggregate mixture. Therefore, optimizing the aggregate gradation will minimize the void content and the required paste in the mixture, producing more economic and durable concrete (Quiroga and Fowler 2004).

Like some other state transportation agencies, ALDOT classifies aggregates into two categories: coarse and fine. However, this can lead to gradations where intermediate-sized particles are scarce or absent, and this in turn can lead to harsh, low-workability concrete (Cramer et al. 1995). ALDOT Standard Specification (2012) states coarse and fine aggregates shall be graded between the limits specified in Subarticle 801.11(d) and 802.09, which are similar to the limits in ASTM C33 and AASHTO M6 and M80. However, using aggregates that meet the requirements of ASTM C 33, AASHTO M6 and M80 may not necessarily produce satisfactory concrete mixtures because the grading limits happen to be too broad to guarantee optimum packing density (Mehta and Monteiro 2014).

Specifications for the fine aggregate fraction of concrete have been developed almost exclusively on the basis of experience with natural fine aggregate, since it was virtually the only type initially utilized (Fowler and Ahn 2001). Clean natural fine aggregates consist of rounded particles that provide good workability. When small particles in the size of the minus 200 mesh are present, the particles are frequently clay or silt and may be deleterious in concrete. These particles can have a negative impact on the workability and performance of the concrete mixture. Therefore, current specifications, including ASTM C33 and most state departments of transportation, limit the percentage of these particles allowed in fine aggregate used for portland cement concrete (Fowler and Ahn 2001). In addition, softer sands such as carbonate sands are known to polish when used in portland cement concrete pavements and thus provide less long-term skid resistance than harder siliceous sands (Fowler and Rached 2012). Many states have

therefore banned the use of carbonate fine aggregates in pavements or require blending these aggregates with harder aggregates to meet certain limits (Fowler and Rached 2012). However, the deposits of natural fine aggregates are slowly depleting, which necessitates the increasing use of manufactured fine aggregates. The first commercial use of manufactured fine aggregate was made in the early 1930s (Fowler and Ahn 2001). Current usage of these aggregates is over 100 times the amount in the 1930s and represents approximately 20 percent of total concrete fine aggregate requirements (Fowler and Ahn 2001). These particles are different from natural fine aggregate in mineralogy, shape, and size distribution. These aggregates are processed from quarried stone that is crushed using mechanical means. Manufactured fine aggregate particles are angular and the crushing process normally generates 10 to 20 percent of particles that pass the No. 200 sieve (Fowler and Ahn 2001). When manufactured fine aggregate is used for ALDOT projects, their standard specification limits the amount of particles passing the No. 200 sieve to five percent, if the materials are dust-of-fracture. In addition, manufactured fine aggregate from crushed limestone is not allowed to be used in bridge decks or concrete pavement, due to perceived issues related to reduced skid resistance.

1.2 PROJECT OBJECTIVES

This research project has been developed to investigate the use of optimized aggregate gradations and manufactured fine aggregate in portland cement concrete. The experimental work and research in this thesis has been performed to address the following primary objectives:

- Quantify the effect of using optimized aggregate gradations on the fresh and hardened concrete properties,
- Evaluate the effectiveness of using various methods to optimize the aggregate gradation,
- Evaluate the effect of using manufactured sands with their typical high percentages of microfines on the performance of concrete,
- Evaluate ALDOT specification limit on maximum percent microfines permissible in concrete applications.

1.3 RESEARCH APPROACH

The experimental work was limited to laboratory work where various concretes were made and tested. The experimental work was separated into two phases, in order to organize the testing of concrete applications in optimized aggregate gradations and manufactured fine aggregate. The first phase consisted of proportioning methods and comparing optimum and gap-graded aggregate gradations. The second phase consisted of using manufactured fine aggregate with increased percentages of particles passing the No. 200 sieve. Aggregates from sources across Alabama were obtained for test mixtures in both phases. The test mixtures were prepared in sequence by the type of coarse aggregate. Once all the test mixtures for one type of coarse aggregate were completed, the next coarse aggregate mixtures began. In this process, both phases were completed simultaneously.

1.4 ORGANIZATION OF THESIS

Chapter 2 of this report summarizes the literature reviewed to help reach the objectives of this project. Background information is provided for aggregate grading and current proportioning methods to optimize the concrete's gradation. In addition, manufactured fine aggregate and dust-of-fracture mineral filler are introduced. Their effects on concrete performance, based on past research, are presented. The experimental plan for the research work is discussed in chapter 3. Overviews of the phases are covered, along with mixture preparations, aggregate proportioning, and the tests completed on the mixture samples. The results and analytical study are described in chapter 4. The data from phases I and II are presented and discussed independently, and the statistical procedures are described for each test. A summary of the research work and highlights of any conclusions that were found are discussed in chapter 5. Further recommendations for additional research are also presented. Appendix A contains the data for the fresh properties testing, Appendix B contains the data for the mechanical properties testing, and Appendix C contains the data for the durability properties testing. In addition, Appendix D provides before and after pictures of samples during abrasion testing from the CTL Group.

CHAPTER 2

LITERATURE REVIEW

2.1 INTRODUCTION

Aggregate, the main constituent of concrete, constitutes 60 to 80 percent of the total volume of concrete. Proper selection of the type and particle size distribution of the aggregates affects the workability and the hardened properties of the concrete (Rached et al. 2009). With the exception of water, aggregate is the least expensive component of portland cement concrete. Conversely, cement is the most expensive component and is responsible for approximately 60 percent of the total cost of materials (Fowler and Ahn 2001). Using more aggregate reduces the amount of paste (cement and water), which reduces the cost of producing concrete. In addition, most of the durability problems (shrinkage and freeze-thaw) of hardened concrete are caused by cement. Furthermore, cement production is a key source of carbon dioxide emissions, and reducing its usage promotes sustainability (Rached et al. 2009).

Supplies of natural sands and gravels are becoming difficult to obtain due to environmental limitations and depletion of resources, leading to the use of manufactured fine aggregate (MFA) (Quiroga and Fowler 2007). MFA is a fine aggregate processed from quarried stone that is crushed and classified to obtain a controlled gradation. It requires sieving out excess fine material called dust-of-fracture mineral filler, or

microfines in order to meet the requirements of specifications (Fowler and Ahn 2001). Microfines are viewed as a waste material due to the possibility of deleterious clay being present within them. This chapter presents information regarding these topics.

2.2 SHAPE AND TEXTURE

The shape and surface texture of aggregate particles influence the properties of fresh concrete more than hardened concrete. Compared to smooth and rounded particles, rough-textured, angular, and elongated particles require more cement paste to produce workable concrete mixtures, thus increasing the cost (Mehta and Monteiro 2014). The shape refers to the geometric profile of the aggregate, with it being round, angular, elongated, or flaky. Descriptions of the particle shape are shown in Figure 2-1. The sphericity in the chart measures how equal are the length, width, and height. This value increases as the three dimensions approach equal values (Rached et al. 2009). Natural aggregates tend to be more rounded and less angular, while manufactured aggregates tend to be more angular with well-defined edges. Methods used to measure the shape of aggregates are the elongation factor and flatness factor. An elongated aggregate is defined as a particle that has a length/width ratio greater or equal to 3, while a flat particle is define as a particle that has a width/thickness ratio greater or equal to 3 (Rached et al. 2009). An excess of poorly shaped particles could reduce the strength of concrete through the increase of water demand. According to Shilstone (1990), flaky and elongated particles can affect the ability of fresh concrete to flow and contribute to harshness.

Round or nearly cubical shaped aggregates are desirable due to the ease in which they move in the mixing and handling process (Rached et al. 2009).

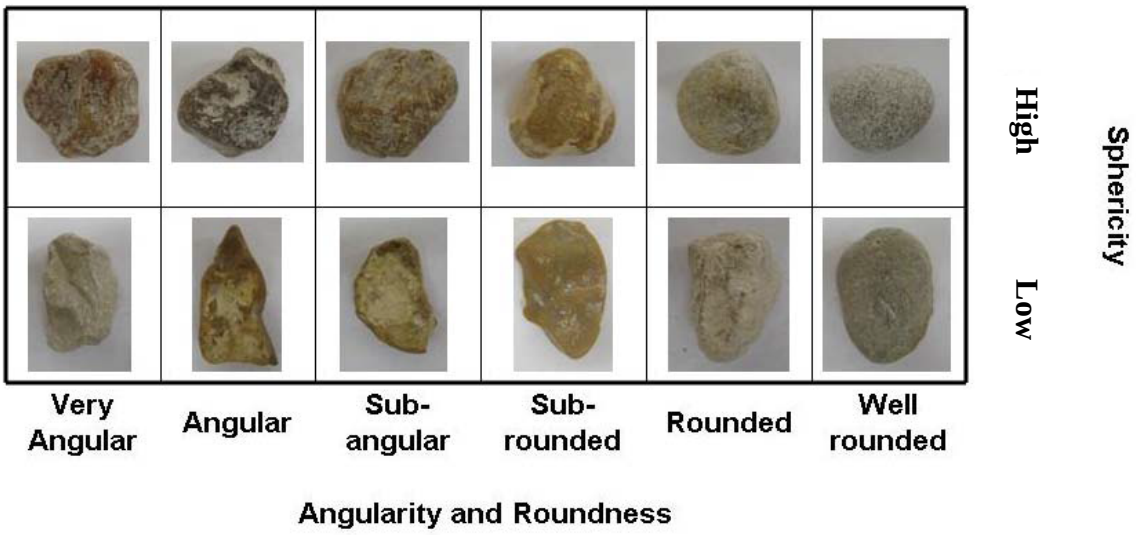

Figure 2-1: Illustrations of particle shapes modified from Rached et al. 2009

The surface texture also impacts the concretes workability and strength. It has been observed that a concrete mixture containing a rough-textured or crushed aggregate would show somewhat greater strength (especially tensile strength) at early ages than a corresponding concrete containing smooth or naturally weathered aggregate of similar mineralogy (Mehta and Monteiro 2014). This is due to the bond matrix between the cement and the aggregate particles. Natural aggregates have a smoother surface than manufactured or crushed aggregates. Although rougher textures lead to better bond between paste and aggregate, they also lead to harsher mixtures, as texture roughness

increases, the internal friction increases between the aggregates, and therefore more paste is needed to achieve a given workability (Rached et al. 2009).

2.3 AGGREGATE GRADING

Grading is the distribution of particles of granular materials among various size ranges, usually expressed in terms of cumulative percentage larger or smaller than each of a series of sizes of sieve openings, or the percentage between certain range of sieve openings (Mehta and Monteiro 2014). Figure 2-2 depicts the particle size distribution of aggregates typically used to produce concrete. The size distribution or grading divides aggregates for concrete applications in three categories (Quiroga and Fowler 2004):

- Coarse aggregate: material retained by No. 4 sieve.
- Fine aggregate: material passing No. 4 sieve and retained in No. 200 sieve.
- Dust-of-Fracture Miner Filler (Microfines): material passing No. 200 sieve.

Figure 2-2: Particle size ranges (Kosmatka et al. 2001)

Grading or particle size distribution affects significantly some characteristics of concrete like packing density, voids content, and, consequently, workability, segregation, durability, and some other characteristics of concrete (Quiroga and Fowler 2004). The size distribution of the fine aggregate plays an even more important role than the coarse aggregate. For example, very coarse sands produce harsh and unworkable concrete mixtures, and very fines sands increase the water demand. Concrete mixtures that do not have a large deficiency or excess of any particular aggregate size, produce the most workable and economical concrete mixtures (Mehta and Monteiro 2014). These concrete mixtures are economical because they require less cement paste, since cement can be 10 to 15 times as much as the price of aggregates. In order to reduce the paste content, the void content of the concrete needs to be reduced. The packing ability of the aggregate

particles can increase or reduce the void content, and therefore the surface area that the cement paste needs to coat. A well-graded aggregate, as opposed to a single-sized aggregate, will have a greater packing density. The smaller aggregates will fill in the voids created by the larger aggregates (Lamond and Pielert 2006). The effect of uniformly graded coarse and fine aggregates as opposed to the combined gradation of these two aggregate sizes and their respected void contents are shown in Figure 2-3. The liquid in the graduates represent the void content. If more volume of aggregate can be packed in a certain volume of concrete, less paste will be required (Quiroga and Fowler 2004).

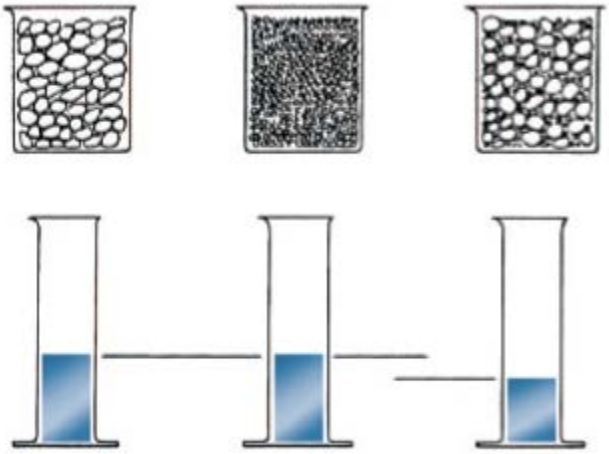

Figure 2-3: Void-content of equal absolute volumes of aggregates (Kosmatka et al. 2001)

The first step in developing mixture proportions is to identify the factors that affect durability for the projected service requirements (Shilstone and Shilstone 1993). Aggregate grading can have a large impact on the durability factors of concrete such as

permeability, shrinkage, and abrasion resistance. The combined particle distribution has a major influence on the permeability due to its effect upon compatibility. The high frequency of small, impermeable 3/8” to No. 16 sieve particles tends to block the movement of water through channels (Shilstone and Shilstone 1993). Shrinkage affects durability in that the resulting cracks provide channels through which water and deleterious materials can migrate (Shilstone and Shilstone 1993). Shrinkage is related mainly to the removal of absorbed water from the hydrated cement paste (Mehta and Monteiro 2014). At a constant water-cementitious material ratio, the lower the amount of cement, the lower the amount of shrinkage will occur (Shilstone and Shilstone 1993). Another important durability factor is abrasion resistance. Aggregate grading is important to prevent the wearing of concrete surfaces. As the paste wears in concrete, the only source of defense is from the aggregates. Where there is a high amount of 3/8” to No. 16 sieve size particles there will be little increase in abrasive wear. Concrete that has a high amount of 1/2” and larger coarse aggregate particles and a deficiency in coarse sand particles tends to wear rapidly in the valleys between the coarser sizes (Shilstone and Shilstone 1993).

2.3.1 OPTIMIZED CONCRETE MIXTURE PROPORTIONS

Cramer (1995) states that an ideal gradation is defined as a precise mixture of particle sizes that leads to the most workable, durable, and strongest concrete possible from given aggregate sources. In contrast, an optimized gradation is defined as one where practical and economic constraints are combined with attempts to obtain and use a mixture of aggregate particles sizes that will lead to improved workability, durability, and strength.

Shilstone (1990) suggests that the slump of a concrete mixture can be controlled by gradation changes without adjusting the water-cementitious material ratio or affecting the strength. He states, for every combination of aggregate mixed with a given amount of cementitious materials and cast at a constant consistency, there is an optimum combination that can be cast at the lowest water-cementitious ratio and produce the highest strength. Corrections to fill gaps in the aggregate grading can lead to significant increases in workability and finish-ability. The optimized concrete mixture has the least particle interference and responds best to a high frequency, high amplitude vibrator. If there is too much sand; the mixture is sticky, has a high water demand, requires more cementitious materials to produce a given strength, increases pump pressures, and creates finishing problems. If there is not enough sand, the mixture is bony and creates a different set of placing and finishing problems. The paste volume should be no more than is necessary to provide lubrication during placement and bind the inert aggregate particles together to resist the forces that will affect the mass during its service life (Shilestone and Shilstone 2002).

Aggregate grading, shape, and texture are important components in obtaining the optimized concrete mixture. In addition, the optimized concrete mixture must also meet other criteria including durability, strength, workability, construction operations, cost, appearance, early use requirements, rebar spacing, and availability of resources (Quiroga and Fowler 2004). According to Shilstone (1990), the accepted practice of establishing constant mixture proportions by weight contributes to problems arising from variability in aggregates and construction needs. Arbitrary means can be used in order to meet the

criteria required by the concrete. Once a concrete mixture is identified as fulfilling the criteria, that combination of materials and adjustment procedure can be translated into a mathematical or graphical model as a mixture design (Shilstone 1990).

Shilstone and Shilstone (2002) present many case studies where gap grading (especially at the No. 4 and 8 size sieves) and excessive fine sand and cementitious materials content were found to cause problems. After applying corrections to the aggregate grading, these same mixtures resulted in reductions in water demand, improvements in concrete flow and finishability, and increases in strength. In addition, Shilstone (1990) states, there are three principle factors upon which mixture proportions can be optimized for a given need with a given combination of aggregate characteristics. They include the relationship between the coarseness of the two larger aggregate fractions and the fine fraction, the total amount of mortar, and the aggregate particle distribution.

Shilstone and Shilstone (1989) recommend we maximize the cheapest variables and minimize the most expensive variables in the concrete mixture while achieving the best performance. Without a method for quantifying workability and the composition of mixtures, the resolution for many contractors is to just add water, sacrificing important attributes of the concrete.

2.4 PROPORTIONING METHODS

The proportioning of concrete mixtures is the process of arriving at the right combination of cement, aggregates, water, and admixtures for making concrete according to given specifications (Mehta and Monteiro 2014). There are two main purposes of mix

proportioning. One purpose is to obtain a product that will perform according to certain predetermined requirements. Conventionally, the two most essential requirements are the workability of the fresh concrete and the strength of hardened concrete at a specified age. The other purpose of mix proportioning is to obtain a concrete mixture satisfying the performance requirements at the lowest possible cost. The overall objective of proportioning concrete mixtures can therefore be summarized as selecting the suitable ingredients among the available materials and determining the most economical combination that will produce concrete with certain minimum performance characteristics (Mehta and Monteiro 2014).

The task of mixture proportioning is complicated by the fact that certain desired properties of concrete may be oppositely affected by changing a specific variable. For example, adding water to a stiff concrete mixture will improve the workability of fresh concrete, but it will also reduce the strength. With variables that have opposing properties, effective proportioning boils down to the balancing of conflicting requirements (Mehta and Monteiro 2014).

Many methods exist for computing concrete mixture proportions, but it is disputed as to which is best for achieving optimal behavior. Mathematical approaches to determine the correct proportion of component materials of a concrete mixture meeting a given set of specifications generally do not work because the materials vary widely in their characteristics (Mehta and Monteiro 2014). In this report, the following methods were evaluated based on their popularity in the United States.

- ACI 211

- Shilstone Method, and
- Percent Retained Charts.

2.4.1 ACI 211

The recommended method of ACI Committee 21l (2012), Standard Practice for Selecting Proportions for Normal, Heavyweight and Mass Concrete is popular in the United States and other countries. While this method is generally accepted, there has been criticism based on its lack of consideration to the optimization of aggregate gradations. The method is based on an empirical formula that indirectly determines the amount of aggregates in a mixture. The values recommended by ACI assume that the aggregates are well graded and no guidance is given on how to blend two or more aggregates (Rached et al. 2009). Further details of the criticisms will now be discussed.

With the ACI 211 method, the water content is determined from the nominal maximum aggregate size (NMAS). The role of coarse aggregates is shown in Table 2-1. It is used to determine the amount of mixing water required to produce a given slump, depending only on the NMAS. However, it does not address other characterization properties such as shape, texture, and grading as addressed in the previous sections. The surface area of the fine aggregate is addressed through the Fineness Modulus (FM) determined in ASTM C 136 (2014), but this does not represent the packing density. The ACI method considers the FM of the sand and the dry rodded unit weight of the coarse aggregate in selecting the proportion of coarse aggregate, as shown in Table 2-2. As the FM of the sand increases, less coarse aggregate is allowed in order to maintain workability (Richardson 2005). Shilstone and Shilstone (1987) state that Table 2-2 was

developed for concrete placed without the aid of vibration, producing mixtures low in coarse aggregate. Although the surface area method and the FM method have been used to tie gradations to the proportioning of concrete, their downfall is that changes in gradations can render little change in calculated surface area or FM, but the workability of the concrete could be significantly different (Shilstone and Shilstone 1987).

Table 2-1: Approximate Mixing Water for Different NMAS (ACI Committee Report 211-1 2012)

Water, lb/yd^3 of Concrete for Indicated Nominal Maximum Sizes of Aggregate								
Slump, in.	**3/8**	**1/2**	**3/4**	**1**	**1.5**	**2**	**3**	**6**
Non-Air-Entrained Concrete								
1 to 2	350	335	315	300	275	260	220	190
3 to 4	385	365	340	325	300	285	245	210
6 to 7	410	385	360	340	315	300	270	-
More than 7	-	-	-	-	-	-	-	-
Approximate amount of entrapped air in non-air-entrained concrete, percent	3	2.5	2	1.5	1	0.5	0.3	0.2
Air-Entrained Concrete								
1 to 2	305	295	280	270	250	240	205	180
3 to 4	340	325	305	295	275	265	225	200
6 to 7	365	345	325	310	290	280	260	-
More than 7	-	-	-	-	-	-	-	-
Recommend averages total air content, percent for level of exposure:								
Mild Exposure	4.5	4	3.5	3	2.5	2	1.5	1
Moderate Exposure	6	5.5	5	4.5	4.5	4	3.5	3
Severe Exposure	7.5	7	6	6	5.5	5	4.5	4

Table 2-2: Volume of Coarse Aggregate per Unit of Volume of Concrete (ACI Committee Report 211-1 2012)

Maximum Size of Aggregate (in.)	Volume of Dry-Rodded Coarse Aggregate per Unit Volume of Concrete for Different Fineness Moduli of Sand			
	2.4	2.6	2.8	3
3/8	0.5	0.48	0.46	0.44
1/2	0.59	0.57	0.55	0.53
3/4	0.66	0.64	0.62	0.6
1	0.71	0.69	0.67	0.65
1 1/2	0.75	0.73	0.71	0.69
2	0.78	0.76	0.74	0.72
3	0.82	0.8	0.78	0.76
6	0.87	0.85	0.83	0.81

Other criticisms can be traced to gradation variations. ACI 211 uses ASTM C 33 for requirements on coarse and fine aggregate gradations, as can be seen from Table 2-3 and Table 2-4. The values in this specification are based on a large number of concrete mixtures and are therefore very broad, applying to a number of different proportions to meet the needs of different mixtures. Current ASTM and similar aggregate limits do not contribute to mixture optimization; as such standards do not address gradations of the blends (Shilstone 1990). The standards have often resulted in highly sanded, gap-graded mixtures that are prone to segregation when exposed to vibration (Richardson 2005). These limits are prescriptive specifications as opposed to performance based. Uniformity of the gradations is recommended but it is not enforced nor is the proportions impacted by any gradation optimization.

Table 2-3: Grading Requirements for Fine Aggregate (ASTM C33 2013)

Sieve	Percent Passing
9.5mm (0.375 in.)	100
4.75 mm (No. 4)	95 to 100
2.36 mm (No. 8)	80 to 100
1.18 mm (No. 16)	50 to 85
600 µm (No. 30)	25 to 60
300 µm (No. 50)	5 to 30
150 µm (No. 100)	0 to 10
75 µm (No. 200)	0 to 3

Table 2-4: Grading Requirements for Coarse Aggregates (ASTM C33 2013)

		Amounts Finer than Each Laboratory Sieve (Square-Openings), Mass Percent						
Size Number	Nominal Size (Sieves with Square Openings)	37.5 mm (1.5 in.)	25.0 mm (1 in.)	19.0 mm (0.75 in.)	12.5 mm (0.5 in.)	9.5 mm (0.375 in.)	4.75 mm (No. 4)	2.36 mm (No. 8)
57	25.0 to 9.5 mm (1 to No. 4)	100	95 to 100	…	25 to 60	…	0 to 10	0 to 5
67	25.0 to 9.5 mm (1 to No. 4)	…	100	90 to 100	…	20 to 55	0 to 10	0 to 5

The use of aggregate classified into two categories of coarse and fine can lead to gradations where intermediate-sized particles are scarce or absent, and this is turn can lead to harsh, unworkable concrete (Cramer et al. 1995). To obtain a good size distribution, the entire range of aggregate size fractions should be viewed as a whole rather than two separate entities, coarse and fine aggregate (Quiroga and Fowler 2004). If a mixture is proportioned using ASTM C 33 #57 size coarse aggregate and ASTM C 33 fine aggregate with both gradations running down the middle of the allowable variation for each material, a lot of material will be retained on the 1/2 in., # 30, and #50 sieves,

but there is a lack of material on the #8 sieve (Richardson 2005). The resulting mixture will result in finishing problems. Shilstone (1993) states a typical gradation for the intermediate aggregate expressed as percent passing each sieve is: 3/8" – 100 %, No. 4 – 65 to 95 %, No. 8 – 15 to 40 %, No. 16 – 5 to 15 %, and No. 50 – 0 to 5 %. The intermediate size is often lacking in the coarse and fine fractions, and the voids will have to be filled with sand, cement, and water. By using mortar to fill voids, less of it is available to provide workability, and the mix becomes harsh and difficult to finish (Richardson 2005).

2.4.2 SHILSTONE METHOD

In the late 1960s Shilstone began work on concrete optimization during a project in Saudi Arabia under contract with the U.S. Army Corps of Engineers. The architectural design required construction of white cement cast-in-place concrete, sandblasted to produce a uniform exposed aggregate surface. The investigation objective was to confirm the potential for a contractor to produce the specified finish and compressive strength (Shilstone 1990). In order to complete the project, they began to develop new technology for proportioning concrete with an emphasis on workability and a simple way to select the optimum gradation. This resulted in what is now referred to as the Shilstone Method. It is composed of the Coarseness Factor Chart and 0.45-Power Chart. Shilstone proposes the use of these charts with the focus on using intermediate sized particles (especially the No.4 and No. 8 sizes) to ensure optimized total aggregate gradations. By using Shilstone's method and a third aggregate to achieve a more optimal particle size distribution, the Colorado Department of Transportation reported a 5 percent reduction in

water demand and a 10 percent increase in strength on a bridge deck project (Cramer et al. 1995). Cramer et al. (1995) also reported similar results during a Wisconsin DOT demonstration project. They concluded that the use of optimized total aggregate gradations in place of near-gap-graded gradations resulted in increased compressive strength, reduced water demand, and reduced segregation. Obla et al. (2007) conducted two phases of research to determine the effectiveness of the Shilsone Method on packing density and concrete performance. In the first phase it was concluded that well-graded mixtures obtained through the use of the Shilstone Method and percent retained chart do not lead to maximum aggregate packing density and minimum voids content. In phase two, it was found that well-graded mixtures obtained through the use of the Shilstone Method and percent retained chart resulted in similar water demand, bleeding water amount, compressive strength, and shrinkage as mixtures that did not use the Shilstone Method and percent retained chart. In addition, well-graded mixtures obtained through the use of the Shilstone Method and percent retained chart resulted in improved finishability and less segregation. Based on the results of the study, it was concluded that there is no assurance that a concrete specification that includes the Shilstone Method and percent retained chart will lead to reduced water demand or less shrinkage, as is typically the goal with aggregate grading (Obla et al. 2007). The subsequent sections will discuss the two charts used in the Shilstone method.

2.4.2.1 Coarseness Factor Chart

The Coarseness Factor Chart (CFC) was developed based on hundreds of mixtures and resolved problems found during pumping, placing, finishing, and curling during projects

in the field. The foundational concept of the CFC is the relationship between the amount of fine aggregate required for a mixture to the coarse and intermediate aggregates. Seven independent variables can be coordinated and reported as a single point on the chart (Shilstone 2007). Aggregate grading is based on all of the sieve sizes considered as a whole, as opposed to being coarse and fine aggregates considered as separate fractions. The chart is divided into the three segments of large or quality particles (Q), intermediate or interference particles (I), and fine or workability particles (W). The Q segment is composed of the plus 3/8 in. sieve particles, which are the inert fillers according to Shilstone (1990). The I segment is composed of the minus 3/8 in. to No.8 sieve particles. These sizes contribute to fill voids and aid in the flow of concrete and workability according to Shilstone (1990). The W segment is composed of the minus No. 8 sieve particles which give the mixture workability, because the particles function as do ball bearings in machinery (Shilstone 1990). The Coarseness Factor Chart gives the relationship between the modified workability factor (WF) and the coarseness factor (CF) that can be computed from Equations 2-1 and 2-2 (Quiroga and Fowler 2007).

$$WF(\%) = W \times 100 + \frac{(C - 564)}{94} \times 2.5 \qquad \textbf{Equation 2-1}$$

Where,

W = minus No. 8 sieve particles, and

C = amount of cementitious material per cubic yard of concrete.

$$CF(\%) = 100\frac{Q}{Q + I} \qquad \textbf{Equation 2-2}$$

Where,

Q = plus 3/8 in. sieve particles, and

I = minus 3/8 in. and plus No. 8 sieve particles

The research that led to this chart was based on mixtures with six U.S. bags of cement, which corresponds to 564 lb/yd^3. A change in one bag of cement (94 lb.) necessitates a change of 2.5 percent points on the Y-axis; either added or subtracted (Shilestone and Shilstone 2002). As cementitious materials are increased, the fine aggregate content should be reduced to maintain the same workability factor and vice versa (ACI Committee 302 2004). The Coarseness Factor Chart divided into five zones is shown in Figure 2-4. Each zone is broken down as follows (Rached et al. 2009):

Zone I (CF of 75 or greater) – This zone includes mixtures that are gap-graded and have a high potential for segregation due to poor combined aggregate grading with a deficiency in intermediate particles. These mixtures are not cohesive, so a clear separation between the coarse particles and the mortar can be seen as the concrete is deposited from the chute (ACI Committee 302 2004).

Zone II (CF between 45 and 75) - This is the optimum zone, for mixtures with NMAS from 1-1/2 to 3/4 inch. These mixtures generally produce consistent, high quality concrete. Field observations with multiple materials and construction methods have produced outstanding results when the CF is approximately 60 and the adjusted WF is approximately 35 (ACI Committee 302 2004). Aggregate gradations that fall in this box have a better chance of meeting project requirements.

Zone III (CF less than 45) - This zone is an extension of Zone II for ½ inch and finer aggregate mixtures.

Zone IV – These mixtures have excessive fines leading to a high potential for segregation during consolidation and finishing. Mixtures in this zone will produce variable strength and may result in high permeability and shrinkage.

Zone V – This zone contains mixtures with too much coarse aggregate and is also referred as non-plastic.

Shilstone uses a trend bar, seen in Figure 2-4, to divide Zone V from the other zones in order judge whether a mixture will be sandy or rocky. The diagonal trend bar defines a region, if made with gravel or cubical shaped crushed material, and with well-graded natural sand, are in near perfect balance to fill voids with aggregate. Combined aggregate gradations that fall within this region reflect maximum packing within the concrete volume (ACI Committee 302 2004). Mixtures that plot inside of the trend bar will require a minimum amount of water but will exhibit poor finishability and cannot be pumped. The material should be placed with bottom-drop buckets and consolidated with large vibrators (Richardson 2005). Shilstone (2007) states the trend bar location reflects the changes in fine aggregate requirement as the two coarser sizes become finer. A mixture with a CF of 100 has no intermediate particles so it is gap-graded; while a mixture with a CF of 0 is a pea gravel mixture with nothing retained on the 3/8 inch sieve.

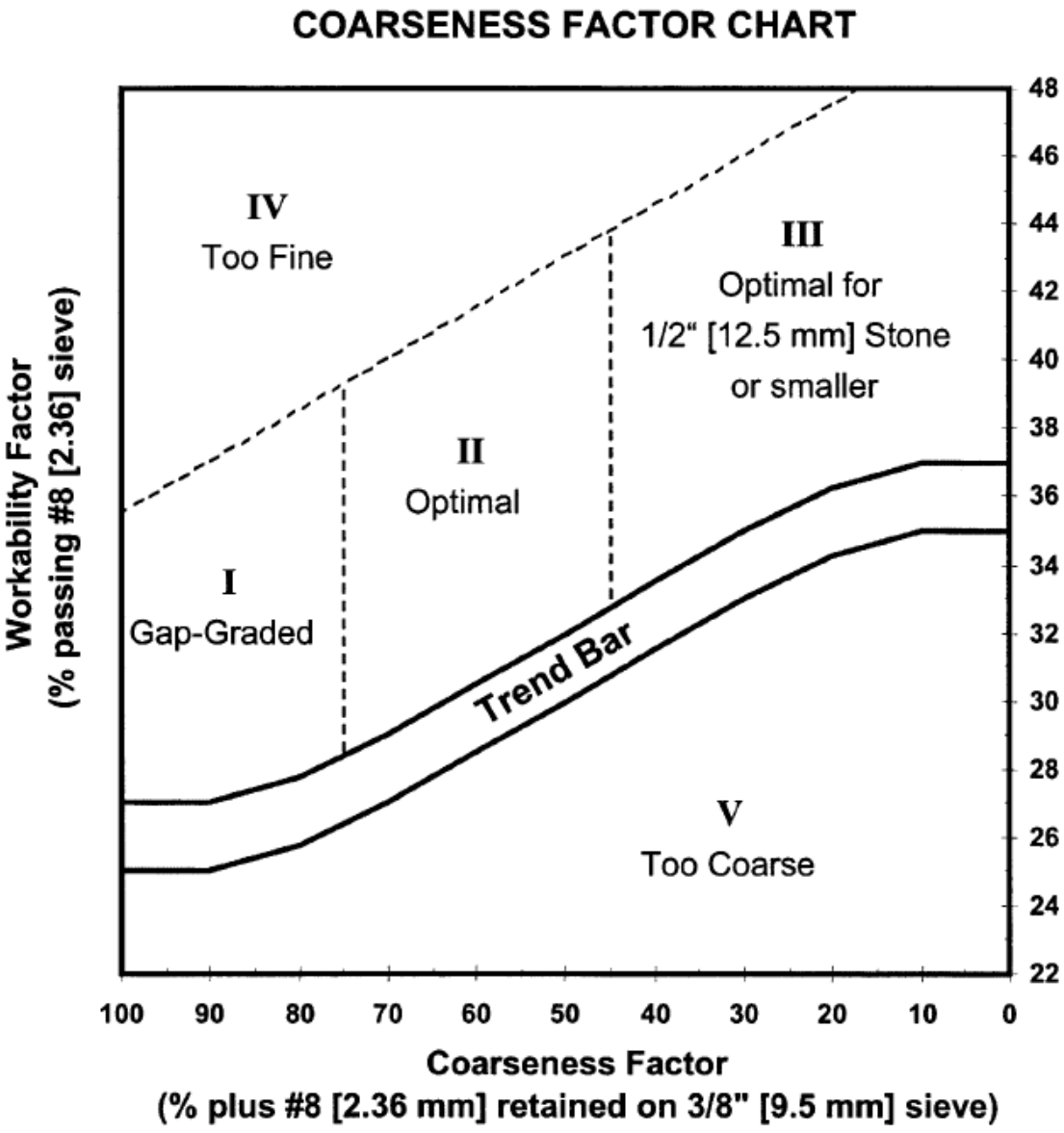

Figure 2-4: Coarseness Factor Chart (ACI Committee 302 2004)

Benefits of the CFC can be seen in cases reported by Shilstone and Shilstone (1996). A low slump mixture placed in Canada segregated as it was dropped into the dump truck. This problem was predicted by its position on the CF chart (CF=83,

WF=31). A second mixture located in Texas, segregated, again as predicted by the CF chart (CF=78, WF=29), as it was placed from a conveyor belt. In a separate case, a mixture was produced using the ACI 211 method that consisted of a gap-graded, two aggregate mixture (CF= 79, WF=37). By adding intermediate aggregates the CF and WF were adjusted to 58 and 36 respectfully, and 23 pounds per yard less water was used at the same slump with the finishability improved (Richardson 2005).

2.4.2.2 0.45-Power Chart

The 0.45-Power Chart, shown in Figure 2-5 is like a semi-log sheet except the spacing is based on the sieve opening in microns to the 0.45-power (Shilestone and Shilstone 2002). It has been widely used by the asphalt industry to determine the best combined grading to reduce voids and the amount of asphalt in a mixture. ACI 302 (2004) states the 0.45-Power Chart is created by plotting the mathematically combined percent passing for each sieve on a chart having percent passing on the y-axis and sieve sizes raised to the 0.45-power on the x-axis. The optimum gradation line is then plotted from the origin of the chart to the sieve one size larger than the first sieve to have 90 percent or less of the aggregate passing. The optimum gradation line can also be generated from Equation 2-3 (Montana Department of Transportation n.d.).

$$\%\text{Passing} = \left(\frac{d}{D}\right)^{0.45} \qquad \textbf{Equation 2-3}$$

Where,

d= Square Opening of the sieve size being considered, and

D= Square opening of the nominal maximum sieve size

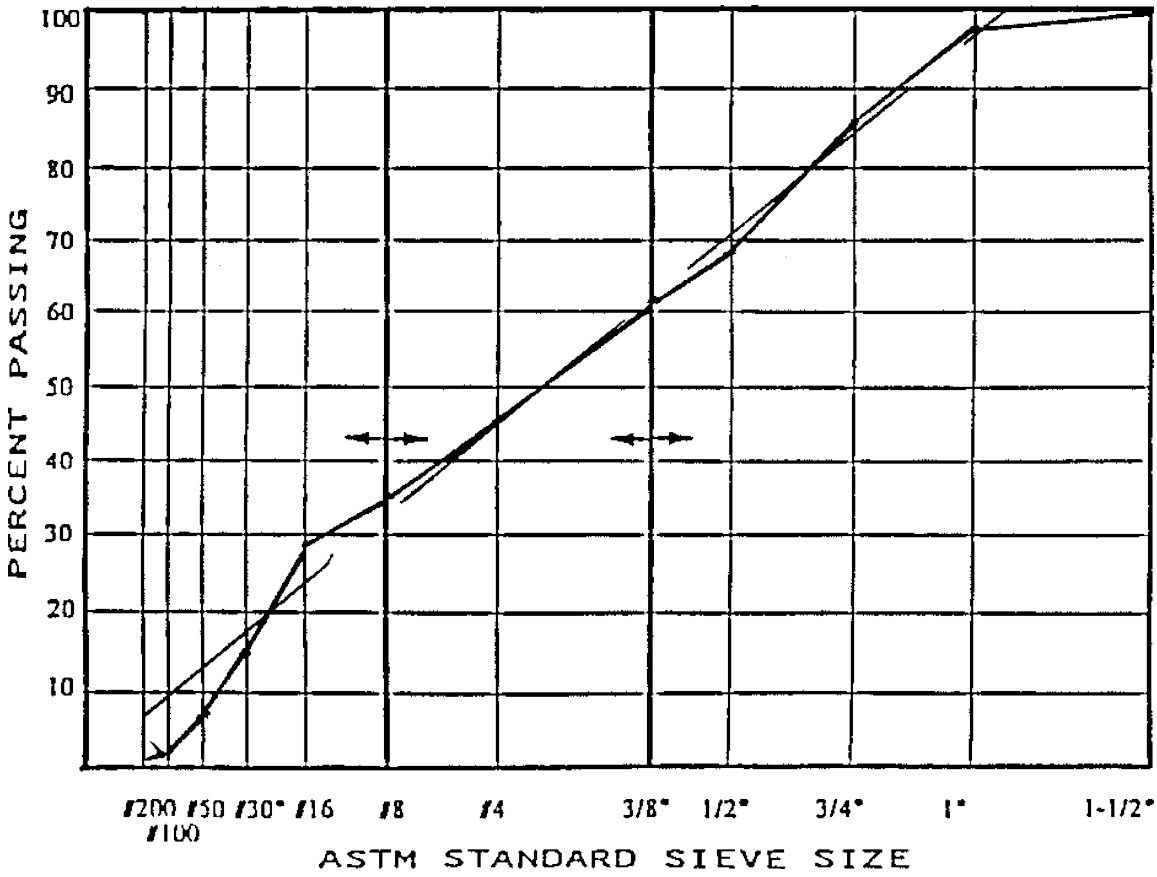

Figure 2-5: 0.45-Power Chart (Shilestone and Shilstone 2002)

A straight line on this chart defines the densest aggregate grading for asphalt. Because asphalt includes fine mineral filler while concrete includes cementitious materials, fewer fine particles passing the No. 8 sieve are necessary for concrete mixtures (ACI Committee 302 2004). Therefore, a perfect match to the 0.45-power line is not ideal for concrete applications. The grading curve for the portion of the combined aggregate passing the No. 30 sieve will typically fall below the optimum gradation line to allow

space for cementitious materials in the final mix (Montana Department of Transportation n.d.).

The power line should not have major dips or rises from the optimum gradation line. Any deviations can help to identify gradation problems. Gradings that zigzag across the line are undesirable (ACI Committee 302 2004). A severe S-shaped curve on the chart would indicate that the gradation is gap-graded. Combined aggregates that plot above the optimum gradation line will tend to be stiff and may require high doses of high-range water-reducing admixture (HRWRA), while blends that plot below the line are too coarse and tend to segregate (Montana Department of Transportation n.d.). The limits for the 0.45-Power Chart should be within ± 7 points from the optimum gradation line according to the Montana Department of Transportation (n.d.). The chart has also been made with tolerance lines starting at zero and extending to the intersection of the 100 percent passing line of the next sieve size smaller and larger than the optimum aggregate line. The grading curve for the portion of the combined aggregate passing the No. 30 sieve will typically fall below the 0.45-power line to allow space for the cementitious materials in the mixture (Montana Department of Transportation n.d.).

2.4.3 PERCENT RETAINED CHART

A more detailed analysis of aggregate gradation can be done using the Percent Retained Chart, shown in Figure 2-6. The Percent Retained Chart is a plot of the percentage of aggregate retained on each individual sieve. The chart can be used to indicate mixes that should be workable and have reasonably low water demand (Montana Department of Transportation n.d.). This chart can provide a tolerance of acceptable uniformity of

distribution of the total combined aggregate particles found in the mixture (ACI Committee 302 2004). Peaks and valleys are more accurately define when plotted on the chart (Shilestone and Shilstone 2002). Shilstone (1993) states when there is a large amount of aggregates retained on the coarser sieves, a deficiency of particles retained on the intermediate sieves (No. 4 and 8), and a large amount retained on the smaller sieves, that mixture can be expected to contribute to problems. ACI 302 (2004) outlined similar occurrences frequently occurring in the U.S. that led to problems associated with cracking, curling, blistering, and spalling of concrete. When there is a deficiency in particles on each of two adjacent sieve sizes but abundance on the sieves adjacent to each, the adjacent sizes tend to balance the two-point valley (ACI Committee 302 2004). If the deficiency extends to three adjacent sieves, then problems will tend to exist. Shilstone (1990) has defined the optimum graded mixture to have a rounded look, with no peaks or valleys existing.

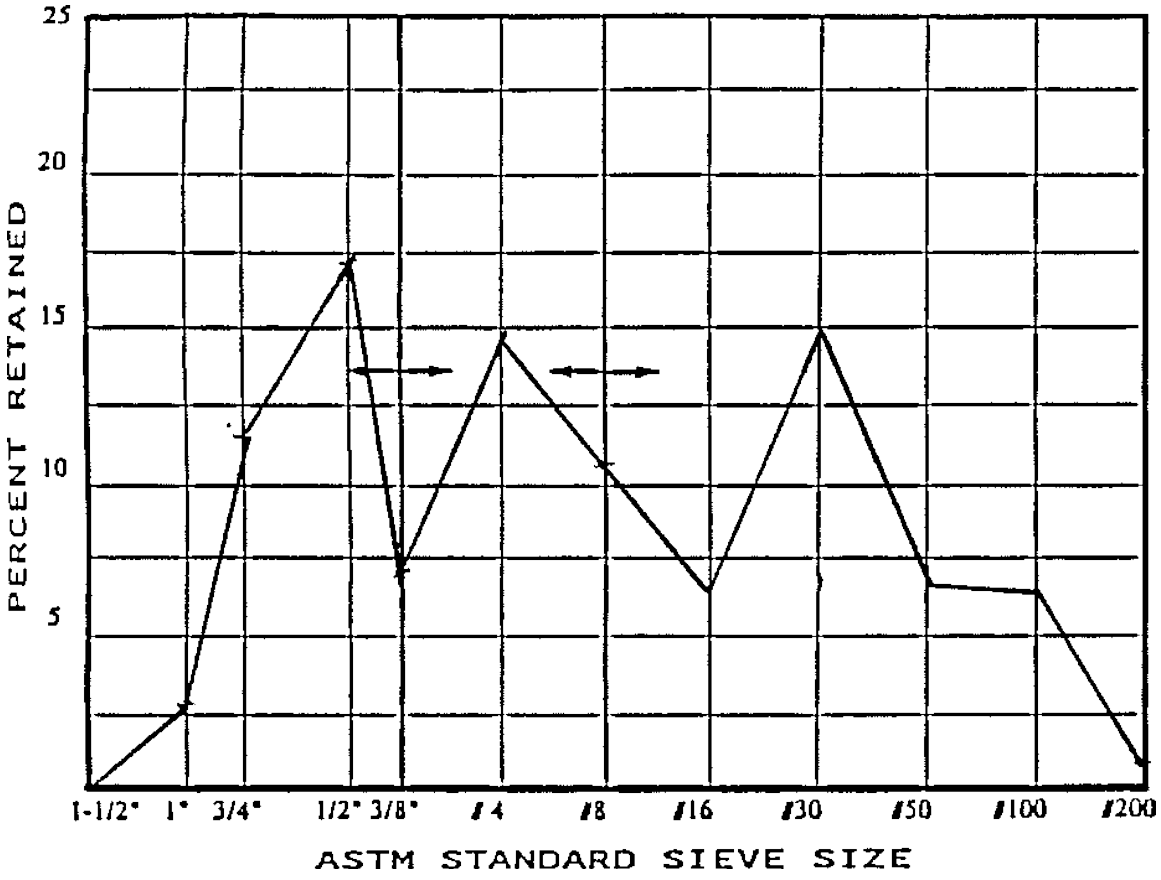

Figure 2-6: Percent Retained Chart (Shilestone and Shilstone 2002)

Tolerances and limits to the Percent Retained Chart are not definite; consequently there are many gradation bands that exist. Shilstone (2007) suggests that the sum of the percent of aggregate retained on two adjacent sieves should not be less than 13 percent of the combined aggregate. According to ACI 302 (2004) gradations requiring between 8 and 18 percent for larger top size aggregates such as 1-1/2 in. or 8 and 22 percent for smaller maximum-size aggregates such as 1 or 3/4 in. retained on each sieve below the top size and above the No. 100 sieve have proven satisfactory in reducing water demand

while providing good workability. The guide line in ACI 302 is based on the data found from J.A. Hollands work with aggregate gradations. Holland (1990) had comparable results to Shilstone's combined aggregate work. During his research he found when he required the total percentage of aggregate to be between 8 and 18 percent his results were good. When he widened the percentages to 6 and 22 percent the results were worse when compared to the 8 and 18 percent limit. Based on his findings, it is generally accepted that Holland is credited with establishing the 8-18 specification. The aggregate bands are thought to be guides in mixture proportioning, as they may not be easily attainable using available local resources (ACI Committee 302 2004).

2.5 MANUFACTURED FINE AGGREGATES

Diminishing natural sand resources and available alkali-silica reactivity-free quarries have increased efforts to identify substitutes for natural sand as a constituent of Portland cement concrete (Dilek 2013). Manufactured fine aggregate (MFA) is produced from the process of crushing rock or gravel to obtain particles that completely pass the 3/8 inch sieve, which results in more angular particles compared to the rounded particles found in natural sand. The use of MFA has been increasing due to the depletion of natural sources. MFA is also referred to as stone sand, crusher sand, crushed fine aggregate, specification sand, or manufactured sand (Fowler and Ahn, An Experimental Study on the Guidelines for Using Higher Contents of Aggregate Microfines in Portland Cement Concrete 2001).

There are two products that result from the manufacturing of MFA: dust-of-fracture mineral filler and ground limestone. According to ACI 211 (2015), mineral filler is defined as a finely divided mineral product at least 65 percent of which passes the No.

200 sieve. Ground limestone is a purposefully manufactured fine product composed primarily of calcium carbonate and with particles sized within narrow ranges. Although ground limestone typically falls within the definition of mineral filler, it is dealt with separately from other mineral fillers. It is manufactured under controlled conditions to be a consistent product. Dust-of-fracture mineral filler consisting primarily of calcium carbonate is not considered ground limestone (ACI 211.7R 2015).

2.5.1 DUST-OF-FRACTURE MINERAL FILLER

The production of MFA usually results in 10-20 percent of dust-of-fracture mineral filler, commonly referred to as microfines. This material is made up of particles that pass the No. 200 (75 µm) sieve. ACI 211 (2015) states dust-of-fracture mineral filler is influenced by many factors, including the equipment used in crushing and the geology of the parent rock. The particle shape can range from flat and elongated to cubical. In natural sand, similar sized particles are mostly clay. When clay and silt occur in natural sands in sufficient quantities, they are deleterious. Even small quantities of clay can cause a dramatic increase in water demand and a reduction in durability. Many think that because MFA has larger percentages of dust-of-fracture mineral filler, it cannot be used for concrete purposes until it has been cleaned of this material. Large amount of dust-of-fracture mineral filler is separated from MFA in order to produce concrete quality sand, which increases costs. It is estimated that 110 million tons of dust-of-fracture mineral filler is produced annually and 80 million tons is not marketed, increasing the environmental impact as the material piles up (Saeed et al. 1997). Figure 2-7 shows an example of a discard stockpile of dust-of-fracture material for long-term storage. Because

the fines are often composed exclusively of rock dust rather than the silts and clays that often occur in natural sands, the use of this material should not be discouraged. The dust-of-fracture material can still produce undesirable effects. Due to their small particle size, they possess a large surface area and require relatively high water content in concrete mixtures (Abou-Zeid and Fakhry 2003). In order to maintain workability and consistency, an increase in the amount admixtures has been associated with the use of MFA with high percentages of dust-of-fracture material. MFA characteristics of grading, shape, and texture as well as the amount and type of dust-of-fracture material have a significant effect on fresh concrete properties such as water demand, admixtures demand, workability, and finishability (Quiroga et al. 2006).

Figure 2-7: Dust-of-fracture mineral filler (ACI 211.7R 2015)

Important relationships exist when using mineral fillers in concrete mixtures that include powder and paste content. ACI 211 (2015) states the powder content is the volume of cement, supplementary cementitious materials, and other mineral fillers in a concrete mixture. In addition, the paste content is the volume of powder and water in a concrete mixture. Dust-of-fracture mineral fillers are similar in size to cementitious materials, but they are often accounted for as part of the fine aggregate volume instead of being considered as part of the powder content. When mineral fillers are added by replacing the fine aggregate volume, the paste volume is increased and the water-powder ratio is decreased. This procedure results in the reduction of workability. In contrast, the dust-of-fracture mineral fillers can be accounted for as part of the powder and paste volume. By replacing part of the powder volume with dust-of-fracture mineral fillers, the water-powder ratio is held constant and changes in the workability are typically much less and are predominantly a function of the particle size distribution, shape characteristics, and clay content of the mineral fillers (Koehler and Fowler, Dust-of-Fracture Aggregate Microfines in Self-Consolidating Concrete 2008).

2.5.2 EFFECT ON CONCRETE PROPERTIES

Most of the previous research done with MFA has shown that concrete properties are not negatively affected, and in some cases are enhanced. However, research has found properties can be adversely affected. It is believed that the effect on concrete properties depends on the percentage of dust-of-fracture mineral filler in the MFA used. The

following sections will discuss the conclusions made in previous research on concrete properties with the use of MFA.

2.5.2.1 Strength

According to ACI 211 (2015), mineral filler can contribute to concrete strength by increasing the overall packing density, providing nucleation sites for cement hydration, or reacting chemically with certain chemical constituents of cement. These mechanisms strongly depend on particle size. Particles must be smaller than cement particles in order to provide a substantial number of nucleation sites for hydration (ACI 211.7R 2015). The mineral filler can also improve workability, which will reduce the water demand and increase the strength.

In research conducted by Quiroga et al. (2006), it was concluded that good quality concrete can be made with MFA with partial replacement of the fine aggregate with dust-of-fracture mineral filler as high as 15 percent. The results showed that most concrete made with MFA surpassed the concrete made with natural sand. Fowler and Rached (2011) used dust-of-fracture mineral filler as part of the powder content which also resulted in an increase in compressive strength. In separate studies, Stewart et al. (2007) using mortar samples with dust-of-facture mineral filler used as part of the fine aggregate volume and Menadi et al. (2009) using concrete samples with mineral fillers included as fine aggregate volume, found slightly less compressive strengths for mixtures containing 15 percent dust-of-fracture mineral filler compared to the control. During concrete mixtures Stewart et al. (2007) found no change in compressive strengths. When comparing the results of a mixture with no dust-of-fracture mineral filler and a mixture

with 5 percent dust-of-fracture (include in the fine aggregate volume) at the same water-cement ratio, Abou-Zeid and Fakhry (2003) found a 7 percent gain in the 28-day compressive strength with the mixture including the dust-of-fracture mineral filler. Topcu and Ugurlu (2003) concluded that there was an improvement in compressive strength from replacing sand with the addition of mineral filler, but improvements were only true for the maximum values of 7-10 percent of the mineral filler. Celik and Marar (1996) found similar results shown in Figure 2-8, concluding that increasing the dust content up to 10 percent improved compressive strength of concrete, but greater dust contents than 10 percent decreased the strength. In mortar testing conducted by Kenai et al. (2008), results showed that in general, the influence of mineral filler on the compressive strength is stronger in the range of 5-10 percent as replacement of sand. The inclusion of mineral filler beyond this range can lead to a lower compressive strength compared to mortars without the dust-of-fracture mineral filler at all ages. Katz and Baum (2006) performed compressive tests using cubes with mixtures accounting for dust-of-fracture mineral filler as part of the fine aggregate volume. Most of the mixtures exhibited an increase of up to 30 percent in their compressive strength as a result of the addition of mineral filler. Most of the improvement occurred with a relatively small addition of fines, and strength did not change much at greater fines contents (Katz and Baum 2006). Among those who found overall negative results in compressive strength at any percentage of mineral filler used was research done by Ahmed and El-Kourd (1989). The mixtures incorporated different percentages of dust-of-fracture mineral filler as a replacement of fine aggregate. Two tests were done using mineral filler, with the first performed with natural fine

aggregate and the second done using MFA. Both tests showed the strength decreasing linearly with increasing percentage of the mineral filler, but the test done using MFA performed better than the tests using natural fine aggregate.

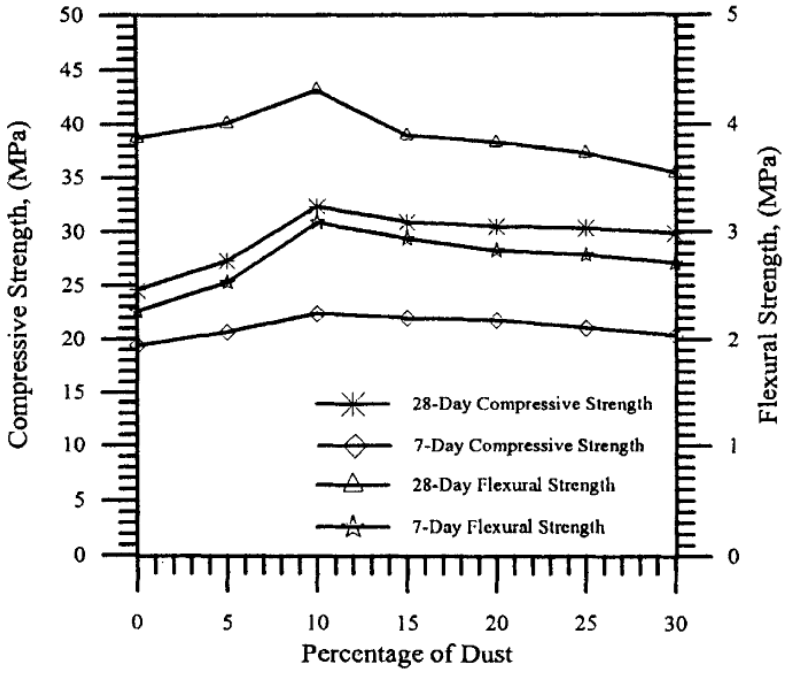

Figure 2-8: Compressive and flexural strengths of concrete with mineral filler (Celik and Marar 1996)

Fowler and Ahn (2001) concluded that the usual proportional relationship between compressive and flexural strength does not apply to MFA concrete, since some characteristics of MFA (such as greater microfines, particle shape and texture) improves flexural capacity compared to natural fine aggregate. Quiroga et al. (2006) found that all mixtures incorporating MFA had a greater flexural strength than the control mixture, with

five out of the 10 mixtures having approximately 20 percent more strength than the control. Stewart et al. (2007) found dust-of-fracture mineral fillers incorporated into mixtures at levels up to 15 percent of the fine aggregate volume had slightly greater and less strengths, depending on which source of mineral filler was used. The flexural strength was found to decrease with an increasing uncompacted void content. Abou-Zeid and Fakhry (2003) showed that some increase in flexural strength is attributed with mineral filler, but this relationship is less pronounced in mixtures incorporating admixtures. Topcu and Ugurlu (2003) found that the flexural strength increased for all mixtures, unlike with the compressive testing where an increase was only shown in mixtures incorporating mineral filler at levels of 7-10 percent. Celik and Marar (1996) found similar results to the compressive testing shown in Figure 2-8, in which strength increases were found up to 10 percent and any further increase in the percentage of mineral filler decreased the strength. Ahmed and El-Kourd (1989) also found similar results to their compressive testing, showing that the 28-day flexural strength decreases linearly with increasing mineral filler addition into the fine aggregate volume.

2.5.2.2 Drying Shrinkage

Research has shown that use of mineral filler as a portion of the fine aggregate typically results in equal or greater shrinkage. This change in shrinkage is usually attributed to the greater powder content in the concrete mixture (ACI 211.7R 2015). The water demand is the most influencing factor affecting drying shrinkage, therefore, to reduce the shrinkage effect in MFA concrete, chemical admixtures can be used to reduce the amount of water (Fowler and Ahn 2001).

In the study conducted by Quiroga and Fowler (2007) drying shrinkage did not increase significantly in mixtures with high microfines as compared with mixtures without microfines. In a mixture of fine aggregate with 20 percent mineral filler, an increase of 11 percent in drying shrinkage was found when compared to the control. In a study done by Quiroga et al. (2006), half the MFA mixtures (unmodified with additional mineral filler percentages) resulted in less drying shrinkage, but two mixtures showed 50 percent greater drying shrinkage strains than the control. In the study conducted by Fowler and Rached (2011), mineral fillers were proportioned by reducing water and cement contents. This condition resulted in constant water-cementitious ratio and lower water-powder ratio. The illustration, shown in Figure 2-9 was made to better display Fowler and Rached's experimental set-up. In using the mineral fillers as part of the powder, results showed that shrinkage decreased as the mineral fillers percentage increased for 30 percent replacement of cement and water. Drying shrinkage originates from the cement paste, therefore these results are expected. Celik and Marar (1996) found increasing the mineral filler content up to 10 percent increased the drying shrinkage. As this limit was exceeded, the shrinkage decreased. In the study conducted by Katz and Baum (2006), slightly greater concrete shrinkage was found when HRWRA was used to keep the slump constant. The shrinkage was also dictated by the mineral filler size. For coarser sized mineral filler particles, the shrinkage was less affected regardless of the fine aggregate replacement percentage compared to finer size mineral filler particles. Ahmed and El-Kourd (1989) found that the drying shrinkage strains increased with increasing replacement of fine aggregate with mineral filler.

w (water) c (cement)	↓ ↓	→	w/cm = constant (water-cementitous material ratio)
w (water) c (cement) mf (mineral filler)	↓ ↓ ↑	→	w/p ↓ (water-powder ratio)

Figure 2-9: Dust-of-fracture mineral filler proportioning

2.5.2.3 Chloride Ion Permeability

Table 2-5 shows values for testing the rapid penetration of concrete according to ASTM C1202 (2006). Typical concrete has moderate permeability, ranging from 2000-4000 coulombs according to the standard. Research has generally found concrete that is composed of MFA has reduced values of chloride ion permeability. It is thought that the dust-of-fracture particles fill the voids between aggregates, creating a less permeable concrete (Fowler and Ahn 2001).

Table 2-5: Chloride Ion Permeability Based of Charge (ASTM Standard C1202 2006)

Charge Passed (coulombs)	Chloride Ion Permeability
> 4000	High
2000-4000	Moderate
1000-2000	Low
100-1000	Very Low
<100	Negligible

The studies of Quiroga and Fowler (2007) and Quiroga et al. (2006), both found that concrete with MFA with dust-of-fracture mineral filler had reduced chloride ion permeability than concrete without mineral filler. Fowler and Ahn's (2001) study also agreed with the Quiroga studies that dust-of-fracture mineral filler will result in less permeability, when used at constant water-cementitious ratio and no water reducing admixtures. The research also included a case study using No. 57 limestone, where MFA concrete with 13 and 17 percent mineral filler showed less permeability than the control mixture. However, for a mixture involving 20 percent mineral filler, the permeability was slightly greater than the control mixture. In the study conducted by Menadi et al. (2009), the results show a slight increase in Rapid Chloride-Ion Penetration Test (RCPT) values at 15 percent mineral filler in MFA, which were in agreement with those obtained by Bonavetti et al. (2000), who reported an increase of RCPT values for concrete containing 10 and 20 percent limestone filler as replacement of cement. Menadi et al. (2009) states, the greater permeability of concrete with limestone fines could limit its use in structures exposed to marine environment. This disagrees with the study done by Fowler and Rached (2011), where RCPT values slightly increased with the addition of all mineral fillers to the powered content, but at 30 percent replacement the permeability decreased, as shown in Figure 2-10. The study by Celik and Marar (1996) use water permeability to test the durability of concrete made with MFA with added mineral filler contents. The highest permeability occurred with the mixture that had no mineral filler within the MFA. The lowest permeability occurred with the mixture that had 30 percent mineral filler added to the MFA. The study found that the addition of dust-of-fracture mineral filler

improves the impermeability of concrete because it blocks the passages connecting capillary pores and the water channels. Kenai et al. (2008) found concrete mixtures incorporating MFA with limestone fines as fine aggregate replacement resulted in greater RCPT values than concrete without the fines.

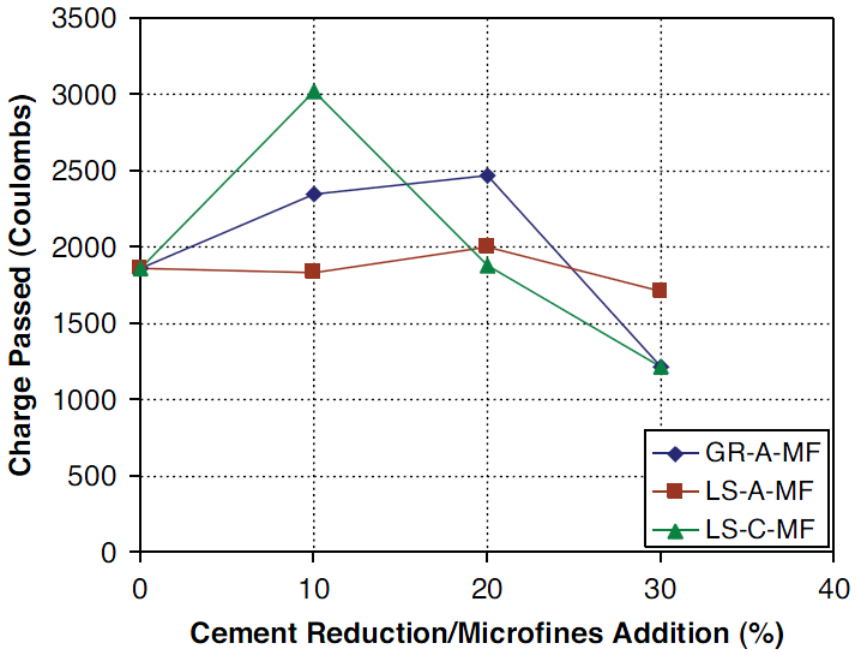

Figure 2-10: Effect of microfines replacement rate on permeability (Fowler and Rached 2011)

2.5.2.4 Abrasion Resistance

Data have shown that mineral filler can affect abrasion resistance positively or negatively. ASTM C33 (2013) limits the amount of dust-of-fracture material finer than the No. 200 sieve in MFA to 5 percent of the fine aggregate mass in structures subjected

to abrasion, and 7 percent in all other structures. Bakke (2006) stated the failure of concrete to resist abrasion can be traced to cumulative effects such as soft aggregate and improper curing or finishing of concrete surfaces. In addition, the compressive strength is one of the most important factors. The abrasion resistance of concrete is thought to increase with an increase in compressive strength (Bakke 2006).

In the study conducted by Fowler and Ahn (2001), all 10 of the MFA mixtures containing dust-of-fracture mineral fillers as part of the fine aggregate showed less 28-day abrasion loss than that of the control concrete. This is in agreement with the studies conducted by Stewart et al. (2007) and Quiroga et al. (2006), which both showed greater resistance to abrasion as compared to the control mixtures for mineral filler contents added as part of the fine aggregate volume. In a separate study involving SCC, Koehler and Fowler (2008) found that the use of mineral filler as part of either the aggregate or powder volume generally resulted in reduced abrasion loss at constant water-cementitious ratio. Celik and Marar (1996) used impact resistance rather than abrasion resistance for durability testing. A maximum blow count of 81 was reached with the mixture containing MFA with addition of 5 percent mineral filler in relation to the fine aggregate volume. For greater mineral filler contents the impact resistance decreased and reached a minimum blow count of 33 for the 30 percent mineral filler mixture. The findings disagree with the theory that abrasion resistance increases with an increase in compressive strength. The highest compressive strength was recorded in the mixture containing 10 percent mineral filler. This may be due to the different test procedures. Impact resistance may not correlate with strength the same way as abrasion resistance.

2.5.3 LIMITS ON DUST-OF-FRACTURE MINERAL FILLER

Many construction material specifications limit the amount of very fine materials for use in concrete of good quality, which limits how much mineral filler can be used. This can make products containing increased quantities of mineral filler difficult to use. This often leads to an overabundance of these materials in long-term storage at quarries (ACI 211.7R 2015). ASTM C 33 (2013) allows a maximum of 7 percent (5 percent for concrete subject to abrasion) mineral filler if they are essentially free of clay or shale. Historically, the reason for this limit is that most deleterious clay or silt that may be present in an aggregate will be removed along with this size fraction (Stewart et al. 2007). Other reasons include high water content in concrete mixtures from increased surface area (due to the mineral filler's small size). Also, it is argued that fines act as a thin insulating film over larger aggregate particles, leading to a reduced bond between aggregates and the surrounding cement paste (Abou-Zeid and Fakhry 2003). As a result, such specifications severely limit the amount of mineral filler that can be used, even though greater mineral filler contents can improve the properties and the performance of the resulting concrete and reduce the cost (Quiroga et al. 2006). Furthmore, the use of these by-product materials results in sustainable use of resources.

As of the start of this research in January 2014, specifications within the United States geographically related to this research were outlined based on their limits to dust-of-fracture mineral filler. The results are shown in Table 2-6, which includes 12 state specifications from department of transportation (DOT) agencies. From the states that provided limits of mineral filler use in their DOT specifications, 6 out of the 10 allow a

greater percentage than what ASTM or AASHTO recommend. This is not unusual as reported by Quiroga and Fowler (2004), other specifications have greater limits. In their research, they state that 5 countries that have greater limits than what ASTM presents. They include the Spanish Concrete Standard (15 percent), the Indian specification (15-20 percent), the Australian specification (25 percent if agreed by client, and no more than 5 percent of entire aggregate), and the French standard (12-18 percent). All the percentages are based on the total fine aggregate mass.

Table 2-6: Limits of Dust-of-Fracture Mineral Filler

Specification	Dust-of-Fracture Mineral Filler Allowed (Percentage of Sand by Volume)
AASHTO	5 % deleterious substances not subjected to abrasion passing the 75 µm sieve. 4 % deleterious substances subjected to abrasion passing the 75 µm sieve. Failing aggregates can be used if strength is not less than 95% at seven days.
ASTM	3 % passing the 75 µm sieve for concrete subjected to abrasion. 5 % passing the 75 µm sieve for concrete not subjected to abrasion. 5 % passing the 75 µm sieve for concrete subjected to abrasion with manufactured sand. 7 % passing the 75 µm sieve for concrete not subjected to abrasion with manufactured sand. Failing aggregates can be used if fresh and hardened properties are shown suitable.
Alabama DOT	2.5 % passing the 75 µm sieve (for natural sand) 5 % passing the 75 µm sieve (for manufactured sand)
Arkansas DOT	Not Listed
Florida DOT	4 % passing the 75 µm sieve (for silica sand) 5 % passing the 75 µm sieve (for RipRap) 15 % passing the 75 µm sieve (for local materials)
Georgia DOT	3 % passing the 75 µm sieve (for natural concrete sand) 4 % passing the 75 µm sieve (for natural mortar sand) 5% passing the 75 µm sieve (for standard manufactured concrete sand) 9 % passing the 75 µm sieve (for fine manufactured concrete sand)
Louisiana DOT	3 % passing the 75 µm sieve
Mississippi DOT	Not Listed
North Carolina DOT	8 % passing the 75 µm sieve
South Carolina DOT	3 % passing the 75 µm sieve (for natural sand) 10 % passing the 75 µm sieve (for manufactured sand)
Tennessee DOT	3 % passing the 75 µm sieve
Texas DOT	3 % passing the 75 µm sieve (for natural sand) 6 % passing the 75 µm sieve (for manufactured sand)
Virginia DOT	0 % passing the 75 µm sieve
West Virginia DOT	10 % passing the 75 µm sieve (for mortar sand)

ASTM C33 (2013) was developed prior to such large volumes of MFA produced today, and is based primarily for natural sand (Fowler 2009). ASTM C33 (2013) is used in conjunction with ACI 211.1. In May 2015, the American Concrete Institute published ACI 211.7R, called Proportioning Concrete Mixtures with Ground Limestone and Other Mineral Fillers. The intent is to supplement ACI 211.1 in order to give a better guide on how to proportion these materials for concrete mixtures. With the acceptance of this specification, there will be a positive push towards using MFA in future concrete applications. Along with providing a general background about mineral filler and ground limestone, the guide also presents how the materials may impact concrete. It also offers modified versions of ACI 211.1 proportioning method for both materials. Some of the highlights of the updated procedure, in reference to dust-of-fracture mineral filler include modifications to estimating the mixing water, selecting the water-cementitious ratio, calculation of mineral filler content, and estimating the coarse aggregate content. The modifications to each step are as follows:

When estimating the mixing water using this procedure, ACI 211.7R (2015) states that the addition of mineral filler may increase or decrease the amount of water needed for a given workability, depending on the shape, size, particle size distribution, and clay content of the mineral filler. Any decrease in workability may be offset by the use of water reducing admixtures. The standard goes on to state that for mineral filler, the powder content should be treated as if it is cementitious material when computing the admixture dosage per cubic yard.

In discussing the modifications to the selection of water-cement ratio or water cementitious ratio, ACI 211.7R (2015) begins by stating mineral filler is not a cementitious material, but it has been shown to increase the strength and durability of concrete. Therefore, a greater ratio may be used than in a corresponding concrete mixture without mineral filler.

ACI 211.7R (2015) details how to calculate the amount of dry and wet mineral filler used for a concrete mixture in a series of equations. In the case of wet mineral filler, the amount is determined after calculating the fine aggregate content and then done in the same way as the dry material. For dry mineral filler, the standard treats the material as a powder and uses the following equations (ACI 211.7R 2015):

$$\text{mineral filler} = \frac{(\text{cementitious material})(\text{percent mineral filler})}{(100\% - \text{percent mineral filler})} \qquad \textbf{Equation 2-4}$$

$$\text{mineral filler} = (\text{powder})(\text{percent mineral filler}) \qquad \textbf{Equation 2-5}$$

$$\text{powder} = \frac{(\text{water})}{w/p} \qquad \textbf{Equation 2-6}$$

$$\text{cementitious materials} = \text{powder} - \text{mineral filler} \qquad \textbf{Equation 2-7}$$

When estimating the coarse aggregate content, mineral filler is addressed in wet and dry conditions. For the dry condition, a decrease of 0.20 in the fineness modulus is called for when using Table 6.3.6 in ACI 211.1 (2012). ACI 211.7R (2015) states the increased fineness associated with the use of mineral filler may enable a reduction in the amount of fine aggregate and a concurrent increase in the amount of coarse aggregate.

For wet mineral filler, the fineness modulus is addressed through the combined aggregate gradation of the MFA and the mineral filler it contains.

These modifications allow for an increased use in MFA, but the original limit on mineral fillers from ASTM C33 (2013) still applies. Although these modifications cannot get around the low limits given within ASTM, the problem is addressed by blending wet MFA and the mineral fillers it contains with other sand. Table 2-7 gives an example of how multiple sands can be blended in order to meet project limits.

Table 2-7: Combined fine aggregate gradations (ACI 211.7R 2015)

	Cumlative percent passing		Combined sand gradation (by mass), percent							
			Sand 1	70	60	50	40	30	25	20
Sieve Size	Sand 1	Sand 2	Sand 2	30	40	50	60	70	75	80
3/8 in.	100	100		100	100	100	100	100	100	100
No. 4	96	98		97	97	97	97	97	97	97
No. 8	72	85		76	77	78	80	81	82	82
No. 16	50	66		55	57	58	60	61	62	63
No. 30	38	44		40	40	41	42	42	43	43
No. 50	29	20		26	25	24	23	23	22	22
No. 100	24	5		18	16	15	13	11	10	9
No. 200	19	1.6		14	12	10	9	7	6	5
Fineness modulus	2.92	2.82		2.89	2.88	2.87	2.86	2.67	2.66	2.65
Specific gravity (saturated surface-dry)	2.77	2.62		2.73	2.71	2.7	2.68	2.67	2.66	2.65
Absorption, percent	0.69	1		0.78	0.81	0.85	0.88	0.91	0.92	0.94

2.5.4 DUST-OF-FRACTURE CHARACTERIZATION TESTS

Dust-of-fracture mineral filler should be characterized to evaluate if it can be used for concrete or to determine the maximum amount in which it can be used (Quiroga and Fowler 2007). Some types can result in very high water demand and their use in concrete may not be suitable. The mineral filler, which results from the crushing of a parent aggregate to produce MFA, can be derived from many types of sedimentary, igneous, and metamorphic rock types and differ widely in characteristics. The main characteristics affecting concrete properties are particle morphology (shape, angularity, and texture), mineralogy, particle size, particle size distribution, deleterious materials, and density (ACI 211.7R 2015). Several tests have been used to characterize dust-of-fracture mineral filler. Some of the most frequently used tests in previous research studies will now be discussed.

2.5.4.1 Vicat Test

The packing degree is important when determining the suitability of mineral filler. Rounded particles usually require less water and have a greater packing degree. The behavior of mineral filler in concrete mixtures is best described by the wet packing density, which is determined using the Vicat test (Quiroga and Fowler 2004). The Vicat test for mineral filler is similar to the test that is used for consistency of cement pastes. The test method is used to determine the amount of water required to meet a target consistency. It is expected that the greater the water demand in the test, the greater the water demand in concrete (Quiroga and Fowler 2007). In research conducted by Quiroga et al. (2006) it was determined from the samples tested, mineral filler from limestone

resulted in the highest packing density and mineral filler from granite had the lowest. The slump flows for the limestone mixtures were twice as great as the granite and required 25 percent less admixture. The test was also run on cement and fly-ash for comparison. A relationship between the water-reducing admixture dosage and the packing density was also established, although it is stated that this relationship is not general and only valid for the specific conditions of the research mixtures. The dosage of admixture was chosen to reach a target slump, shown in Figure 2-11. It was concluded that the wet packing of microfines and cementing materials obtained from the Vicat test is a good predictor of the effect on concrete water demand.

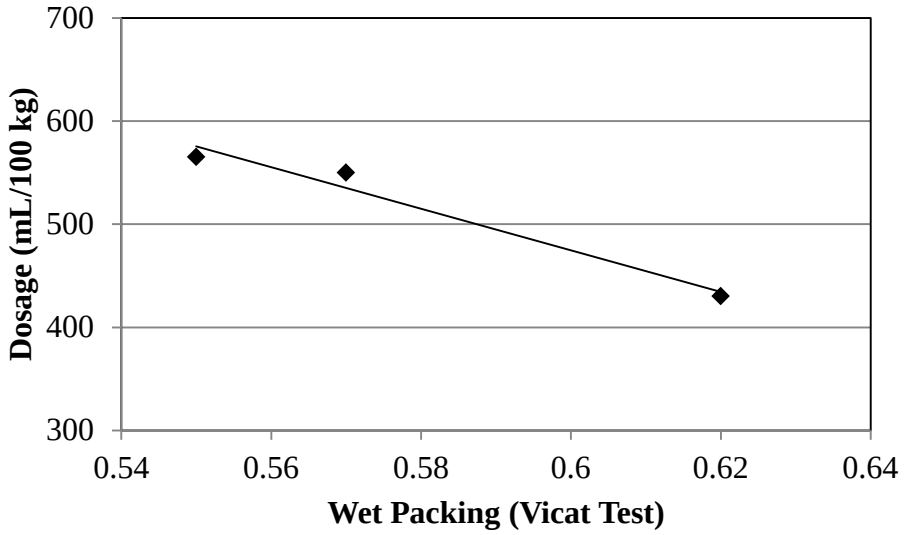

Figure 2-11: Dosage of water-reducer versus packing density (Quiroga et al. 2006)

2.5.4.2 Laser Size Distribution

ACI 211.7R (2015) states the combined particle size distribution of all solid particles, including mineral fillers strongly affects concrete workability. Given the influence of particle size and particle size distribution on concrete properties, maintaining consistency of these characteristics is important. Therefore, the particle size distribution of mineral filler relative to other constituent materials should be considered (ACI 211.7R 2015). In research conducted by Stewart et al. (2007), laser size diffraction was used to test different sources of mineral fillers and cement for comparison. This method was determined to be the most appropriate for characterizing portland cement, and since mineral filler and cement have similar sizes, it was adopted for the study. The results of the size distribution data determined by laser diffraction are shown in Figure 2-12. The mineral fillers tested included limestone, gneiss, and granite from three different sources. It can be seen that the granite (GR03) sample has a greater percentage of small particles than the other mineral fillers tested. In some samples, the test measures particles that are greater than 75 μm; this is likely due to some elongated particles that slipped through the sieve openings during processing (Stewart et al. 2007). Using the data from the laser diffraction test, relationships can be correlated with concrete properties. The granite sample that had the greatest percentage of small particles also had the lowest chloride penetration value. It was also found that samples which have a larger percentage of large particles in the mineral filler had greater strengths. The laser size distribution test is a good method for determining mineral filler characterizations and the particle size distribution, but is not always available. In most instances, samples need to be shipped to

laboratories for testing. When this is not possible, tests that are more simple and inexpensive can be used to give a good indication of mineral fillers and their effects on concrete performance.

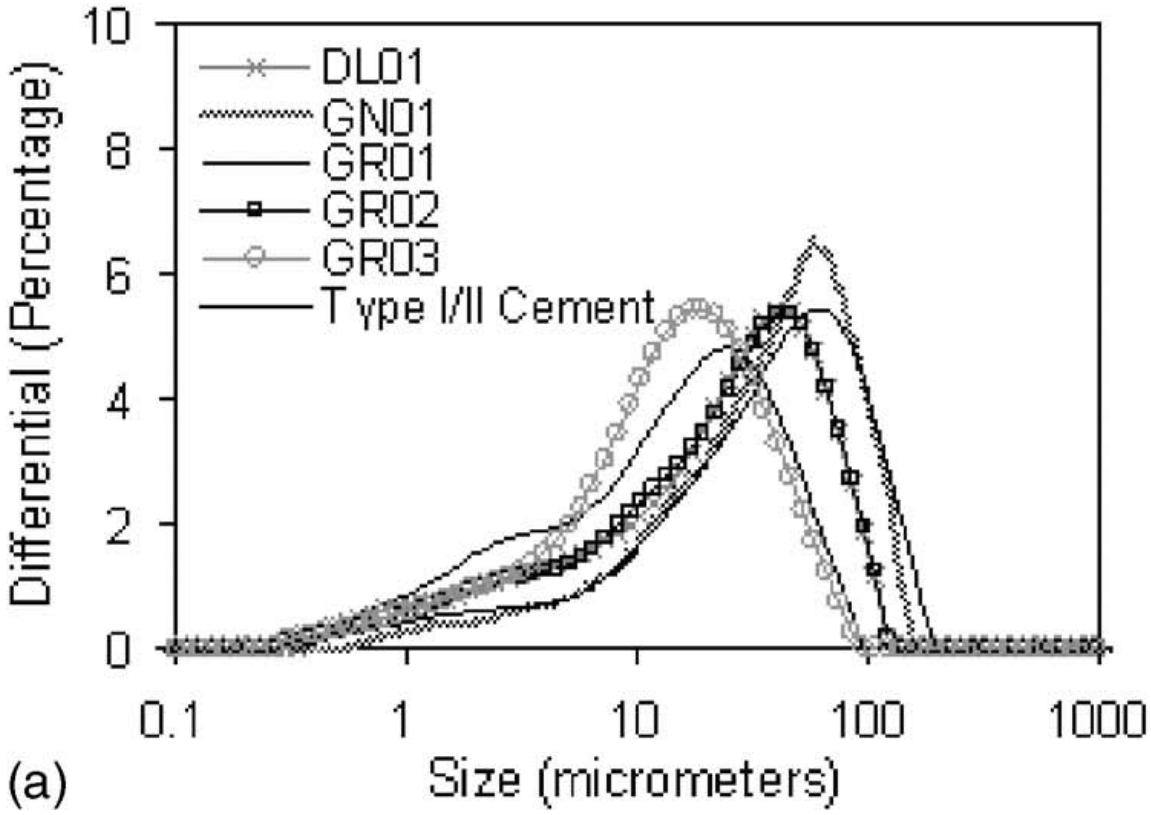

Figure 2-12: Laser particle distribution results (Stewart et al. 2007)

2.5.4.3 Clay Material - Methylene Blue Test

An important factor to consider when using MFA is the possibility of clay or other deleterious material presence. There are three possible forms of particles finer than 75

μm (No. 200 sieve). They include clay, silt, and dust that all have different effects on concrete. Clay is defined as hydrous aluminum-phyllosilicates with certain layered structures (composed of tetrahedral and octahedral sheets and exchangeable cations) that exhibit plasticity in presence of water (ACI 211.7R 2015). They are typically less than 2 μm in size, but Norvell et al. (2007) believes that clays should be classified based on their mineralogy and not size because this would limit the use of the potentially beneficial mineral filler. Limiting the amount of fine material does not prevent detrimental effects of clay on concrete properties. Even if the quantity of mineral filler material is very low, the clay content may be high, and the compressive strength is generally negatively affected (Topcu and Demir 2008).

The most harmful aspect of clay is its ability to exchange cations. This process is done in order to balance the charge of the clay. The cations are readily exchanged with organic compounds, such as water reducing admixtures, which makes the admixtures unavailable for lubricating the fresh concrete (Topcu and Demir 2008). This exchange necessitates the use of more water reducing admixtures, as the majority is being used up by the clay. In addition to the cation exchange, clays swell when they absorb water (water that is not released) and can create a weak bond between the aggregate and the cement. The clay mineral coats the outside of the aggregates and produces a weak bond, resulting in increased shrinkage values and decreased strengths (Topcu and Demir 2008). However, not all clays are equal. The most damaging clays are found to belong to the smectite group, which includes montmorillonite. Other forms of clay, including kaolinite and illite are found to be less detrimental. Shen et al. (2012) even found that the

substitution of kaolin clay can increase the strength of portland cement concrete. Results from a study done by Maldonado et al. (1994) are shown in Figure 2-13. The research highlighted concrete composed of mineral filler results in increased tensile strength up to 20 percent, while concrete made of kaolinite and montmorillonite dropped in strength right away. Less than 5 percent was enough to cause a decrease in the tensile strength by 10 percent.

The ability to exchange cations also provides the basis for detecting the presence of clay minerals. Clay minerals adsorb methylene blue (a cationic dye) when in the form of an aqueous solution. This gives a means to measuring the clay content by measuring the surface area. The greater the surface area of a sample, the more methylene blue will be needed to cover the clay particles (Yool et al. 1998). This method to characterize the clay content is named the Methylene Blue Value (MBV) and dates back to the 1940s for original use in asphalt. It is standardized as AASHTO T330 (2007). An increase in the amount of clay material increases the MBV. It was observed in multiple research studies, as stated in Topcu and Demir (2008) that the MBV changes independently of the mineral filler content and is related to the clay content. Sand replaced with montmorillonite at 1 and 4 percent has MBVs near or greater than 20 mg/g, while kaolinite and illite replacement results in much lower MBV values (Norvel et al. 2007). Differences between clays MBV are due to the surface area and number of cation exchange sites. According to AASHTO T330 (2007), aggregates with MBVs less than 6 mg/g are considered excellent and will not cause problems in asphalt concrete. The MBV has been found to be a good indicator of clay, but the relationship between the MBV and concrete properties has not

been fully developed. Researchers have observed correlations between MBV and properties such as workability and drying shrinkage, but generally stop short of being able to predict performance based on MBV alone (Pike 1992). For this reason, it is believed the test should only be used as a screening process of MFA.

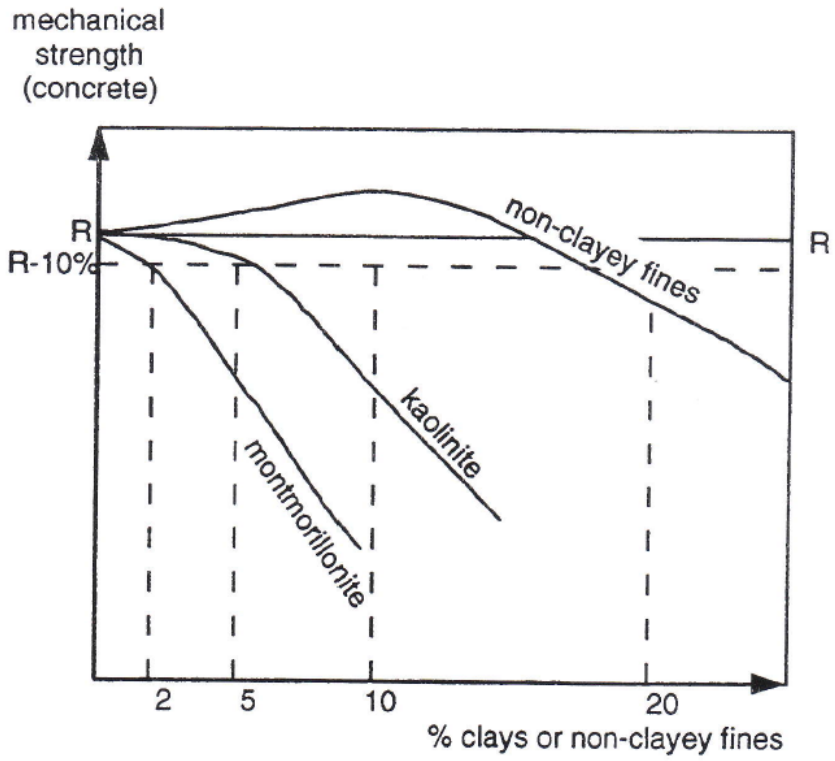

Figure 2-13: Influence of clay and mineral filler (Maldonado et al. 1994)

2.6 WORKABILITY

ACI (2013) defines workability as the property of freshly mixed concrete or mortar that determines the ease with which it can be mixed, placed, consolidated, and finished to a

homogeneous condition. Other terms that are commonly associated with workability include flowability, consistency, pumpability, plasticity, compactability, stability, and finishability. These are all qualitative definitions and give no attempt to describe behavior in a quantitative way. The use of these terms in inaccurate ways has led to much confusion in workability measurement. This is due to the fact that workability is broadly defined throughout the industry because no test exists that can measure all of its aspects.

The most common test used to describe workability is ASTM C143 (2012), or the slump test. Over the years, this test has taken on even more meaning. As Shilstone (1988) states, for some it is a reflection of the amount of water in a mixture, and may be used as an indicator of expected strength. This myth originated from laboratory use, and with only minor changes in the materials, it may hold some truth. However, for the majority of concrete mixtures this is false thinking. The slump test is easy to perform so it is a simple solution to a complex materials equation; unfortunately it obscures the variations that occur in the concrete manufacturing process (Shilstone 1988). Popovics (1994) states the slump test does provide some information about workability and qualitative information with regard to mix cohesiveness, but only on a "within-batch" basis. Therefore, the test should not be used to compare two separate mixtures, especially on a quantitative basis. While two mixes being sampled may both have the same slump, one mix may lose all cohesive properties when subjected to the slightest vibration just as the other may remain stationary at the initial slump; in this case the slump test would not reveal such behavior (Quiroga and Fowler 2004). In order to properly describe the workability of concrete mixtures, a test needs to use quantitative values so the results can

be easily passed on and understood. In addition, the test should have a theoretical basis in order to avoid any subjective assessments. By strictly conforming to a standard, the test can be easily repeated with little error. Specifically, concrete workability should ideally be described in terms of fundamental flow properties (Koehler and Fowler 2003).

2.6.1 RHEOLOGY

Rheology is the study of the flow of matter and its deformation. Using rheological properties to measure the workability of fresh concrete gives a better description of the flow behavior, which can be standardized across the concrete industry (Koehler and Fowler 2003). In order to analyze concrete through rheological properties, concrete should be viewed as a fluid material. This states that it will continuously deform under an applied shear stress. A flow curve can then be generated, using the shear stress and the shear rate. The resulting linear relationship is called Newton's Law of Viscous Flow, where the shear stress is proportional to the shear rate, and the constant of proportionality is called the viscosity. A substance that obeys this law is referred to as a Newtonian liquid (Tattersall 1991). Most workability tests fail in quantifying concrete properly because they measure a single parameter, which is an accurate way to measure a Newtonian fluid. Concrete does not behave in this simplistic manner, as water would.

Concrete possesses a yield stress, or minimum stress that must be exceeded to initiate flow (Koehler and Fowler 2003). Tattersall (1991) states the mere fact that a slump test can be carried out at all, or that the material can stand in a pile and resist flow under the influence of its own self-weight, proves this true. In order to display the yield stress a different relationship must be utilized. The use of only one parameter cannot

accurately display the differences between concrete mixtures, as shown in Figure 2-14. Therefore, Tattersall suggests the use of the Bingham model to describe the concrete behavior with two parameters. The shear stress on a material is the sum of the yield stress and plastic viscosity, which is proportional to the shear rate. The relationship developed by the Bingham model is shown in Figure 2-15. The initial shear stress required to start the flow is symbolized by τ_0. Other research has shown that the rheology of concrete is better described by the Herschel-Bulkley model. This model is more complex and better suited for highly flowable mixtures (self-compacting concrete) that have nonlinear flow curves. Using the Bingham model equation to represent a concrete mixture with a nonlinear flow curve not only gives an inaccurate indication of viscosity but can also result in an erroneous yield stress when the linear flow curve is extrapolated to the shear stress axis (Koehler and Fowler 2003). This research will focus on the Bingham model because it has been found to be appropriate for the majority of concrete mixtures.

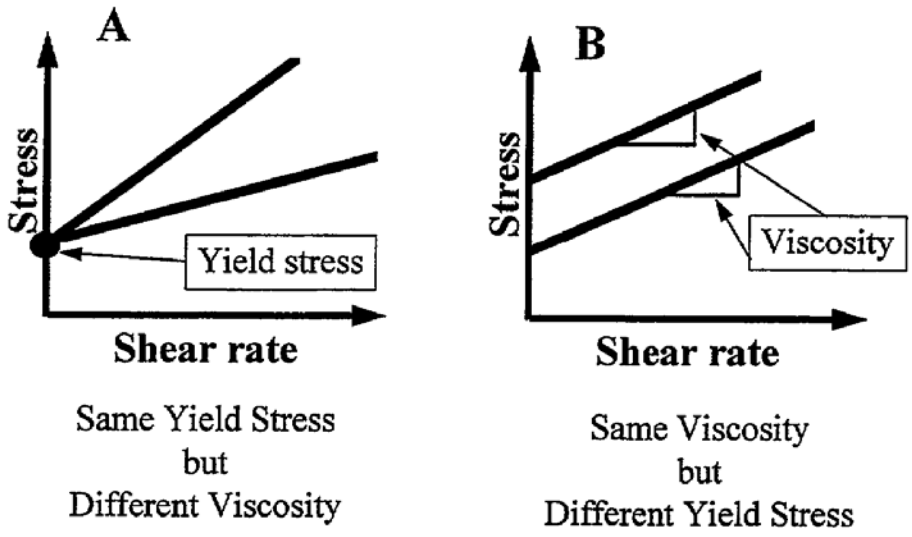

Figure 2-14: Concrete rheology using two parameters (C. F. Ferraris 1996)

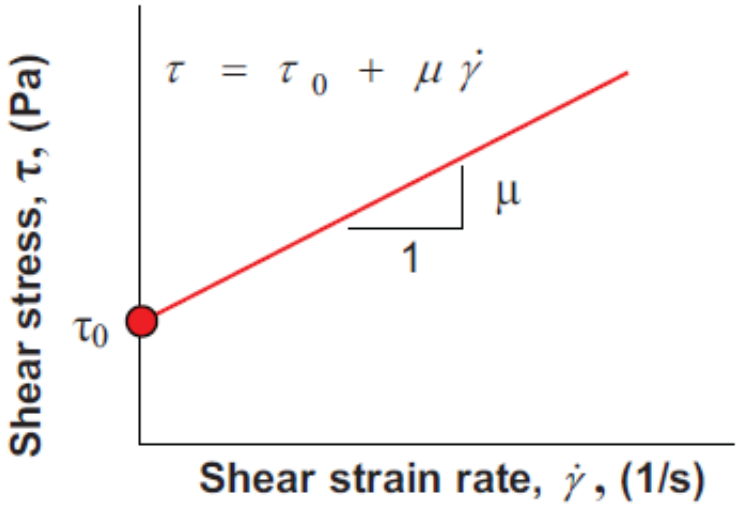

Figure 2-15: Bingham model (Germann Instuments 2014)

2.6.2 TEST METHODS

Many tests methods exist for testing concrete mixtures for both field and laboratory applications. Few of these tests have been used on a widespread basis throughout the industry, with exception to the slump test. Even as concrete workability is further studied and more is learned about rheology, the slump test is the predominate procedure used. Koehler and Fowler (2003) state, the advent of high-performance concrete mixtures that are susceptible to small changes in mixture proportions has made monitoring workability even more critical.

Workability tests have generally been able to fit into one of two categories, one- or two-parameter tests. One-parameter tests measure only one point on the flow curve (either the viscosity or shear stress), while two-parameter tests measure both rheological parameters, or values that can be related to the parameters. Typically two-parameter tests measure multiple points by varying the shear rate in order to provide a more complete description of the flow curve (Koehler and Fowler 2003). One-parameter tests have the advantage of being very quick and simple, but they lack information regarding rheological properties. Examples of one- and two-parameter tests include the slump test and a rotational rheometer, respectfully. Further separation between workability tests is done by splitting them into dynamic and static groups. Dynamic tests submit concrete to energy through actions such as vibrating, jolting, or applying a shear force in order to promote flow. Static tests, as implied, lack movement and rely on concrete to flow under its own weight. Testing for this research project focused on popular tests that have been used in similar projects. Due to the high prices of rheometers, simple and inexpensive

tests were chosen in order to gather results on both rheological properties. The slump test was also conducted for consistency purposes. Further discussion on these tests will now be provided.

2.6.2.1 Vebe Test

The Vebe test is standardized in ASTM C187 (2011). It is a dynamic test that subjects concrete to vibration in order to measure the amount of energy required to reshape concrete. Use of this test has mainly been in laboratory applications due to the heavy equipment involved and the needed source of power. The apparatus is shown in Figure 2-16. The test is conducted by first performing a slump test within an outer cylindrical container, and then measuring the time it takes for the concrete to remold to the shape of the cylinder. A clear plastic disk is seated on top of the subsiding concrete and dictates the end of the test when it is covered in cement grout. The main criticism to this test is that the start is ill-defined because the vibration takes times to build up, and the end-point is ill-defined because the rate of wetting of the disc with grout decreases with time and may even reach zero before the whole area is covered (Tattersall 1991). However, the test is easy to perform and the results are obtained directly.

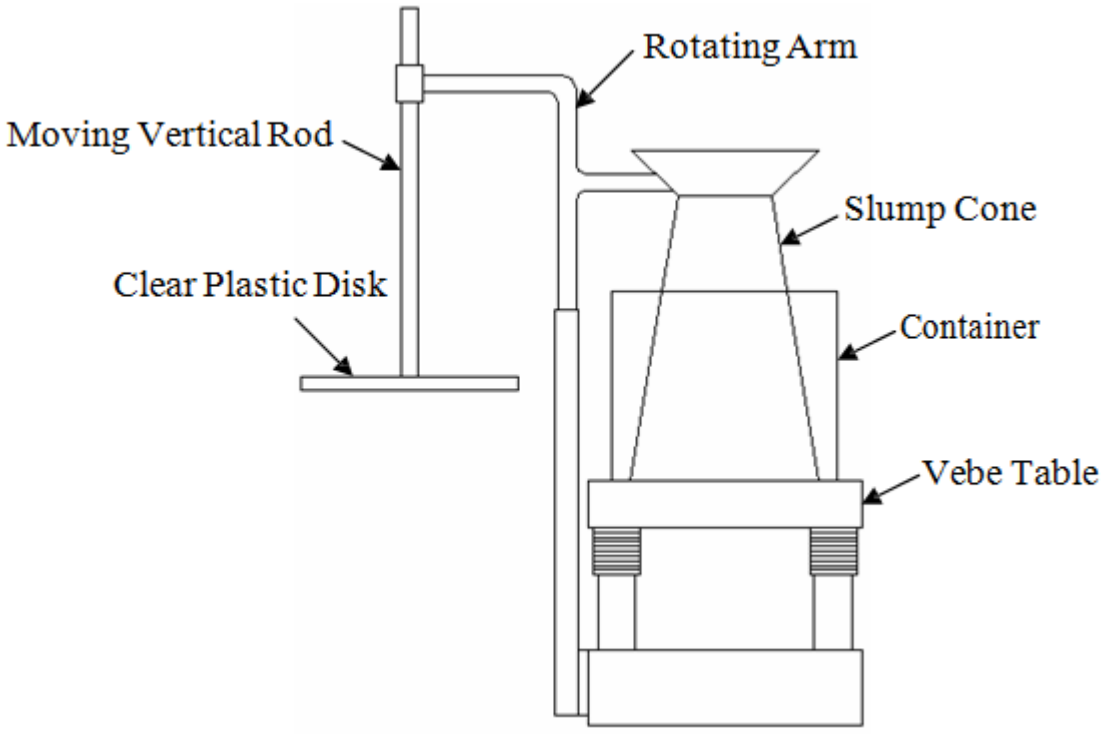

Figure 2-16: Vebe Consistometer (Koehler and Fowler 2003)

2.6.2.2 Modified Slump Test

In order to generate flow curves, rotational rheometers have been found to be very good tools. The measurement of rheological properties can be done easily and accurately, but the equipment is expensive and should only be used by trained personnel. Therefore, there is a need for a simple, inexpensive device for making rapid and reliable measurements in the field (Ferraris and de Larrard 1997). While the slump test has been found to correlate to the yield stress, none of the current field tests have been found to correlate to the plastic viscosity of concrete. Dynamic tests such as the Vebe

Consistometer are not useful for characterizing the rheological parameters because the results cannot be compared in terms of the Bingham model.

Ferraris and de Larrard (1998) developed the modified slump apparatus, shown in Figure 2-17 in order to evaluate the yield stress and plastic viscosity of fresh concrete. The test is similar to ASTM C143 (2012) with the exception of a vertical rod and steel disk in the center of the slump cone. The yield stress is measured based on the final slump. In order to keep the test simple, plastic viscosity is based on the average rate of slumping in the slump test. It is measured by the time required for the disk to reach an intermediate height on the rod. Ferraris and de Larrard (1998) state, recording the slump as a function of time would require a complete recording with electronic data acquisition, and interpreting the resulting curve would be too complex. The intermediate height of 100 mm was chosen in order to avoid small slump times, which would result in poor precision. An intermediate height which is too large can cause the elimination of all concrete with smaller slumps; therefore this was also taken into consideration.

One possibility of error was whether or not the disk stayed in contact with the concrete during the duration of the test. The theoretical time for the disk, subjected to gravity, to free fall 100 mm is found to be 0.14 seconds ($\sqrt{2h/g}$). Ferraris and de Larrard (1998) measured the disk to fall in 0.15 and 0.16 seconds without concrete. Therefore, it was concluded that separation of the disk and concrete was unlikely. The other possibility of error came from the increase of vertical stress on the concrete due to the disk mass and the reduction of the final slump due to the friction of the concrete with the rod. To verify

that these errors are negligible, comparisons were made on concrete mixtures using both the modified slump test apparatus and the standard slump test. The results are shown in Figure 2-18. The best fit line passing through the origin has a slope of 1.01 and a standard error of 0.03 (Ferraris and de Larrard 1998). It was concluded that the slumps measured with the two tests are identical.

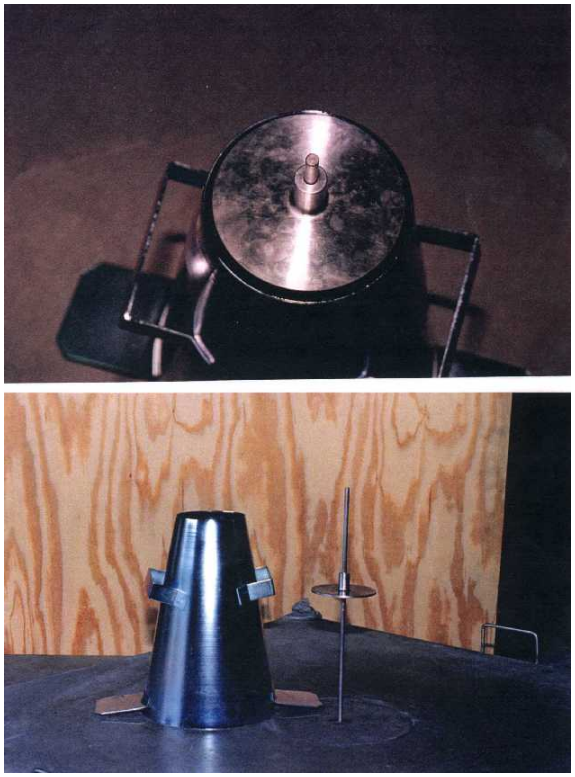

Figure 2-17: Modified slump test apparatus (Ferraris and de Larrard 1998)

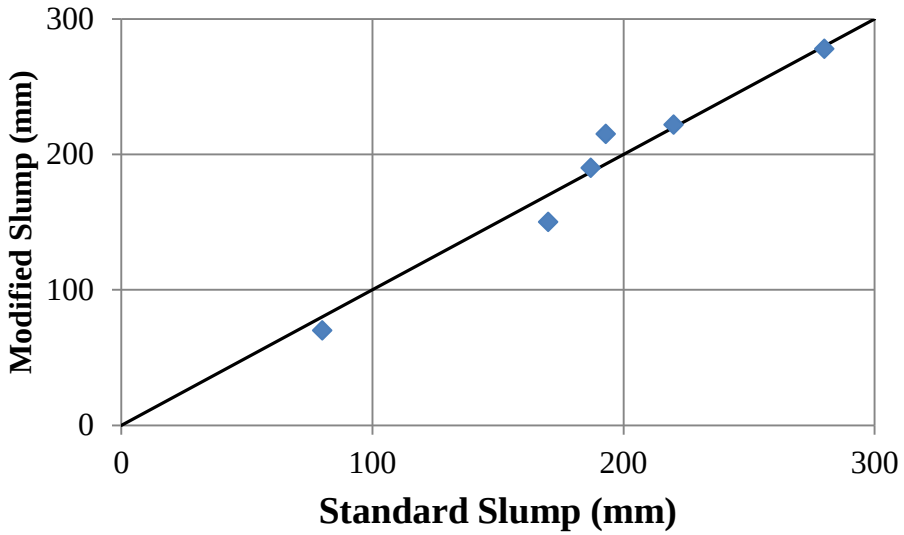

Figure 2-18: Comparison of modified slump with standard slump (Ferraris and de Larrard 1998)

2.7 SUMMARY

Concrete optimization can improve fresh and hardened properties and reduce the total cost of production. By properly proportioning aggregates, cement and admixture dosages can both be reduced. Not only does optimization benefit costs, it can provide an environmental benefit. The production of cement results in carbon dioxide emissions that are harmful to the environment. Reducing these emissions promotes sustainability in concrete production. The physical properties of the aggregates, mainly the shape and texture are important variables in concrete optimized aggregate gradations. Rounded aggregates will produce a more workable concrete, while angular aggregates will cause the mixture to be harsher. Also important is the aggregate gradation. The aggregate

grading or particle size distribution will directly impact the packing density and void content. The distribution of the aggregates will determine whether a mixture has a high packing density and be well-graded or a low packing density and be gap-graded. Gap-graded mixtures will produce undesirable results, while a well-graded mixture will perform much better in terms of fresh and hardened concrete properties. Several proportioning methods have been proposed for use, but not all result in concrete optimization. The use of the Shilstone Method along with the percent retained charts has been found to result in well-graded concrete gradations. As can be seen from Table 2-8, these proportioning methods have many advantages relative to concrete properties.

The use of manufactured fine aggregates is attracting more interest due to the steady depletion of natural fine aggregates. There is not widespread use of MFA due to the perceived negative drawbacks. The drawbacks of dust-of-fracture mineral filler are assumed to be

- Particles of this size may lead to reduced workability due to large surface area,
- Very fine particles tend to adhere to the surface of larger particles and prevent proper bonding between cement paste and the aggregate, and
- Clay particles present within the dust-of-fracture mineral filler material.

MFA result in 10-20 percent composition of dust-of-fracture mineral filler that are the main source for the assumed drawbacks. However, research studies have found that the use of MFA with their varying percentages of mineral filler can actually improve concrete properties. Incorporating this material not only reduces the reliance of concrete production on natural fine aggregates, but also utilizes a waste material. Currently, in

order to use MFA concrete quarries first wash the aggregates to clean them of mineral filler. The mineral filler is then stored on site long-term, awaiting disposal. This has caused the accumulation of approximately 500 million tons of mineral filler nationally per year. In addition, many specifications have strict limits on the use of MFA. In order to use this material, these limits must allow for greater percentages of mineral filler. This adjustment to the concrete industry has begun with the production of ACI 211.7R (2015), but other states must also address their standards. The addition of increased percentages in standards must be done with caution due to the possible negative results from the material. Characterization tests have been found to identify harmful materials versus beneficial materials within MFA and mineral fillers.

Table 2-8: Summary of Concrete Properties

Property	Trend Relative to Shilstone Method	Reference	Trend Relative to Percentage of Mineral Filler in Manufactured Sand	Reference
Fresh Properties				
Slump	↑	Richardson (2005), J. Shilestone (1990), Shilstone and Shilestone (1993), Shilestone and Shilestone (2002), Cramer et al. (1995)	↓ at all percentages	Quiroga et al. (2006), Quiroga and Fowler (2007), Stewart et al. (2007), Fowler and Rached (2011), Celik and Marar (1996)
Workability	↑	Richardson (2005), Silestone (1990), Shilstone and Shilestone (1993), Shilestone and Shilestone (2002), Cramer et al. (1995)	↓ at all percentages	Quiroga et al. (2006), Quiroga and Fowler (2007), Stewart et al. (2007), Fowler and Rached (2011), Celik and Marar (1996)

Notes:
↑ - Increase in Property
↓ - Decrease in Property

Table 2-9: Summary of Concrete Properties Continued

Property	Trend Relative to Shilstone Method	Reference	Trend Relative to Percentage of Mineral Filler in Manufactured Sand	Reference
Hardened Properties				
Compressive Strength	↑	Richardson (2005), Shilestone (1990), Shilestone and Shilestone (2002), Cramer et al. (1995)	↑ up to 10 %	Quiroga et al. (2006), Stewart et al. (2007), Topcu and Ugurlu (2003), Celik and Marar (1996)
Flexural Strength	↑	Richardson (2005), Shilestone (1990), Shilestone and Shilestone (2002)	↑ up to 15 %	Quiroga et al. (2006), Stewart et al. (2007), Topcu and Ugurlu (2003)
Drying Shrinkage	↑	Richardson (2005), Shilstone and Shilestone (1993)	↑ at all percentages	Quiroga and Fowler (007), Katz and Baum (2006), Ahmed and El-Kourd (1989)
Chloride Ion Permeability	↑	Richardson (2005), Shilstone and Shilestone (1993)	↓ at all percentages	Quiroga and Fowler (2007), Quiroga et al. (2006), Fowler and Ahn (2001), Celik and Marar (1996)
Abrasion Resistance	↑	Shilstone and Shilestone (1993)	↑ up to 15 %	Stewart et al. (2007), Quiroga et al. (2006), Fowler and Ahn (2001)

Notes:
↑ - Increase in Property
↓ - Decrease in Property

CHAPTER 3

EXPERIMENTAL PLAN

3.1 INTRODUCTION

Based on the topics covered in the literature review, an experimental plan was established to cover gaps found in previous research and produce additional data to achieve the objectives of this study. It has been established that optimizing aggregate gradations is best at utilizing cement and other concrete mixture materials more efficiently while producing workable concrete. Lower water-cementitious material ratios are achieved, while maintaining the workability of the concrete. Many have suggested the use of the Shilstone Method in addition to the percent retained charts. These methods were further studied in order to compare results from previous research, quantify their effectiveness, and evaluate the potential benefits from their use. In addition, the use of MFAs for concrete applications was studied. Current specifications strictly limit the amount of dust-of-fracture mineral filler within MFA. The effect of dust-of-fracture mineral filler on concrete properties is controversial. The use of MFA with its typical percentage of dust-of-fracture mineral filler within the gradation were studied, along with increased percentages to explore its beneficial use to produce economical and sustainable concrete, and evaluate the limits of maximum percent of dust-of-fracture mineral filler for use in specifications. This chapter presents the experimental plan, standards, testing equipment, mixture proportions, and raw materials used in order to carry out this research project.

3.2 OVERVIEW OF EXPERIMENTAL PLAN

The concrete produced during this research was chosen to represent typical bridge deck and other surfaces exposed to traffic constructed by Alabama Department of Transportation (ALDOT). Mixture proportions targeted 28-day strengths of 4000-5000 psi with a slump ranging from 4-7 inches. During the development of the experimental plan, it was decided to split the project into two phases to cover both studies of optimized aggregate gradation and MFA with dust-of-fracture mineral filler addition. In total 34 mixtures were conducted, including three duplicate mixtures. All mixtures took place in the Auburn University Structural Engineering and Materials Lab.

Phase I focused on the aggregate optimization portion of the research. The experimental plan for phase I is shown in Figure 3-1. It consisted of two groups with different types of coarse aggregates. Both groups were divided into two subgroups, differentiated by their nominal maximum aggregate size (NMAS). Each subgroup had four different combined aggregate gradation blends.

Phase II focused on the MFA and dust-of-fracture mineral filler portion of the research. It was split into two groups, separated by the type of coarse aggregate. The groups were then divided into five subgroups, differentiated by additions of dust-of-fracture mineral filler. The experimental plan for phase II is shown in Figure 3-2. Phase II also included five separate mixtures to evaluate the impact of using dust-of-fracture mineral filler on the abrasion resistance. The mixtures were separated by additions of dust-of-fracture mineral filler. The experimental plan for the abrasion testing mixtures is shown in Figure 3-3. Characterization tests were also performed on the MFA dust-of-

fracture mineral filler and then compared to results from natural fine aggregate mineral filler, cement, and fly ash.

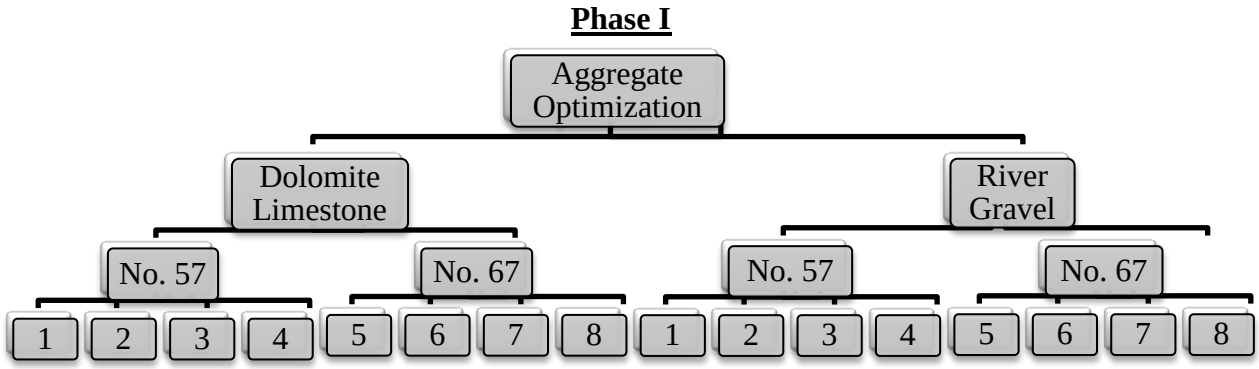

Figure 3-1: Phase I experimental plan

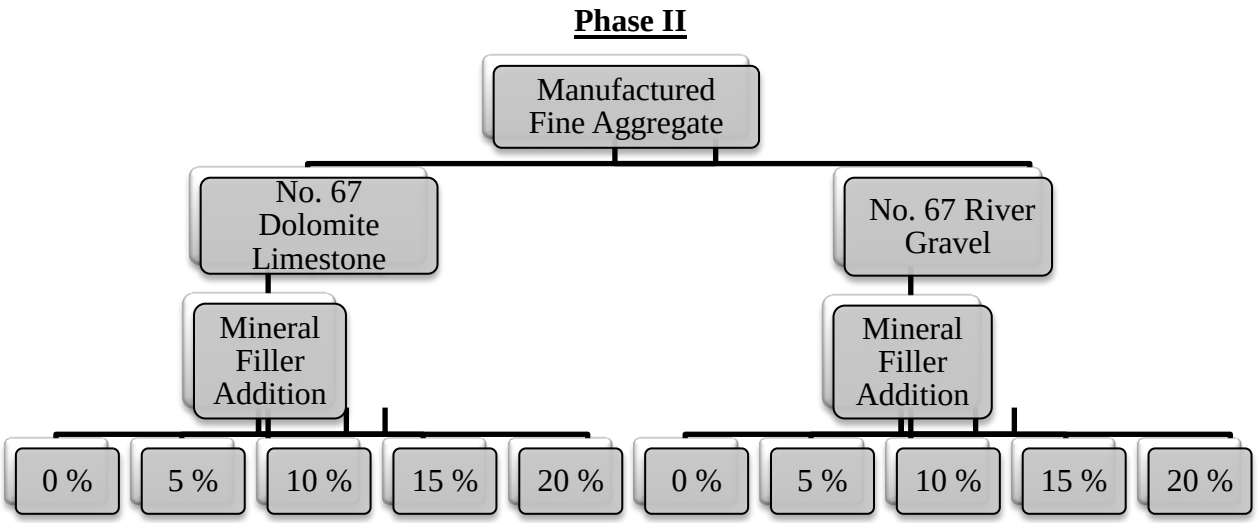

Figure 3-2: Phase II experimental plan

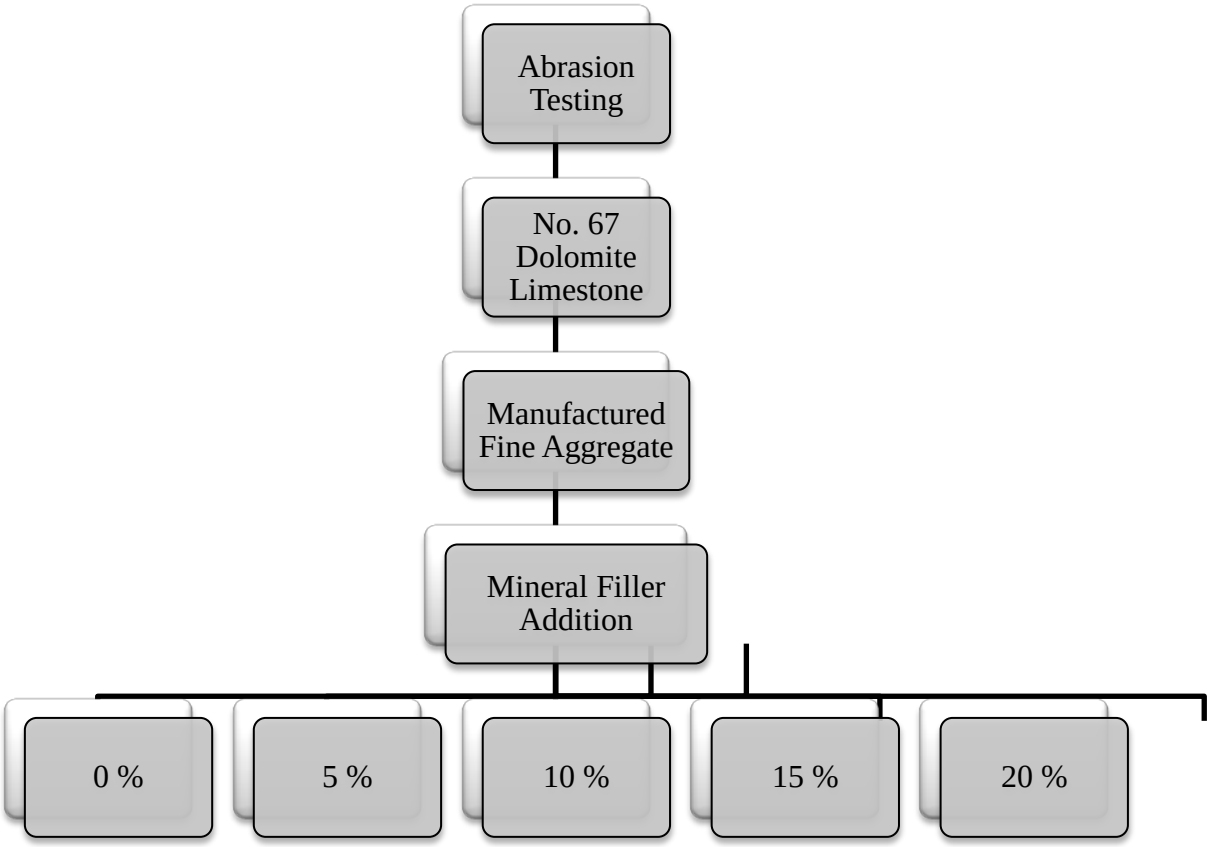

Figure 3-3: Abrasion testing experimental plan

3.3 PHASE I EXPERIMENTAL PLAN

Phase I focused on evaluating methods to optimize the concrete properties by changing the combined aggregate gradation. The variables in phase I included type of coarse aggregate, NMAS, combined aggregate gradation, and the amount of low-range water-reducing admixtures. The coarse aggregates used were dolomite limestone (DL) and river gravel (RG). The NMAS used for the research included No. 57 and No. 67 sizes. RG and DL were chosen as the types of coarse aggregate because they are the most frequently

used in ALDOT projects. The different NMAS were chosen based upon their popularity nationwide in the transportation industry.

Constants in phase I included type I cement, Class F fly ash, type of fine aggregate and the water-cementitious materials ratio (w/cm). Fly ash was included in the experiment because most present-day concrete mixtures involve fly ash. The fly ash is not expected to change any of the variables based on its interaction with MFA dust-of-fracture mineral filler.

Adjustments were made to the combined aggregate gradations through the Shilstone Method and the percent retained chart. When using the coarseness factor chart, the target was to have a mixture located in each of the zones, indicating whether the mixture was sandy, gap-graded, well-graded, or rocky. Zone III was not a targeted zone because it is used to describe smaller NMAS mixtures, which is out of the scope of this research. The target zones on the coarseness factor chart are shown in Figure 3-4. When using the 0.45-power chart areas 1 and 2 were targeted, as shown in Figure 3-5. The goal was to have gradations that were spaced both far and close to the max density line. When using the percent retained chart, the target was to have mixtures that were gap-graded, well-graded, and optimum-graded. A general schematic of how each type of gradation might look is shown in Figure 3-6.

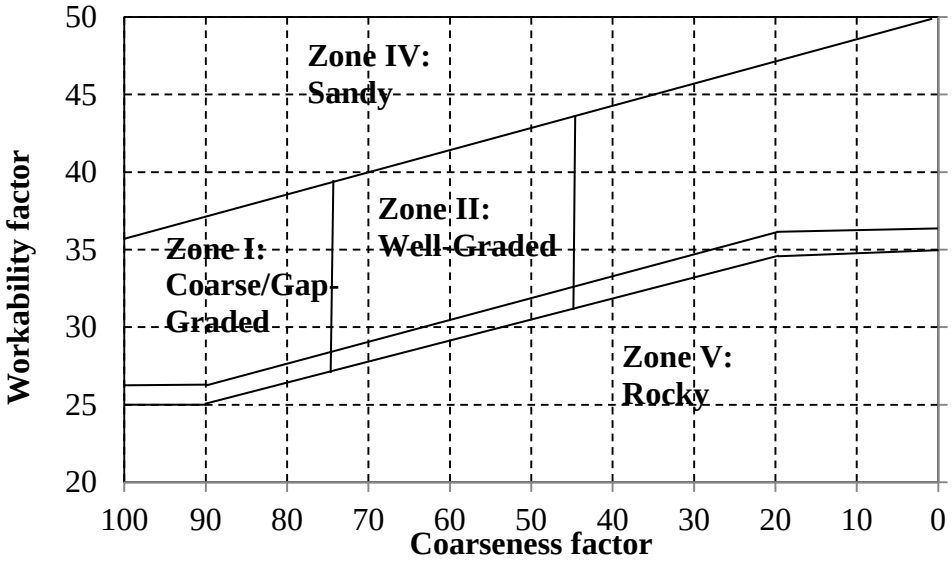

Figure 3-4: Target zones on the coarseness chart

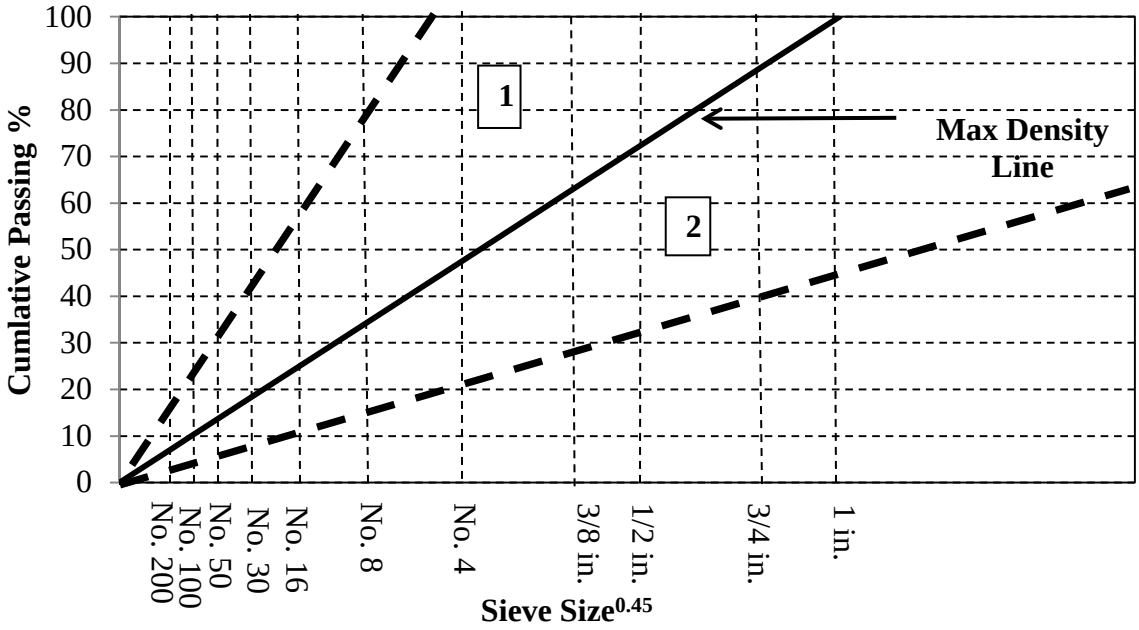

Figure 3-5: Target areas on the 0.45 power chart

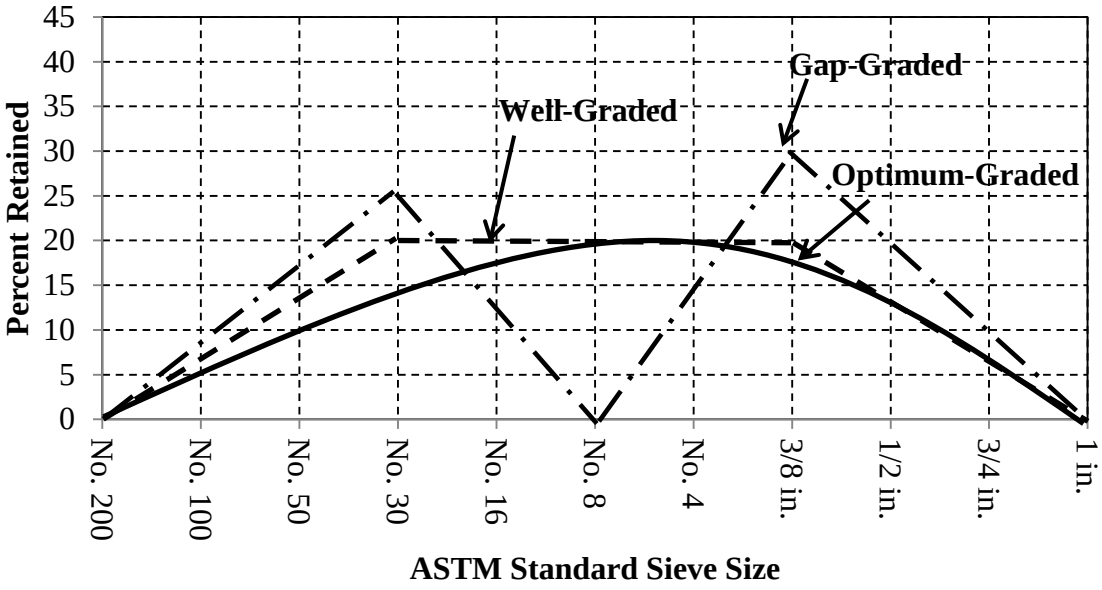

Figure 3-6: Target gradations on the percent retained chart

In order to quantify the effect of different combined aggregate gradations on concrete, fresh and hardened concrete properties were measured. Among the fresh properties tested were air content, workability (vebe consistometer, modified slump, assessment rating, and slump test), and unit weight. The hardened properties of concrete tested included drying shrinkage, compressive strength, splitting tensile strength, modulus of elasticity, and chloride ion permeability. Each of the hardened properties had specific ages at which the concrete was tested. The schedule of testing is shown in Table 3-1. Three samples were used to test each property at all test dates.

Table 3-1: Phase I Hardened Properties Testing Schedule

Tested Property	Concrete Age at Testing (Days)
Compressive Strength	7, 28, 91
Splitting Tensile Strength	7, 28, 91
Modulus of Elasticity	7, 28, 91
Drying Shrinkage	4, 7, 14, 28, 56, 112, 168
Chloride Ion Permeability	91

3.3.1 CONCRETE PROPORTIONS FOR PHASE I

The mixture proportions for phase I can be seen in the following tables. The water content and cementitious materials remained unchanged during all mixtures in order to keep a constant water-cementitious materials ratio. The target air content changed slightly as testing progressed to more closely match the measured results. The water-reducing admixture was altered during testing in order to obtain the target slump, stated in Section 3.2.

Table 3-2: Phase I Dolomitic Limestone No. 57 Mixture Proportions and Properties

Item	DL No. 57 Blend 1	DL No. 57 Blend 2	DL No. 57 Blend 3	DL No. 57 Blend 4
Water Content (lb/yd^3)	275	275	275	275
Cement Content (lb/yd^3)	465	465	465	465
Class F Flyash Content (lb/yd^3)	155	155	155	155
SSD Coarse Aggregate (lb/yd^3)	1,960	1,649	1,444	1,608
SSD Fine Aggregate (lb/yd^3)	1,240	1,530	1,698	1,546
Water-Reducing Admixture (oz/yd^3)	43.4	27.3	37.8	32.2
Target Total Air Content (%)	2	2	3	3
Water-cementitious materials ratio (w/cm)	0.44	0.44	0.44	0.44

Table 3-3: Phase I Dolomitic Limestone No. 67 Mixture Proportions and Properties

Item	DL No. 67 Blend 5	DL No. 67 Blend 6	DL No. 67 Blend 7	DL No. 67 Blend 8
Water Content (lb/yd^3)	275	275	275	275
Cement Content (lb/yd^3)	465	465	465	465
Class F Flyash Content (lb/yd^3)	155	155	155	155
SSD Coarse Aggregate (lb/yd^3)	1,937	2,186	1,922	1,730
SSD Fine Aggregate (lb/yd^3)	1,217	985	1,231	1,410
Water-Reducing Admixture (oz/yd^3)	32.2	37.8	37.8	32.2
Target Total Air Content (%)	3	3	3	3
Water-cementitious materials ratio (w/cm)	0.44	0.44	0.44	0.44

Table 3-4: Phase I River Gravel No. 57 Mixture Proportions and Properties

Item	RG No. 57 Blend 1	RG No. 57 Blend 2	RG No. 57 Blend 3	RG No. 57 Blend 4
Water Content (lb/yd^3)	275	275	275	275
Cement Content (lb/yd^3)	465	465	465	465
Class F Flyash Content (lb/yd^3)	155	155	155	155
SSD Coarse Aggregate (lb/yd^3)	1,804	1,470	1,688	1,802
SSD Fine Aggregate (lb/yd^3)	1,203	1,540	1,320	1,203
Water-Reducing Admixture (oz/yd^3)	21.7	43.4	21.7	10.5
Target Total Air Content (%)	3	3	3	3
Water-cementitious materials ratio (w/cm)	0.44	0.44	0.44	0.44

Table 3-5: Phase I River Gravel No. 67 Mixture Proportions and Properties

Item	RG No. 67 Blend 5	RG No. 67 Blend 6	RG No. 67 Blend 7	RG No. 67 Blend 8
Water Content (lb/yd^3)	275	275	275	275
Cement Content (lb/yd^3)	465	465	465	465
Class F Flyash Content (lb/yd^3)	155	155	155	155
SSD Coarse Aggregate (lb/yd^3)	1,536	1,534	2,005	1,925
SSD Fine Aggregate (lb/yd^3)	1,471	1,473	1,000	1,078
Water-Reducing Admixture (oz/yd^3)	32.2	27.3	32.2	21.7
Target Total Air Content (%)	3	3	3	3
Water-cementitious materials ratio (w/cm)	0.44	0.44	0.44	0.44

3.4 PHASE II EXPERIMENTAL PLAN

Phase II focused on MFA and the effects on concrete from the addition of dust-of-fracture mineral filler. The variables in the experiment included the percentage of dust-of-fracture mineral filler, type of coarse aggregate, and the amount of water-reducing admixture. The dust-of-fracture mineral filler addition was done in intervals of five percent of the fine aggregate (by mass), ranging from zero to twenty percent. The types of coarse aggregate used included dolomitic limestone and river gravel. The type of water-reducing admixture was alternated between low-range, mid-range, and high-range as the addition of dust-of-fracture mineral filler increased. This is because the workability of fresh concrete decreases as the percentage of dust-of-fracture mineral filler increases (Quiroga et al. 2006). The use of only one water-reducing admixture would not allow a consistent slump to be reached. The constants in the experiment included the type of fine aggregate (MFA), Type I cement, Class F fly ash, w/cm, gradation, and NMAS. The NMAS was chosen to only include No. 67 aggregates because the size and gradation of the aggregates was not the focus in this phase.

Five additional batches were made in order to test for abrasion resistance. The need for additional batches to test for abrasion was due to size constraints of the concrete mixer. These batches were made to reproduce the concrete of phase II; however, only dolomitic limestone coarse aggregate was used. Natural fine aggregate was not chosen for abrasion resistance testing because it is not a perceived problem for this material. In ASTM C33 (2013), a foot-note is made to limit dust-of-fracture mineral filler in MFA subjected to abrasion. There is no such note for natural fine aggregate.

In order to evaluate the effects dust-of-fracture mineral filler have on concrete applications, fresh and hardened concrete properties were measured. The fresh measured concrete properties included air content, workability (vebe consistometer, modified slump, assessment rating, and slump test), and unit weight. The measured hardened concrete properties included drying shrinkage, compressive strength, splitting tensile strength, modulus of elasticity, chloride ion permeability, and abrasion resistance. Three samples were tested for each property at the concrete ages shown in Table 3-6.

Table 3-6: Phase II Hardened Concrete Properties Testing Schedule

Tested Property	Concrete Age at Testing (Days)
Compressive Strength	7, 28, 91
Splitting Tensile Strength	7, 28, 91
Modulus of Elasticity	7, 28, 91
Drying Shrinkage	4, 7, 14, 28, 56, 112, 168
Chloride Ion Permeability	91
Abrasion Resistance	91

3.4.1 CONCRETE PROPERTIES FOR PHASE II

The mixture proportions for phase II can be seen in the following tables. The water content and cementitious materials remained unchanged during all mixtures in order to keep a constant water-cementitious materials ratio. The type of water-reducing admixture was changed as the percentage of dust-of-fracture mineral filler increased, and the dosage was altered during testing in order to obtain the target slump, stated in Section 3.2.

Table 3-7: Phase II Dolomitic Limestone Mixture Proportions and Properties

Item	DL No. 67 0%	DL No. 67 5%	DL No. 67 10%	DL No. 67 15%	DL No. 67 20%
Water Content (lb/yd^3)	275	275	275	275	275
Cement Content (lb/yd^3)	465	465	465	465	465
Class F Flyash Content (lb/yd^3)	155	155	155	155	155
SSD Coarse Aggregate (lb/yd^3)	1,947	1,957	1,957	1,957	1,957
SSD Fine Aggregate (lb/yd^3)	1,234	1,246	1,246	1,246	1,246
Water-Reducing Admixture (oz/yd^3)	32.2	35.3	43.4 (Mid-Range)	43.4 (Mid-Range)	37.8 (High-Range)
Target Total Air Content (%)	3	2.5	2.5	2.5	2.5
Water-cementitious materials ratio (w/cm)	0.44	0.44	0.44	0.44	0.44

Table 3-8: Phase II River Gravel Mixture Proportions and Properties

Item	RG No. 67 0%	RG No. 67 5%	RG No. 67 10%	RG No. 67 15%	RG No. 67 20%
Water Content (lb/yd^3)	275	275	275	275	275
Cement Content (lb/yd^3)	465	465	465	465	465
Class F Flyash Content (lb/yd^3)	155	155	155	155	155
SSD Coarse Aggregate (lb/yd^3)	1,797	1,797	1,797	1,797	1,797
SSD Fine Aggregate (lb/yd^3)	1,234	1,234	1,234	1,234	1,234
Water-Reducing Admixture (oz/yd^3)	32.2	32.2	32.2 (Mid-Range)	27.3 (Mid-Range)	19.2 (High-Range)
Target Total Air Content (%)	3	3	3	3	3
Water-cementitious materials ratio (w/cm)	0.44	0.44	0.44	0.44	0.44

3.5 MIXTURE PREPARATION

This section will discuss the methods used to produce the various mixtures previously discussed, procedures followed for mixing and making concrete samples, test methods followed for evaluating concrete properties, and details regarding the raw materials.

3.5.1 MIXING PROCEDURE

Two separate batch sizes were used during the research. They were conducted in a 12 ft^3 concrete mixer in a laboratory environment. Phase I and II both used 5 ft^3 of concrete for each batch. Five separate 3 ft^3 batches had to be made for abrasion resistance testing. A smaller volume was not chosen for the abrasion testing mixtures because the materials would not properly blend if there is not an adequate volume in the mixer.

The batched material was placed in the mixing area and separated into sections of water, butter material (fine aggregate, cement, and water), aggregates, and cementitious material. ASTM C192 (2015) was followed when mixing concrete and making all test specimens. Minor adjustments were made to the mixing procedure based on outcomes from trial batching. An outline of the mixing procedure is as follows:

- The concrete mixer was first buttered with a coating of mortar. The butter mixtures were proportioned to represent the concrete batch. This is done to compensate for the loss of mortar that adheres to the side of the mixer. Once completed, the mixer was started and the aggregates were added.
- Next, 80 percent of the total water was added to the mixture and mixed for 2 minutes before adding all cementitious material. The remaining amount of water was then added.
- After mixing the concrete for a minute, the water reducing admixture was added with syringes and mixed for two minutes before shutting the mixer off and resting for three minutes. Once completed, the mixer was switched on for an additional two minutes. The concrete was then evaluated to determine whether it was suitable, or if more water-reducing admixture would be needed.

3.5.2 TRIAL BATCHING

Four trial batches were initially completed before phase I and II were started. These were done to practice all tests and procedures, and to make necessary adjustments to batch proportions. It was not practical to trial every test batch, therefore a dolomitic limestone blend and river gravel blend with NMAS of No. 67 were completed for phase I. Both coarse aggregates with MFA and five percent dust-of-fracture mineral filler addition were completed for phase II. Outcomes from trial batching included adjustments to admixture dosage.

3.5.3 RAW MATERIALS

All materials used to produce concrete samples will be discussed in this section. The materials were locally available and were either purchased or donated for research use.

Proper inspection and identification of each material was conducted upon arrival to the laboratory.

3.5.3.1 Cementitious Material

The cementitious material used for this research involved Type I cement and Class F fly ash. The cement was purchased from the Cemex supply company in Demopolis, Alabama. It was delivered to the laboratory on a pallet in 94-pound bags. The mill test report certified that the cement was within the standards of ASTM C150 (2012). The Class F fly ash was purchased from the Boral Bowen Plant in Stilesboro, Georgia. It was delivered on a pallet in 70-pound bags. An analysis report from the plant certified that the fly ash was within standards of ASTM C618 (2012).

3.5.3.2 Coarse Aggregate

The coarse aggregate used for this project consisted of No. 57 and No. 67 dolomitic limestone and river gravel, donated by the Sherman Industries Ready Mixed Concrete Plant. The dolomitic limestone for the No. 57 and No. 67 size aggregates were from APAC Midsouth Aggregates in Auburn, Alabama (ALDOT ID 1604). The No. 57 river gravel was from Lambert Materials Wiregrass Polly Pit in Shorter, Alabama (ALDOT ID 1762). The No. 67 river gravel was from Foley Materials Company in Shorter, Alabama (ALDOT ID 1481). All coarse aggregates were compared to ASTM C33 (2013) using ASTM C136 (2014) procedures for sieving the aggregates. The gradations were graphed along with the grading requirements reported by the standard. The results are shown in Figure 3-7 through Figure 3-10.

3.5.3.3 Fine Aggregate

The fine aggregate for the project consisted of natural fine aggregate and MFA. The natural fine aggregate was donated by the Sherman Industries Ready Mixed Concrete Plant. It was from Foley Materials Company in Shorter, Alabama (ALDOT 1481). The MFA with dust-of-fracture mineral filler was donated by the Vulcan Materials Company in Calera, Alabama. Both fine aggregates were compared to ASTM C33 (2013) using ASTM C136 (2014) and ASTM C117 (2004) procedures for sieving the aggregates. Their gradations were graphed along with the grading requirements reported by the standard. The results are shown Figure 3-11 and Figure 3-12.

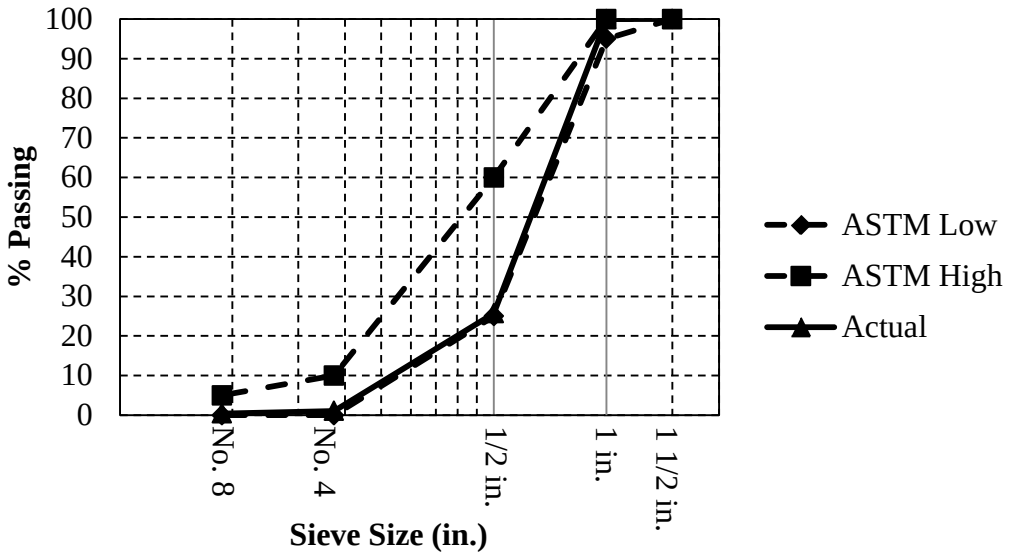

Figure 3-7: No. 57 dolomite limestone gradation

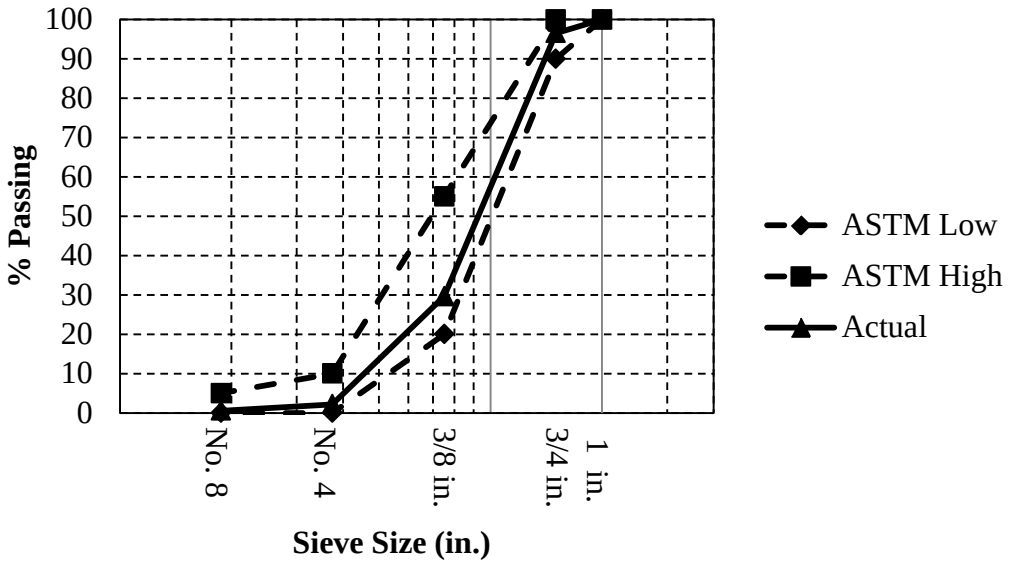

Figure 3-8: No. 67 dolomite limestone gradation

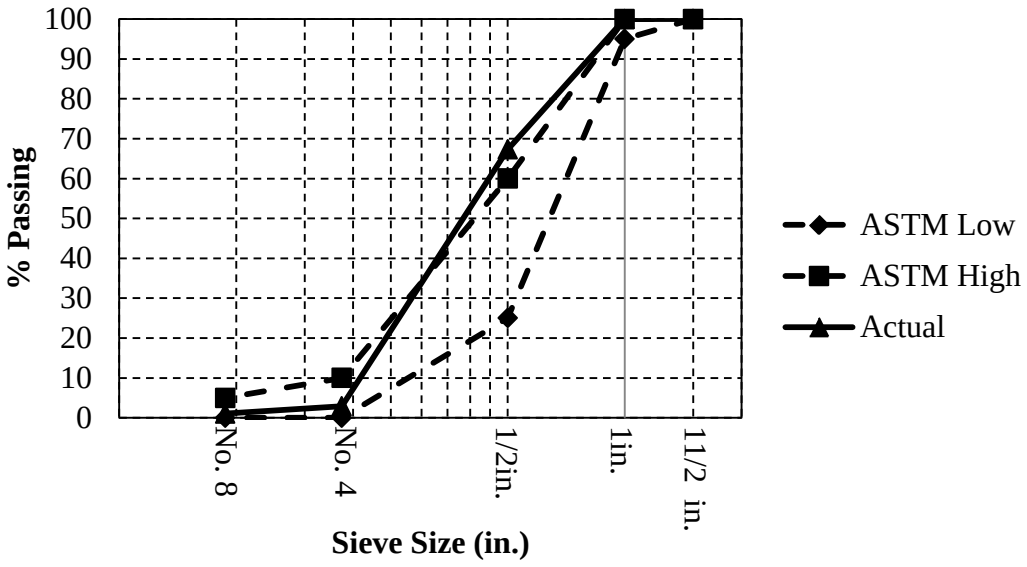

Figure 3-9: No. 57 river gravel gradation

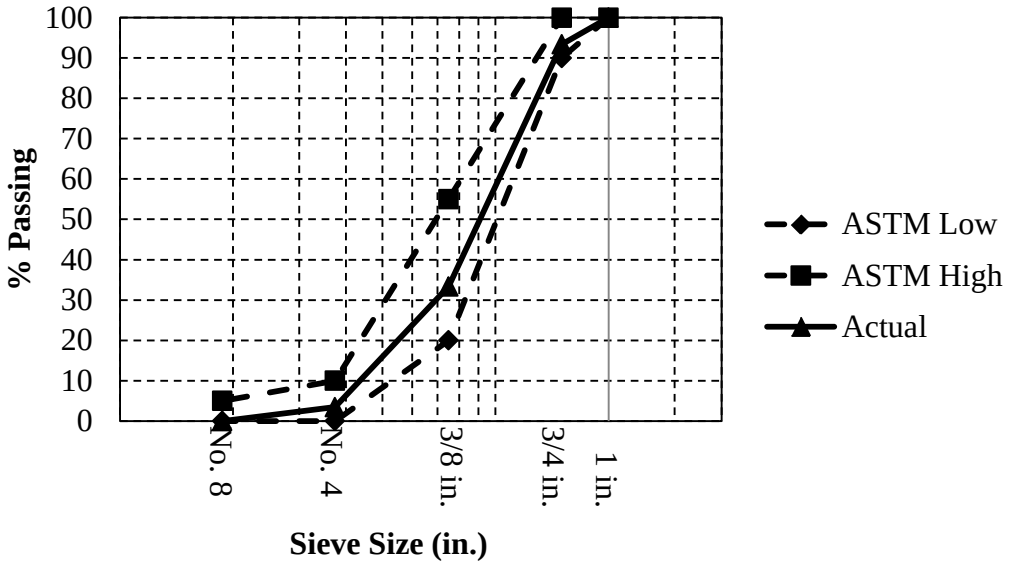

Figure 3-10: No. 67 river gravel gradation

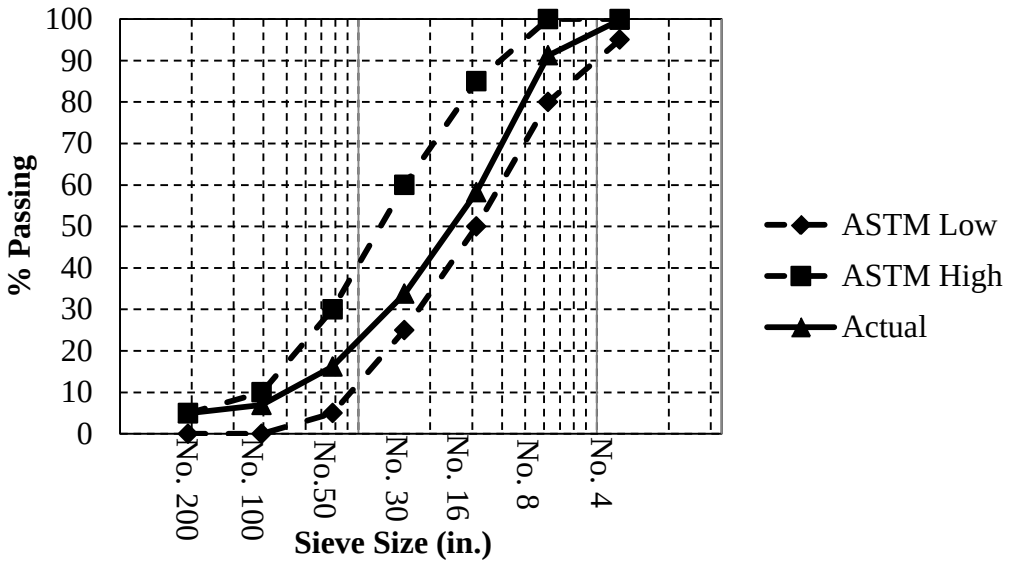

Figure 3-11: Natural fine aggregate gradation

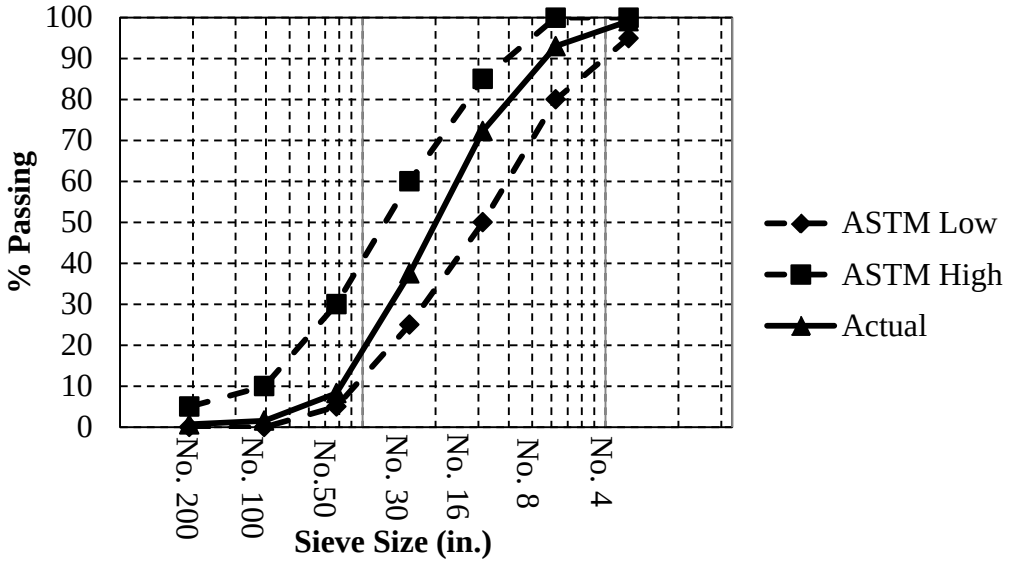

Figure 3-12: Manufactured fine aggregate gradation

3.5.3.4 Chemical Admixtures

There were three types of water-reducing admixtures used to control the workability of the concrete. All three types were products from Master Builders Solution by BASF. In phase I, only a normal-range water-reducing admixture was used. In phase II, all three water-reducing admixtures were used in order to counteract the dust-of-fracture mineral filler effects on workability. For dust-of-fracture mineral filler additions of zero and five percent, a normal-range water-reducing admixture was used. For dust-of-fracture mineral filler additions of 10 and 15 percent, a mid-range water-reducing admixture was used. For the dust-of-fracture mineral filler addition of 20 percent, a high-range water-reducing admixture was used. The details of the chemical admixtures used can be found in Table 3-9.

Table 3-9: Water-Reducing Admixtures

Water-Reducer Classification	ASTM C494 Classification	BASF Product
Normal-Range	Type A, Type B, Type D	Pozzolith® 322N
Mid-Range	Type A, Type F	MasterPolyheed® 1025
High-Range	Type A, Type F	MasterGlenium® 7500

3.5.4 AGGREGATE PROPORTIONING

In both phases specific aggregate gradations were prepared using a mechanical sieve shaker, shown in Figure 3-13. Sieving followed the procedures outline in ASTM C136 (2014). Sieve sizes were then selected based on ASTM C33 (2013). The sieve sizes used

included 1 in., 3/4 in., 1/2 in., 3/8 in., No. 4, No. 8, No. 16, No. 30, No. 50, No. 100, and No. 200.

Figure 3-13: Mechanical sieve shaker

3.5.4.1 Phase I

Aggregate proportioning in phase I focused on producing stock piles of each sieve size. It was necessary to obtain large quantities of each size to produce aggregate blends in the target locations on the proportioning charts. The first step was to dry the aggregates in preparation for the mechanical shaker. Aggregate samples were dried to a constant mass at a temperature of 230 ± 9 °F. Once cooled, the aggregates could be sieved. Upon completion, aggregates were placed into 5-gallon buckets and stacked according the size

and type. The following figures show the different stockpiles produced. After stockpiles were produced, the necessary amount of material on each sieve was determined for the mixtures.

Figure 3-14: Dolomitic limestone and river gravel aggregates separated by sieve size

Figure 3-15: Stockpiles of sieved aggregates

3.5.4.2 Phase II

Aggregate proportioning in phase II focused on the addition of dust-of-fracture mineral filler to the MFA. The MFA supplied for the research had an average composition of five percent dust-of-fracture mineral filler within the gradation. To obtain MFA without dust-of-fracture mineral filler, all material passing the No. 200 sieve had to be removed. This was done using a mechanical shaker. All material retained on the No. 200 sieve or larger was kept and recombined. All material that passed the No. 200 sieve was removed. For the mixtures that included dust-of-fracture mineral filler at five percent of the fine aggregate, no additional preparation was required. The other mixtures required adding dust-of-fracture mineral filler to meet contents of 10, 15, and 20 percent of the fine aggregate (by mass). Dust-of-fracture mineral filler was sieved and collected at the quarry where the MFA originated. It was then delivered to the laboratory in 5-gallon buckets.

The procedure for dust-of-fracture mineral filler (MF) addition first required drying both the MFA and the dust-of-fracture mineral filler. This allowed for easy batching calculations and ensured no surplus of water would be added to the mixture. The aggregates were dried in an oven to a constant mass at a temperature of 230 ± 9 °F. Next, the amount of additional dust-of-fracture mineral filler was calculated based on the current amount of mineral filler (MF) within the MFA. The quantities of material required for the three mixtures of each coarse aggregate type in phase II are shown in Table 3-10 and Table 3-11 .

Table 3-10: Dolomite Limestone Dust-of-Fracture Mineral Filler Additions

10 % Mix		**15 % Mix**		**20 % Mix**	
MFA (pcy)	1246	MFA (pcy)	1246	MFA (pcy)	1246
MF (MF) Addition	10%	MF (MF) Addition	15%	MF (MF) Addition	20%
MF in MFA (pcy)	70	MF in MFA (pcy.)	70	MF in MFA (pcy)	70
Added MF (pcy)	55	Added MF (pcy)	117	Added MF (pcy)	179
Total Material (pcy)	1301	Total Material (pcy)	1363	Total Material (pcy)	1425

Table 3-11: River Gravel Dust-of-Fracture Mineral Filler Additions

10 % Mix		**15 % Mix**		**20 % Mix**	
MFA (pcy)	1234	MFA (pcy)	1234	MFA (pcy)	1234
MF (MF) Addition	10%	MF (MF) Addition	15%	MF (MF) Addition	20%
MF in MFA (pcy)	69	MF in MFA (pcy.)	69	MF in MFA (pcy)	69
Added MF (pcy)	54	Added MF (pcy)	116	Added MF (pcy)	178
Total Material (pcy)	1288	Total Material (pcy)	1350	Total Material (pcy)	1412

After the proportions were calculated, the MFA was then combined with the required amount of dust-of-fracture mineral filler in a concrete mixer, shown in Figure 3-16. The mixer was switched on to rotate the material for a period of ten minutes. Once the material was combined, it was emptied into a wheelbarrow. A mass equal to the dust-of-fracture mineral filler originally added was removed to get the total amount of material back to the batching proportion. This was done by placing a 5-gallon bucket on a scale and removing the required combined material from the wheelbarrow into a waste bucket, shown in Figure 3-16.

Figure 3-16: Combining material (left) and removing extra material (right)

3.6 FRESH CONCRETE PROPERTY TESTING

This section will discuss the procedures used to sample the concrete during the fresh state and also evaluate the workability. Previous studies have found that rheometers deliver the best results in terms of workability. However, these instruments are costly and were not reasonable to use for this research. The tests for this research were chosen based on their ability to measure the viscosity and yield stress of the concrete. The concrete produced was expected to be of low and moderate workability due to poor gradations and the addition of dust-of-fracture mineral filler. This type of concrete would typically be vibrated in the field to overcome the initially high yield stress. A dynamic test simulates similar field conditions, using vibration to consolidate the concrete. The industry

common slump test, outlined in ASTM C143 (2012) was also used to give an initial reading of the concrete's consistency during the mixing process.

3.6.1 MODIFIED SLUMP TEST

The modified slump test (Ferraris and de Larrard 1998) is a method that was used to determine the plastic viscosity and yield stress of concrete. Before starting the test it was necessary to gather the following components; a horizontal base plate with a 14-inch long rod in the middle, mold for the slump test, sliding disk, rod to consolidate the concrete, ruler to measure the slump, and a stopwatch. The test measures the rate of slumping with a disk, to be made of steel with the dimensions outline in Figure 3-17. The disk has a rubber O-ring seal to prevent fine materials from interfering with the fall of the disk. After preliminary tests were conducted with the apparatus during trial batches, the disk would not slide on the rod after it came in contact with the concrete. Removing the O-ring seal allowed larger aggregates to lodge in between the disk and the rod. Therefore, a modification was made by the author to permit a frictionless surface for the disk to freely travel with the movement of the concrete. The rod was removed from the base plate and a back board with indication lines was made to measure when to stop timing the concrete flow. The modified slump test apparatus with back board is shown in Figure 3-18. On the bottom of the board, a start line was added to match the height of the base plate. The next line is eight inches from the start line that indicates the stopping point of timing. The last line is measured 12 inches up from the start line. This height matches that of the slump mold when placed on top of the base plate. In addition, instead of timing during the test, a video camera was used to record the slump. The video was later played back in slow

motion to give a more exact reading on the time to reach a slump of 4 inches. The setup of with the modifications to the test is shown in Figure 3-19.

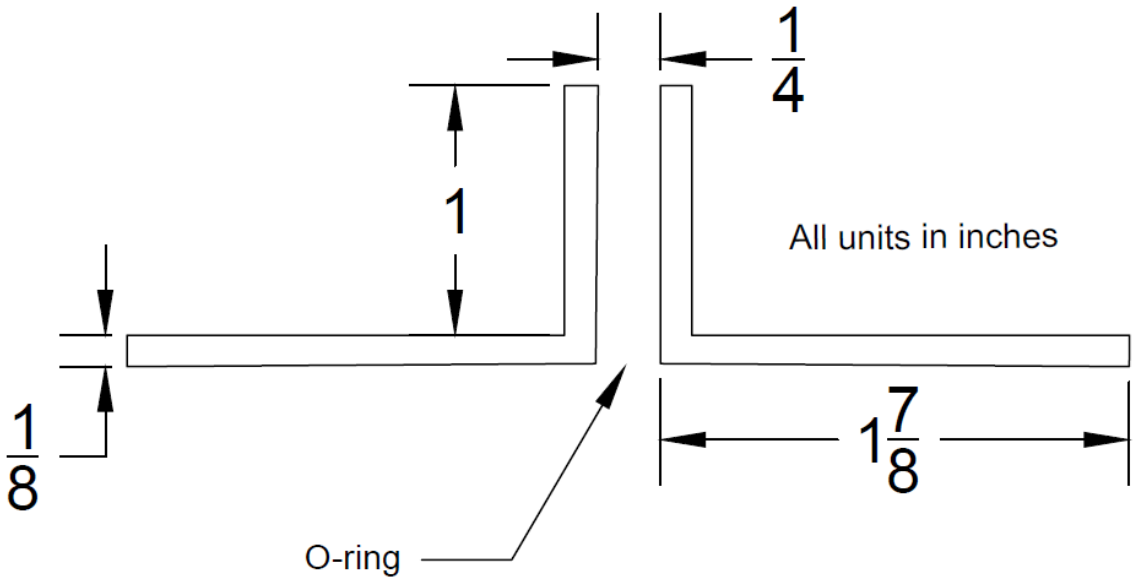

Figure 3-17: Modified slump test disk apparatus dimensions

Figure 3-18: Modified slump test with additional modifications

Figure 3-19: Modified slump test setup

The placement of the concrete was done in the same manner as in the standard slump test ASTM C143 (2012). The process for the test was adopted from the procedure Ferraris and de Larrard (1998) outlined.

- The mold and base plate are dampened. The mold is then secured by a clamping arrangement to the base plate.
- The mold is filled in 3 layers, rodding each layer 25 times and then the top surface of concrete is to be stroked off.
- The disk is placed on top of the concrete with the mold still in place on the base plate. Start the video camera.
- Raise the mold vertically. Start stopwatch during video playback.
- While the concrete is slumping, continue to observe the disk to make sure it remains in contact with the concrete. During video playback, stop the stopwatch as soon as the disk crosses the indication line.
- Once the slump has stabilized, or no later than one minute after the start of the test, measure the slump with a ruler.

A schematic of the procedure is shown in Figure 3-20. Calculation of the plastic viscosity and the yield stress are done using the following equations. They were derived using finite element analysis, based on Ferraris and de Larrard (1998) results from the modified slump and rheometer tests. These equations are to be used only with final slumps of 200 mm (8 inches) or less. Additional equations are available for mixtures that have larger slumps, but they are outside the range of this research.

$$\tau_0 = \frac{\rho}{347}(300 - s) + 212$$ **Equation 3-1**

Where,

τ_0 = yield stress (Pa), and

ρ = density of the concrete (kg/m^3), and

s = final slump (mm).

$$\mu = 25 \cdot 10^{-3} \rho T$$ **Equation 3-2**

Where,

μ = plastic viscosity (Pa·s), and

T = slump time required for disk to reach stopping point (s).

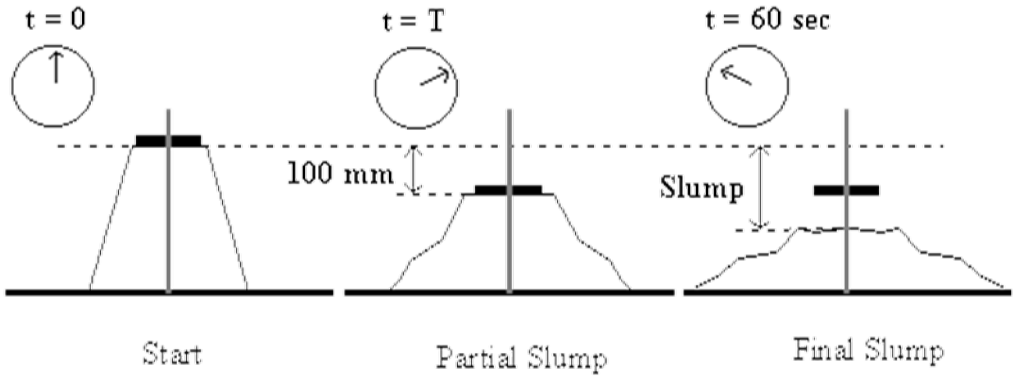

Figure 3-20: Schematics of the modified slump test from Ferraris and de Larrard (1998)

3.6.2 VEBE TEST

The vebe test is a method used to determine the workability of concrete in a fresh state (Tattersall 1991). It is a dynamic test that operates at a frequency of 50 Hz to consolidate the concrete. The vebe consistometer is shown in Figure 3-21. The consistometer can be considered in three parts which includes the vibrating table, container assembly, and the measuring head. The container has an internal diameter of 240 ± 5 mm (9 1/2 inches) and a height of 200 ± 2 mm (8 inches). The measuring head includes a scale with intervals of 5 mm (1/5 inch). Attached to the bottom of the bar is a transparent disc and weight of approximately 6 pounds. The principle of the test is to carry out a normal slump test after which the sample of concrete is vibrated to remold the material. The time taken for the vibrator to achieve a preset amount of remolding is called the vebe time (ELE International 2002).

Figure 3-21: Vebe Consistometer

The test is not meant for concrete that has a vebe time less than 5 seconds or more than 30 seconds, which translates to a slump of approximately 2 inches or less. Concrete used for slip forming is usually applied to this testing method. The concrete for this research was expected to have greater slumps than outlined in the vebe test procedure. Therefore, a modification was made to remove the weight on top of the disc. This would allow the concrete to settle in a slower time and give a more precise reading, considering the slump of these mixtures. The procedure is outline in the British Standard (2009) as follows:

- Firmly fix the container to the vibrating table. Dampen the mold and place it inside the container. Swing the funnel into position over the mold and lower onto the mold. Tighten the screw so that the mold cannot rise from the bottom of the container.
- Fill the mold with concrete in the same manner outline in ASTM C143 (2012), in three layers while compacting each layer with 25 strokes of the compacting rod.
- After the top layer has been tamped, loosen the screw and raise the funnel and swing it out of the way and tighten the screw in the new position.
- Strike off the concrete level with the top of the mold. Remove the mold from the container by raising it carefully in a vertical direction, performing the operation in two to five seconds.
- If the concrete shears, as shown in Figure 3-22b, collapses, as shown in Figure 3-22c, or slumps to the extent that it touches the wall of the container, record the fact.
- Swing the transparent disc over the top of the concrete and lower the disc until it comes into contact with the concrete. Provided there has been a true slump, when the disc touches the highest point of the concrete, read and record the value of the slump

from the scale. Loosen the screw to allow the disc to easily slide down into the container to rest fully on the concrete.

- Start the vibration of the table and the timer simultaneously. As soon as the lower surface of the disc is fully in contact with the cement grout, stop the timer and switch off the vibrating table. Record the vebe time to the nearest second. The entire test should take no longer than five minutes.

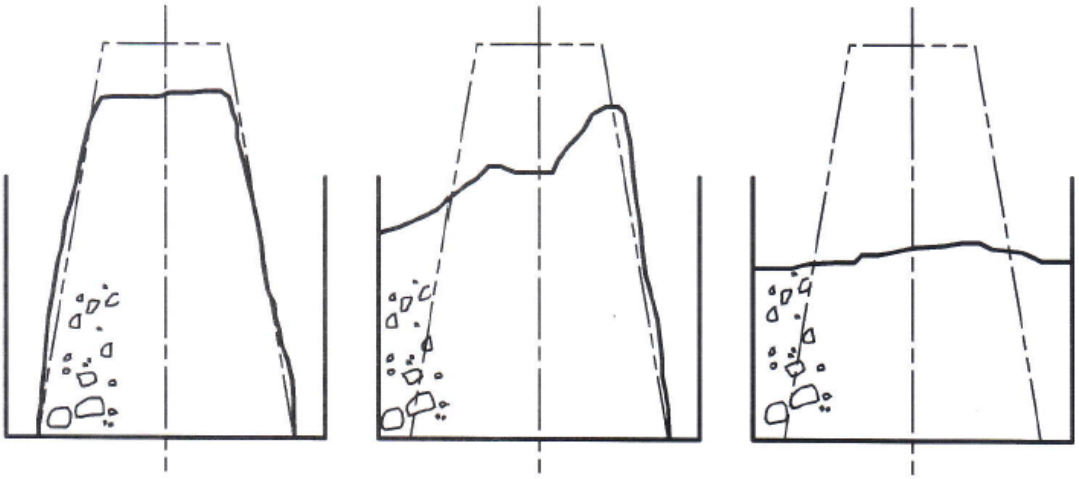

a) True Slump c) Shear Slump b) Collapse Slump

Figure 3-22: Forms of vebe slump (EN 12350-3 2009)

3.6.3 ASSESSMENT RATING

The third workability test of the fresh concrete was a scaling system to be filled out by the workers handling the concrete. The objective was to have a combination of ratings and average the scores to grade the workability of each mixture. The workers individually rated the concrete and were not informed about the variables of the mixture. They were

aware which phase was being tested, but they did not know any specifics about the mixture. Two workers were helping with the mixtures throughout both phases. In order to have a consistent point of view on the workability of the concrete, the target was to keep the same workers during the duration of the project. However, one worker had to leave before the end of the research.

While filling out the worksheet, the workers were asked to judge the concrete based on three categories. They included scooping, rodding, and troweling as shown in Figure 3-23. The categories were picked to best relate properties of workability to the work required during the completion of a mixture. The scooping category can be related to flow of concrete. It is classified as the ease with which the concrete is transported or placed into a mold or formwork. The rodding category can be related to the consolidation of the concrete. The troweling category can be related to the finishability of the concrete. It is classified as the quality of finish to the concrete without creating bug-holes or other surface defects, and the ease to achieve the finish. The overall rating system was scaled 0 through 10, with 10 meaning the concrete performed very poorly in the given category. The rating for the mixture was then obtained by adding up each category. The two overall ratings, provided by each worker, were then averaged to give the final grading for the mixture. The workers also had the opportunity to leave additional comments if they felt it was necessary to describe the workability of the mixture.

Mix number:

Date:

Name:

Workability Assessment		
Categories	Scale (0-10) 0 = Best 10 = Worst	Additional Comments
Scooping (Ease of putting scoop into concrete and taking it out)		
Rodding (Ease of concrete compaction with rod)		
Troweling (How sticky the concrete is and how easily you can finish it)		

Total =

Figure 3-23: Workability assessment worksheet

3.6.4 SAMPLING

In addition to the ASTM C143 (2012) slump test, used to initially sample the fresh state of the concrete as mentioned in Section 3.6, other standard tests were used to assess the fresh concrete properties. They included the standard method for unit weight of concrete outlined in ASTM C138 (2014), the standard method for air content outline in ASTM

C231 (2010), and the standard method for temperature outline in ASTM C1064 (2012). The procedure for making and storing test specimens was also done according to common standards.

3.7 HARDENED CONCRETE PROPERTY TESTING

Hardened concrete property testing was used to determine the effect the variables from both phases had on the concrete. Sections 3.3 and 3.4 outline the schedules that were used for each test specimen. This section will discuss the procedures that were followed and the specimen preparation required.

3.7.1 COMPRESSION STRENGTH TESTING

Compressive testing was conducted with unbonded caps using elastomeric pads. Pads were made of neoprene and a pad durometer of 70 met the cylinder strength that would be tested. The pads were placed in two metal retainers used to support and align the cylinder. The dimensions conformed to those required in ASTM C1231 (2013). Before performing a test, cylinder ends were examined for any depressions that exceeded 0.2 inches using a straight edge. Any irregularities were corrected by grinding the surfaces. Powder was then applied to the ends of the cylinder in order to reduce any friction that might occur from the roughened surfaces. Testing was conducted using a Forney compression machine, following the procedure outline in ASTM C39 (2015). The load rate was applied at 35 ± 7 psi/s and the type of fracture pattern was noted. An example of a proper fracture pattern is shown in Figure 3-24.

Figure 3-24: Compression testing fracture pattern

3.7.2 SPLITTING TENSILE STRENGTH TESTING

Splitting tensile testing was conducted in accordance to ASTM C496 (2011). The test applies a diametric compressive force along the length of the specimen, creating tensile stresses on these planes. Tensile failure occurs rather than compressive failure because the areas of load application are in a state of triaxial compression, thereby allowing them to withstand much greater compressive stresses than would be indicated by a uniaxial compressive strength test (ASTM C496 2011). To accommodate the height of the sideways placed cylinder, a metal block was used in the Forney compressive machine. An aligning jig, consisting of a frame and top bearing block, was then used to center the cylinder. The top bearing block of the jig was centered beneath the bearing block of the Forney compressive machine, as shown in Figure 3-25. Two bearing strips were placed in between the specimen and the jig, on top and bottom. The bearing strips were 0.125 inch

thick plywood conforming to ASTM C496 (2011). A load rate of 100-200 psi/min was applied to the specimen until failure. The failure pattern often resulted in two equal halves with a thin strip in between, as shown in Figure 3-26.

Figure 3-25: Splitting tensile testing arrangement

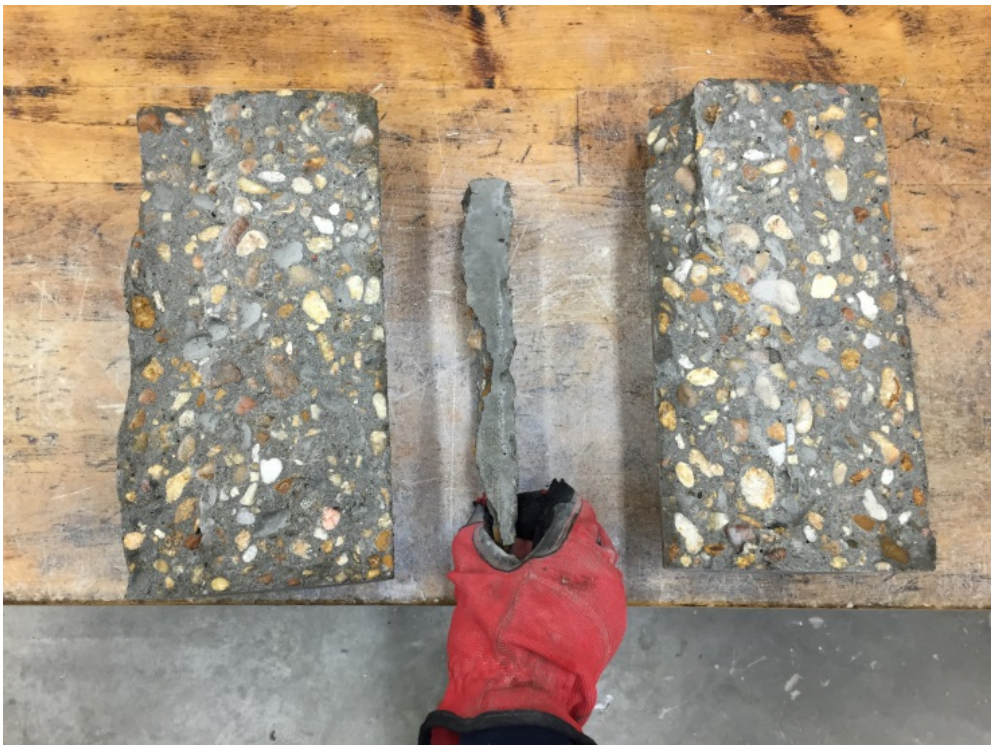

Figure 3-26: Splitting tensile fracture

3.7.3 MODULUS OF ELASTICITY TESTING

Testing for the modulus of elasticity for the concrete specimens were done in accordance to ASTM C469 (2014). The specimen is prepped in the same manner as in Section 3.7.1 with unbonded caps. Before applying the top cap, a compressometer is mounted onto the specimen to measure the strain. A specimen with the compressometer installed is shown in Figure 3-27. Before performing the test, a companion cylinder is used to determine the ultimate compressive strength. Separate specimens are then loaded until the applied load is equal to 40 percent of the ultimate strength, operating at the same load rate specified in Section 3.7.1. The test was performed three times on two cylinders (first cycle results were discarded per specification requirements), and the results were averaged.

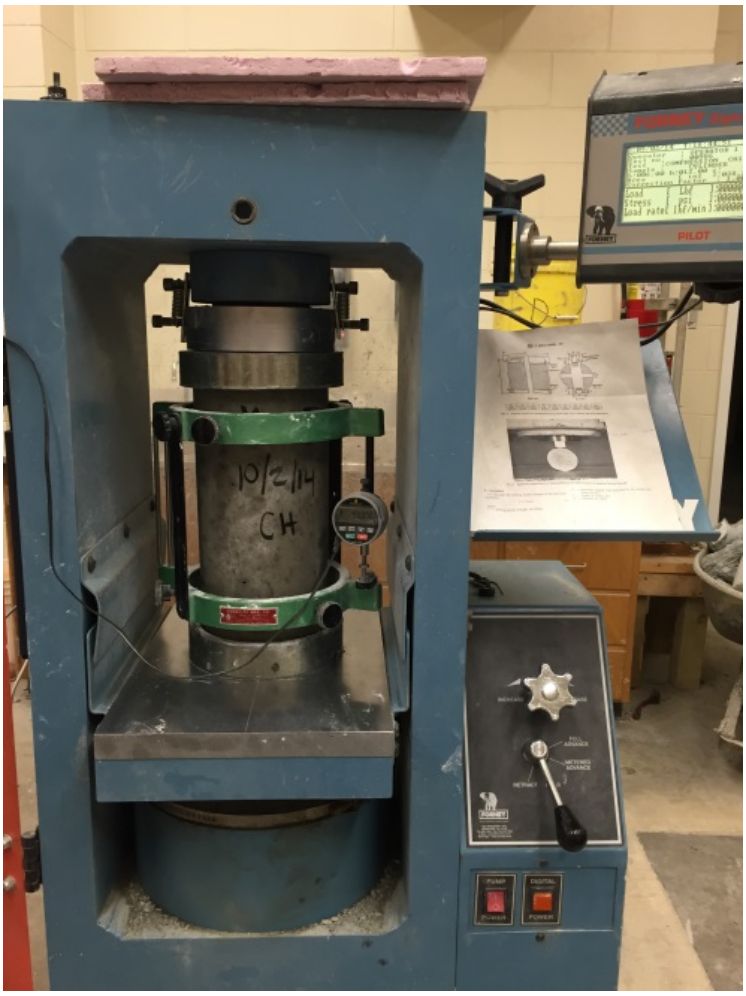

Figure 3-27: Modulus of elasticity testing

3.7.4 DRYING SHRINKAGE TESTING

Testing for the length change of the hardened concrete followed the procedures outlined in ASTM C157 (2008). Three prisms were measured at the specified dates for each phase, shown in Table 3-1 and Table 3-6. Readings were conducted using a length comparator. Before recording the length change of a specimen, the comparator dial was read using the reference bar. Then two readings were conducted with the specimen in the length comparator, as shown in Figure 3-28. Specimens were then returned to the air

storage room located in the Auburn University Structures and Materials Laboratory, shown in Figure 3-29.

Figure 3-28: Shrinkage prism loaded into comparator

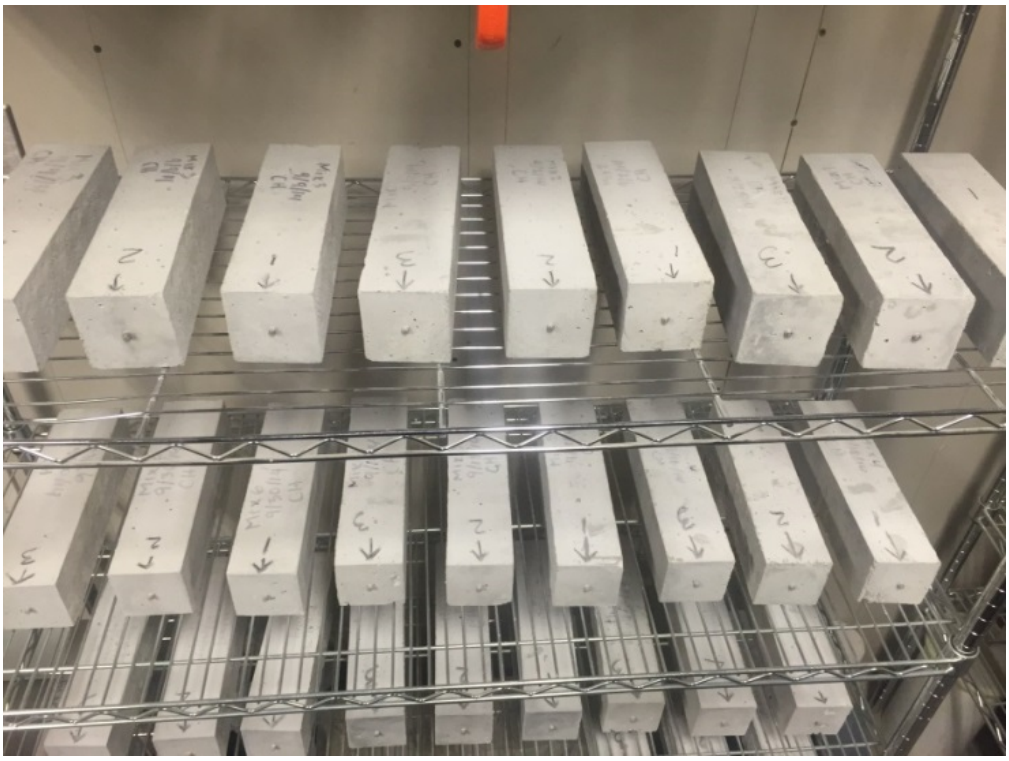

Figure 3-29: Drying shrinkage prisms stored in drying room

3.7.5 CHLORIDE ION PERMEABILITY TESTING

Testing the permeability of the concrete specimens was conducted following the procedures in ASTM C1202 (2006). All specimens cured until they reached an age of 91 days. At this age the 4 x 8 inch cylinders were trimmed to a 2 inch testing size using a water-cooled diamond saw. Next, the specimens were washed of any slurry and laid out to dry for one hour. Specimens were then placed into a plastic bowl and vacuum pumped for three hours to remove all water from the samples. After this period the plastic container was filled with distilled water, while the pump remained on for an additional hour. The pump was then switched off and the specimens were left submerged and uncovered for 18 ± 2 hours. After, specimens were removed from the water and the

surfaces were wiped dry. A plastic ring was then placed over the middle of the specimens and secured with rubber O-rings. Sealant molds were then placed over each rubber O-ring. For each specimen, one sealant mold was filled with NaCl solution, and the other was filled with NaOH solution. The prepared specimens were then connected to a power supply set to 60 volts, as shown in Figure 3-30. The test then ran for six hours, and the final amount of charge that passed through the specimens was recorded.

Figure 3-30: Specimens connected to power supply

3.7.6 ABRASION RESISTANCE TESTING

Testing for abrasion resistance of concrete specimens was conducted following ASTM C779 (2012). The Auburn University Laboratory did not have the equipment needed for the test, therefore after specimens were cured they were sent to CTL Group to be tested. The equipment used to test for the wear of the concrete followed procedure A, the revolving-disk machine, in ASTM C779 (2012). This option is known to produce the

most consistent results. It operates by sliding and scuffing steel disks in conjunction with abrasive grit in a circular motion, shown in Figure 3-31. The depth of wear is reported at 0, 5, 15, 30, and 60 minutes of abrasion. The abrasive mode of the procedure best simulates wear by medium tire-wheeled traffic (Karl 2006).

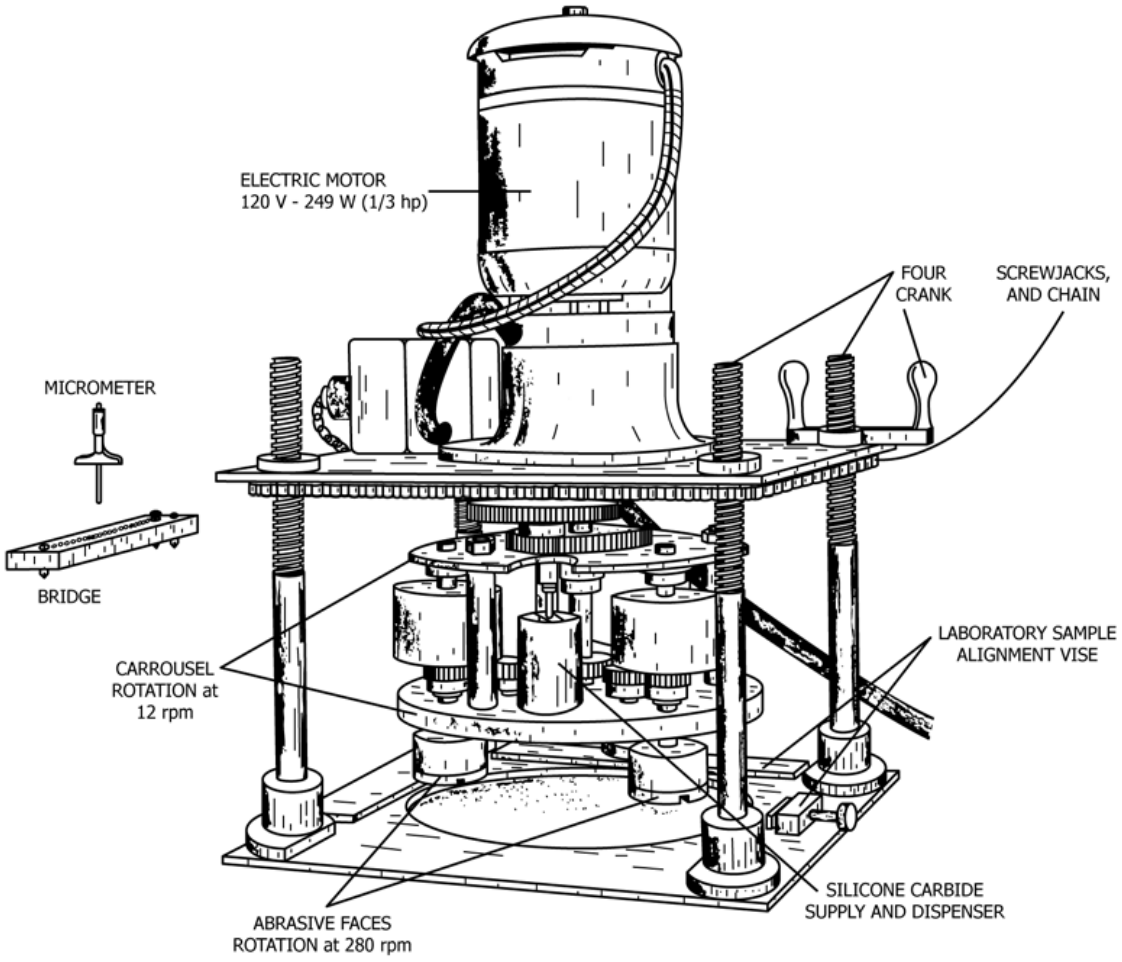

Figure 3-31: Revolving disk abrasion test machine (ASTM C779 2012)

The test specimens were required to have dimensions of at least 12 x 12 x 3 inches. Formwork was designed to produce three specimens and be reusable to make all

the specimens for phase II. A sketch of the formwork with its dimensions is shown in Figure 3-32.

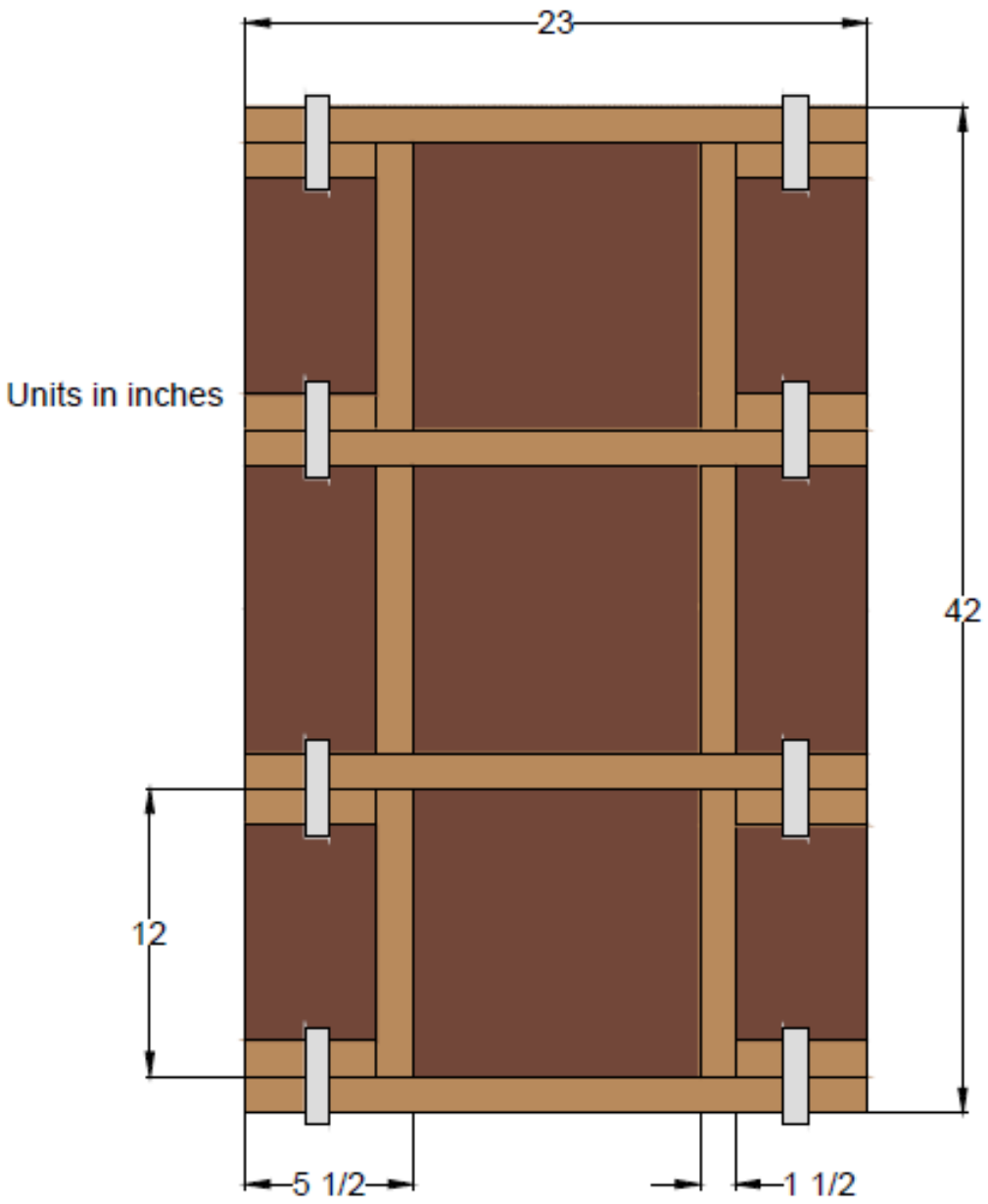

Figure 3-32: Abrasion formwork dimensions

Figure 3-33: Abrasion testing formwork

Casting the specimens for abrasion testing followed the procedures in ASTM C192 (2015). The specimens were made in 2 layers with 72 strokes per layer using a 5/8 inch diameter rod. After each layer was rodded, the outside surfaces of the formwork were lightly tapped using a rubber mallet 10 to 15 times to close any holes left by rodding. The top of the concrete surface was then finished using a woodened trowel. Upon the concrete reaching final set, a final finish was applied to the surface using a metal trowel. Once the concrete reached final set, wet burlap was placed on the surface of the concrete and plastic then covered the burlap to prevent evaporation of water. After the concrete reached an age of 7 days, the specimens were stripped from the formwork and

placed into the curing room with the cylinders until they reached an age of 28 days. They were then air cured in the laboratory until they were shipped to CTL Group. The specimens in the laboratory are shown in Figure 3-34.

Figure 3-34: Abrasion specimens air cured in laboratory

3.8 RAW MATERIAL CHARACTERIZATION TESTING

Three tests were conducted to characterize both types of fine aggregate by their water demand, packing density, shape, and amount of clay content. Tests were also run on the cement and fly ash for comparison purposes. This section will discuss the details of these tests.

3.8.1 METHYLENE BLUE TEST

Testing for the detection of harmful clays followed the procedures outlined in AASHTO T330 (2007). The natural fine aggregate passing the No. 200 sieve and the dust-of-

fracture mineral filler were both tested and compared. A test slurry must first be made that consists of water and fine aggregate. A methylene blue solution is then incrementally added to the test slurry until the endpoint is reached, as shown in Figure 3-35. The endpoint is indicated by removing a drop of the slurry and observing a light blue halo formed around the sample drop, as shown in Figure 3-36. A high methylene blue value (MBV) indicates a large amount of clay or organic matter present in the sample (AASHTO T330 2007). Table 3-12 relates the MBVs to their expected fresh and hardened concrete performance. The equation to calculate the MBV is shown below.

$$M = \frac{CV}{W} \qquad \textbf{Equation 3-3}$$

Where,

M = MBV in mg of solution per g of the minus No. 200 material, and

C = mg of Methylene Blue/mL of solution, and

V = mL of Methylene Blue solution required for titration, and

W = grams of dry material

Figure 3-35: Titrating methylene blue solution into slurry

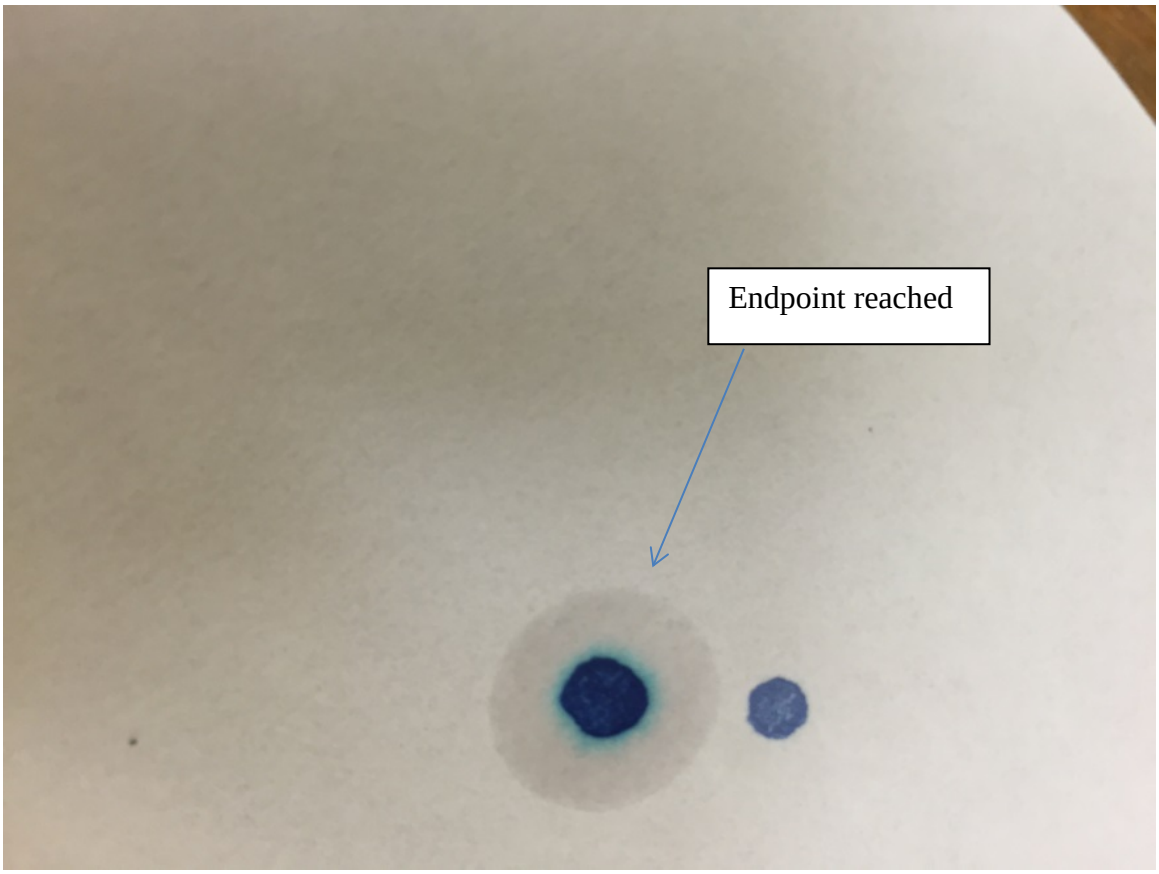

Figure 3-36: Methylene blue endpoint

Table 3-12: Expected Performance of Methylene Blue (AASHTO T330 2007)

Methylene Blue (mg/g)	Expected Performance
≤ 6	Excellent
7-12	Marginally acceptable
13-19	Problems/possible failures
≥ 20	Failure

3.8.2 VICAT TEST

The test to determine the normal consistency of hydraulic cement is outlined in ASTM C187 (2011). Enough water is combined with the cement sample to settle the Vicat apparatus 9-11 mm within 30 seconds, as shown in Figure 3-37. This test also included additional powder samples in order to evaluate the wet packing density. The wet packing density can be related to the water demand, as stated in Section 2.5.4.1. Samples included cement, Class F fly ash, dust-of-fracture mineral filler, and mineral filler from the natural fine aggregate.

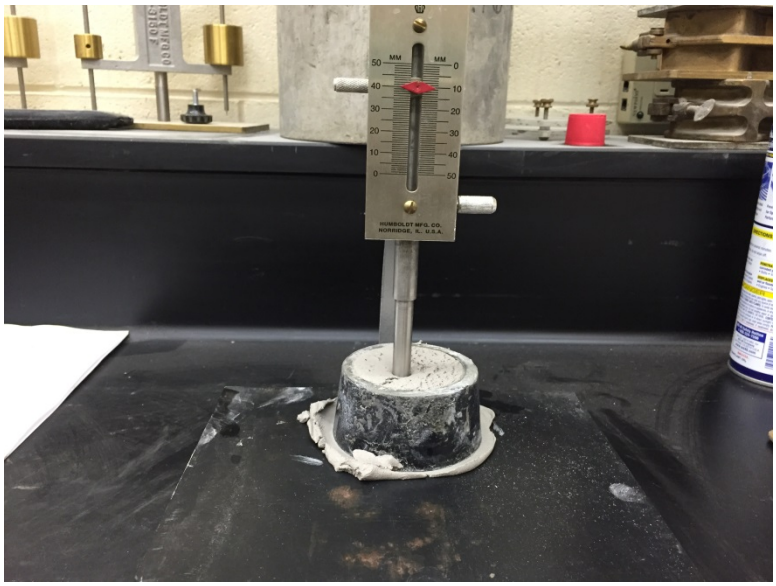

Figure 3-37: Testing for wet packing density using Vicat apparatus

To run the test, 650 grams of powder is measured, mixed with water and formed into a paste ball in accordance to the standard. The ball is then quickly pushed into a plastic ring and the plunger of the Vicat apparatus is released. The amount of water found

to give the paste a normal consistency can then be used in the following equation (ASTM C187 2011).

$$\phi = \frac{V_{solids}}{V_{total}} = \frac{1}{1 + \frac{W_w}{W_{mf}} \cdot SG_{mf}} \qquad \textbf{Equation 3-4}$$

Where,

ϕ = packing degree, and

W_w = weight of water, and

W_{mf} = weight of mineral filler, and

SG_{mf} = specific gravity of mineral filler

3.8.3 PARTICLE SIZE DISTRIBUTION

In order to determine the combined particle distribution of all material smaller than the No. 200 sieve, the fine aggregates and cementitious material were analyzed using laser diffraction. This requires specialized and precise equipment that was not accessible to the Auburn University laboratory. Therefore, samples were sent to the CTL Group in Skokie, Illinois. The samples included dust-of-fracture mineral filler, mineral filler obtain from the natural fine aggregate, cement, and fly ash. The cementitious material was tested for comparison purposes. Particle size distribution testing was conducted using Malvern Mastersizer 2000 testing equipment. The sample sizes were 10 grams and tested in a dry state. The results provide a graphical particle size distribution curve ranging from 2000 micrometers to 0.02 micrometers.

3.9 RAW MATERIAL CHARACTERIZATION TEST RESULTS

The Vicat test was used to determine the wet packing density, as stated in Section 3.8.2. The results from the test are shown in Figure 3-63. It can be seen that the MFA material passing the No. 200 sieve resulted in the highest packing density, which was 20 percent greater than the packing density for the natural fine aggregates passing the No. 200 sieve. It can also be seen that the packing density of fly ash is greater than cement.

The results are similar to what Quiroga and Fowler (2007) found. In their study, the packing densities included 0.62 for dolomitic limestone MFA dust-of-fracture mineral filler, 0.51 for cement, and 0.62 for Class F fly ash. The study concluded that the packing density is best at describing the behavior and water demand of the material. A relationship may also exist between the dosage of water-reducing admixture and the packing density, as stated in Section 2.5.4.1.

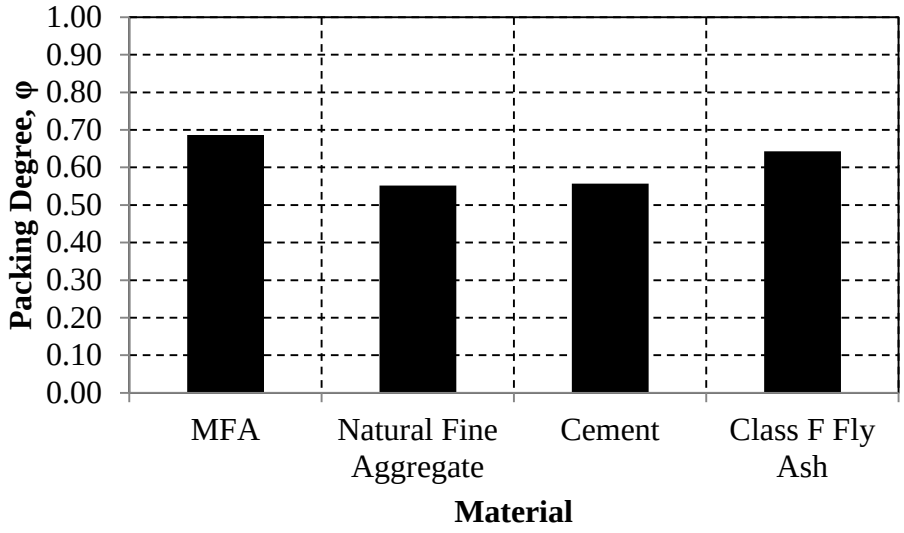

Figure 3-38: Vicat packing degree

The particle size distribution was measured using a laser size analyzer, as stated in Section 3.8.3. The results of the test are listed in Table 3-16 and plotted in Figure 3-64. It can be seen that cement and fly ash have similar particle size distributions. In addition, the MFA dust-of-fracture mineral filler and natural fine aggregate dust-of-fracture mineral filler are both smaller than the cementitious materials. When comparing the MFA and natural fine aggregate dust-of-fracture mineral fillers, the MFA has the smaller distribution of particles. The volume of the MFA dust-of-fracture mineral filler has 26 percent of the material between the sizes of 3 and 30 micrometers, compared to the natural fine aggregate that has 13 percent, as seen in Table 3-16.

Table 3-13: Particle Size Analysis

	Cumulative Volume under Stated Size (%)			
Size of Particles (µm)	MFA	Natural Fine Aggregate	Cement	Class F Fly Ash
45	39.37	30.14	86.93	77.85
30	34.33	14.15	74.02	65.89
10	21.35	4.85	40.52	32.64
7	16.96	3.11	32.73	23.23
3	8.39	1.55	17.74	8.31
1	2.91	0.25	5.77	2.33
3-30 µm	25.94	12.6	56.28	57.58

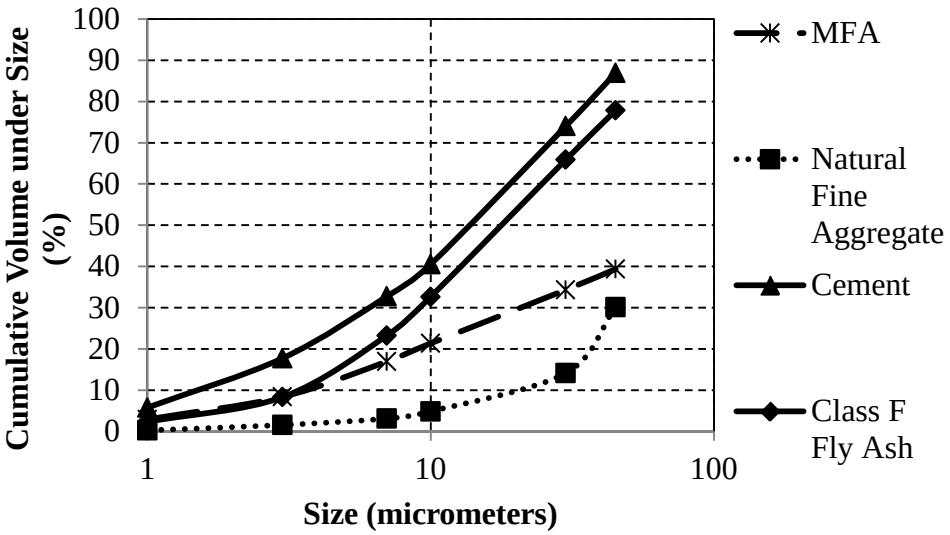

Figure 3-39: Particle size distribution plot

The MBV was determined as stated in Section 3.8.1. The values for the dust-of-fracture mineral fillers can be seen in Table 3-17. According to AASHTO T330 (2007), aggregates with MBVs less than 6 mg/g are considered free of deleterious material. The MBV's for both dust-of-fracture mineral fillers were under 6 mg/g, therefore they can be considered free of deleterious material and do not present any problems to the concrete. The MBV for the MFA dust-of-fracture mineral filler was less compared to the natural fine aggregate dust-of-fracture mineral filler. It is thought the reason for this result is due to the larger particle size distribution for the natural fine aggregate dust-of-fracture mineral filler. An increase in surface area may lead to an increase in the amount of methylene blue required to coat the particles (Quiroga and Fowler 2004). In addition, the MBV's found for this project for the MFA dust-of-fracture mineral filler were smaller

than the results from Vulcan Materials Company, but both results were significantly under the 6 mg/g limit.

Table 3-14: Methylene Blue Values for Dust-of-Fracture Mineral Filler

Type of Dust-of-Fracture Mineral Filler	**MB Solution Required for Titration (ml)**			**MBV (mg/g)**
	Test 1	Test 2	Test 3	
MFA	1.5	1.5	1.5	0.75
Natural Fine Aggregate	4	3.5	4	1.92

CHAPTER 4

EXPERIMENTAL RESULTS AND DISCUSSION OF RESULTS

4.1 INTRODUCTION

The laboratory testing results of the fresh and hardened concrete properties from phases I and II are presented in this chapter. The data were statistically analyzed in order to determine correlations, in accordance with the project objectives listed in Section 1.2. This chapter presents data using the Shilstone Method and the percent retained chart in phase I, and the effects from increasing the percentage of dust-of-fracture mineral filler in fine aggregate during phase II.

4.2 SUMMARY OF COLLECTED DATA

Three different tests were used to measure the workability of the fresh concrete, as discussed in Section 3.6. The hardened concrete properties were measured using mechanical and durability tests, as discussed in Section 3.7. The data were collected and graphed and all statistical analysis was performed with the statistical computing and graphics language R®. If correlations were found between the recorded data, graphs and plots of averages were made to show the relationship. All fresh property raw data are presented in Appendix A. Mechanical property raw data are presented in Appendix B. Durability property raw data are presented in Appendix C, and corresponding abrasion test pictures are presented in Appendix D.

4.3 PRELIMINARY DATA REVIEW

Prior to data analysis, the results were examined to check for any outlying values. Data points that are distant from other observations can cause the test average to be skewed. Outliers were identified in accordance to ASTM C670 (2013) Standard Practice for Preparing Precision and Bias Statements for Test Methods for Construction Materials. ASTM specifications provide precision limitations on physical properties of concrete. The single-operator precision range and coefficient of variation for several physical properties are shown in Table 4-1. The difference in the results relative to their control mixtures were compared to the values shown in Table 4-1. The precision ranges were also used to determine the level of practical significance in the concrete results.

Table 4-1: Single-Lab Precision for Hardened Concrete Properties

Property	ASTM Specification	Coefficient of Variation	Range[1]	Maximum Strain Range[1]
Compressive Strength	C39	2.4%	7.8%	-
Splitting Tensile Strength	C496	5.0%	16.5%	-
Modulus of Elasticity	C469	4.3%	11.9%	-
Shrinkage	C157	-	-	0.0277%
RCPT	C1202	12.3%	41.0%	-
Abrasion	C779	5.51%	18.2%	-

[1]Calculated using multiplier of coefficient of variation in ASTM C 670

The shrinkage data set contained 609 values with 0 being identified as outliers. The RCPT data set contained 87 values with 0 being identified as outliers. The abrasion data set contained 15 values with 0 being identified as outliers. The compressive strength testing data set contained 261 values with 0 being identified as outliers. The splitting

tensile strength testing data set contained 261 values with 5 being classified as probable outliers. The outliers were removed from the data set before further analysis was completed. The modulus of elasticity testing data set contained 174 values with 1 being identified as a probable outlier. In this instance, the identified outlying value was noted during testing, due to the use of a different compressometer. This value was removed from the data set before further analysis was completed.

4.4 PHASE I DATA AND DISCUSSION OF RESULTS

Evaluating the effectiveness of using the Shilstone Method and the percent retained chart to quantify the effect of using optimized aggregate gradations in concrete was completed during the phase I analysis. In order to quantify the potential benefits of using optimized aggregate gradations in concrete, fresh and hardened properties were tested. This section presents the data and corresponding analysis.

The Shilstone Method consists of the CFC and the 0.45-Power chart. These charts, along with the percent retained chart can be found in the following figures for each of the mixtures used in phase I. In addition, Table 4-2 provides information on whether or not mixtures pass ASTM C33 (2013) gradation limits and if they are optimized gradations. The mixtures in phase I were compared by analyzing mixtures that had optimized aggregate gradations against mixtures that did not have optimized aggregate gradations. The optimized aggregate gradations fell within the limits of the Shilstone Method and the percent retained chart. In order to fall within the limits of the Shilstone Method, a mixture was located in zone II of the CFC and was within 15 percent of the power line on the 0.45-Power chart. In order to fall within the limits of the percent

retained chart, the percentage of aggregates retained between the 1/2 inch sieve and the No. 50 sieve were within the 8-22 percent limit. In addition, adjacent sieves were within 10 percentage points of each other, as defined in Section 2.4.3.

Table 4-2: Mixture Acceptance Reference

Mixture	ASTM C33 Coarse Aggregate Gradation	ASTM C33 Fine Aggregate Gradation	Optimized Aggregate Gradation
DL No. 57 Blend 1	✓	✓	
DL No. 57 Blend 2			✓
DL No. 57 Blend 3	✓	✓	
DL No. 57 Blend 4	✓		✓
DL No. 67 Blend 1	✓	✓	
DL No. 67 Blend 2		✓	
DL No. 67 Blend 3	✓		
DL No. 67 Blend 4	✓		✓
RG No. 57 Blend 1		✓	
RG No. 57 Blend 2	✓	✓	
RG No. 57 Blend 3			✓
RG No. 57 Blend 4	✓	✓	
RG No. 67 Blend 1	✓	✓	
RG No. 67 Blend 2	✓	✓	
RG No. 67 Blend 3	✓		✓
RG No. 67 Blend 4	✓		

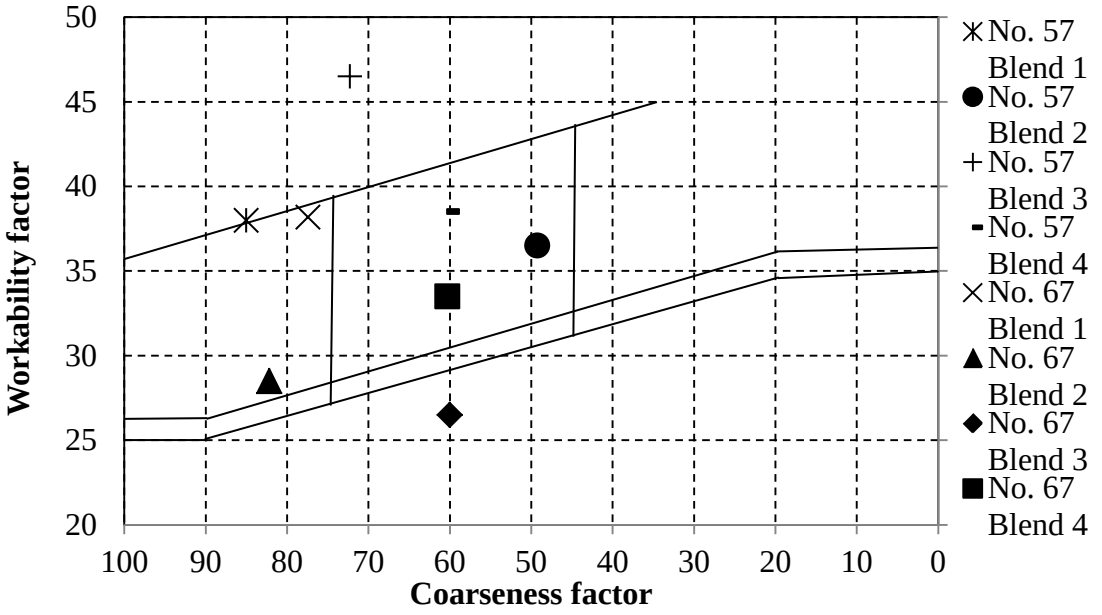

Figure 4-1: Dolomitic limestone CF chart

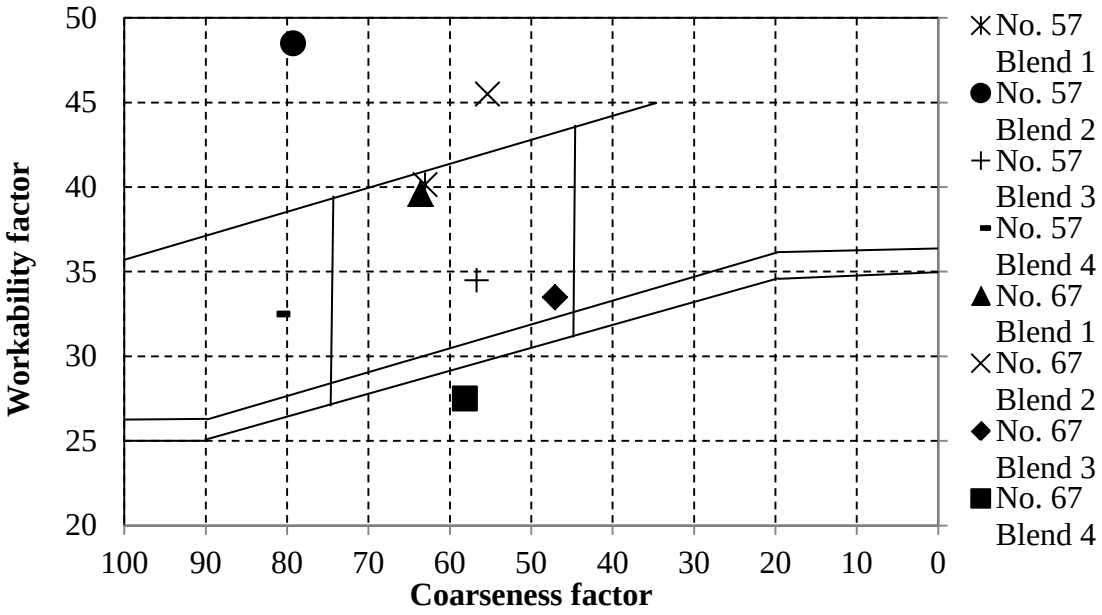

Figure 4-2: River gravel CF chart

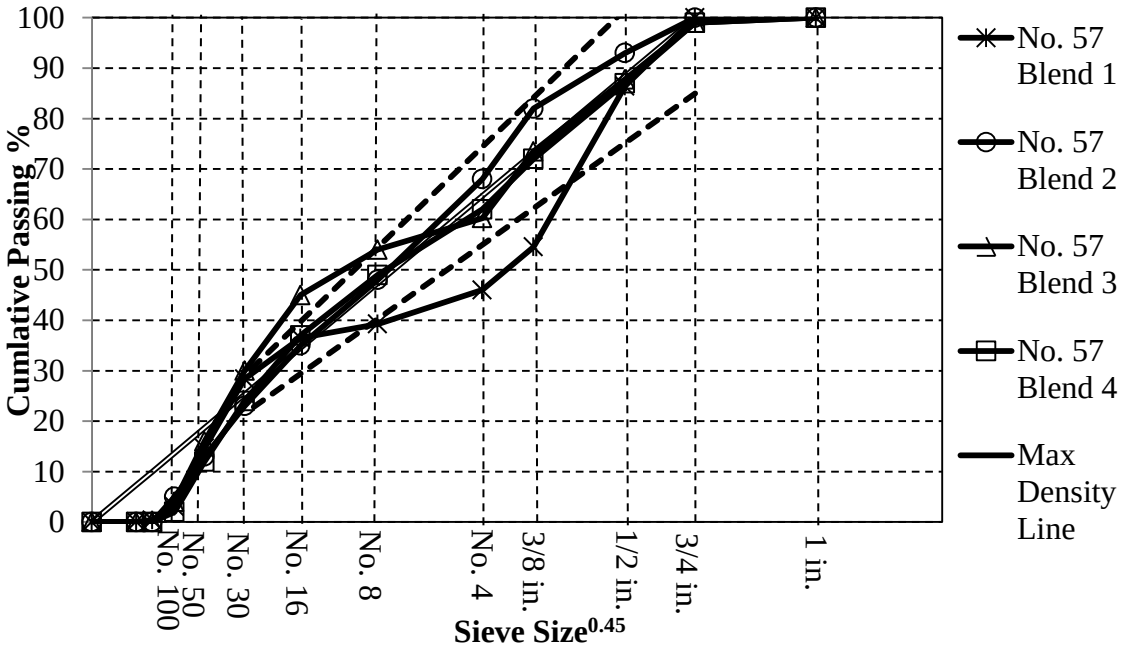

Figure 4-3: Dolomitic limestone 0.45-Power chart

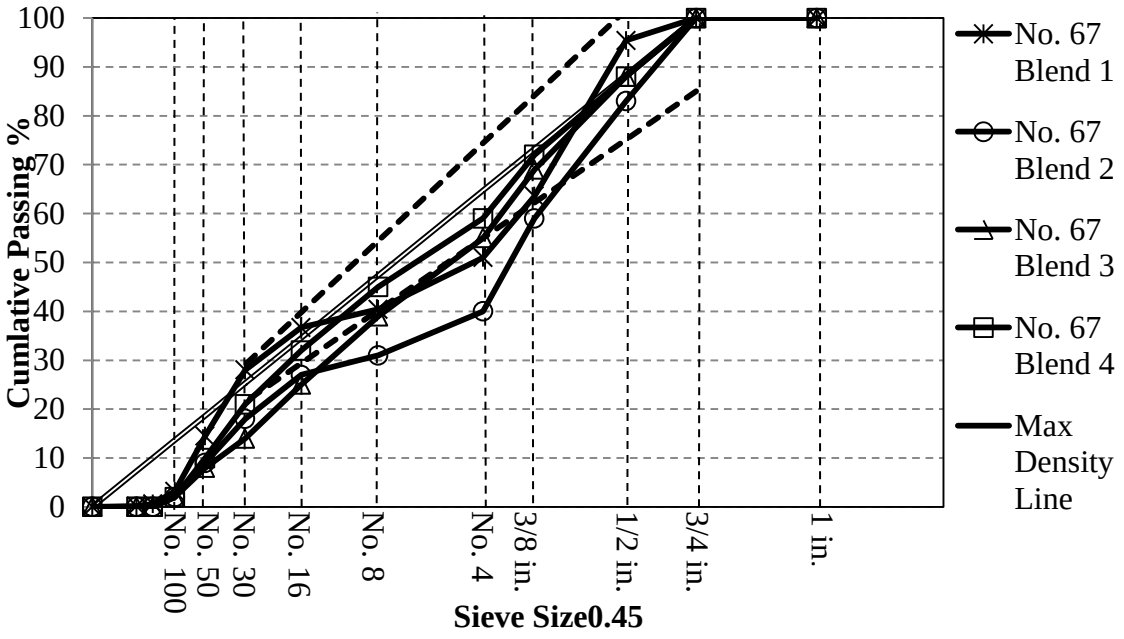

Figure 4-4: Dolomitic limestone 0.45-Power chart

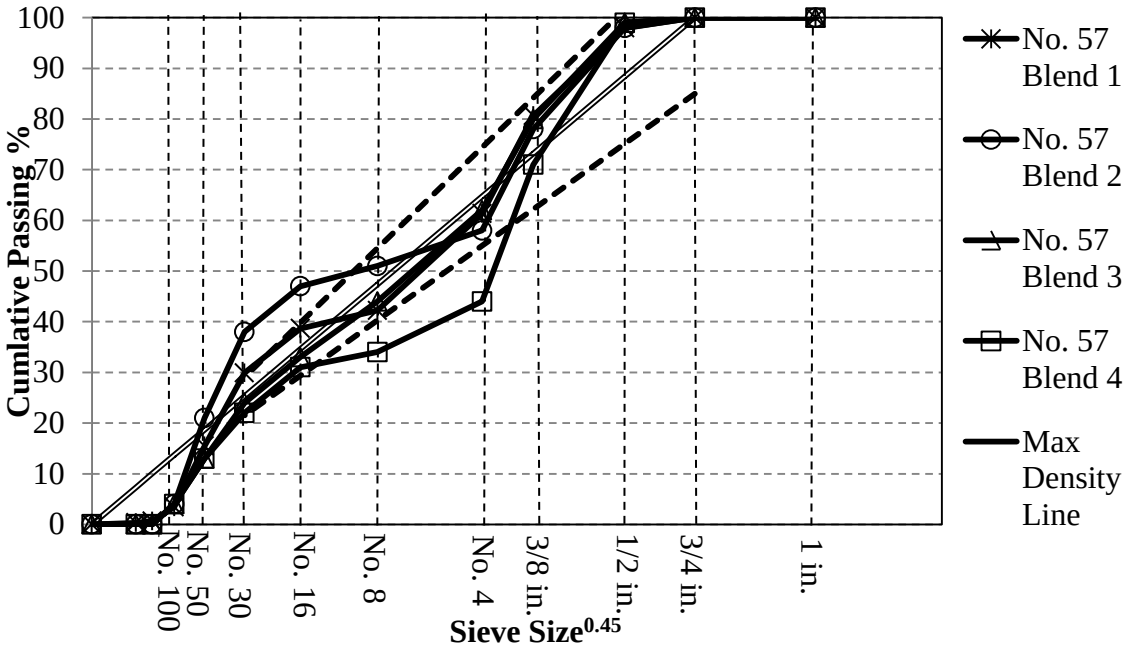

Figure 4-5: River gravel 0.45-Power chart

Figure 4-6: River gravel 0.45-Power chart

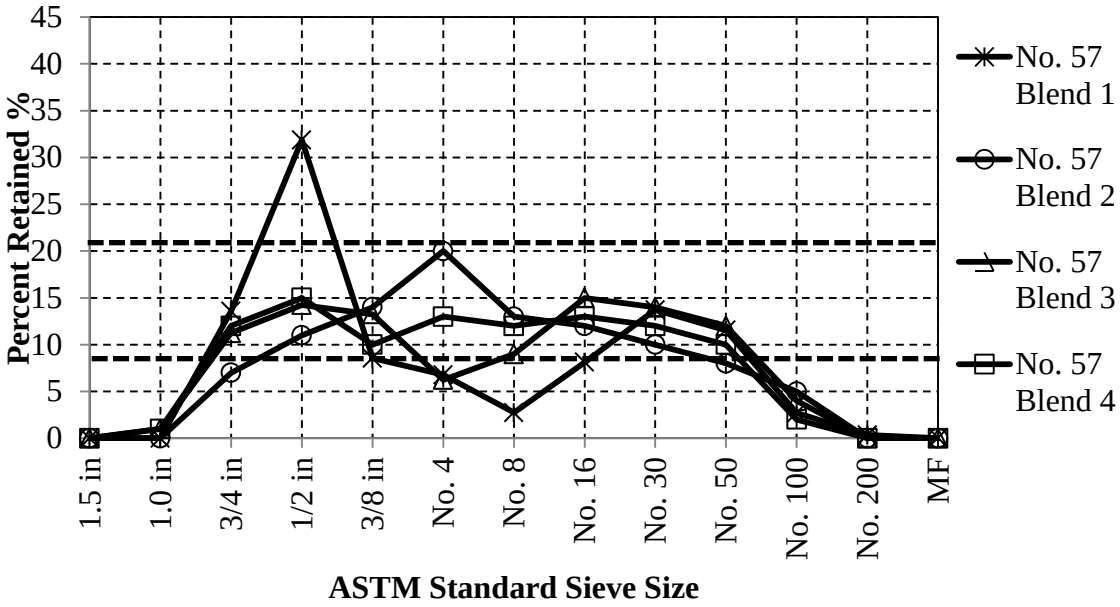

Figure 4-7: Dolomitic limestone percent retained chart

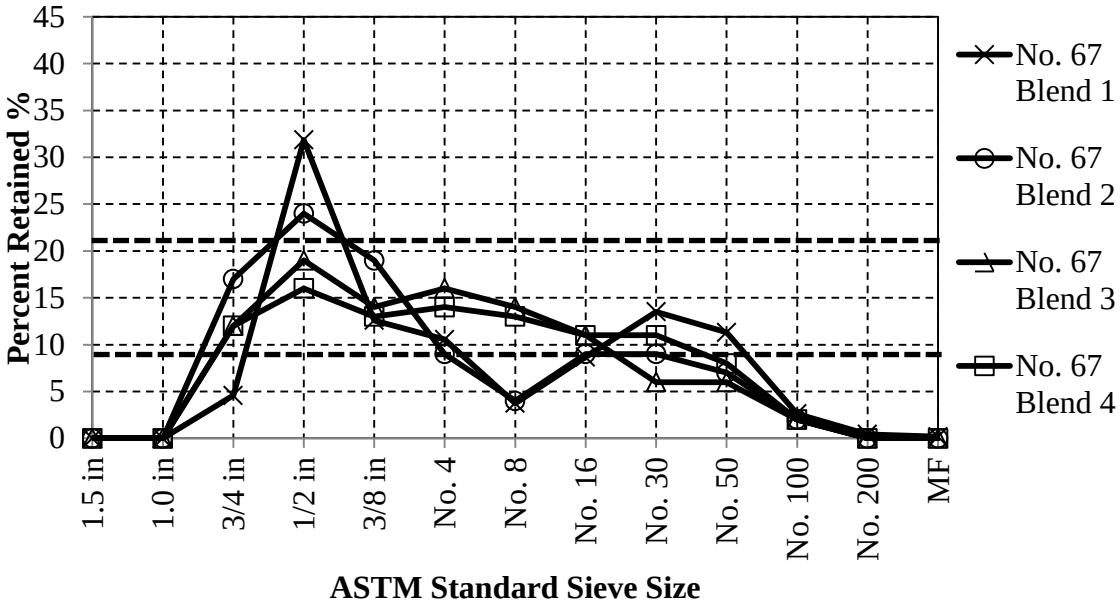

Figure 4-8: Dolomitic limestone percent retained chart

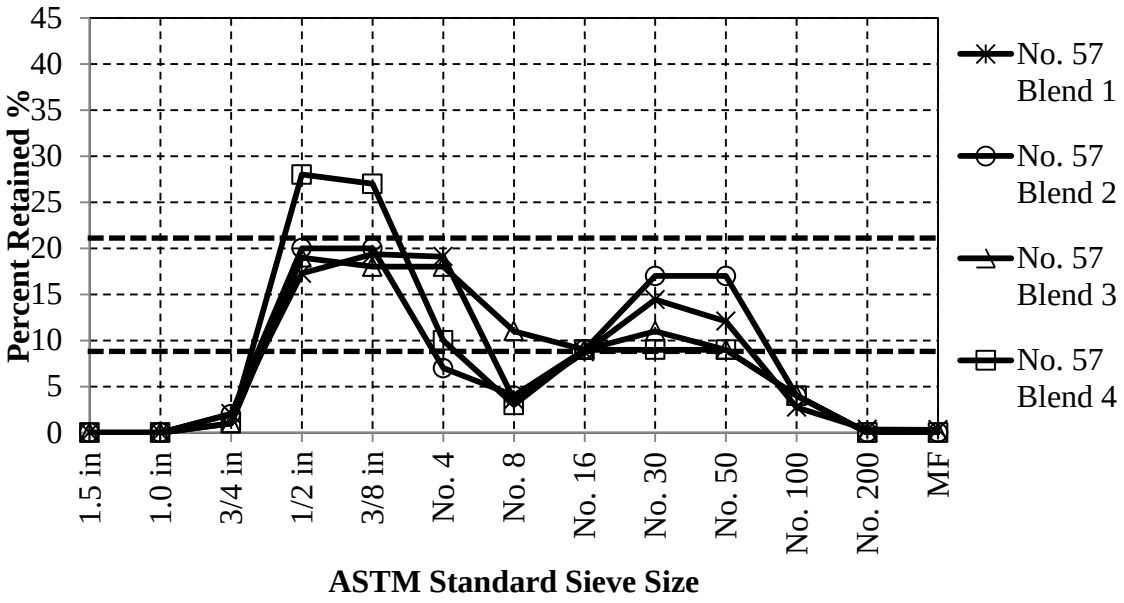

Figure 4-9: River gravel percent retained chart

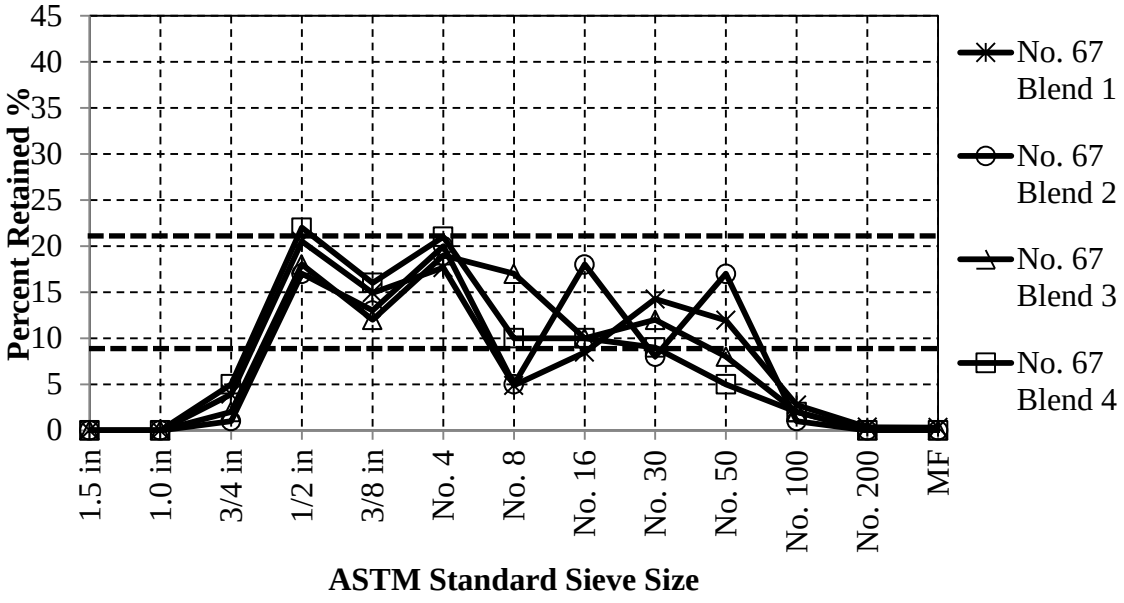

Figure 4-10: River gravel percent retained chart

4.4.1 EFFECT ON FRESH CONCRETE PROPERTIES

The effect of the two proportioning methods on obtaining workable concrete was evaluated through three tests. These tests included the modified slump test, the vebe test, and the workability assessment rating. For analysis purposes, only the vebe time and the workability rating were statistically analyzed. These two methods generate data that can compare differences in values. The data generated using the modified slump test served the purpose to measure yield stresses and plastic viscosities, to help assess the rheology of these concretes.

A statistical analysis was performed to identify which variables had a significant impact on the measured results. A test of hypothesis is a method for using sample data to decide between two competing hypotheses under consideration. It is initially assumed that one hypothesis is correct (null hypothesis). The sample data is then considered, and the null hypothesis is rejected in favor of the competing claim if there is convincing evidence against the null hypothesis (Devore and Farnum 2005). The test of hypothesis is carried out by employing a test statistic, or the function of the data that is computed and used to decide between the null and alternative hypotheses. The convincing evidence is provided by the p-value, which is the probability of obtaining a test statistic at least as contradictory to the null hypothesis as the value that actually resulted. The smaller the p-value, the more contradictory the data is to the null hypothesis (Devore and Farnum 2005). An independent two sample t-distribution was used for the analysis of the fresh properties. The test used a confidence interval, which is the degree of reliability of the confidence level, of 95 percent. This implies that 95 percent of the samples would give an interval that included the mean, and only 5 percent of all samples would yield an

erroneous interval (Devore and Farnum 2005). Therefore, when evaluating the p-value, a value below 0.05 indicates there is a significant difference between values. The p-values for all the mixtures tested in Phase I relative to the measured fresh properties are shown in Table 4-2.

Table 4-3: Summary of Phase I Fresh Property P-values

Variables Compared	P-value
Vebe Time (DL vs. RG)	0.4545
Vebe Time (No. 57 vs. No. 67)	0.2547
Vebe Time (Optimized Gradations vs. Non-Optimized)	0.0218
Workability Rating (DL vs. RG)	0.3263
Workability Rating (No. 57 vs. No. 67)	0.6834
Workability Rating (Optimized Gradations vs. Non-Optimized)	0.0048

In order to analyze the effect the proportioning methods had on the concrete workability, the data were first analyzed to determine whether there was a difference between the measured properties from concrete made from different coarse aggregate types and different NMAS. It was determined that at a 95 percent confidence level no difference existed between either the coarse aggregate type or the NMAS. Next the data were analyzed to determine if a difference existed between mixtures that had optimized aggregate gradations and mixtures that did not have optimized aggregate gradations. Optimized aggregate gradations fell within the limits of the Shilstone Method and met the 8-22 limits on the percent retained chart, as described in Section 4.4. A difference was

found between the data for these mixtures at a 95 percent confidence level for both the vebe times and workability ratings.

The first test that will be presented is the vebe test. The objective was to determine the amount of time it takes a clear plastic disk to be covered in cement grout, while subjected to vibration, as detailed in Section 2.6.2.1. The data for the vebe times are shown in Table A-1. The mixtures with the largest slumps did not always have the smallest vebe time, indicating that the mixtures reacted differently to the vibration. Three of the vebe slumps were mistakenly not recorded.

After determining that the vebe times from optimized aggregate gradations were statistically different from vebe times from the non-optimized gradations, as shown from the p-value in Table 4-3, Figure 4-11 was made to graphically present these results. The horizontal x-axis represents the mixture and the vertical y-axis represents the vebe time. The mixtures labeled with diagonal stripes represent the optimized aggregate gradations. These mixtures displayed the lowest measured vebe times. This is in agreement with the findings from Richardson (2005) and Cramer (1995). These studies found that mixtures resulted in better flow and reduced water demand from using optimized total aggregate gradations. In addition, Shilstone (1990) states that the optimized concrete mixture has the least particle interference and responds best to vibration. Therefore, it can be concluded that optimized aggregate gradations will aid in lowering vebe times.

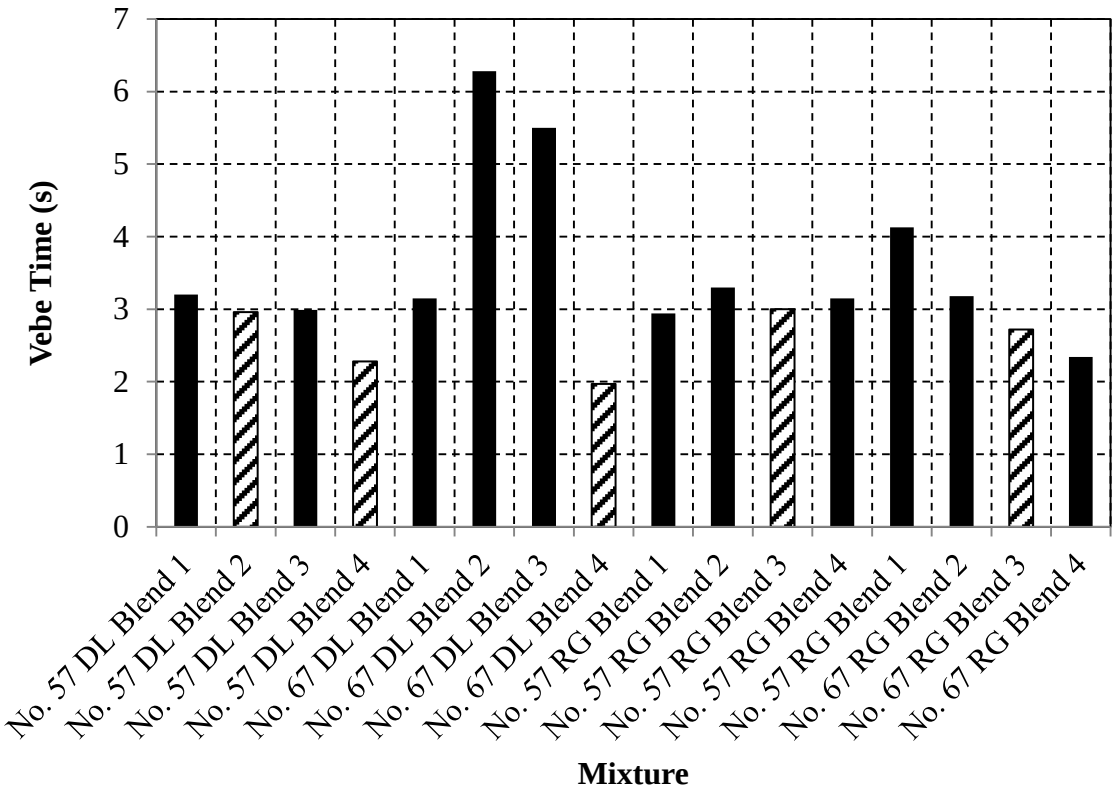

Figure 4-11: Plot of phase I vebe times

The workability assessment rating was a scaling system completed by the workers handling the concrete. For this rating assessment, ratings and average scores were combined to grade each mixture, as described in Section 3.6.3. The data for the workability ratings are shown in Table A-3. In addition to reporting the workability rating, workers provided a comment in relation to the mixture if it performed exceedingly good or bad. Three mixtures from dolomitic limestone had comments. They included No.67 blends 2-4. Blend 2 was stated as having excess coarse aggregate, segregating, and sticking to the trowel. This mixture was located in zone I of the CFC, and classifies as coarse gap-graded. Blend 3 was also stated as having excess coarse aggregate and

segregation. This mixture was located in zone V of the CFC and classifies as rocky. Blend 4 was stated as having performed the best out of all dolomitic limestone mixtures, with ease in scooping and rodding. This mixture was located in zone II of the CFC and classifies as optimum graded. Two mixtures from river gravel mixtures had comments. They included No. 57 blend 4 and No. 67 blend 4. The No. 57 blend 4 was stated as being difficult to trowel due segregation, but was still workable. This mixture was located in zone I of the CFC and classifies as coarse gap-graded. The No. 67 blend 4 was stated as being very difficult to trowel and finish, due excess coarse aggregate. This mixture was located in zone V of the CFC and is classified as rocky. The dolomitic limestone No. 57 blends 2-4 do not have workability ratings because the workability assessment was incorporated into the testing procedures after these mixtures were completed. Blend 1 has a workability rating because this blend was chosen as a duplication mixture.

After determining that the workability assessment ratings for the optimized aggregate gradations were statistically different from the ratings obtained from the non-optimized gradations, as shown from the p-value in Table 4-3, Figure 4-12 was made to graphically present these results. The horizontal x-axis represents the mixture and the vertical y-axis represents the workability rating. The mixtures labeled with diagonal stripes represent the optimized aggregate gradations. These mixtures displayed the lowest workability ratings recorded. This is in agreement with Shilstone (2007), stating that the use of the CFC will resolve pumping, placing, and finishing problems. Therefore, it can be concluded that optimized aggregate gradations aid in producing better workability assessment ratings.

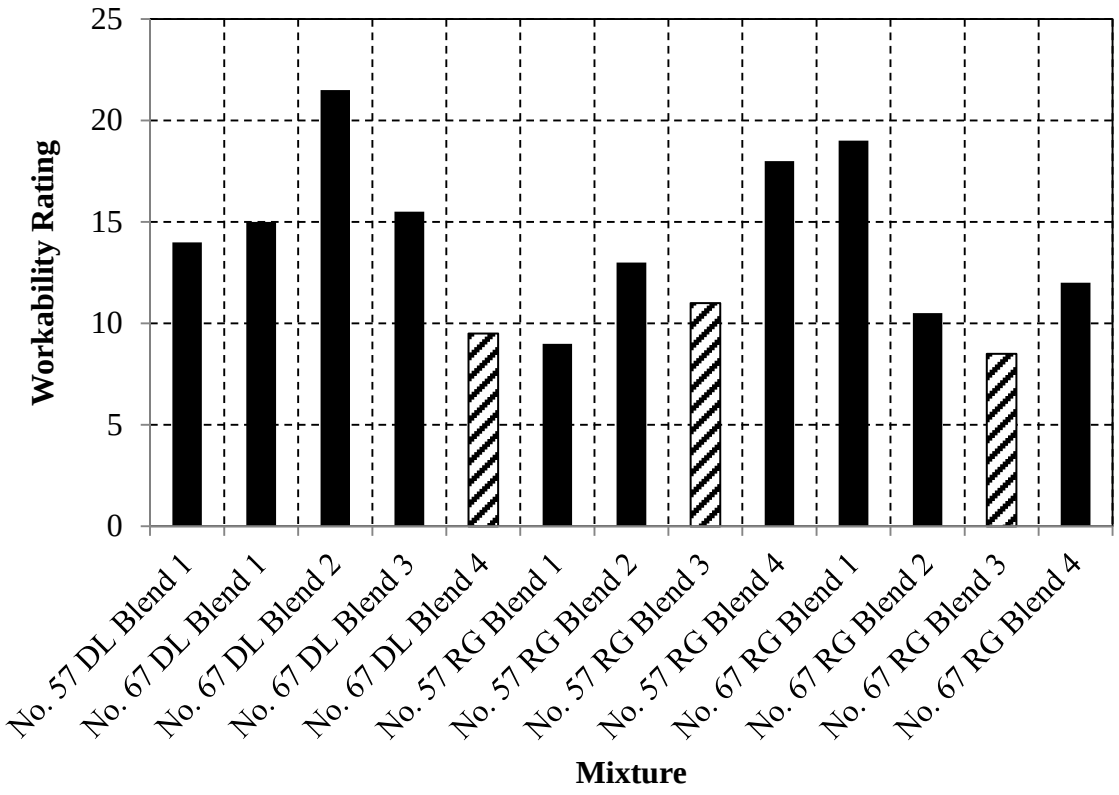

Figure 4-12: Plot of phase I workability ratings

The flow behavior of the concrete mixtures was evaluated through the use of the modified slump test. The flow curves, as described in Section 2.6.1, for the dolomitic limestone and river gravel mixtures can be seen in Figure 4-13 and Figure 4-14. The optimized aggregate gradations are labeled by double black lines in Figure 4-13 and Figure 4-14. The data for the dolomitic limestone mixtures and river gravel mixtures can be found in Table A-5. All mixtures are not represented with flow curves. Some mixtures did not reach the 4 inch slump limit required by the test. Therefore, the plastic viscosities could not be calculated, as described in Section 3.6.1.

The dolomitic limestone mixtures resulted in greater yield stresses and greater plastic viscosities, compared to the river gravel mixtures. This is in agreement with Rached et al. (2009) and Shilstone (1990), who state angular and rougher textured aggregates will affect the ability of fresh concrete to flow and contribute to harsh mixtures. When looking at the dolomitic limestone mixtures, the optimized aggregate gradation is clearly different from the other mixtures. It has the lowest yield stress, meaning this mixture required the least amount of shear stress to initiate the flow of the concrete. The optimized aggregate gradation also had the highest plastic viscosity. A low plastic viscosity increases the likeliness of segregation occurring (Germann Instuments 2014). When looking at the river gravel mixtures, the optimized gradations have greater plastic viscosities than 2 out of the 3 non-optimized gradations. Therefore, these mixtures are less prone to segregation. The results are in agreement with Shilstone and Shilstone (2002). In their case study, they proved moving an aggregate gradation into zone II of the CFC prevented segregation. Therefore, optimized aggregate gradations have a beneficial impact on the concrete flow behavior.

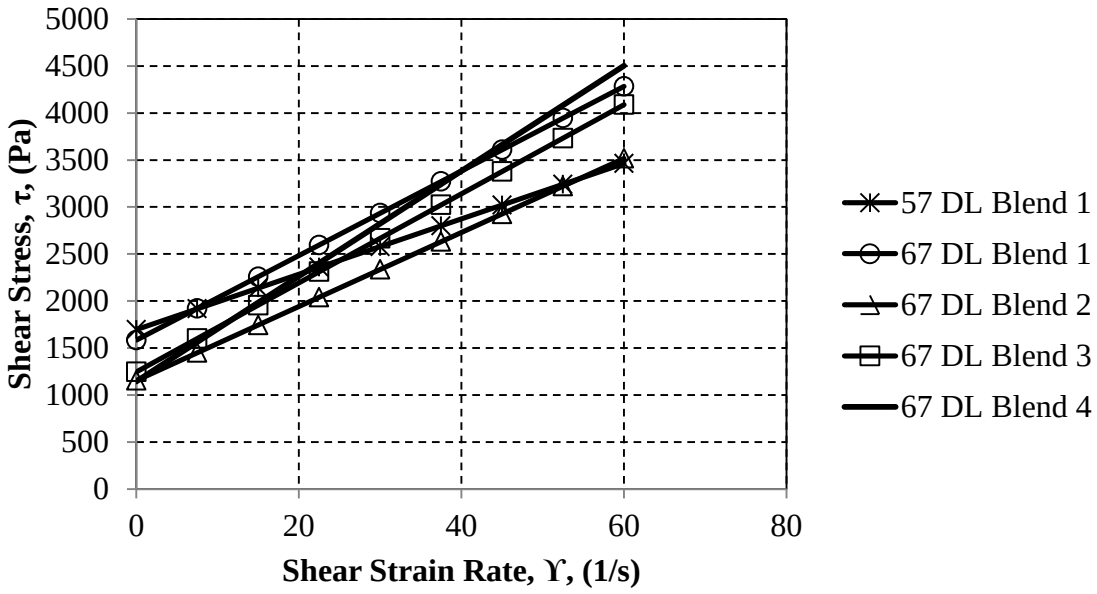

Figure 4-13: Flow curve for dolomitic limestone mixtures

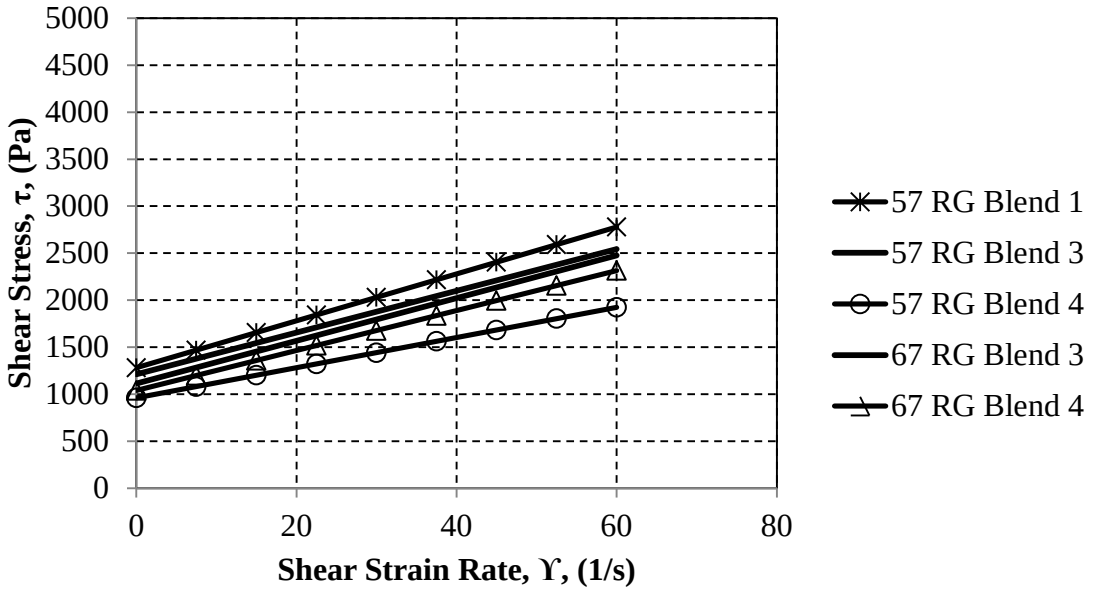

Figure 4-14: Flow curves for river gravel mixtures

4.4.2 EFFECT ON HARDENED CONCRETE PROPERTIES

The hardened properties were split into two categories while analyzing the data. The categories included mechanical properties (compression strength, splitting tensile strength, and modulus of elasticity) and durability properties (drying shrinkage and RCPT). The effects from the proportioning methods on each mixture will be discussed in the following sections.

4.4.2.1 Mechanical Properties

A statistical analysis was performed to identify which variables had a significant impact on the measured results. When analyzing the mechanical properties, a two-factor analysis of variance (ANOVA) statistical test was used for comparing variables. This is a statistical tool used to analyze data from experiments and make decisions about whether given factors have a statistically significant impact on a response variable (Devore and Farnum 2005). This test was used instead of the t-test because each mechanical property had results that needed to be compared at three different ages (7, 28, and 91-day values). The t-test is only capable of comparing variables at a single level. The ANOVA test was used at a confidence interval of 95 percent. Therefore, when evaluating the p-value, a value below 0.05 indicates that there is a significant difference between values. The p-values for the mechanical properties are shown in Table 4-4.

Table 4-4: Summary of Phase I Mechanical Property P-values

Property	Variables Compared	P-value
Compressive Strength	DL vs. RG	0.000753
	No. 57 vs. No. 67 (DL)	0.941
	No. 57 vs. No. 67 (RG)	0.210
	Optimized Gradations vs. Non-Optimized (DL)	0.259
	Optimized Gradations vs. Non-Optimized (RG)	0.533
Splitting Tensile Strength	DL vs. RG	1.40E-07
	No. 57 vs. No. 67 (DL)	0.123
	No. 57 vs. No. 67 (RG)	0.0423
	Optimized Gradations vs. Non-Optimized (DL)	0.000361
	Optimized Gradations vs. Non-Optimized (RG No. 57)	0.0900
	Optimized Gradations vs. Non-Optimized (RG No. 67)	0.948
Modulus of Elasticity	DL vs. RG	2.00E-16
	No. 57 vs. No. 67 (DL)	0.273
	No. 57 vs. No. 67 (RG)	6.94E-09
	Optimized Gradations vs. Non-Optimized (DL)	0.160
	Optimized Gradations vs. Non-Optimized (RG No. 57)	0.332
	Optimized Gradations vs. Non-Optimized (RG No. 67)	0.533

In order to analyze the effect the proportioning methods had on the concrete strength and modulus of elasticity, the data were first analyzed to determine whether or not there was a difference in behavior for mixtures with different coarse aggregate types and different NMAS. For all properties, a difference existed between the different coarse aggregates. No difference existed between the NMAS for dolomitic limestone mixtures. However, a difference did exist between NMAS for river gravel mixtures, except for compression strengths. The data were analyzed to determine if a difference existed between mixtures that had optimized aggregate gradations and mixtures that did not. Optimized aggregate gradations fell within the limits of the Shilstone Method and met the 8-22 limits on the percent retained chart, as described in Section 4.4. It was found at a 95 percent confidence level that no difference existed between the data obtained for the optimized and non-optimized concrete mixtures.

The growth in compressive strength for the dolomitic limestone and river gravel mixtures can be seen in Figure 4-15 through Figure 4-18. The data for the compressive strengths can be found in Table B-1, Table B-2, Table B-4 and Table B-5. No mixtures performed exceedingly good or bad, as can be seen from the statistics. The dolomitic limestone mixtures generally produce greater compressive strengths than the river gravel mixtures, as expected. The dolomitic limestone No. 57 mixtures were within the test's 7.8 percent range of the control. The dolomitic limestone No. 67 blend 1 mixture achieved greater compressive strengths than the other dolomitic limestone mixtures. Based on the statistics in Table 4-4, the differences in strength are not significant, but the 91-day compressive strength for blend 2 is more than 900 psi less than the control, which is outside the range for the test. Blend 2 is a non-optimized gradation. Blend 1 was the

control and was located on the border of zone I of and II of the CFC. The river gravel No. 57 blend 2 achieved greater compressive strengths than the other river gravel mixtures. Based on the statistics in Table 4-4, the differences in compressive strength are not significant, but the 91-day compressive strength for blend 2 is more than 700 psi greater than the control, which is outside the range for the test. This mixture was located in zone IV of the CFC. The river gravel No. 67 mixtures were within the test's 7.8 percent range of the control.

After comparing the data, changing the optimized aggregate gradations did not have a significant impact on the compressive strengths of the concrete mixtures. This is in agreement with the results of Obla et al. (2007). In the study, 6 out of 9 mixtures produced using the Shilstone Mixture and percent retained chart, had a strength that was within 300 psi of the control. One mixture had a strength that was more than 300 psi greater and 2 mixtures had a strength that was more than 300 psi less than the control (Oblat et al. 2007). Therefore the differences in compressive strength with optimized aggregate gradations are not significant.

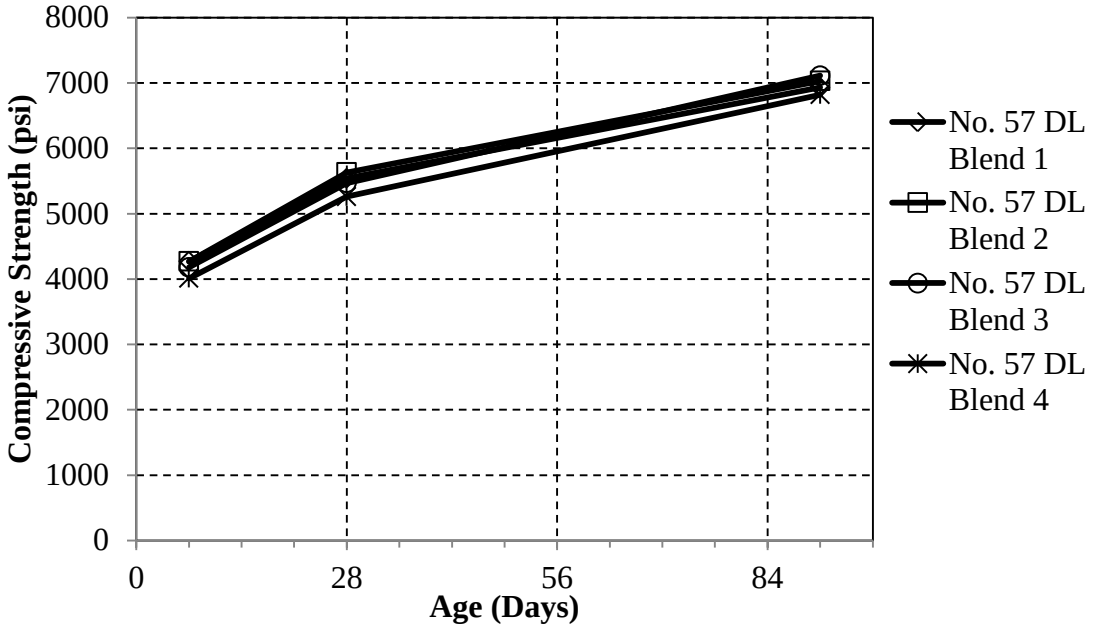

Figure 4-15: Dolomitic limestone No. 57 compressive strengths

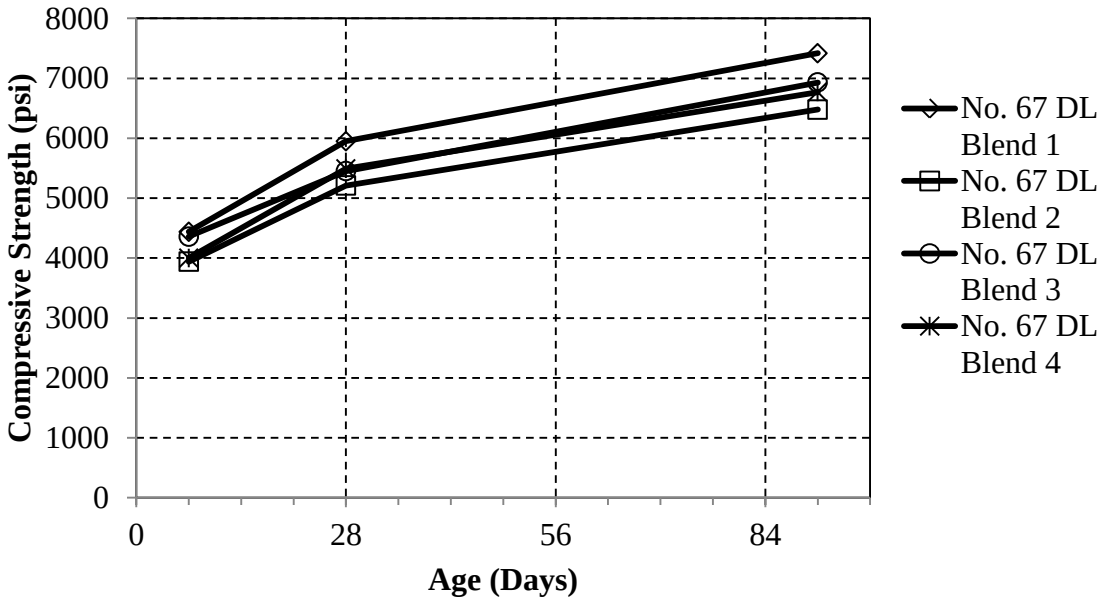

Figure 4-16: Dolomitic limestone No. 67 compressive strengths

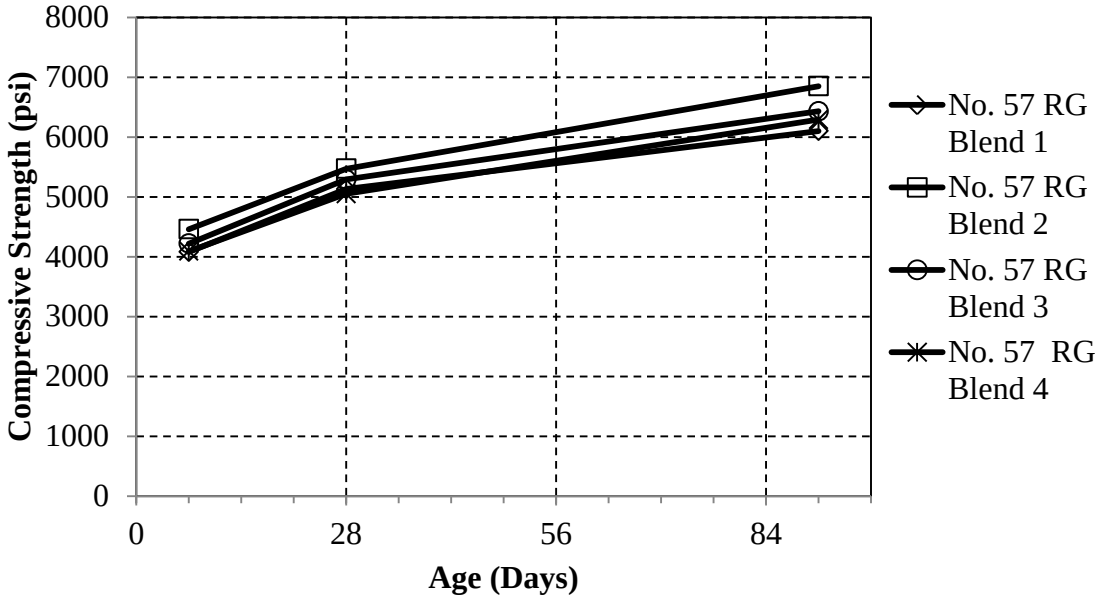

Figure 4-17: River gravel No. 57 compressive strengths

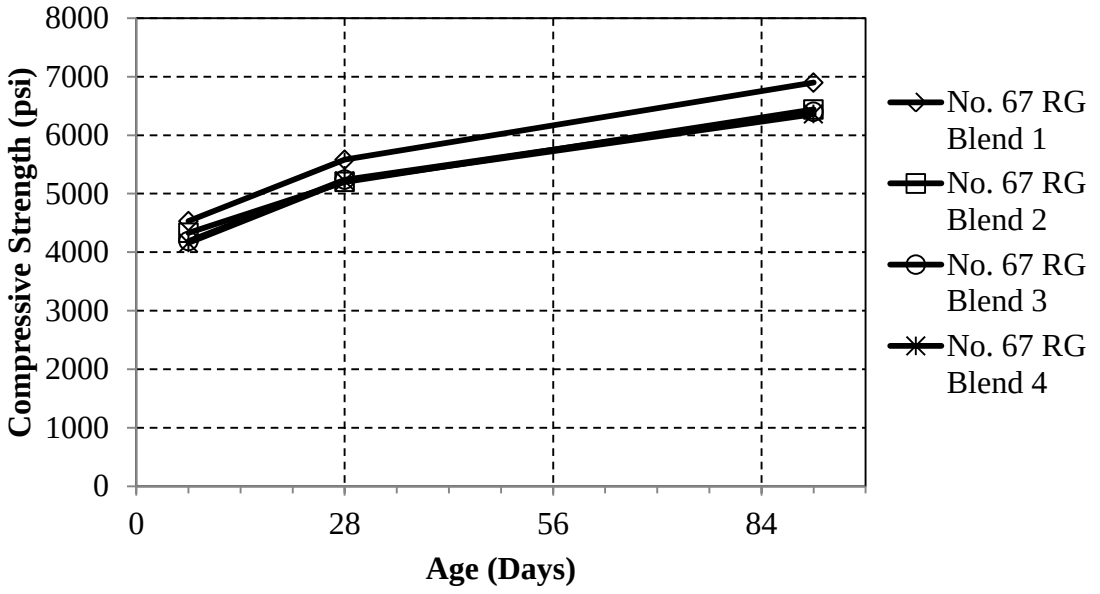

Figure 4-18: River gravel No. 67 compressive strengths

The growth in splitting tensile strength for both dolomitic limestone and river gravel mixtures can be seen in Figure 4-19 through Figure 4-22. The data for the splitting tensile strengths can be found can be found in Table B-1, Table B-2, Table B-4 and Table B-5. The dolomitic limestone No. 57 mixtures were within the test's 16.5 percent range of the control. The 91-day splitting tensile strengths for the dolomitic limestone No. 67 blends 2 and 4 are more than 100 psi less than the control, which is outside the range for the test. This difference is also shown in Table 4-3. Blend 2 is a non-optimized gradation and blend 4 is an optimized gradation. The 91-day splitting tensile strength for the river gravel No. 57 blend 2 is slightly greater than the test's 16.5 percent range compared to the control. This is a non-optimized gradation, located in zone IV of the CFC. The river gravel No. 67 mixtures are within the test's 16.5 percent range of the control. Therefore, the optimized aggregate gradations did not have a significant impact on the splitting tensile strength. In the literature review the studies changed the water-cementitious materials ratio. In this study the water-cementitious materials ratio was kept constant; therefore the research conclusions cannot be compared.

The predictability of the splitting tensile strength measured for all concrete can be seen in Figure 4-23 and Figure 4-24. In order to quantify the percentage of error between the measured data and the predicted data, the unbiased estimate of the standard deviation, Sj, for the error was calculated. Equation 4-1, taken from McCuen (1985), was used for this calculation. The values for the unbiased estimate of standard deviation for all concrete mixtures are shown in Table 4-5. There is not a significant difference in the prediction accuracy between the optimized gradations and the gradations that meet ASTM C33, as shown in Table 4-2. This proves that the proportioning methods stated in

this research can be used in conjunction with the equation recommended by Raphael (1984) for determining the splitting tensile strength.

$$S_j = \sqrt{\frac{1}{n-1}\sum_i^n \Delta_i^{\,2}} \qquad \textbf{Equation 4-1}$$

Where,

S_j = unbiased estimate of the standard deviation (percent),

n = number of data points (unitless), and

Δ_i = absolute error (percent)

The absolute error was calculated using the following equation:

$$\Delta_i = \frac{\left|(S_i)est - (S_i)m\right|}{(S_i)m} \times 100 \qquad \textbf{Equation 4-2}$$

Where,

Δ_i = absolute error (percent),

$(S_i)est$ = value of the predicted data point, and

$(S_i)m$ = value of measured data point

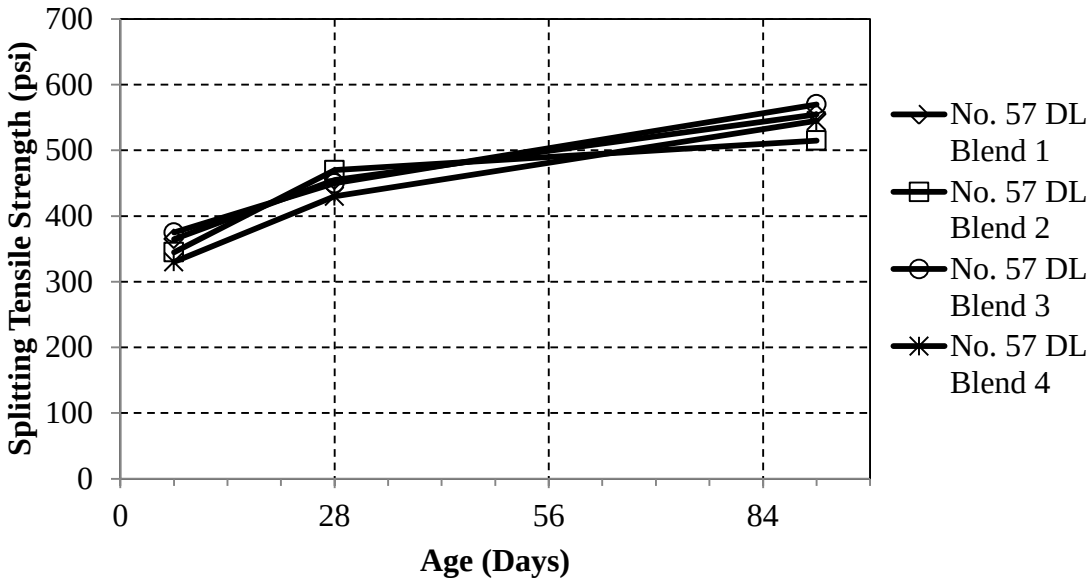

Figure 4-19: Dolomitic limestone No. 57 splitting tensile strength

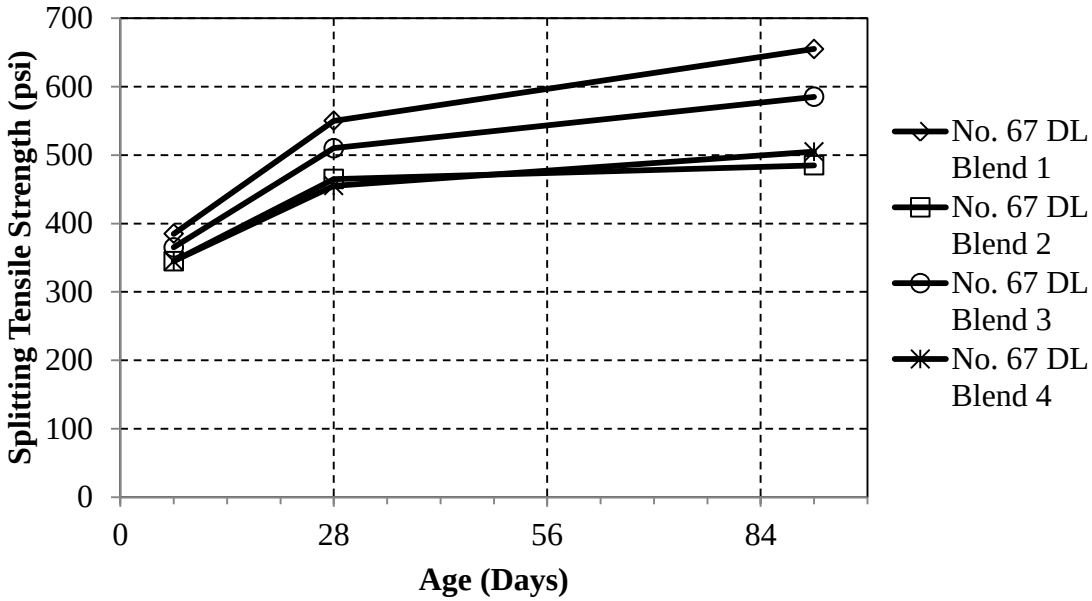

Figure 4-20: Dolomitic limestone No. 67 splitting tensile strength

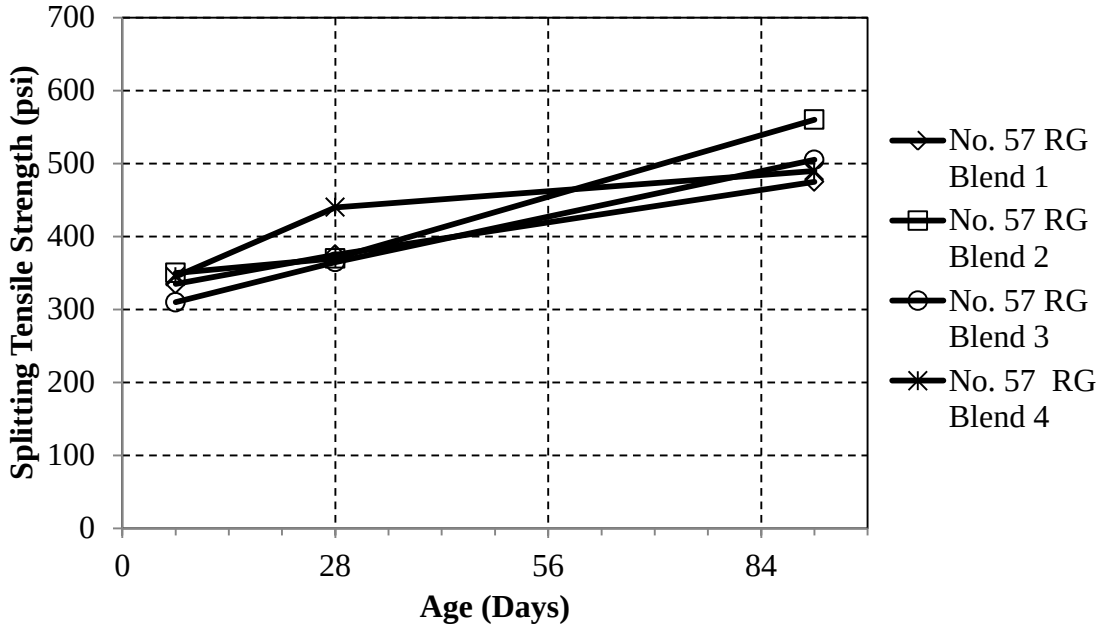

Figure 4-21: River gravel No. 57 splitting tensile strength

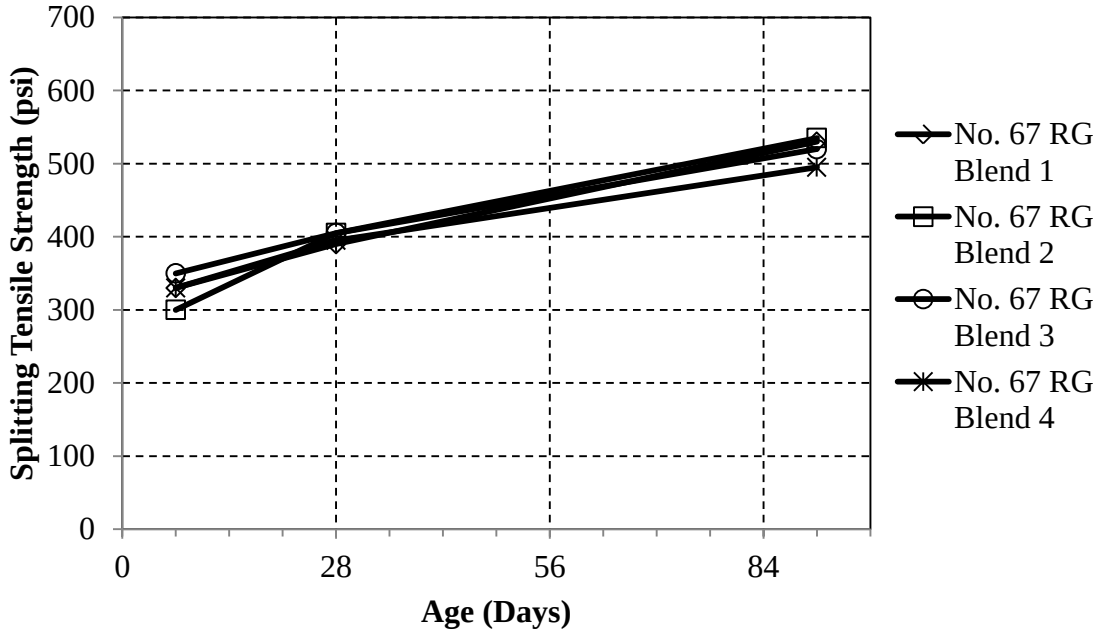

Figure 4-22: River gravel No. 67 splitting tensile strength

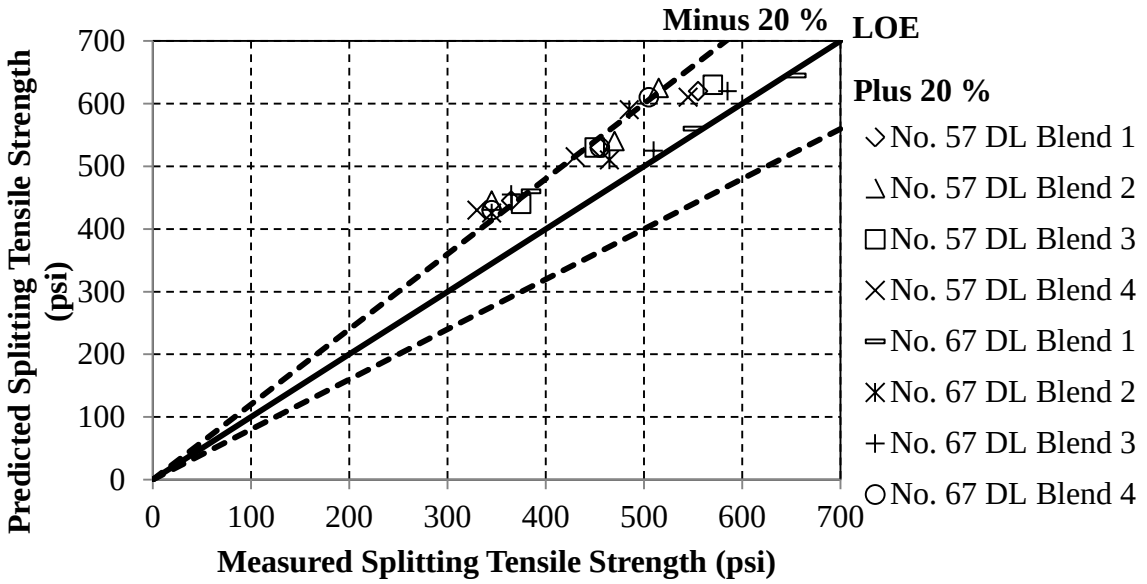

Figure 4-23: Dolomitic limestone predicted versus measured splitting tensile strength

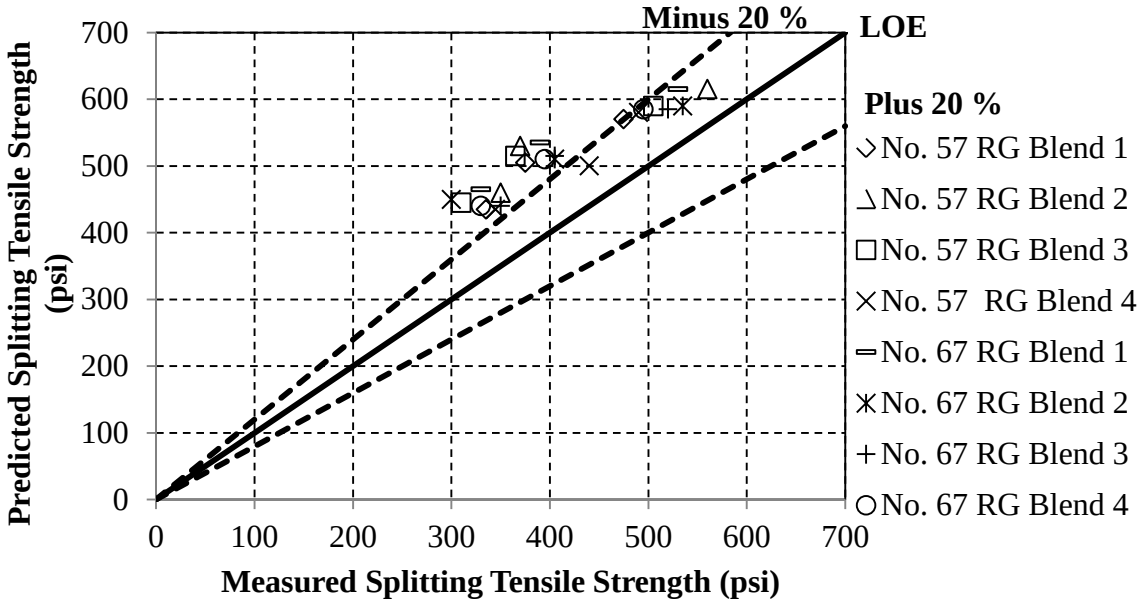

Figure 4-24: River gravel predicted versus measured splitting tensile strength

Table 4-5: Phase I Unbiased Estimate of the Standard Deviation of Splitting Tensile Strengths

Blends	Sj (%)			
	DL No. 57	DL No. 67	RG No. 57	RG No. 67
1	21.1	13.9	35.3	40.7
2	27.6	23.5	38.4	40.5
3	19.1	18.1	44	27.9
4	26.9	25.6	24.5	33.9

The modulus of elasticity (MOE) plots for the dolomitic limestone and river gravel mixtures can be seen in Figure 4-25 through Figure 4-28. The data for the MOE of all mixtures can be found in Table B-3 and Table B-6. The dolomitic limestone mixtures have greater MOE's than the river gravel mixtures. This is expected based on the measured compressive strengths, which are used in ACI Building Code 318 (2011) equation for determining the modulus of elasticity. The dolomitic limestone No. 57 blend 4 was slightly less than the test's 11.9 percent range when compared to the control mixture. This blend was an optimized gradation mixture. All other mixtures for dolomitic limestone and river gravel were within the test's 11.9 percent range when compared to the control mixtures. Therefore, the optimized aggregate gradations did not have a significant impact on the modulus of elasticity for the concrete mixtures.

The predictability of the mixtures' MOE with ACI Building Code 318 (2011) equation can be seen in Figure 4-29 and Figure 4-30. In order to quantify the percentage of error between the measured data and the predicted data, the unbiased estimate of the

standard deviation, Sj, for the error was calculated. Equation 4-1, taken from McCuen (1985), was used for this calculation. The values for the unbiased estimate of standard deviation for all concrete mixtures are shown in Table 4-6. There is not a significant difference in the prediction accuracy between the optimized gradations and the gradations that meet ASTM C33 (2013), as shown in Table 4-2. This proves that the ACI Building Code 318 (2011) equation for determining the MOE can be used for optimized aggregate gradations with the same accuracy as mixtures currently meeting the limits specified in ASTM C33 (2013).

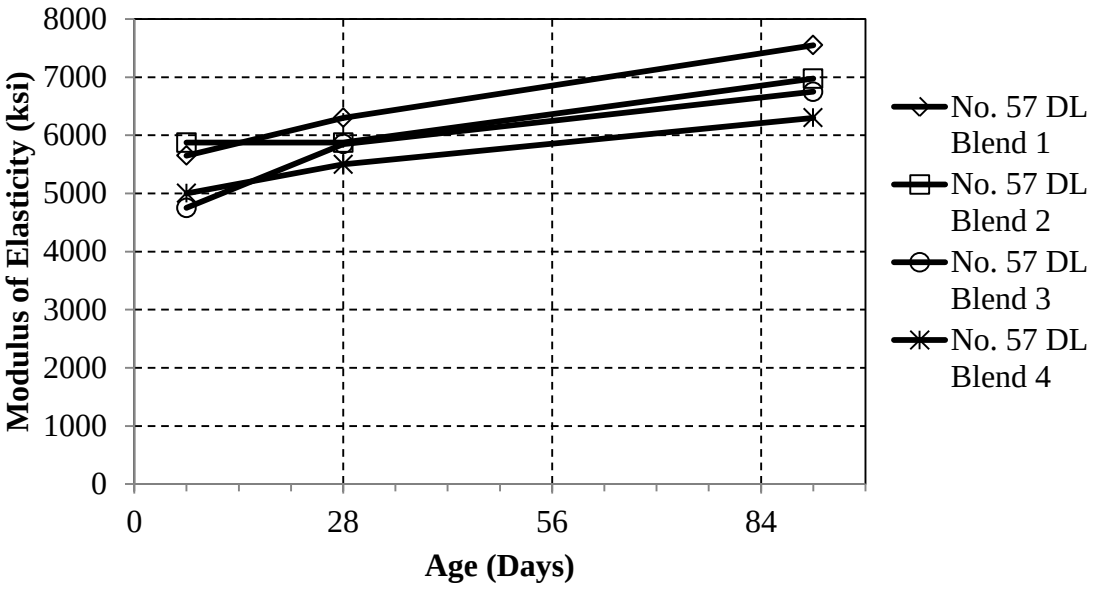

Figure 4-25: Dolomitic limestone No. 57 modulus of elasticity

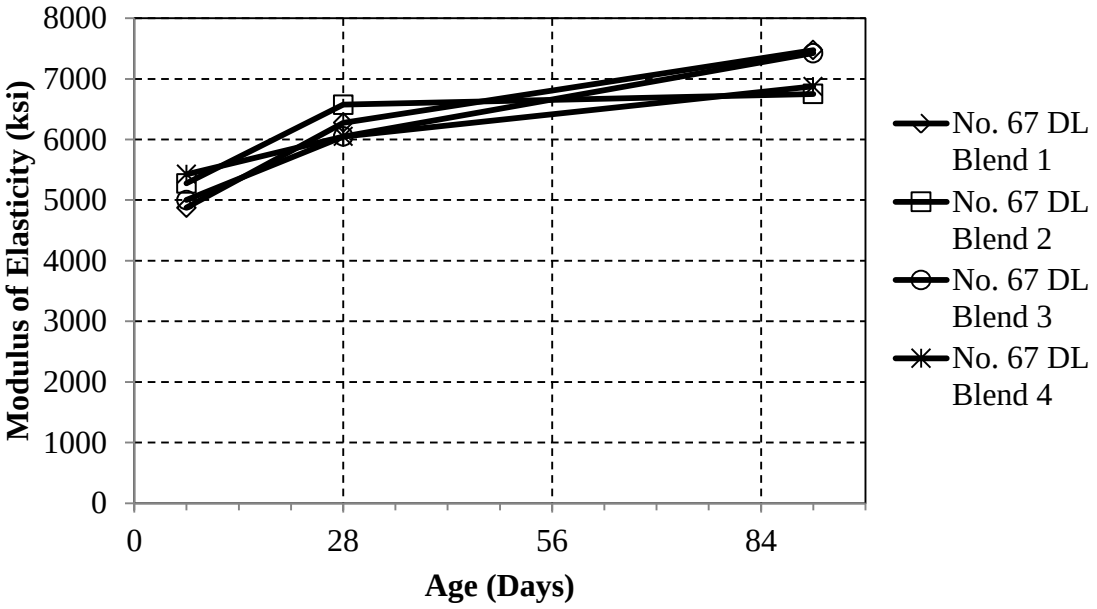

Figure 4-26: Dolomitic limestone No. 67 modulus of elasticity

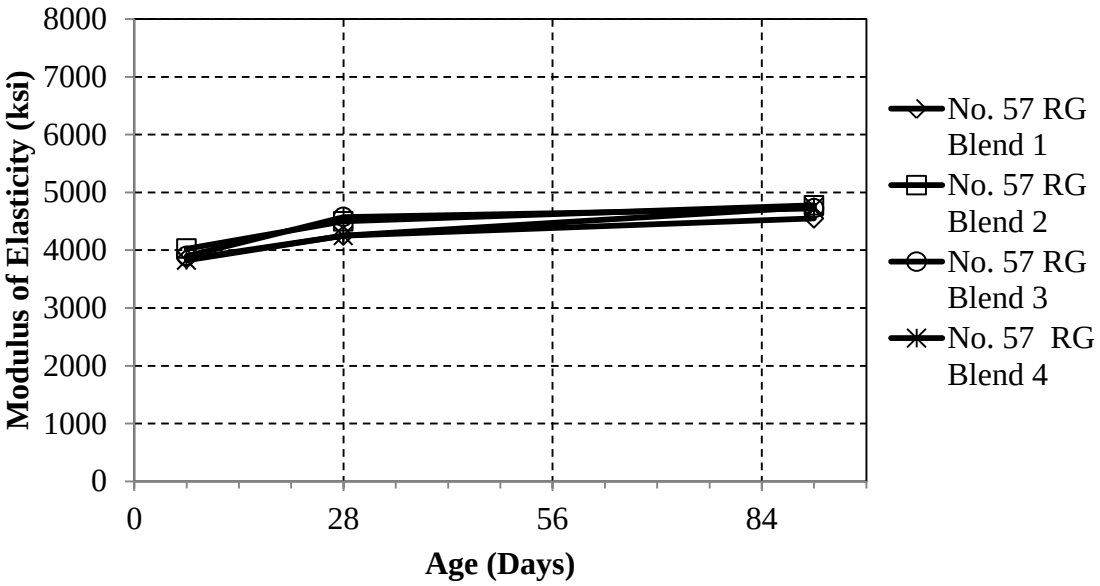

Figure 4-27: River gravel No. 57 modulus of elasticity

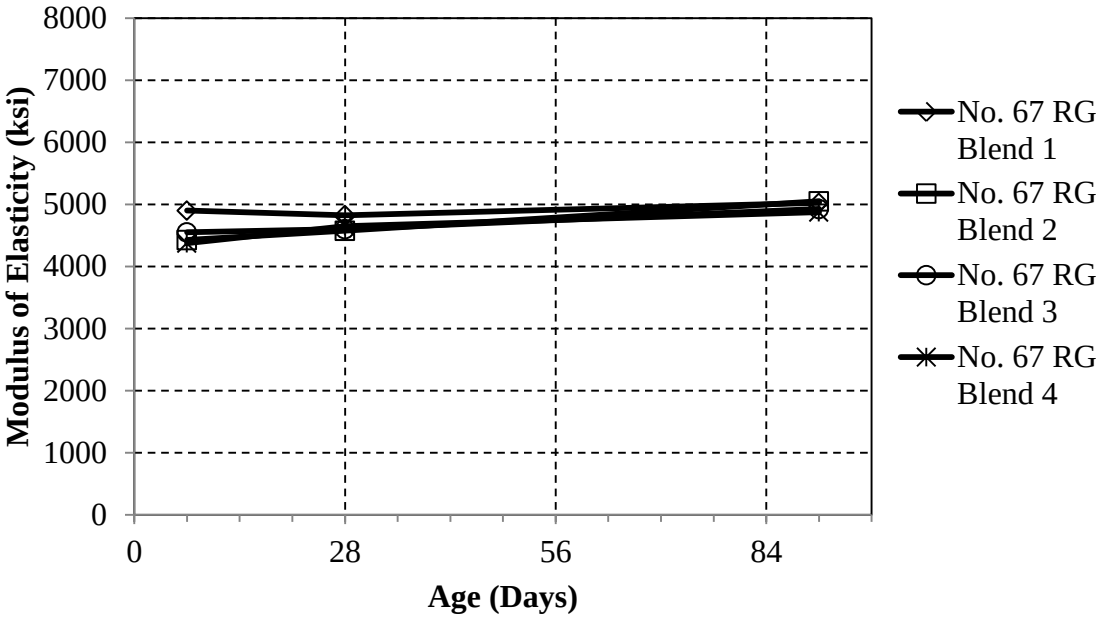

Figure 4-28: River gravel No. 67 modulus of elasticity

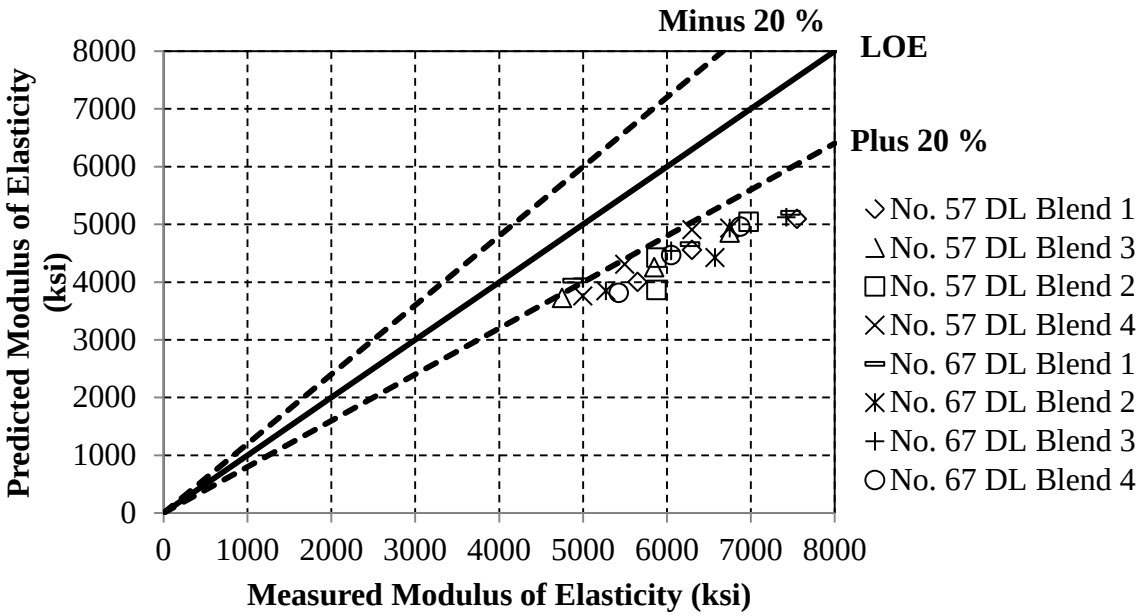

Figure 4-29: Dolomitic limestone predicted versus measured modulus of elasticity

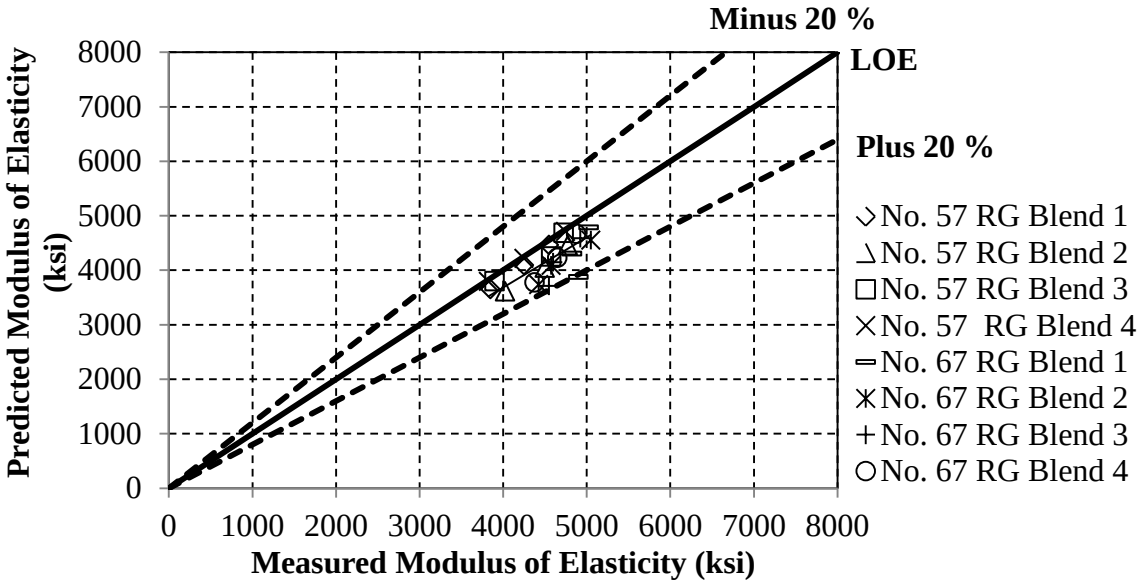

Figure 4-30: River gravel predicted versus measured modulus of elasticity

Table 4-6: Phase I Unbiased Estimate of the Standard Deviation of Modulus of Elasticity

Blends	Sj (%)			
	DL No. 57	DL No. 67	RG No. 57	RG No. 67
1	36.6	30.8	4.6	17.0
2	35.7	35.6	11.2	15.1
3	31.6	31.1	5.3	15.6
4	28.1	34.2	1.0	12.0

4.4.2.2 Durability Properties

In order to validate any conclusions between the durability property data, the values were statistically analyzed. When analyzing the shrinkage data, a two-factor ANOVA statistical test was used for comparing variables. This test was used instead of the t-test because the shrinkage data were composed of strain measurements at 7 different ages (4, 7, 14, 28, 56, 112, and 168-day strains). The ANOVA test used a confidence interval of 95 percent. An independent two sample t-distribution was used for the analysis of the RCPT data. The values for the RCPT test were only measured at an age of 91 days. The test used a confidence interval of 95 percent. The p-values for the durability properties are shown in Table 4-7.

Table 4-7: Phase I Durability Property P-values

Property	Variables Compared	P-value
Shrinkage	No. 57 vs. No. 67 (DL)	0.0103
	Optimized Gradations vs. Non-Optimized (DL No. 57)	0.34
	Optimized Gradations vs. Non-Optimized (DL No. 67)	0.948
	Optimized Gradations vs. Non-Optimized (RG No. 57)	0.646
RCPT	DL vs. RG	2.64E-10
	No. 57 vs. No. 67 (DL)	0.00835
	No. 57 vs. No. 67 (RG)	0.06
	Optimized Gradations vs. Non-Optimized (DL No. 57)	0.3313
	Optimized Gradations vs. Non-Optimized (DL No. 67)	0.3397
	Optimized Gradations vs. Non-Optimized (RG No. 57)	0.02261
	Optimized Gradations vs. Non-Optimized (RG No. 67)	0.7745

In order to analyze the effect the proportioning methods had on the mixtures, it was first determined whether there was a difference in RCPT values between coarse aggregate types and the NMAS. It was determined that a difference in results existed between the coarse aggregates and NMAS at a 95 percent confidence level. The drying shrinkage data was only analyzed whether there was a difference between the NMAS for the dolomitic limestone mixtures, due to a malfunction in the gauge that caused errors in the river gravel data. Next, the data were analyzed to determine whether the optimized

aggregate gradations versus the non-optimized aggregate gradations performed differently. Optimized aggregate gradations fell within the limits of the Shilstone Method and met the 8-22 limits on the percent retained chart, as described in Section 4.4. The differences found between the data will now be discussed.

The amount of shrinkage during a 168 day interval was measured, as described in Section 3.7.4. Due to a malfunction with the shrinkage gauge, readings between April 2015 and May 2015 were measured inaccurately. These data were removed, causing some of the mixtures to not obtain the full 168-day drying shrinkage development. The drying shrinkage data that were affected included the No. 57 river gravel (112-168 day) and No. 67 river gravel (56-168 day). Due to the lack of accurate data for the No. 67 river gravel, these mixtures were not analyzed for drying shrinkage.

Plots of the unaffected shrinkage strains can be seen in Figure 4-31 through Figure 4-33. The shrinkage data for these mixtures can be found in Table C-2 through Table C-4. Based on the statistics in Table 4-7, the differences in shrinkage are not significant, but the 168-day shrinkage strain for No. 57 blend 3 is more than 30 microstrains greater than the control, which is outside the range for the test. This mixture was a non-optimized gradation and located in zone IV of the CFC, meaning it was a sandy mixture. The dolomitic limestone No. 67 blend 2 168-day shrinkage strain is more than 30 microstrains less than the control, which is outside the range for the test. This mixture was a non-optimized gradation and located in zone I of the CFC, meaning it was a rocky mixture. The 56-day shrinkage strain for the river gravel No. 57 blend 4 is more than 30 microstrains less than the control, which is outside the range for the test. This

mixture was a non-optimized gradation and located in the extreme area of zone IV in the CFC. Due to the gauge malfunction, more data is needed to verify these differences.

After comparing the data, changing the optimized aggregate gradations did not have a significant impact on the shrinkage strains of the concrete mixtures. This is in agreement with the results of Obla et al. (2007). The study found that out of 13 optimized gradations, 12 had an average length change that was within 0.005 percent of the control. Out of 11 non-optimized gradations, 7 had an average length change that was within 0.005 percent of the control mixture (Obla et al. 2007). Therefore the differences in drying shrinkage with optimized aggregate gradations are not significant.

In addition to the shrinkage plots, the predictability of the shrinkage with the equations from ACI Committee 209 (1997) for each mixture was measured. The results can be seen in Figure 4-35 through Figure 4-37. In order to quantify the percentage of error between the measured data and the predicted data, the unbiased estimate of the standard deviation, Sj, for the error was calculated. Equation 4-1, taken from McCuen (1985), was used for this calculation. The drying shrinkage values for the unbiased estimate of standard deviation are shown in Table 4-8. There is not a significant difference in the prediction accuracy between the optimized gradations and the gradations that meet ASTM C33 (2013), as shown in Table 4-2. This proves that the predictability of the shrinkage with the equations from ACI Committee 209 (1997) can be used for optimized aggregate gradations with the same accuracy as mixtures currently meeting the limits specified in ASTM C33 (2013).

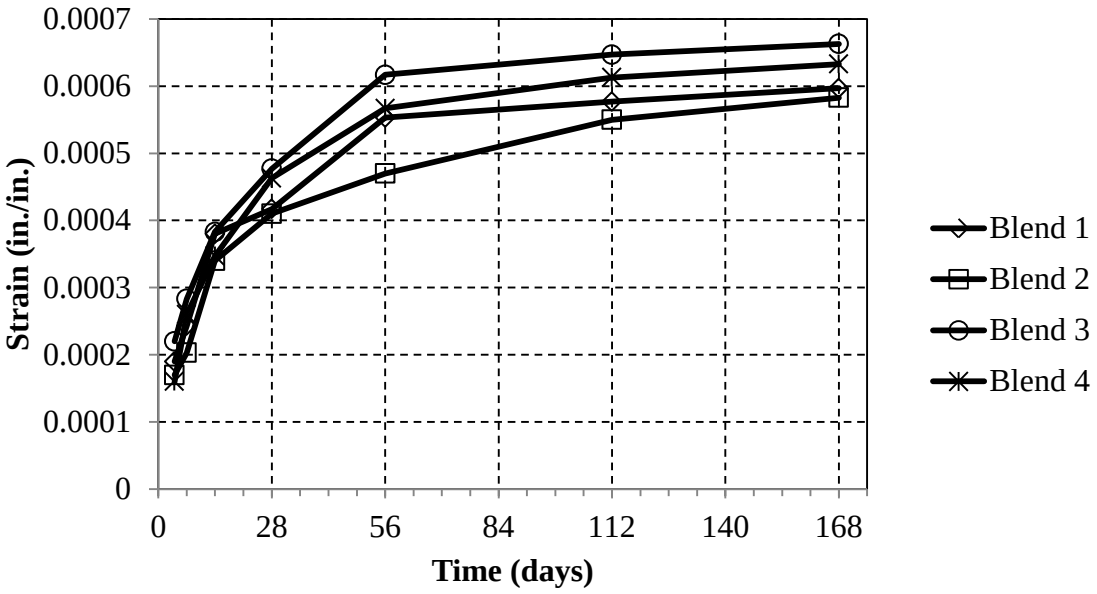

Figure 4-31: Dolomitic limestone No. 57 shrinkage strains

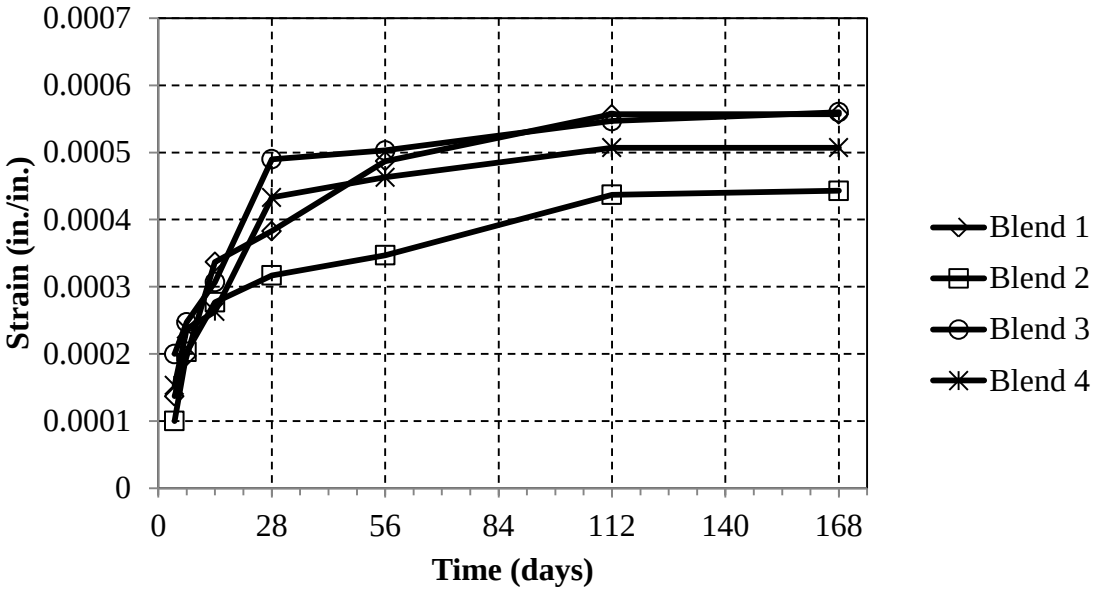

Figure 4-32: Dolomitic limestone No. 67 shrinkage strains

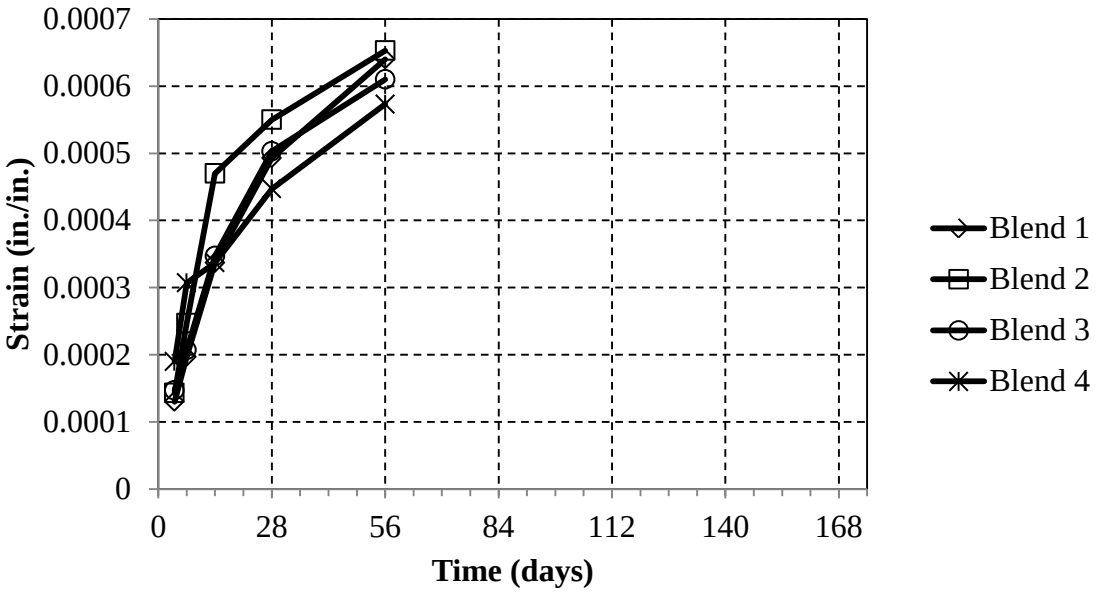

Figure 4-33: River gravel No. 57 shrinkage strains

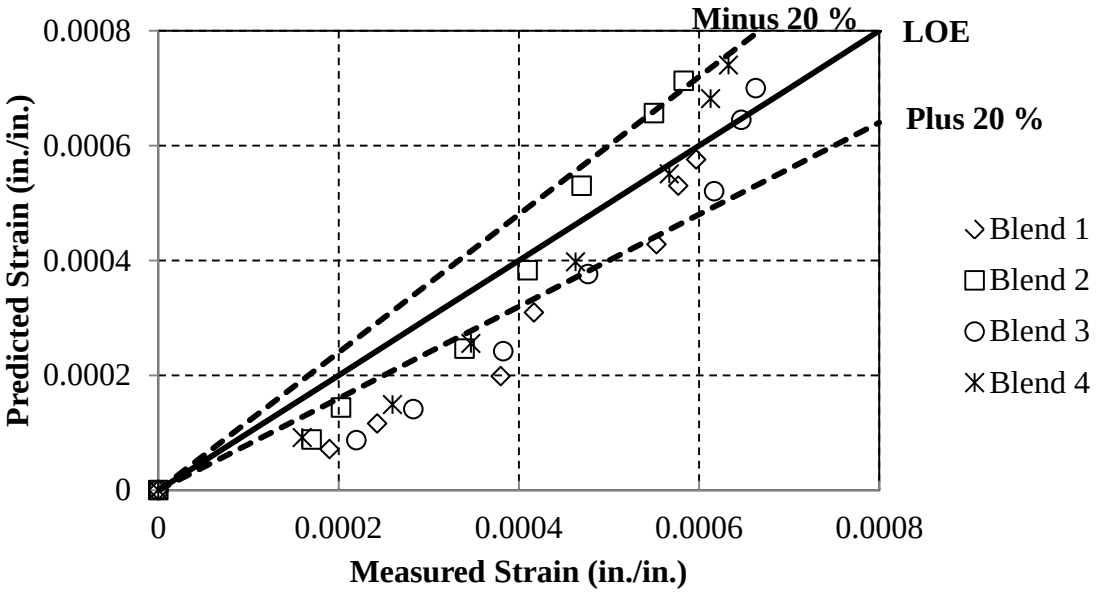

Figure 4-34: Dolomitic No. 57 predicted versus measured shrinkage strains

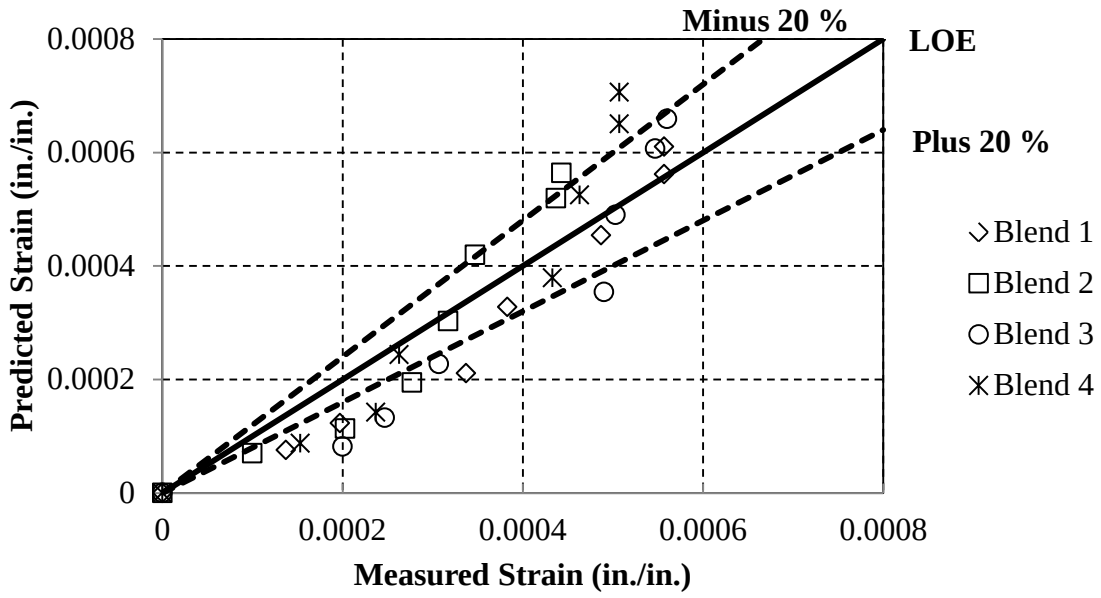

Figure 4-35: Dolomitic limestone No. 67 predicted versus measured shrinkage strains

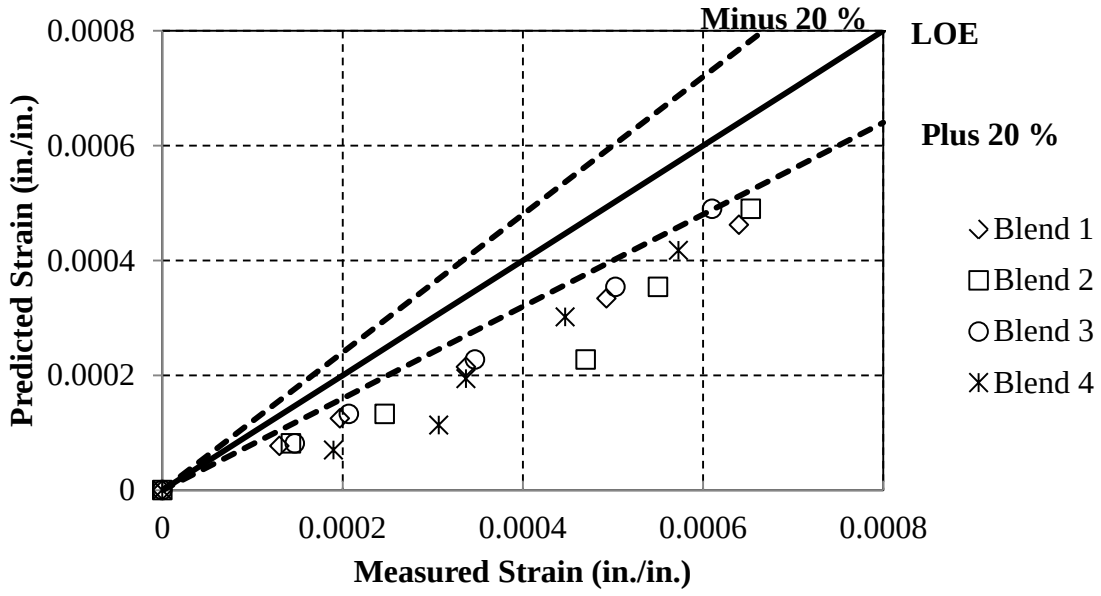

Figure 4-36: River gravel No. 57 predicted versus measured shrinkage strains

Table 4-8: Phase I Unbiased Estimate of the Standard Deviation of Drying Shrinkage

Blends	Sj (%)		
	DL No. 57	DL No. 67	RG No. 57
1	41.2	29.4	39.1
2	28.9	29.7	46.2
3	31.1	35.4	37.8
4	28.7	32	53.8

The next durability property that was analyzed was the RCPT test, as described in Section 3.7.5. The values of charges passed through the concrete (in coulombs) were graphed for each mixture, as seen in Figure 4-39 through Figure 4-42. The data for the RCPT values of all mixtures are shown in Table C-1. The optimized aggregate gradations are labeled with diagonal stripes. All dolomitic limestone mixtures were within the test's 41 percent range when compared to the control mixtures. The river gravel No. 57 blend 4 was slightly less than the test's 41 percent range when compared to the control mixture, which can also be seen from the statistics in Table 4-7. This blend was a non-optimized gradation mixture. All other mixtures for river gravel were within the test's 41 percent range when compared to the control mixtures. Therefore, the optimized aggregate gradations did not have a significant impact on the RCPT values for the concrete mixtures.

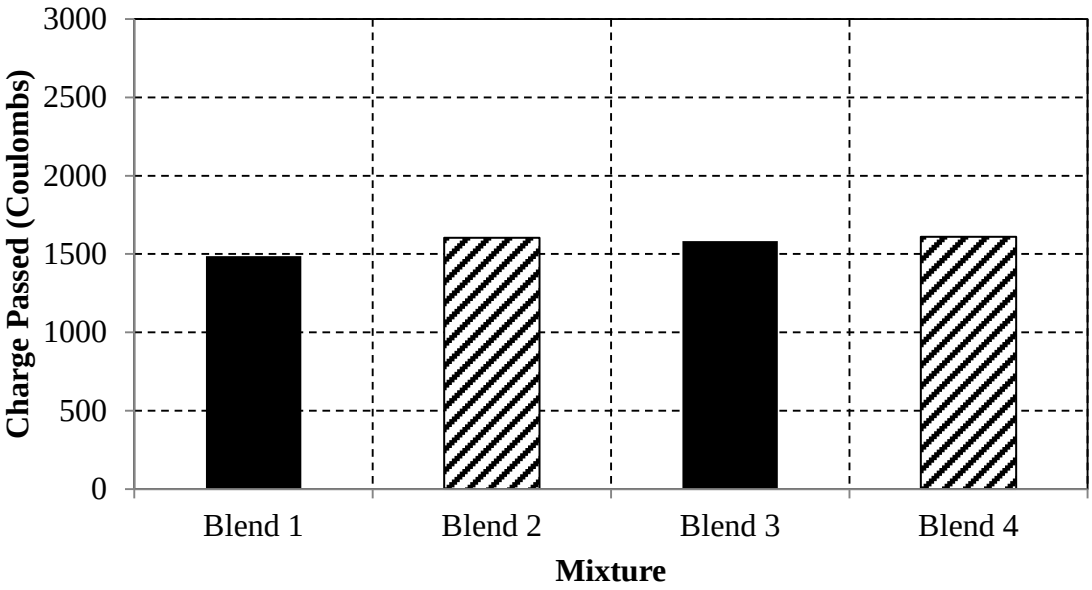

Figure 4-37: Dolomitic limestone No. 57 RCPT values

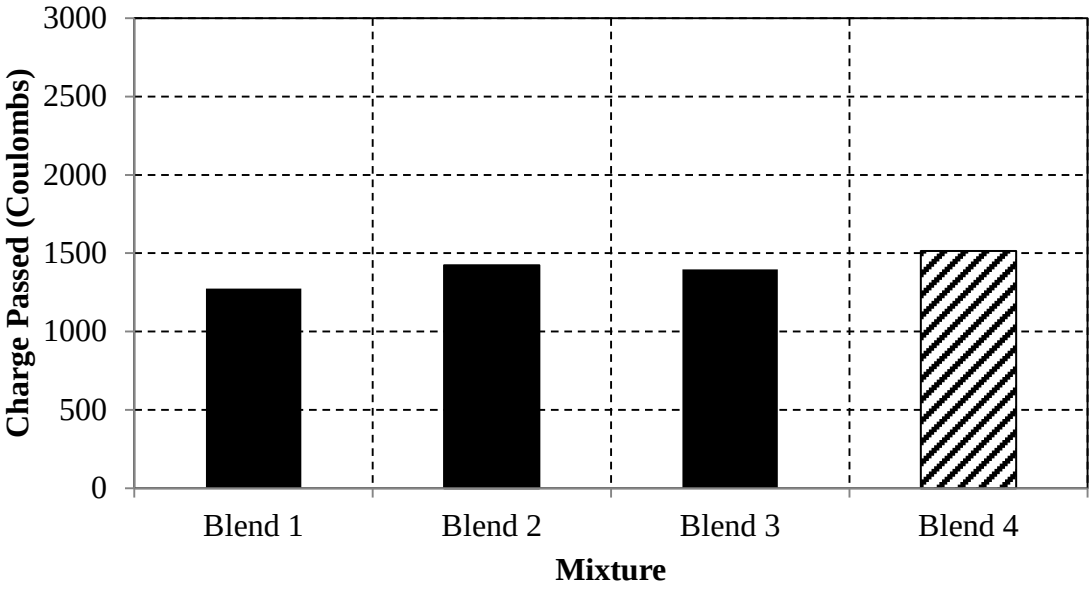

Figure 4-38: Dolomitic limestone No. 67 RCPT values

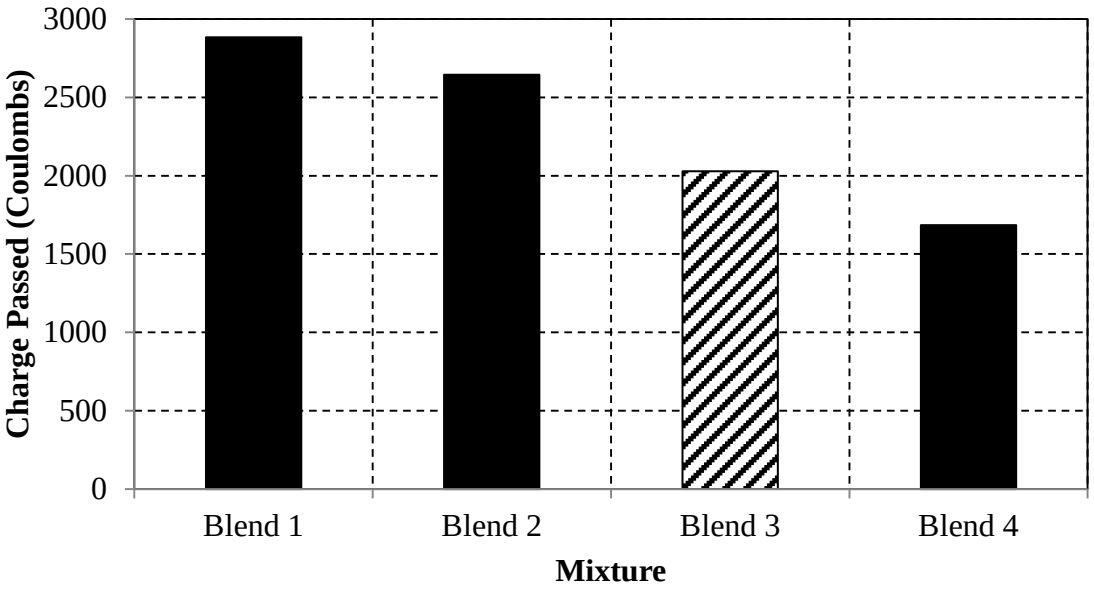

Figure 4-39: River gravel No. 57 RCPT values

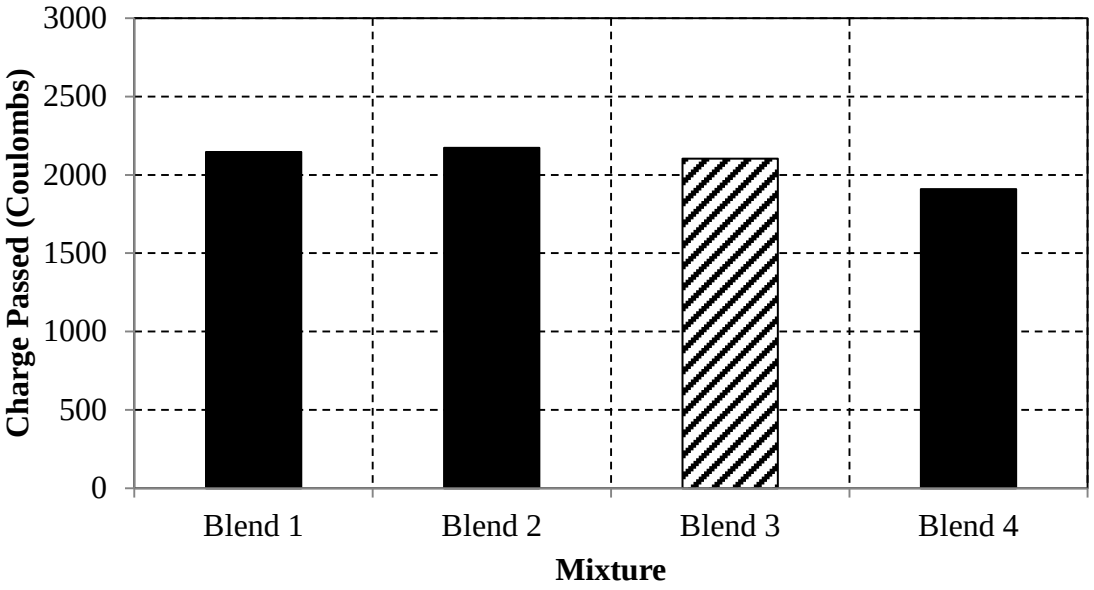

Figure 4-40: River gravel No. 67 RCPT values

4.5 PHASE II DATA AND DISCUSSION OF RESULTS

The effect of varying percentages of dust-of-fracture mineral filler in concrete was completed during the phase II analysis. In order to evaluate the effects in concrete, fresh and hardened properties were tested. In addition, tests were run on the dust-of-fracture mineral filler and compared to the mineral filler within the natural fine aggregate, as shown in Section 3.9. This was done in order to characterize the aggregates and to screen for harmful substances. This section presents the data and corresponding analysis.

4.5.1 EFFECT ON FRESH PROPERTIES

Concrete mixtures were made with increasing percentages of dust-of-fracture mineral filler, and the effect on workability was evaluated through three tests. The tests used during this phase were identical to the tests used in phase I, as stated in Section 4.4.1. Currently, for concrete with MFA, ASTM and ALDOT allow dust-of-fracture mineral filler up to five percent if subjected to abrasion. AASHTO does not mention a specific limit for dust-of-fracture mineral filler, but does have a limit for deleterious material. It also states any fine aggregate which fails the grading limits may be used, provided that the strength is not less than 95 percent at seven days in accordance with T71 (AASHTO M6 2013). Therefore, this study used the zero percent dust-of-fracture mineral filler mixture and the five percent dust-of-fracture mineral filler as the control mixtures. These mixtures are within the limits of ASTM and ALDOT, as shown in Table 4-9. These two mixtures were used to compare the effects of increasing dust-of-fracture mineral filler.

Table 4-9: Acceptable MFA Gradations in Accordance to ASTM C33 (2013) and ALDOT (2012) Standards

Mixture	Within Dust-of-Fracture Mineral Filler Limits
DL No. 67 0 %	✓
DL No. 67 5 %	✓
DL No. 67 10 %	
DL No. 67 15%	
DL No. 67 20 %	
RG No. 67 0 %	✓
RG No. 67 5 %	✓
RG No. 67 10 %	
RG No. 67 15%	
RG No. 67 20 %	

To validate conclusions, statistical conclusions were first made. An independent two sample t-distribution was used for the analysis of the fresh properties. The test used a confidence interval of 95 percent, as done in the phase I fresh properties analysis. The p-values for the fresh properties are shown in Table 4-9.

Table 4-10: Summary of Phase II Fresh Property P-values

Variables Compared	P-value
Vebe Time (DL vs. RG)	0.266
Vebe Time (0-5 % vs. 10-20 %)	0.1678
Vebe Time (0-5 % vs. 10-15 %)	0.2578
Vebe Time (0-5 % vs. 10 %)	0.7154
Workability Rating (DL vs. RG)	0.1172
Workability Rating (0-5 % vs. 10-20 %)	0.3191
Workability Rating (0-5 % vs. 10-15 %)	0.3185
Workability Rating (0-5 % vs. 10 %)	0.5619

In order to analyze the effect of increasing the percentage of dust-of-fracture mineral filler, it was first determine whether a difference existed between the coarse aggregate types. No difference was present between the dolomitic limestone and river gravel mixtures. Next, it was determined whether a difference existed between mixtures that incorporated the allowable percentage of dust-of-fracture mineral filler (zero and five percent) and the mixtures that had increased percentages of dust-of-fracture mineral filler. In order to determine whether a threshold existed, mixtures containing the highest percentages of dust-of-fracture mineral filler were removed from the analysis at five percent increments of the fine aggregate volume. Therefore, if a lower percentage

mixture performed well, but at increased percentages of dust-of-fracture mineral filler the properties began to decrease, this trend could be detected.

The first test presented for the phase II fresh properties is the vebe test. The data for the vebe times are shown in Table A-2. After determining there was not a significant difference between the control mixtures and the mixtures incorporating increased percentages of dust-of-fracture mineral filler at any level, Figure 4-43 was made to graphically present the data. The control mixtures, which had zero and five percent dust-of-fracture mineral filler within the fine aggregate, are shown with diagonal lines. The mixtures that had greater percentages of dust-of-fracture mineral filler had silimar vebe times, when compared to the control mixtures. As the percentage of dust-of-fracture mineral filler was increased, the type of water-reducing admixture was changed from normal, mid, and high-range in order to counteract the effects of the dust-of-fracture mineral filler on workability, as stated in Section 3.5.3.4. The studies presented in the literature review stated the use of MFA with dust-of-fracture mineral filler result in lower slumps and workability, but these studies did not use water-reducing admixtures. Quiroga et al. (2006) conducted two projects, one that incorporated admixtures and one that did not. In the project that incorporated water-reducing admixtures, it was concluded that the tendency of MFA with high microfines to increase the concrete water demand can be counteracted by means of water-reducing admixtures. Therefore, it can be concluded that by using water-reducing admixtures in concrete mixtures that incorporate dust-of-fracture mineral filler up to 20 percent, no significant change will occur in the vebe time, which is shown in Table 4-9

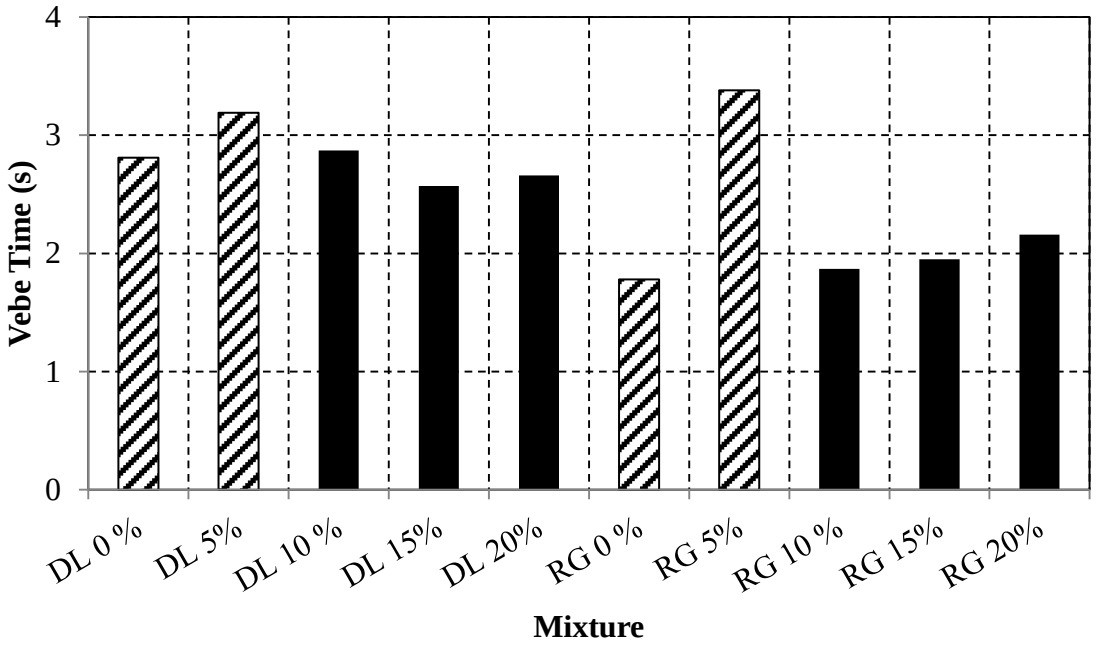

Figure 4-41: Plot of phase II vebe times

The next test analyzed in phase II fresh properties is the workability assessment rating. The data for the workability assessment rating test are shown in Table A-4. In addition to reporting the workability assessment rating, workers provided comments in relation to the mixture's workability if it performed exceedingly well or bad. Two dolomitic limestone mixtures had comments. They included the zero percent control mixture and the 15 percent dust-of-fracture mineral filler mixture. The control mixture was stated as difficult to scoop. When pushing the scoop into the concrete, it was increasingly difficult to remove the scoop due to the sticky consistency of the mixture. The mixture incorporating 15 percent dust-of-fracture mineral filler was stated to be easy to scoop, but the mixture remained sticky. Four river gravel mixtures had comments from the workers handling the concrete. They included the control mixtures, 10 percent

mixture, and 15 percent dust-of-fracture mineral filler mixture. The control mixtures were stated to be difficult to finish by troweling due to the sticky consistency of the mixtures. The 10 percent dust-of-fracture mineral filler mixture had comments regarding difficulty in scooping due to the sticky consistency, but it was assessed to be better than the control mixtures. The 15 percent dust-of-fracture mineral filler mixture was also stated to be difficult to scoop due to the sticky consistency of the mixture. After determining there was not a significant difference in the workability assessment rating between the control mixtures and the mixtures incorporating increased percentages of dust-of-fracture mineral filler, Figure 4-44 was made to graphically present the data. The control mixtures are shown with diagonal lines.

ACI 211 (2015) states, when mineral fillers are added by replacing the fine aggregate volume, the paste volume is increased and the water-powder ratio is decreased. This procedure results in the reduction of workability. Stewart et al. (2007) also found that microfines increased the demand of mid-range water-reducing admixture to achieve a constant flow when compared to the control mixture. This is in agreement with the results from this research, as increased doses and strength of water-reducing admixture were necessary. This allowed the workability of the mixtures incorporating increased dust-of-fracture mineral filler to perform similar to the mixtures currently acceptable in ASTM and ALDOT standards. Therefore, it can be concluded that by using water-reducing admixtures in concrete mixtures that incorporate up to 20 percent dust-of-fracture mineral filler, the workability assessment rating will not be sacrificed.

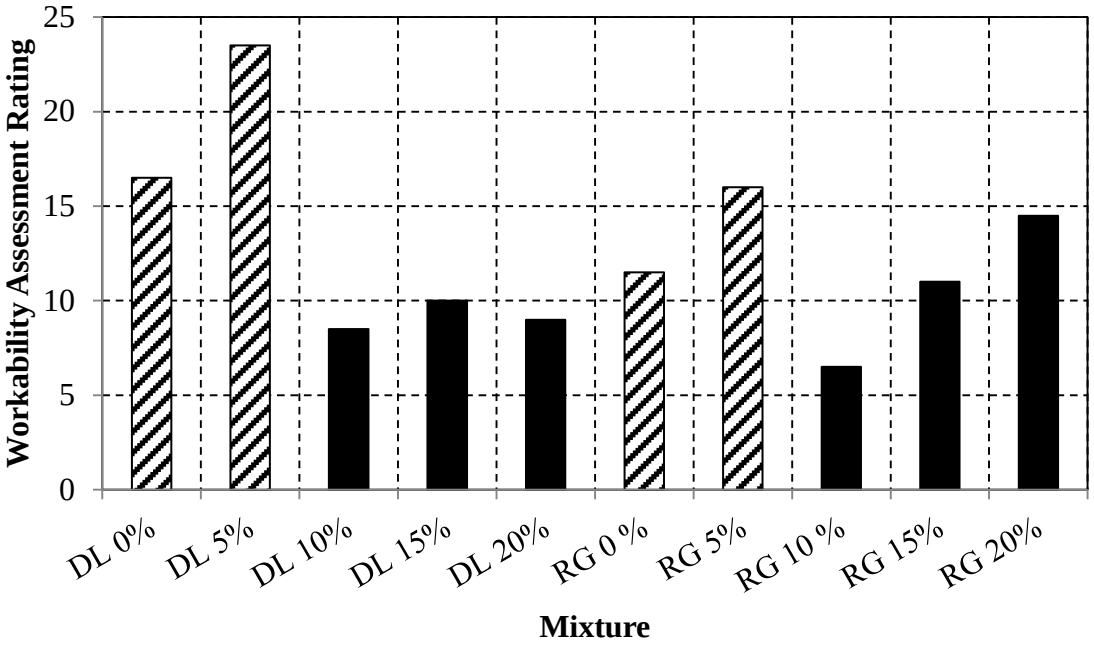

Figure 4-42: Plot of phase II workability ratings

The flow behavior of the concrete mixtures was evaluated through the use of the modified slump test, as stated in Section 3.6.1. Data for the yield stresses and plastic viscosities of each mixture are shown in Table A-6. The flow curves for the dolomitic limestone and river gravel mixtures can be seen in Figure 4-13 and Figure 4-14. The dolomitic limestone mixtures displayed similar yield stresses, but the plastic viscosity of the zero percent control mixture was significantly larger. The use of higher strength water-reducing admixtures in the mixtures incorporating increased percentages of dust-of-fracture mineral filler offset the likely increase in yield stress and plastic viscosity. The RG mixtures all displayed similar yield stresses and plastic viscosities.

Koehler and Fowler (2008) found that the use of a high-range water-reducing admixture reduced the yield stress in concrete, and did not change the plastic viscosity

compared to the control mixture, when the dust-of-fracture mineral filler was used as part of the paste volume. The use of high-range water reducing admixture with mixtures incorporating dust-of-fracture mineral filler as part of the aggregate volume reduced the yield stress, but increased the plastic viscosities when compared to the control mixture. During this study, it was found that the use of water-reducing admixtures offset any increase in yield stress and plastic viscosity, caused by the increase amount of dust-of-fracture mineral filler. The mixtures incorporating increased percentages of dust-of-fracture mineral filler remained unchanged, when compared to the control mixtures. Therefore, it can be concluded that concrete mixtures made with MFA within the allowable limits for dust-of-fracture mineral filler will have similar flow curves to mixtures incorporating percentages up to 20 percent of dust-of-fracture mineral filler with the appropriate use water-reducing admixtures.

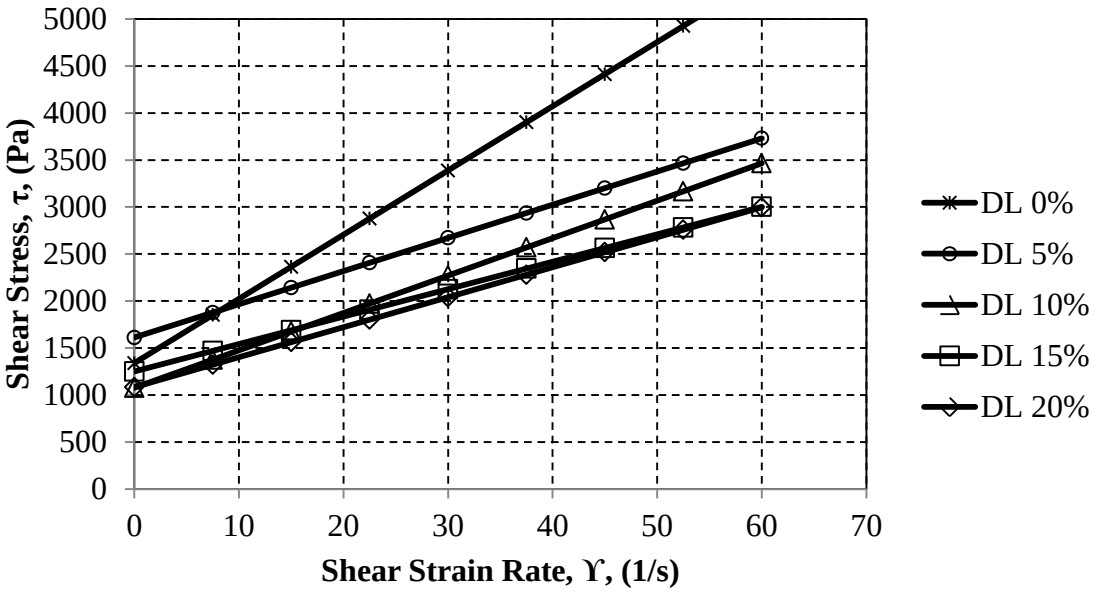

Figure 4-43: Flow curves for dolomitic limestone mixtures

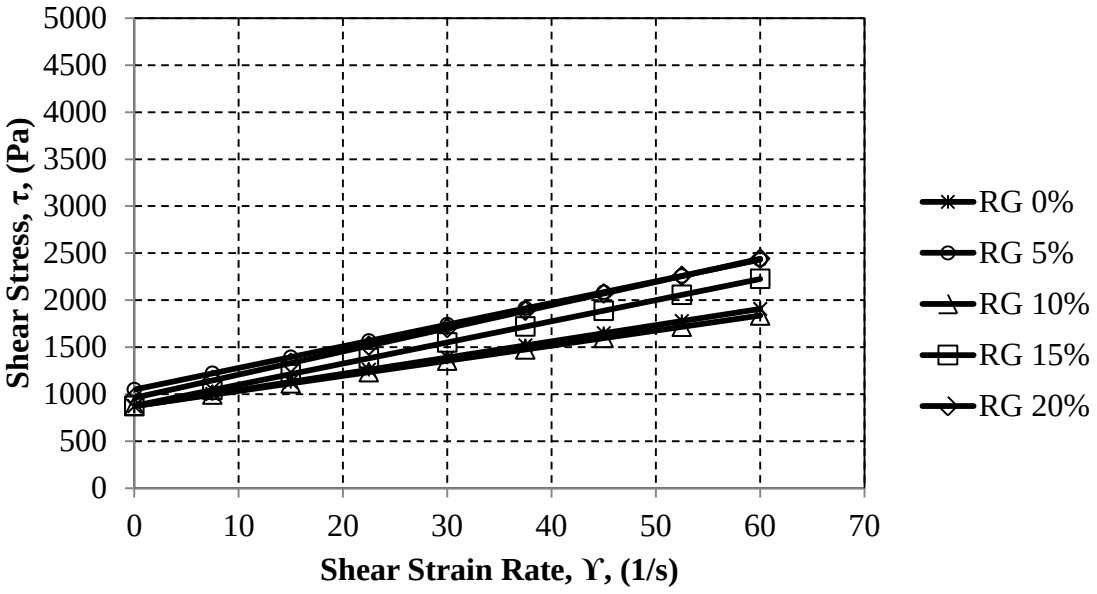

Figure 4-44: Flow curves for river gravel mixtures

4.5.2 EFFECT ON HARDENED PROPERTIES

The hardened properties for phase II were split into two categories. The categories included mechanical properties (compression strength, splitting tensile strength, and modulus of elasticity) and durability properties (drying shrinkage, RCPT, and abrasion resistance). The effects from using increased percentages of dust-of-fracture mineral filler will be discussed in the following sections.

4.5.2.1 Mechanical Properties

The data were analyzed to determine whether a difference existed between the control mixtures and the mixtures that had increased percentages of dust-of-fracture mineral filler. In order to determine whether a maximum limit existed, mixtures containing the highest percentages of dust-of-fracture mineral filler were removed in intervals, as stated during the phase II fresh properties analysis. The differences found in the data will now be discussed.

In order to validate any conclusions between the mechanical property data, the values were statistically analyzed. When analyzing the mechanical properties, an ANOVA statistical test was used for comparing variables, as stated in Section 4.4.2.1. The analysis compared each mechanical property variables at three different ages (7, 28, and 91-day values). A confidence interval of 95 percent was used for the ANOVA test. The p-values for the mechanical properties results are shown in Table 4-10.

Table 4-11: Summary of Phase II Mechanical Property P-values

Property	Variables Compared	P-value
Compressive Strength	DL vs. RG	4.54E-09
	0-5% vs. 10-20% (DL)	0.0645
	0-5% vs. 10-15% (DL)	0.187
	0-5% vs. 10% (DL)	0.722
	0-5% vs. 10-20% (RG)	0.000113
	0-5% vs. 10-15% (RG)	0.00464
	0-5% vs. 10% (RG)	0.00364
Splitting Tensile Strength	DL vs. RG	6.42E-10
	0-5% vs. 10-20% (DL)	0.0485
	0-5% vs. 10-15% (DL)	0.23
	0-5% vs. 10% (DL)	0.584
	0-5% vs. 10-20% (RG)	0.5740
	0-5% vs. 10-15% (RG)	0.2990
	0-5% vs. 10% (RG)	0.6280
Modulus of Elasticity	DL vs. RG	2.00E-16
	0-5% vs. 10-20% (DL)	0.1110
	0-5% vs. 10-15% (DL)	0.1870
	0-5% vs. 10% (DL)	0.1440
	0-5% vs. 10-20% (RG)	0.1080
	0-5% vs. 10-15% (RG)	0.0192
	0-5% vs. 10% (RG)	0.0389

The growth in compressive strength for the dolomitic limestone and river gravel mixtures can be seen in Figure 4-47 and Figure 4-48. The data for the compressive strengths are shown in Table B-7 and Table B-8. The compressive strengths for the dolomitic limestone mixtures were within the test's 7.8 percent range from the control mixtures. The compressive strengths for the river gravel mixtures were also within the test's 7.8 percent range from the 0 percent dust-of-fracture mineral filler control mixture, but the 91-day compressive strength for the 5 percent dust-of-fracture mineral filler control mixture is more than 600 psi greater than the other mixtures, which is outside the range for the test. This difference is also shown by the p-values for the river gravel mixtures in Table 4-10. It is not reasonable to conclude that increasing the percent of dust-of-fracture mineral filler will decrease the compressive strength of concrete. This is because there is almost no difference between the zero percent dust-of-fracture mineral filler control mixture and the mixtures incorporating increased percentage of dust-of-fracture mineral filler.

The results found during the compressive strength testing are in agreement with the studies conducted by Stewart et al. (2007). Stewart et al. (2007) found the compressive strength had no change compared to the control after the addition of dust-of-fracture mineral filler. In addition, using the data from the laser size analyzer in Section 3.9, relationships can be made with the size distribution and how it plays an important role on the strength. ACI 211 (2015) states mineral filler can contribute to concrete strength by providing nucleation sites for cement hydration, but the particles must be smaller than cement particles in order to provide a substantial number of nucleation sites for hydration. The cement particles are significantly smaller than the MFA dust-of-

fracture mineral filler particles, as seen in Figure 3-64. Therefore, the MFA dust-of-fracture mineral filler used in this research should not be expected to contribute to significant strength benefits. Therefore, it can be assumed that using MFA with percentages of dust-of-fracture mineral filler up to 20 percent will not significantly affect the compressive strength of the concrete compared to concrete made with no dust-of-fracture mineral filler.

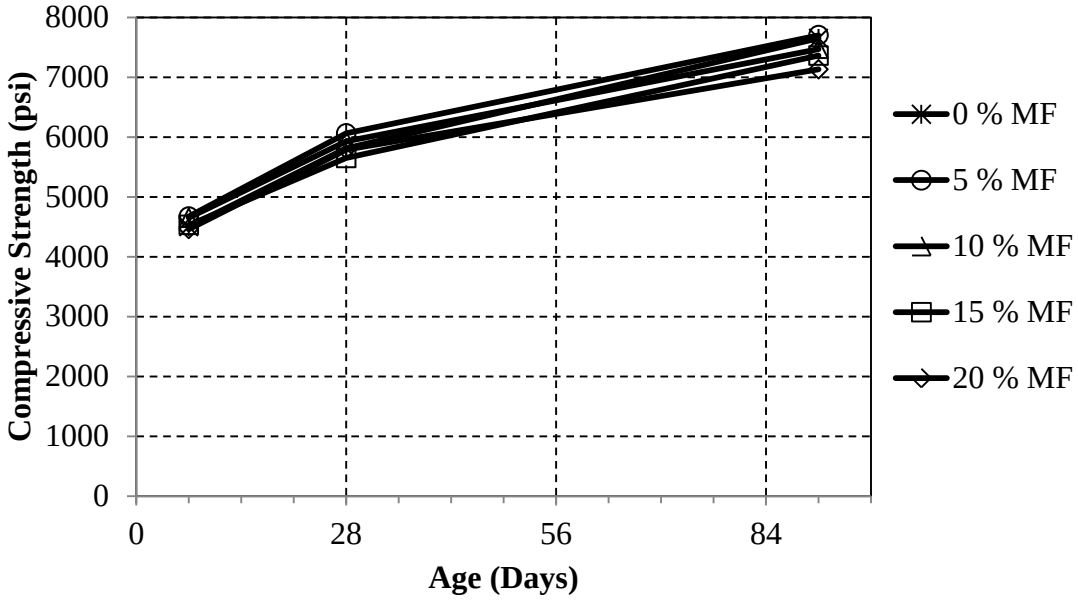

Figure 4-45: Dolomitic limestone compressive strengths

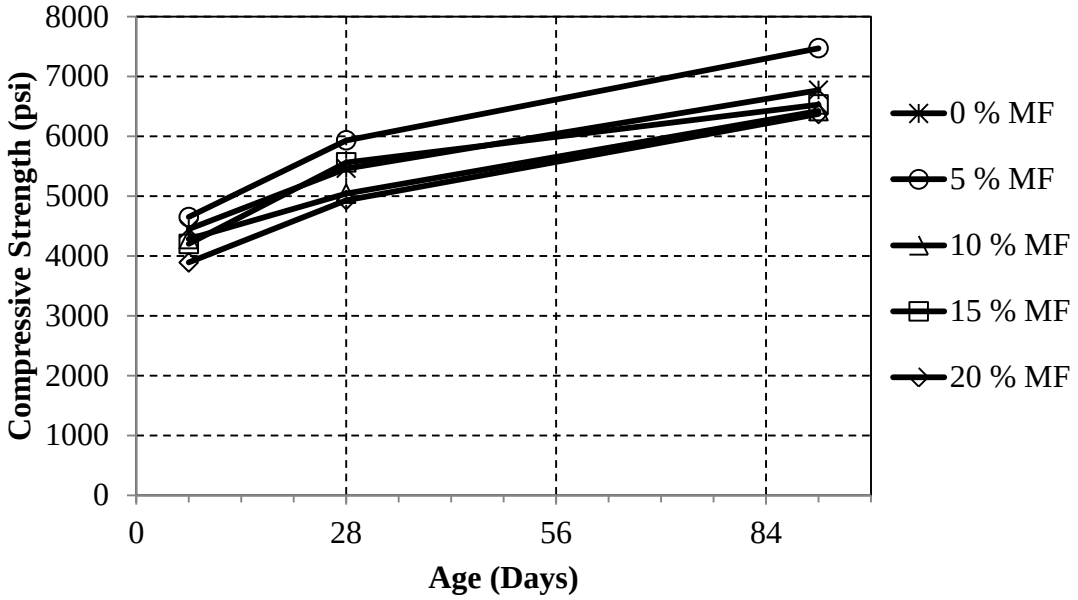

Figure 4-46: River gravel compressive strengths

The splitting tensile strength development for both dolomitic limestone and river gravel mixtures can be seen in Figure 4-49 and Figure 4-50. The data for the splitting tensile strengths are shown in Table B-7 and Table B-8. The dolomitic limestone mixtures had greater splitting tensile strengths than the river gravel mixtures. This is expected due to the larger compressive strengths of the dolomitic limestone mixtures, which are used in the equation recommended by Raphael (1984) for determining the splitting tensile strength. The 7-day splitting tensile strength for the dolomitic limestone 5 percent dust-of-fracture mineral filler mixture had outliers; therefore this data point was not used. In addition, the 28-day splitting tensile strength for the dolomitic limestone 20 percent dust-of-fracture mineral filler mixture had outliers; therefore this data point was not used. The dolomitic limestone 20 percent dust-of-fracture mineral filler was significantly less than the rest of the mixtures. This is the reason for the small p-value in Table 4-10. However, the dolomitic limestone 10 and 15 percent dust-of-fracture mineral filler mixtures performed equally as well as the control mixtures. Therefore, going to 20 percent dust-of-fracture mineral filler in the dolomitic limestone mixtures caused the splitting tensile strength to decrease. The river gravel mixtures all had similar strengths, considering the precision of this test.

These results are in agreement with the studies discussed in the literature review. Stewart et al. (2007) found dust-of-fracture mineral fillers incorporated into mixtures at levels up to 15 percent of the fine aggregate volume had similar flexural strengths to the control mixture. The use of water-reducing admixtures is also thought to have an effect on the results of the test. Abou-Zeid and Fakhry (2003) showed that some increase in flexural strength is attributed with mineral filler, but this relationship is less pronounced

in mixtures incorporating admixtures. In addition, Celik and Marar (1996) found a decrease in flexural strength when the dust-of-fracture mineral filler in the concrete was increased over 10 percent. Therefore, it can be assumed that using MFA with percentages of dust-of-fracture mineral filler up to 15 percent will not significantly affect the splitting tensile strength of the concrete compared to concrete made with no dust-of-fracture mineral filler. Greater percentages may be used if further evidence is found to demonstrate that 20 percent dust-of-fracture mineral filler mixture can be used without affecting the splitting tensile strength.

The predictability of all mixtures' splitting tensile strength with the equation recommended by Raphael (1984) can be seen in Figure 4-51 and Figure 4-52. In order to quantify the percentage of error between the measured data and the predicted data, the unbiased estimate of the standard deviation, Sj, for the error was calculated. Equation 4-1, taken from McCuen (1985), was used for this calculation. The values for the unbiased estimate of standard deviation are shown in Table 4-12. The strengths are predicted close to a ± 20 percent error and have similar Sj values to the accepted mixtures, as shown in Table 4-9. The dolomitic limestone 20 percent dust-of-fracture mineral filler mixture was the only mixture with a significantly larger Sj value when compared to the control mixtures. This proves that the equation recommended by Raphael (1984) for determining the splitting tensile strength can be used for mixtures that incorporate dust-of-fracture mineral filler up to 15 percent with the same accuracy with mixtures currently accepted in ASTM C33 (2013) and ALDOT (2012).

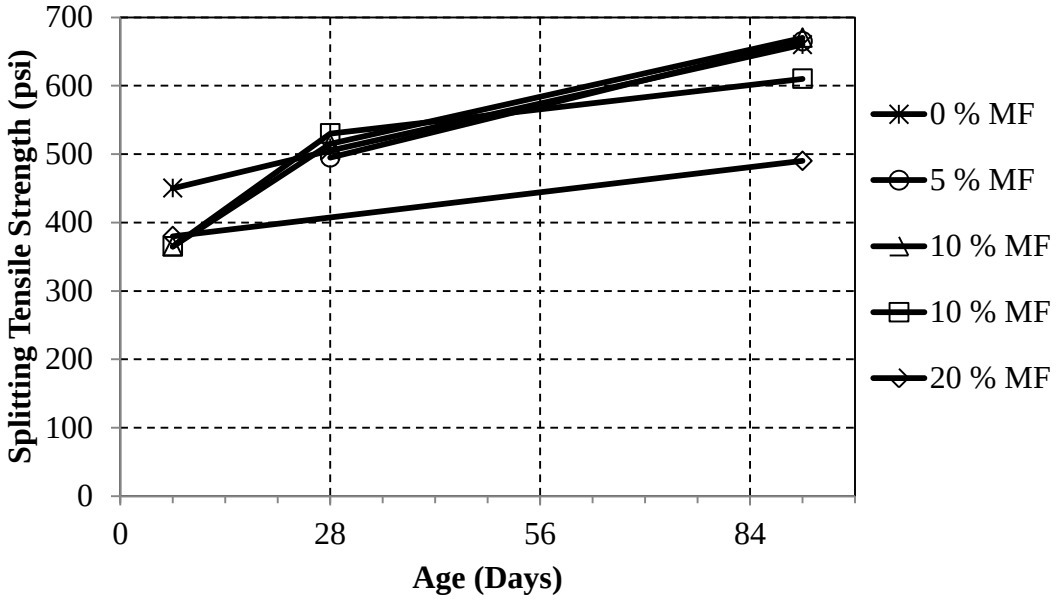

Figure 4-47: Dolomitic limestone splitting tensile strengths

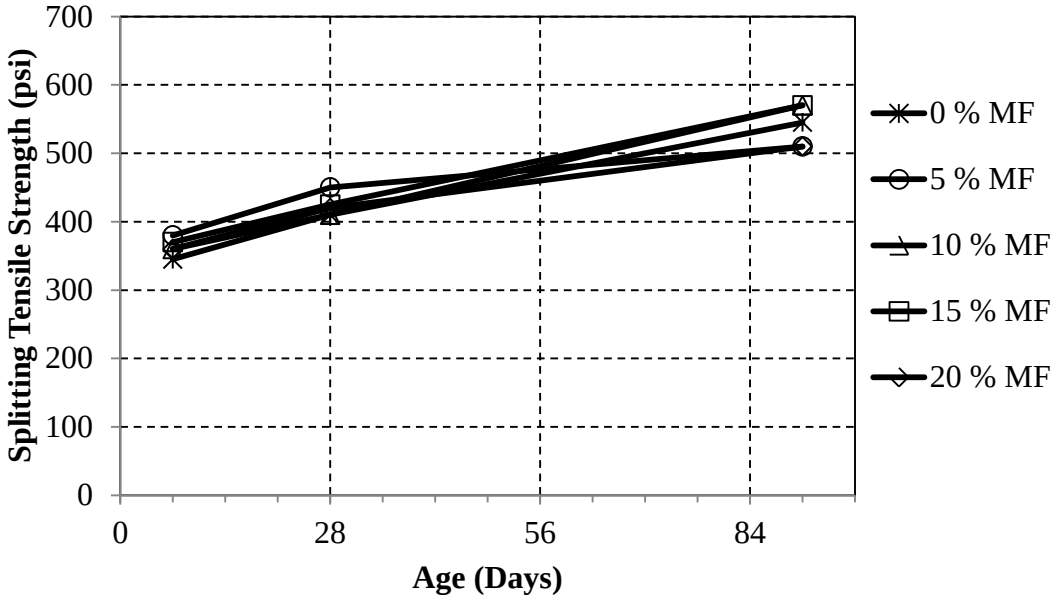

Figure 4-48: River gravel splitting tensile strengths

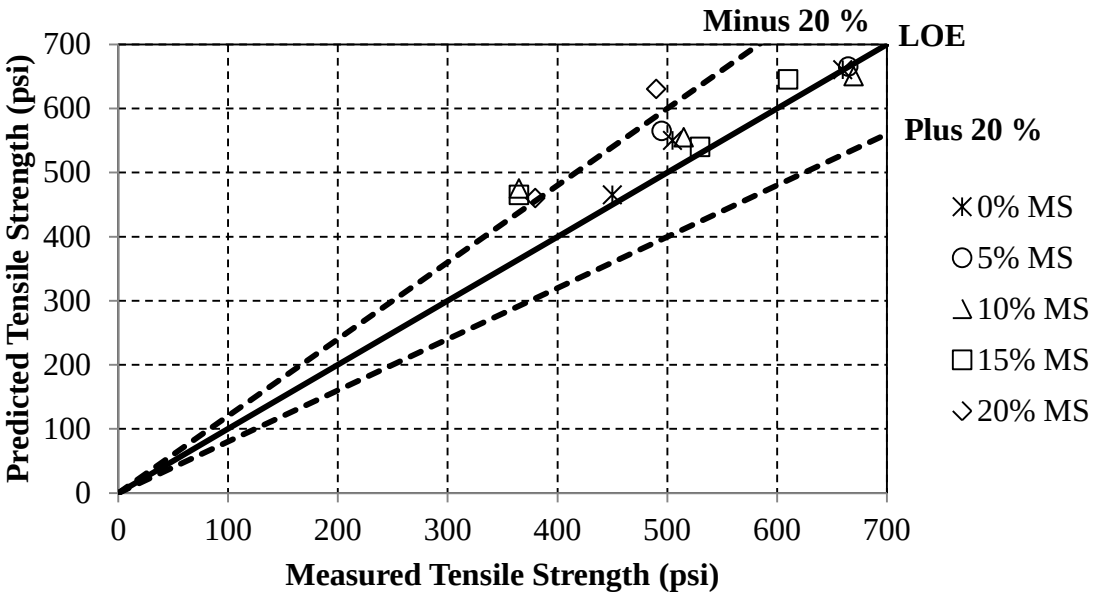

Figure 4-49: Dolomitic limestone predicted versus measured splitting tensile strength

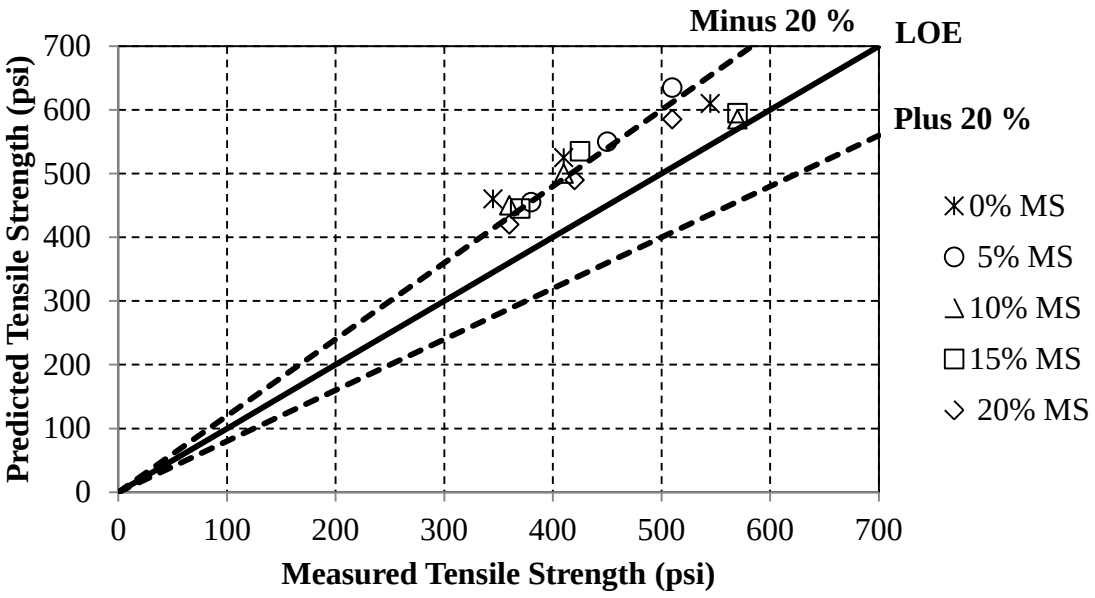

Figure 4-50: River gravel predicted versus measured splitting tensile strength

Table 4-12: Phase II Unbiased Estimate of the Standard Deviation of Splitting Tensile Strengths

MF %	Sj (%)	
	DL No. 67	RG No. 67
0	6.7	32
5	14.1	27.2
10	22.1	23.6
15	19.8	23.5
20	35.5	19.6

The MOE plots for the dolomitic limestone and river gravel mixtures can be seen in Figure 4-53 and Figure 4-54. The data for all the mixtures MOE's are shown in Table B-9. The dolomitic limestone mixtures had greater MOE's than the river gravel mixtures. This is expected due to the larger compressive strengths of the dolomitic limestone mixtures, which are used in the ACI Building Code 318 (2011) equation for determining the MOE. The dolomitic limestone mixtures had similar MOE developments. The 28-day MOE's have greater variation between mixtures, but the 7 and 91-day values are very similar. Based on Table 4-10, the river gravel mixtures had significant differences between the MOE's. However, all MOE's were within the test's 11.9 percent range from the control mixtures.

The predictability of the mixture's MOE with the ACI Building Code 318 (2011) equation can be seen in Figure 4-55 and Figure 4-56. In order to quantify the percentage of error between the measured data and the predicted data, the unbiased estimate of the standard deviation was used, as previously stated. The values for the unbiased estimate of standard deviation are shown in Table 4-13. There is not a significant difference in the prediction accuracy between the mixtures that have increased percentages of dust-of-

fracture mineral filler and the control mixtures that meet ASTM C33 (2013) ALDOT (2012), as shown in Table 4-9. This proves that the ACI Building Code 318 (2011) equation for determining the MOE can be used for mixtures with dust-of-fracture mineral filler percentages up to 20 percent with the same accuracy as mixtures currently meeting the limits specified in ASTM C33 (2013) and ALDOT (2012). Therefore, it can be assumed that using MFA with percentages of dust-of-fracture mineral filler up to 20 percent will not significantly affect the MOE of the concrete, compared to concrete containing MFA with allowable limits for dust-of-fracture mineral filler.

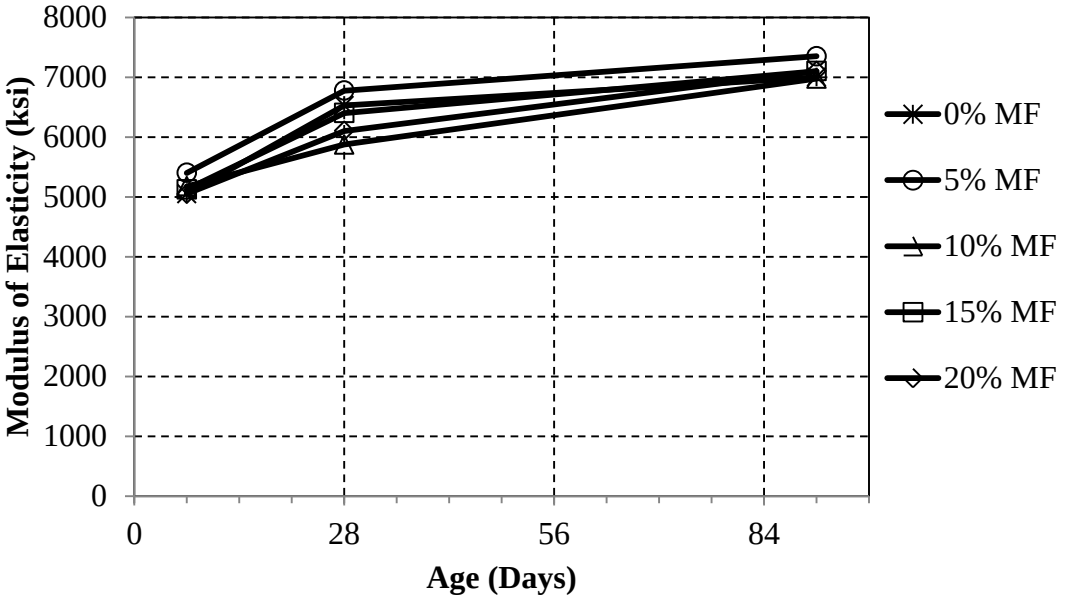

Figure 4-51: Dolomitic limestone modulus of elasticity

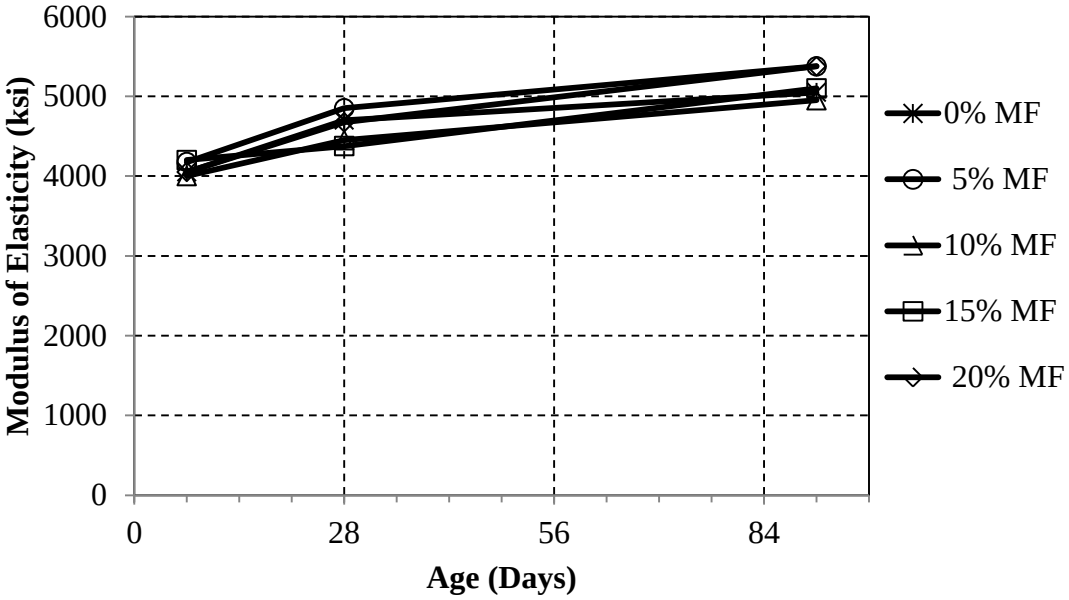

Figure 4-52: River gravel modulus of elasticity

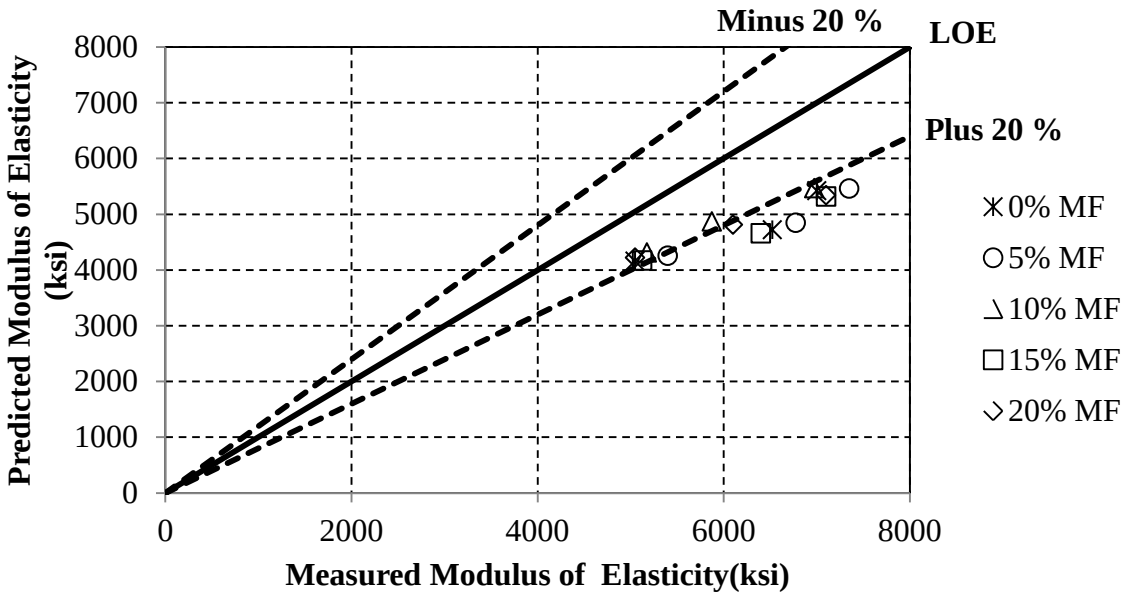

Figure 4-53: Dolomitic limestone predicted versus measured modulus of elasticity

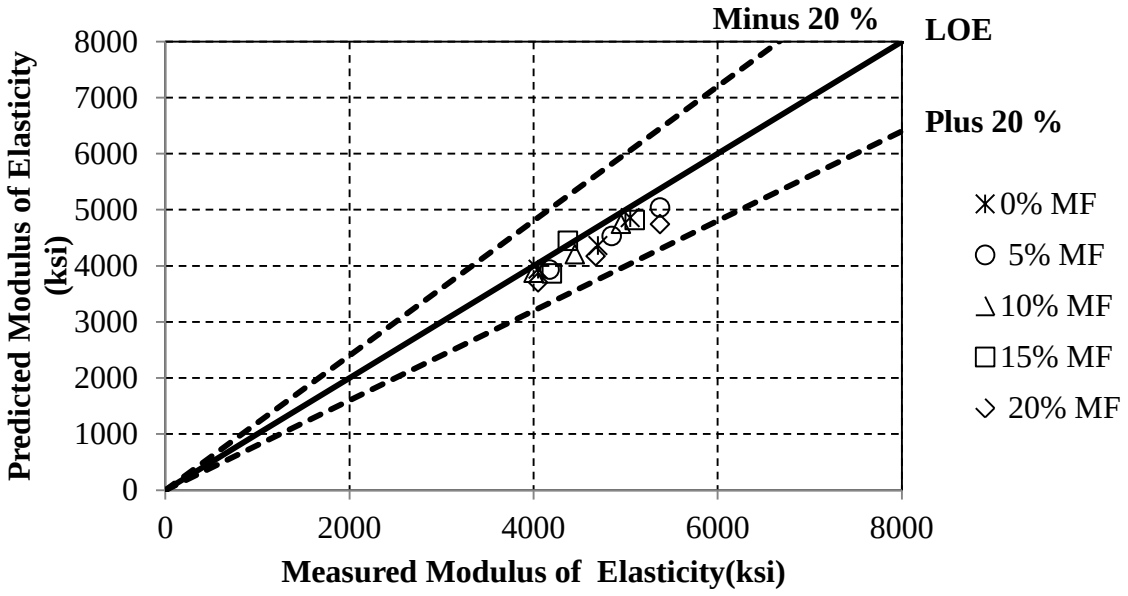

Figure 4-54: River gravel predicted versus measured modulus of elasticity

Table 4-13: Phase II Unbiased Estimate of the Standard Deviation of Modulus of Elasticity

MF %	Sj (%)	
	DL No. 67	RG No. 67
0	28.2	6.1
5	31.0	7.6
10	22.8	5.3
15	29.3	7.0
20	25.8	12.8

4.5.2.2 Durability Properties

In order to validate any conclusions between the durability property data, the values were statistically analyzed. When analyzing the shrinkage data, a two-factor ANOVA statistical test was used for comparing variables. This shrinkage data were composed of strain measurements at 7 different ages (4, 7, 14, 28, 56, 112, and 168-day strains). An independent two sample t-distribution was used for the analysis of the RCPT and abrasion data. The values for these tests were only measured at an age of 91 days. All statistical tests were conducted at a 95 percent confidence interval.

Table 4-14: Phase II Durability Property P-values

Property	Variables Compared	P-value
Shrinkage	0-5% vs. 10-20% (DL)	2.13E-04
	0-5% vs. 10-15% (DL)	0.00445
	0-5% vs. 10% (DL)	0.0309
	0-5% vs. 10-20% (RG)	0.153
	0-5% vs. 10-15% (RG)	0.321
	0-5% vs. 10% (RG)	0.0853
RCPT	DL vs. RG	0.6363
	0-5% vs.10-20%	3.577E-07
	0-5% vs.10-15%	1.60E-05
	0-5% vs. 10%	2.93E-04
Abrasion Resistance	0-5% vs.10-20%	0.0107
	0-5% vs.10-15%	0.0088
	0-5% vs. 10%	0.0013

In order to analyze the effect the dust-of-fracture mineral filler had on the mixtures, it was first determined whether there was a difference in RCPT values between coarse aggregate types. It was determined that there was no difference in results between the coarse aggregates at a 95 percent confidence level. For abrasion testing, only dolomitic limestone mixtures were used, as described in Section 3.4. Next, it was determined whether a difference existed between the control mixtures and the mixtures that had increased percentages of dust-of-fracture mineral filler. In addition, mixtures containing the highest percentages of dust-of-fracture mineral filler were removed in

intervals, as stated during the phase II fresh properties analysis. The drying shrinkage data was only analyzed whether there was a difference between the control mixtures and the mixtures that had increased percentages of dust-of-fracture mineral filler, due to a malfunction in the gauge that caused errors in the data. The differences found in the data will now be discussed.

The amount of shrinkage during a 168 day interval was measured, as described in Section 3.7.4. Due the malfunction previously stated in Section 4.4.2.2, the drying shrinkage data for the river gravel mixtures at an age of 28 days was not used for analysis. Because the malfunction occurred early in the measurements, the later dates were unaffected. In addition, the drying shrinkage data for the dolomitic limestone mixtures at an age of 168 days was not used for analysis. Plots of the unaffected shrinkage strains for the mixtures can be seen in Figure 4-57 through Figure 4-58. The data for the shrinkage strains are shown in Table C-7 and C-8. The dolomitic limestone 20 percent dust-of-fracture mineral filler mixture was the only mixture that was out of the range for the test when compared to the control mixtures, despite what is presented with the statistics in Table 4-12. This mixture had significantly less drying shrinkage than the control mixtures, which is a beneficial effect. The river gravel dust-of-fracture mineral filler mixtures were not within the test range when compared to the control mixtures, but the zero percent dust-of-fracture mineral filler control mixture had the most shrinkage. The 15 percent dust-of-fracture mineral filler mixture also had high shrinkage values, but they were smaller than the values for the zero percent dust-of-fracture mineral filler control mixture. The 20 percent dust-of-fracture mineral filler mixture was within the test

range of the 5 percent control mixture, therefore these differences were not caused by dust-of-fracture mineral filler additions.

The results are in agreement with Quiroga et al. (2006) and Fowler and Rached (2011). Quiroga et al. (2006) found half the MFA mixtures resulted in lower drying shrinkage strains than the control. Fowler and Rached (2011) found shrinkage decreased as the percent of dust-of-fracture mineral filler increased, but during their study the dust-of-fracture mineral filler was proportioned as part of the powder content. This project proportioned dust-of-fracture mineral filler as part of the fine aggregate volume which is different than how Fowler and Rached (2011) incorporated the dust-of-fracture mineral filler. In addition, the size of the dust-of-fracture mineral filler also plays an important role on drying shrinkage, according to Katz and Baum (2006). The study states, for coarser sized mineral filler particles, the shrinkage is less affected regardless of the fine aggregate replacement percentage compared to finer size mineral filler particles. Finer sized mineral filler particles are believed to be the size of the cementitious materials. Using the results shown in Figure 3-64, it can be seen that the MFA dust-of-fracture mineral filler used in this project is coarser than the cementitious materials. Therefore, based on the study by Katz and Baum (2006), the additions of the dust-of-fracture mineral filler should not affect the shrinkage results of the concrete mixtures.

In addition to the shrinkage plots, the predictability of the shrinkage with the equations from ACI Committee 209 (1997) for each mixture was measured. The results can be seen in Figure 4-59 and Figure 4-60. In order to quantify the percentage of error between the measured data and the predicted data, the unbiased estimate of the standard deviation was used, as previously stated. The drying shrinkage values for the unbiased

estimate of standard deviation are shown in Table 4-15. There is not a significant difference in the prediction accuracy between the dust-of-fracture mineral filler mixtures that are outside the allowable limits and the control mixtures that meet ASTM C33 (2013) and ALDOT (2012), as shown in Table 4-9. This proves that the predictability of the shrinkage with the equations from ACI Committee 209 (1997) can be used for mixtures with dust-of-fracture mineral filler percentages up to 20 percent with the same accuracy as mixtures currently meeting the limits specified in ASTM C33 (2013) and ALDOT (2012).

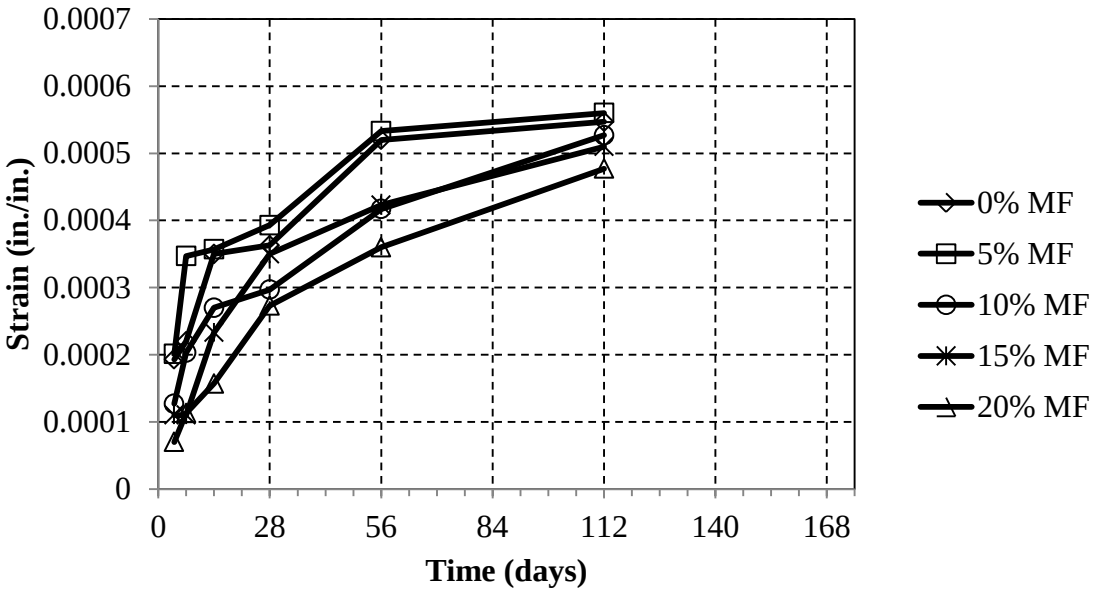

Figure 4-55: Dolomitic limestone shrinkage strains

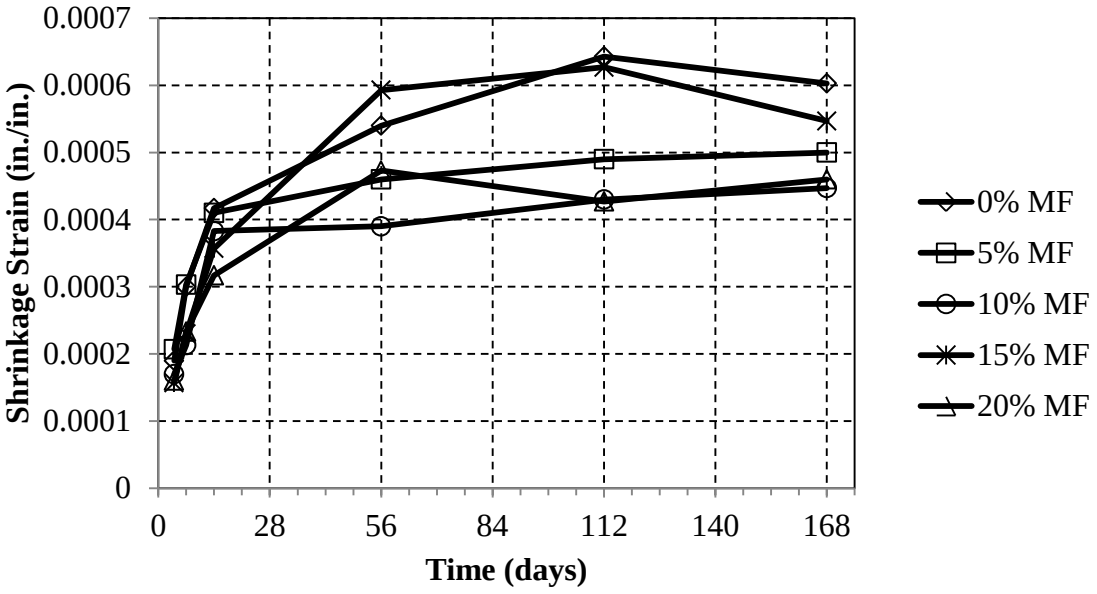

Figure 4-56: River gravel shrinkage strains

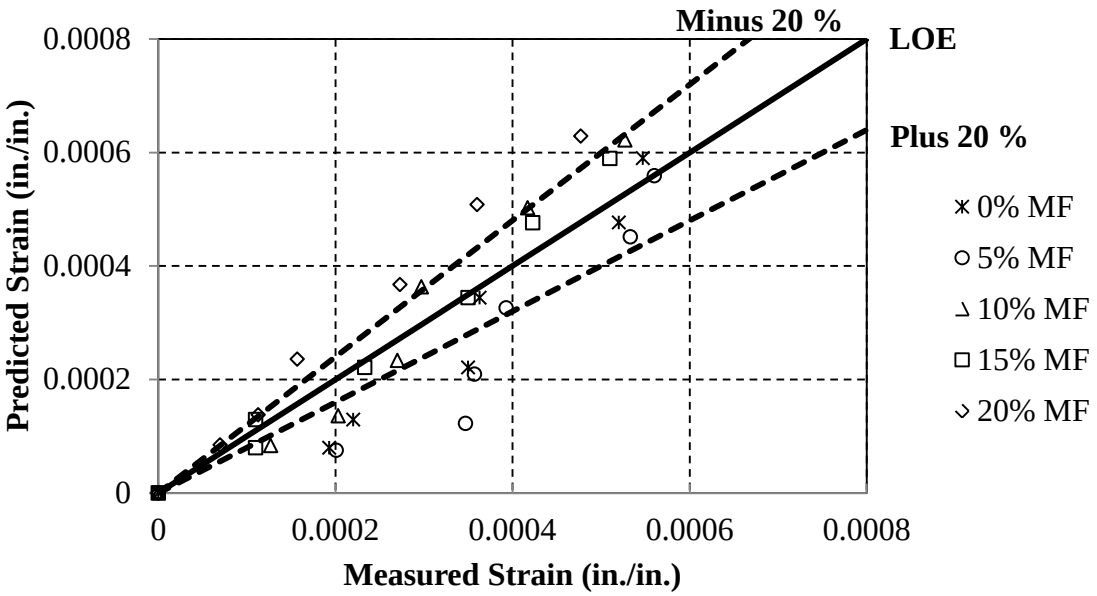

Figure 4-57: Dolomitic limestone predicted versus measured shrinkage strains

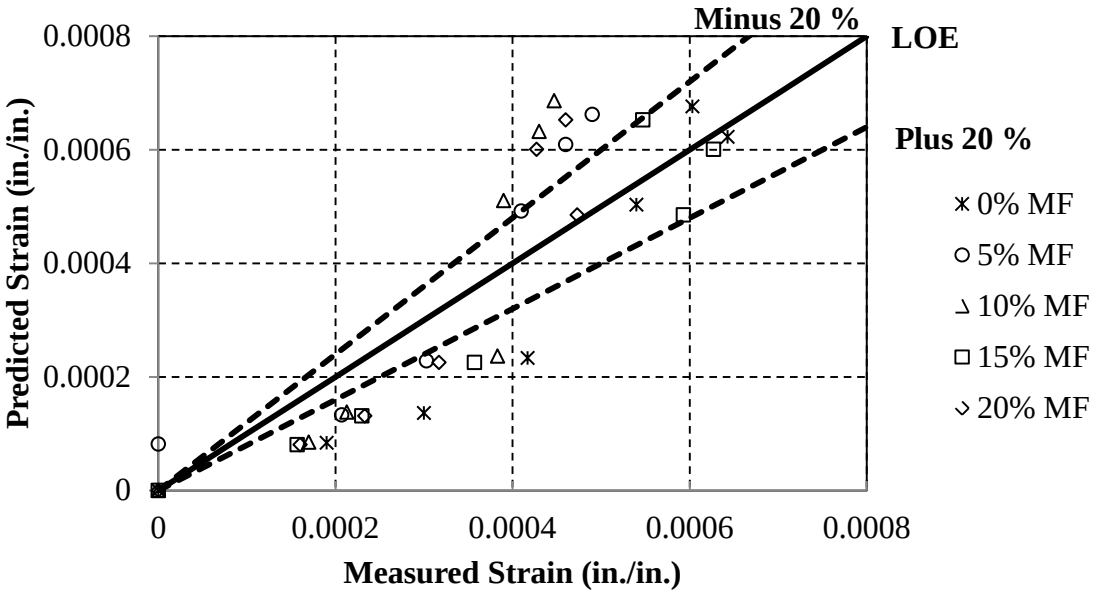

Figure 4-58: River gravel predicted versus measured shrinkage strains

Table 4-15: Phase II Unbiased Estimate of the Standard Deviation of Drying Shrinkage Strain

MF %	Sj (%)	
	DL No. 67	RG No. 67
0	36.6	40.6
5	45.5	45.7
10	27.1	47.4
15	17.3	35.4
20	38.3	41.9

The permeability of concrete was measured using the RCPT test, as described in Section 3.7.5. The values of charge passed through the concrete (in coulombs) were graphed for each mixture and are shown in Figure 4-61. The data for the RCPT values are shown in Table C-6. All mixtures were classified in the low category for chloride ion permeability, as detailed in ASTM Standard C1202 (2006). This is due to the use of fly ash in the mixtures. The particle size distribution of fly ash typically ranges from 1 micrometer to 100 micrometers in diameter, with more than 50 percent by mass less than 20 micrometers. Due to its small particle size and pozzolanic behavior, Class F fly ash has proven to cause pore refinement that reduces the permeability of concrete (Mehta and Monteiro 2014). The dolomitic limestone and river gravel dust-of-fracture mineral filler mixtures were all within the test's 41 percent range when compared to the control mixtures. Therefore, it can be assumed that using MFA with percentages of dust-of-fracture mineral filler up to 20 percent will not significantly affect the permeability of the concrete, compared to concrete containing MFA with allowable limits for dust-of-fracture mineral filler.

The abrasion resistance of the concrete was measured using ASTM C1779 (2012), as stated in Section 3.7.6. The results from this test are shown in Figure 4-62. The control mixtures are shown with diagonal lines. The data for the testing can be found in Table C-9. In addition, before and after test pictures of the samples can be found in Appendix D. The dust-of-fracture mineral filler mixtures were within the test's 18.2 percent range when compared to the control mixtures. MFA with percentages of dust-of-fracture mineral filler up to 20 percent is shown to not significantly affect the abrasion resistance of the concrete compared to concrete made within the allowable limits for dust-of-fracture mineral filler.

ASTM C33 (2013) states, the limit of dust-of-fracture mineral filler should be reduced from 7 to 5 percent in relation to the fine aggregate volume when concrete is subjected to abrasion. This reduction is due to the thought that the particles will have a negative impact, which was not found. Section 6.3 in ASTM C33 (2013) states any fine aggregate which fails to meet the grading requirements shall meet the requirements provided that the supplier can demonstrate that the concrete will have relevant properties at least equal to those of concrete made with the same ingredients. Therefore, the use of the MFA with dust-of-fracture mineral filler with additions up to 20 percent may be appropriate for concrete use, due to similar amounts of wear when compared to the control mixtures.

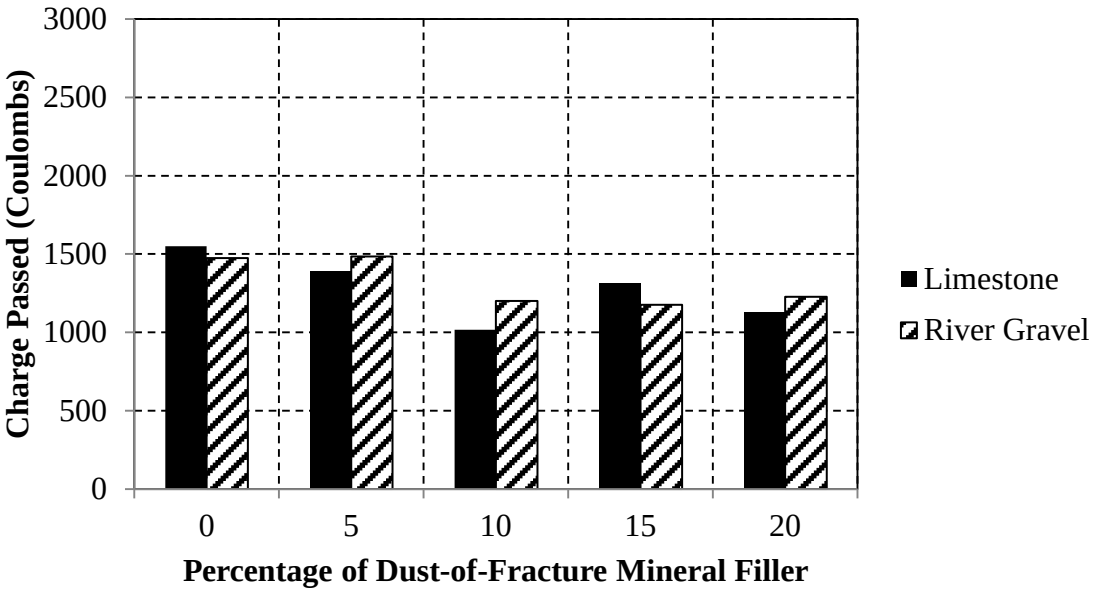

Figure 4-59: RCPT coulomb values for MFA mixtures

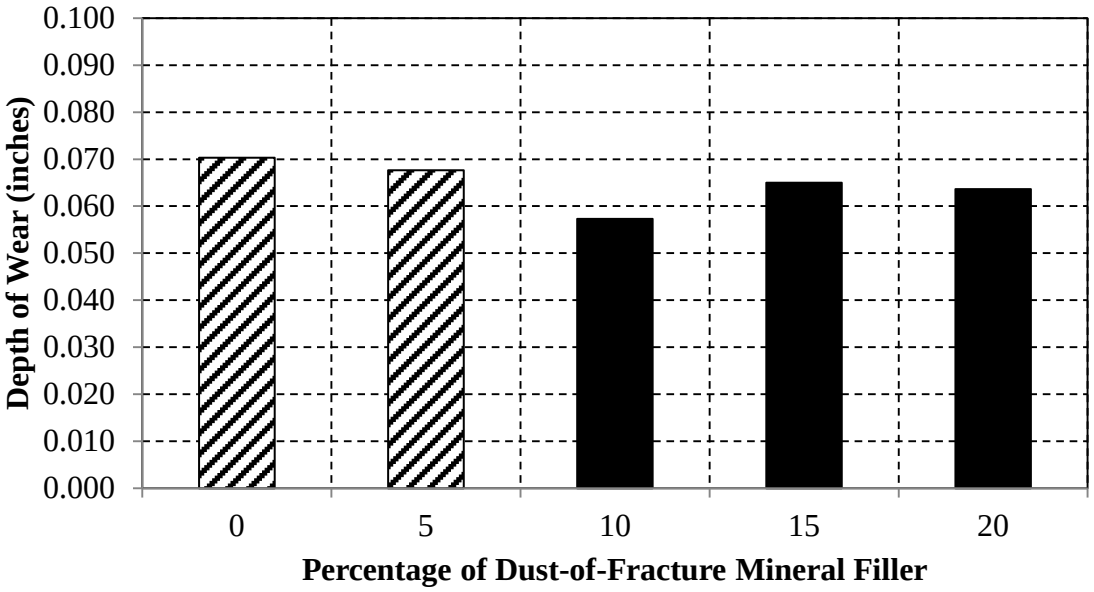

Figure 4-60: Abrasion wear values for dolomitic limestone MFA mixtures

4.6 SUMMARY OF RESULTS

4.6.1 SUMMARY OF PHASE I WORK

From the research conducted in phase I, the following conclusions can be made about optimized aggregate gradations achieved from using the Shilstone Method and percent retained chart.

- Mixtures that met the limits of the proportioning methods produced low vebe times.
- Workability assessment ratings were best among mixtures that met the limits of proportioning methods.
- Mixtures that met the limits of the proportioning methods were least prone to segregation, based on flow curves.
- No change in compressive strength was found for mixtures that met the limits of the proportioning limits.
- No change in splitting tensile strength was found for mixtures that met the limits of the proportioning methods limits. In addition, there is not a significant difference in the prediction accuracy with the equation recommended by Raphael (1984) for determining the splitting tensile strength between the optimized aggregate gradations and the gradations that meet ASTM C33 (2013).
- No change in MOE was found for mixtures that met the limits of the proportioning methods limits. In addition, there is not a significant difference in the prediction accuracy with the ACI Building Code 318 (2011) equation for determining the MOE between the optimized aggregate gradations and the gradations that meet ASTM C33 (2013).

- No change in drying shrinkage was found for mixtures that met the limits of the proportioning methods limits. In addition, there is not a significant difference in the prediction accuracy with the ACI Committee 209 (1997) equations for shrinkage predictability between the optimized aggregate gradations and the gradations that meet ASTM C33 (2013).
- No change in the permeability of the concrete was found for mixtures that met the limits of the proportioning methods limits.

4.6.2 SUMMARY OF PHASE II WORK

From the research conducted in phase II, the following conclusions can be made about the use of MFA and dust-of-fracture mineral filler for concrete use.

- The use of water-reducing admixtures in concrete mixtures incorporating MFA dust-of-fracture mineral filler up to 20 percent will result in similar vebe times as the control mixtures that meet ASTM C33 (2013) and ALDOT (2012).
- The use of water-reducing admixtures in concrete mixtures that incorporate MFA dust-of-fracture mineral filler up to 20 percent will not sacrifice the workability assessment rating, compared to the control mixtures that meet ASTM C33 (2013) and ALDOT (2012).
- The use of water-reducing admixtures in concrete mixtures incorporating MFA dust-of-fracture mineral filler up to 20 percent will result in similar flow curves as the control mixtures that meet ASTM C33 (2013) and ALDOT (2012).
- No change in compressive strength was found for mixtures with MFA dust-of-fracture mineral filler up to 20 percent.

- No change in splitting tensile strength was found for mixtures with percentages of MFA dust-of-fracture mineral filler up to 15 percent. In addition, there is not a significant difference in the prediction accuracy with the equation recommended by Raphael (1984) for determining the splitting tensile strength between the dust-of-fracture mineral filler mixtures and the control mixtures that meet ASTM C33 (2013) and ALDOT (2012).
- No change in MOE was found for mixtures with percentages of MFA dust-of-fracture mineral filler up to 20 percent. In addition, there is not a significant difference in the prediction accuracy with the ACI Building Code 318 (2011) equation for determining the MOE between the dust-of-fracture mineral filler mixtures and the control mixtures that meet ASTM C33 (2013) and ALDOT (2012).
- No change in drying shrinkage was found for mixtures with percentages of MFA dust-of-fracture mineral filler up to 20 percent. In addition, there is not a significant difference in the prediction accuracy with the ACI Committee 209 (1997) equations for shrinkage predictability between the dust-of-fracture mineral filler mixtures and the control mixtures that meet ASTM C33 (2013) and ALDOT (2012).
- No change in permeability was found for mixtures with percentages of MFA dust-of-fracture mineral filler up to 20 percent.
- No change in abrasion resistance was found for mixtures with percentages of MFA dust-of-fracture mineral filler up to 20 percent.

CHAPTER 5

SUMMARY, CONCLUSIONS, AND RECOMMENDATIONS

5.1 SUMMARY OF PROJECT

In total 34 concrete mixtures were developed, produced, and tested for this research. Phase I consisted of 18 mixtures focused on the assessment of various aggregate proportioning methods. Phase II consisted of 16 mixtures focused on evaluating the effect of using MFA dust-of-fracture mineral filler on the performance of concrete. During phase I, 16 different combined aggregate gradations were developed using the Shilstone Method and percent retained chart. The goal was to evaluate the effectiveness of these proportioning methods on the fresh and hardened concrete states and determine if there are any benefits from the use of these methods. During phase II, five different percentages of MFA dust-of-fracture mineral filler were used in concrete mixtures. The goal was to determine whether the use of this material above the current ASTM, AASHTO, and ALDOT limits affected the performance of the concrete, in terms of fresh and hardened concrete states.

For each mixture, the fresh properties were evaluated through the use of the modified slump test, vebe consistometer, and a workability assessment. The hardened properties were evaluated through the use of compressive strength, splitting tensile strength, modulus of elasticity, RCPT, and drying shrinkage testing. In addition, abrasion testing was conducted during phase II, because it is perceived that MFA dust-of-fracture

mineral filler might lead to increased wear, most significantly in dolomitic limestone mixtures.

5.2 RESEARCH CONCLUSIONS

5.2.1 CONCLUSIONS FROM PHASE I

From this research the following conclusions can be made.

- The Shilstone Method has a larger role in developing the optimized aggregate gradation than the percent retained chart, but both methods should be used. The percent retained chart assists the Shilstone Method to verify poor gradations are avoided.
- Combined aggregate gradations that plot inside of zone II of the CFC have the best concrete performance, in terms of fresh properties.
- Optimized aggregate gradations can improve concrete workability. These gradations will benefit the finishability, flow, and compactability of the concrete.
- The optimized aggregate gradation for a concrete mixture responds well to vibration and does not segregate.
- Optimized aggregate gradations do not affect the durability or hardened properties of concrete.
- The use of optimized aggregate gradations for concrete mixtures has no effect on the prediction accuracy of the equations stated in this research.

5.2.2 CONCLUSIONS FROM PHASE II

From this research the following conclusions can be made.

- Good quality concrete can be made with MFA dust-of-fracture mineral filler with amounts as high as 20 percent of the fine aggregate volume.

- Standards should be adjusted to allow greater percentages and more frequent use of dust-of-fracture mineral filler in MFA concrete mixtures.
- Concrete mixtures with MFA dust-of-fracture mineral filler with amounts up to 20 percent will not result in decreased workability, with the use of water-reducing admixtures.
- The mechanical properties of concrete mixtures made with MFA dust-of-fracture mineral filler with amounts up to 15 percent are not affected. Increased amounts of dust-of-fracture mineral filler may be valid, but the splitting tensile strength was found to be significantly decreased in the dolomitic limestone mixture that used 20 percent dust-of-fracture mineral filler addition.
- The durability properties of concrete mixtures made with MFA dust-of-fracture mineral filler with amounts up to 20 percent are not affected.
- Before selecting a MFA to use in a concrete mixture, characterization tests should be conducted on the dust-of-fracture mineral filler particles within it to avoid material that will adversely affect the concrete performance. The dust-of-fracture mineral filler should adhere to the excellent category in AASHTO T330 (2007) that states, aggregates with MBVs less than 6 mg/g are considered free of deleterious material.
- The particle size distribution of the dust-of-fracture mineral filler is an important factor on the concrete performance.

5.3 RESEARCH RECOMMENDATIONS

For successful implementation of phase I applications, further research should be done based on the following recommendations.

- Aggregate blending should be used in order to produce combined aggregate gradations. This procedure is more efficient than sieving aggregates to collect the necessary amounts of individual sieve sizes, for both research and field use. Achieving an optimized aggregate gradation requires blending at least three different sized aggregates, as stated in ACI 302 (2004).
- Explore the ability of lowering the water content in Table 6.3.3 in ACI Committee Report 211-1 (2012) with optimum aggregate gradations, while maintaining constant water-cementitious materials ratio, in order to achieve equal fresh and hardened properties as mixtures that meet Table 6.3.3 from ACI 211.1 (2012).

For successful implementation of phase II applications, further research should be done based on the following recommendations.

- Concrete mixtures incorporating MFA dust-of-fracture mineral filler material as part of the powder volume should be compared to mixtures incorporating MFA dust-of-fracture mineral filler as part of the fine aggregate volume. This procedure presents the best proportioning method for the dust-of-fracture mineral filler material.
- Among the previously stated problems associated with concrete using MFA with dust-of-fracture mineral filler, skid resistance or polish resistance is a cause for concern. While the workability and finishability of concrete can be improved by better proportioning mixtures, skid resistance depends mainly on the mineralogy of the sand. A decrease in skid resistance leads to more incidences of skid-related accidents on highways. Softer sands are known to polish when used in concrete pavements and thus provide less long-term skid resistance (Fowler and Rached

2012). Therefore, skid resistance testing should be conducted on future work involving MFA dust-of-fracture mineral filler.

- The relatively high cost to produce self-consolidating concrete (SCC) hinders the widespread use of such specialty concrete in various segments of the construction industry. The cost is due to greater demand of cementitious materials and chemical admixtures in order to achieve adequate plastic viscosity and low yield stress (Ghezal and Khayat 2002). The addition of cementitious materials and fine powders are used in SCC to reduce the segregation. Ground limestone has been widely used because it is an inert material, therefore will not generate heat. Extensive research is available on ground limestone use in SCC, but little research is available on the use of MFA dust-of-fracture mineral filler in SCC. MFA dust-of-fracture mineral filler could be an economical alternative to the powder content in SCC.

REFERENCES

AASHTO T330. 2007. Standard Method of Test for the Qualitative Detection of Harmful Clays of the Smectite Group in Aggregate Using Methylene Blue. Washington, DC: American Association of State Highway and Transportation Officials.

AASHTO M6. 2013. Fine Aggregate for Hydraulic Cement Concrete. Washington, DC: American Association of State Highway and Transportation Officials.

Abou-Zeid, and Fakhry. 2003. Short-Term Impact of High-Aggregate Fines Content on Concrete Incorporating Water-Reducing Admixtures. *ACI Materials Journal*, 280-285.

ACI 318. 2011. *Building Code Requirements for Structural Concrete and Commentary.* Farmington Hills, MI: American Concrete Institute.

ACI 209. 1997. *Prediction of Creep, Shrinkage, and Temperature Effects in Concrete Structures.* Farmington Hills, MI: American Concrete Institute.

ACI 211.7R. 2015. *Guide for Proportioning Concrete Mixtures with Ground Limestone and Other Mineral Fillers.* Farmington Hills, MI: American Concrete Institute.

ACI Committee 302. 2004. *Guide for Concrete Floor and Slab Construction.* Farmington Hills, MI: American Concrete Institute.

ACI CT-13. 2013. *ACI Concrete Terminology.* Farmington Hills, MI: American Concrete Institute.

Ahmed, A.E., and El-Kourd, A.A. 1989. Properties of Concrete Incorporating Natural and Crushed Stone Very Fine Sand. *ACI Materials Journal*, 417-424.

ALDOT. 2012. *Standard Specifications for Highway Construction*. Montgomergy, AL: Alabama Department of Transportion.

ASTM Standard C33. 2013. Specification for Concrete Aggregates. West Conshohocken, PA: ASTM International.

ASTM Standard C39. 2015. Standard Test Method for Compressive Strength of Cylindrical Concrete Specimens. West Conshohocken, PA: ASTM International.

ASTM Standard C117. 2004. Standard Test Method for Materials Finer than No. 200 Sieve in Mineral Aggregates by Washing. West Conshohocken, PA: ASTM International.

ASTM Standard C127. 2012. Standard Test Method for Density, Relative Density (Specific Gravity), and Absorption of Coarse Aggregate. West Conshohcken, PA: ASTM International, 2012.

ASTM Standard C 128. 2012. Standard Test Method for Density, Relative Density (Specific Gravity), and Absorption of Fine Aggregate. West Conshohcken, PA: ASTM International.

ASTM Standard C136. 2041. Standard Test Method for Sieve Analysis of Fine and Coarse Aggregates. West Conshohocken, PA: ASTM International.

ASTM Standard C138. 2014. Standard Test Method for Density, Yield, and Air Content. West Conshohocken, PA: ASTM International.

ASTM Standard C143. 2012. Standard Test Method for Slump of Hydralic-Cement Concrete. West Conshohocken, PA: ASTM International.

ASTM Standard C150. 2012. Standard Specification for Portland Cement. West Conshohocken, PA: ASTM International.

ASTM Standard C157. 2008. Standard Test Method for Length Change of Hardened Hydraulic-Cement Mortar and Concrete. West Conshohocken, PA: ASTM International.

ASTM Standard C187. 2011. Standard Test Method for Amount of Water Required for Normal Consistency of Hydraulic Cement Paste. West Conshohocken, PA: ASTM International.

ASTM Standard C192. 2015. Standard Practice for Making and Curing Concrete Test Specimens in the Laboratory. West Conshohocken, PA: ASTM International.

ASTM Standard C231. 2010. Standard Test Method for Air Content of Freshly Mixed Concrete by the Pressure Method. West Conshohcken, PA: ASTM International.

ASTM Standard C469. 2014. Standard Test Mthod for Static Modulus of Elasticity and Poisson's Ratio of Concrete in Compression. West Conshohocken, PA: ASTM International.

ASTM Standard C496. 2011. Standard Test Method for Splitting Tensile Strength of Cylindrical Concrete Specimens. West Conshohocken, PA: ASTM International.

ASTM Standard C618. 2012. Standard Specification for Coal Fly Ash and Raw or Calcined Natural Pozzolan for Use in Concrete. West Conshohocken, PA: ASTM International.

ASTM Standard C670. 2013. Standard Practice for Preparing Precision and Bias Statements for Test Methods for Constructin Materials. West Conshohocken, PA: ASTM International.

ASTM Standard C779. 2012. Standard Test Method for Abrasion Resistance of Horizontal Concrete Surfaces. West Conshohocken, PA: ASTM International.

ASTM Standard C1064. 2012. Standard Test Method for Temperature of Freshly Mixed Hydraulic-Cement Concrete. West Conshohcken, PA: ASTM International.

ASTM Standard C1202. 2006. Rapid Chloride Penetrability Test. West Conshohocken, PA: ASTM International.

ASTM Standard C1231. 2013. Standard Practice for Use of Unbonded Caps in Determination of COmpressive Strength of Hardened Concrete Cylinders. West Conshohocken, PA: ASTM International.

Bakke, K.J. 2006. Abrasion Resistance. *Significance of Tests and Properties of Concrete-Making Materials*. West Conshohocken, PA: ASTM International. 184-192.

Bonavetti, V., Donza, H., Rahhal, V., Irassar, E. 2000. Influence on initital curing on properties of concrete containing limestone blended cement. *Cement and Concrete Research*. 703-8.

Celik, T., and Khaled, M. 1996. Effects of Crushed Stone Dust on Some Properties of Concrete. *Cement and Concrete Research*. 1121-1130.

Cramer, S.M., Hall, M., and Parry, J. 1995. Effect of Optimized Total Aggregate Gradation on Portland Cement Conccrete for Wisoconsin Pavements. *Transportation Research Record*. 100-106.

Devore, J., and Farnum, N. 2005. *Applied Statisitics for Engineers and Scientists.* Belmont, CA: Brooks and Cole.

Dilek, U. 2013. Effects of Manufactured Sand Characteristics on Water Demand of Mortar and Concrete Mixtures. *ASTM Journal of Testing and Evaluation*. 1-11.

Ferraris, C.F., and de Larrard, F. 1998. Modified Slump Test to Measure Rheological Parameters of Fresh Concrete. *American Society for Testing and Materials*. 241-247.

Ferraris, C.F. 1996. Measurement of Rheological Properties of High Performacne Concrete: State of the Art Report. Research, Gaithersburg, MAryland: National Institute of Standards and Technology.

Ferraris, C.F., and de Larrard, F. 1997. Testing and Modeling of Fresh Concrete Rheology. NISTIR 6094, Gaithersburg, Maryland: National Institute of Standards and Technology.

Fowler, D.W., and Ahn, N. 2001. An Experimental Study on the Guidelines for Using Higher Contents of Aggregate Microfines in Portland Cement Concrete. ICAR 102-1F Research Report, Austin, Texas: ICAR.

Fowler, D.W., and Rached, M.M. 2001. Optimizing Aggregates to Reduce Cement in Concrete Without Reducing Quality. *Transportation Research Board*. 89-95.

Fowler, D.W. 2009. High Microfines Manufactured Fine Aggregate in Concrete. Concrete Technical Forum. Birmingham: American Concrete Institute, Alabama Chapter. 1-22.

Fowler, D.W., and Rached, M.M. 2012. Polish Resistance of Fine Aggregates in Portland Cement Concrete Pavements. *Transportation Research Board*. 29-36.

Germann Instuments. 2014. ICAR Rheometer. Evanston, Illinois. 618.

Ghezal, A., Khayat, K. 2002. Optimizing Self-Consolidating Concrete with Limestone Filler by usingStatistical Factorial Design Methods. *ACI Materials Journal*. 264-272.

Holland, J.A. 1990. Mixture Optimization. *Concrete International*. 10.

Hover, K.C. 2011. The influence of water on the performance of concrete. *Construction and Building Materials*. 3004-3013.

ICAR. 2003. Measurement of Concrete Workability: Key Principles and Current Methods. ICAR 11th Annual Symposium: Aggregates-Asphalt Concrete. Austin, Texas. 1-17.

Katz, A., and Baum, H. 2006. Effect of High Levels of Fines Content on Concrete Properties. *ACI Materials Journal*. 474-482.

Kenai, S., Menadi, B., Attar, A., and Khatib, J. 2008. Effect of Crushed Limestone Fines on Strength of Mortar and Durability of Concrete. International Conference of Construction and Building Technology. Kuala Lumpur: ICCBT. 205-216.

Koehler, E.P., and Fowler, D.W. 2008. Dust-of-Fracture Aggregate Microfines in Self-Consolidating Concrete. *ACI Materials Journal*. 165-173.

Koehler, E.P., and Fowler, D.W. 2003. Summary of Concrete Workability Test Methods. Research Report, Austin, Texas: ICAR.

Kosmatka, S.H., Kerkhoff, B., and Panarese, W.C. 2001. *Design and Control of Concrete Mixtures.* 14th. Skokie, Illinois: Portland Cement Association.

Lamond, J.F., and Pielert, J.H. 2006. Significance of tests and Properties of Concrete and Concrete-Making Materials. *American Society for Testing and Materials*. 337-354.

Maldonado, A., Orsetti, S., and Tourenq, C. 1994. Standardization and Qualification of Fines in Aggregates in France. Internation Center for Aggregates Research, 4th annual symposium.

McCuen, R.H. 1985. *Statistical Methods for Engineers.* 1st Ed. Prentice hall, Englewood Cliffs, NJ.

Mehta, K.P., and Monteiro, P. 2014. *Concrete Microstructure, Properties, and Materials.* 4. New York: The McGraw Hill Companies.

Menadi, B., Kenai, S., Khatib, J., and Ait-Mokhtar, A. 2009. Strength and durability of concrete incorporating crushed limestone sand. *Construction and Building Materials*. 625-633.

Montana Department of Transportation. Concrete Aggregate Gradation Example. n.d. http://www.mdt.mt.gov/other/const/external/temp_drawings_calc_ex/combined_gradation_example.pdf (accessed June 3, 2015).

Norvell, J.K., Stewart, J.G., Juenger, M., and Fowler, D.W. 2007. Influence of CLay and Clay-Sized PArticles on Concrete Performance. *Journal of Materials in Civil Engineering.* 1053-1059.

Obla, K., Kim, H., and Lobo, C. 2007. Effect of Cpontinuous (Well-Graded) Combined Aggregate Grading on Concrete Performance. National Ready Mixed Concrete Association Research.

Pike, D.C. 1992. Methodologies for assessing the varability of fines in sands used for concrete mortars. PhD Dissertation, Reading, U.K.: Univerity of Reading.

Popovics, S. 1994. The Slump Test is Useless - Or Is It? *Concrete International*. 30-33.

Quiroga, P.N., and Fowler, D.W. 2004. Guidelines for Proportioning Optimized Concrete Mixtures With High Microfines. Austin, Texas: Internatinal Center For Aggregates Research.

Quiroga, P.N., and Fowler, D.W. 2007. Portland cement concrete using high levels of microfines. *Sustainable Construction Materials and Technologies.* 101-106.

Quiroga, P.N., Ahn, N., and Fowler, D.W. 2006. Concrete Mixtures with High Microfines. *ACI Materials Journal*. 258-264.

Quiroga, P.N., and Fowler, D.W. 2004. The Effects of Aggregate Characteristics on The Performance of Portland Cement Concrete. Research Report, Autsin, Texas: International Center for Aggregates Research.

Rached, M., De Moya, M., and Fowler, D.W. 2009. Utilizing Aggregates Characteristics to Minimize Cement Content in Portland Cement Concrete. Austin, Texas: International Center For Aggregates Research.

Raphael. 1984. Tensile Strength of Concrete. *ACI Materials Journal*.

Richardson, D.N. 2005. Aggregate Gradation Optimization. Research Report, Jefferson City, MO: Missouri Department of Transportation.

Saeed, A., Razmi, A., Aki, G., and Hudson, W.R. 1997. Production and Use of By-Product Fines in the USA. Research Report, Austin, Texas: International Center for Aggregate Research.

Shen, J., Zhaoxing, X., Griggs, D., and Shi, Y. 2012. Effects of Kaolin on the Engineering Properties of Porltand Cement Concrete. *Applied Mechanics and Material.* 76-81.

Shilestone, J.M., and Shilestone, J.M. 2002. Performance-Based Concrete Mixtures and Specifications for Today. *Concrete International.* 80-83.

Shilstone, J.M., and Shilstone, J.M. 1993. High Performance Concrete mixtures for Durability. *ACI Materials*. Septmeber. 281-306.

Shilstone, J.M. 1988. Interpresting the Slump Test. *Concrete International*. 68-70.

Shilstone, J.M., and Shilstone, J.M. 1987. Practical Concrete Mixture Proportioing Technology. *Refence Manuel*. Shilstone Software Co.

Shilstone, J.M., and Shilstone, J.M. 1989. Concrete Mixtures and Construction Needs. *Concrete International*. 53-57.

Shilstone, J.M. 2007. Worlwide Standards for Concrete Mixtures for Safe and Durable Runways and Taxiways. International Air Transport Conference. Dallas-Fort Worth Texas: ASCE. 237-250.

Shilstone, J.M. 1990. Concrete Mixture Optimization. *Concrete International: Design and Construction*. 33-39.

Stewart, J.G., Norvell, J.K., Juenger, M., and Fowler, D.W. 2007. Influence of Microfine Aggregate Characteristics on Concrete Performance. *Journal of Materials in Civil Engineering*. 957-963.

Tattersall, G.H. 1991. *Workability and Quality Control of Concrete*. London: Spon Press.

Topcu, B.I., and Demir, A. 2008. Relationship between methylene blue values of concrete aggregates fines and some concrete properties. *Canadian Journal of Civil Engineering*. 379-383.

Topcu, B.I., and Ali, U. 2003. Effect of the use of mineral filler on the properties of concrete. *Cement and Concrete Research*. 1071-1075.

Whitney, D., Fowler, D.W., and Rached, M. 2013. Use of Manufactured Sands for Concrete Pavement. Technical Report, Austin, Texas: ICAR.

Yool, A., Lees, T., and Fried, A. 1998. Improvements to the Methylene Blue Dye Test for Harmful Clay in Aggregates for Concreteand Mortar. *Cement and Concrete Research*. 1417-1428.

Appendix A

FRESH PROPERTIES DATA

Table A-1: Phase I Vebe Time Results

Mixture	Vebe Slump (mm)	Vebe Slump (in.)	Vebe Time (s)
No. 57 DL Blend 1	90	3.5	3.2
No. 57 DL Blend 2			2.96
No. 57 DL Blend 3			2.99
No. 57 DL Blend 4			2.28
No. 67 DL Blend 1	70	2.8	3.15
No. 67 DL Blend 2	95	3.7	6.28
No. 67 DL Blend 3	40	1.6	5.5
No. 67 DL Blend 4	90	3.5	1.97
No. 57 RG Blend 1	125	4.9	2.94
No. 57 RG Blend 2	50	2	3.3
No. 57 RG Blend 3	95	3.7	3
No. 57 RG Blend 4	150	5.9	3.15
No. 57 RG Blend 1	50	2	4.13
No. 67 RG Blend 2	75	3	3.18
No. 67 RG Blend 3	125	4.9	2.72
No. 67 RG Blend 4	145	5.7	2.34

Table A-2: Phase II Vebe Time Results

Mixture	Vebe Slump (mm)	Vebe Slump (in.)	Vebe Time (s)
No. 67 DL 0 %	110	4.3	2.81
No. 67 DL 5%	60	2.4	3.19
No. 67 DL 10 %	130	5.1	2.87
No. 67 DL 15%	150	5.9	2.57
No. 67 DL 20%	140	5.5	2.66
No. 67 RG 0 %	150	5.9	1.78
No. 67 RG 5%	140	5.5	3.38
No. 67 RG 10 %	160	6.3	1.87
No. 67 RG 15%	155	6.1	1.95
No. 67 RG 20%	125	4.9	2.16

Table A-3: Phase I Workability Assessment Results

Mixture	Workability Scale
No. 57 DL Blend 1	14
No. 67 DL Blend 1	15
No. 67 DL Blend 2	21.5
No. 67 DL Blend 3	15.5
No. 67 DL Blend 4	9.5
No. 57 RG Blend 1	9
No. 57 RG Blend 2	13
No. 57 RG Blend 3	11
No. 57 RG Blend 4	18
No. 67 RG Blend 1	19
No. 67 RG Blend 2	10.5
No. 67 RG Blend 3	8.5
No. 67 RG Blend 4	12

Table A-4: Phase II Workability Assessment Results

Mixture	Workability Scale
No. 67 DL 0 %	16.5
No. 67 DL 5%	23.5
No. 67 DL 10 %	8.5
No. 67 DL 15%	10
No. 67 DL 20%	9
No. 67 RG 0 %	11.5
No. 67 RG 5%	16
No. 67 RG 10 %	6.5
No. 67 RG 15%	11
No. 67 RG 20%	14.5

Table A-5: Phase I Flow Curve Data

Mixture	Modified Slump (in.)	Modified Slump (mm)	Slump Time, T (s)	Unit Weight, ρ (lb/ft^3)	Unit Weight, ρ (kg/m^3)	Yield Stress, τ_0 (Pa)	Plastic Viscosity, μ (Pa*s)
No. 57 DL Blend 1	3.5	88.9	0.48	152.02	2439.16	1695.88	29.45
No. 67 DL Blend 1	4	101.6	0.75	149.56	2399.69	1584.04	44.99
No. 67 DL Blend 2	6.5	165.1	0.65	151.04	2423.44	1154.14	39.38
No. 67 DL Blend 3	6	152.4	0.78	151.44	2429.85	1245.56	47.38
No. 67 DL Blend 4	6.5	165.1	0.93	149.44	2397.76	1144.16	55.99
No. 57 RG Blend 1	5.5	139.7	0.43	144.3	2315.29	1281.57	24.95
No. 57 RG Blend 3	6	152.4	0.38	146.44	2349.63	1211.44	22.20
No. 57 RG Blend 4	7.5	190.5	0.27	147.9	2373.06	960.85	16.05
No. 67 RG Blend 3	6.5	165.1	0.39	144.48	2318.18	1113.22	22.72
No. 67 RG Blend 4	7	177.8	0.36	146.52	2350.91	1039.90	21.25

Table A-6: Phase II Flow Curve Data

Mixture	Modified Slump (in.)	Modified Slump (mm)	Slump Time, T (s)	Unit Weight, ρ (lb/ft^3)	Unit Weight, ρ (kg/m^3)	Yield Stress, τ_0 (Pa)	Plastic Viscosity, μ (Pa*s)
No. 67 DL 0 %	5.5	139.7	1.12	152.18	2441.72	1339.98	68.30
No. 67 DL 5%	4	101.6	0.58	152.66	2449.43	1612.48	35.30
No. 67 DL 10 %	7	177.8	0.65	153.12	2456.81	1077.19	39.80
No. 67 DL 15%	6	152.4	0.48	152.20	2442.05	1250.75	29.18
No. 67 DL 20%	7	177.8	0.52	154.24	2474.78	1083.52	31.89
No. 67 RG 0 %	8	203.2	0.29	147.38	2364.71	871.67	17.26
No. 67 RG 5%	7	177.8	0.39	148.06	2375.62	1048.60	23.04
No. 67 RG 10 %	8	203.2	0.27	147.74	2370.48	873.28	16.06
No. 67 RG 15%	8	203.2	0.38	148.34	2380.12	876.96	22.49
No. 67 RG 20%	7.5	190.5	0.42	147.98	2374.34	961.25	24.66

Appendix B

MECHANICAL PROPERTIES RAW DATA

Table B-1: Phase I Dolomitic Limestone Compressive and Splitting Tensile Strength Data

Mixture	Time (days)	Property	Strength (psi)
No. 57 DL Blend 1	7	Compressive	4270
	7	Splitting Tensile	365
	28	Compressive	5540
	28	Splitting Tensile	455
	91	Compression	6930
	91	Splitting Tensile	555
No. 57 DL Blend 2	7	Compressive	4270
	7	Splitting Tensile	345
	28	Compressive	5630
	28	Splitting Tensile	470
	91	Compression	7030
	91	Splitting Tensile	515
No. 57 DL Blend 3	7	Compressive	4180
	7	Splitting Tensile	375
	28	Compressive	5470
	28	Splitting Tensile	450
	91	Compressive	7110
	91	Splitting Tensile	570
No. 57 DL Blend 4	7	Compressive	4010
	7	Splitting Tensile	330
	28	Compressive	5260
	28	Splitting Tensile	430
	91	Compressive	6820
	91	Splitting Tensile	545

Table B-2: Phase I Dolomitic Limestone Compressive and Splitting Tensile Strength Data Continued

Mixture	Time (days)	Property	Strength (psi)
No. 67 DL Blend 1	7	Compressive	4440
	7	Splitting Tensile	385
	28	Compressive	5950
	28	Splitting Tensile	550
	91	Compressive	7420
	91	Splitting Tensile	655
No. 67 DL Blend 2	7	Compressive	3940
	7	Splitting Tensile	345
	28	Compressive	5210
	28	Splitting Tensile	465
	91	Compressive	6480
	91	Splitting Tensile	485
No. 67 DL Blend 3	7	Compressive	4360
	7	Splitting Tensile	365
	28	Compressive	5450
	28	Splitting Tensile	510
	91	Compressive	6930
	91	Splitting Tensile	585
No. 67 DL Blend 4	7	Compressive	4000
	7	Splitting Tensile	345
	28	Compressive	5490
	28	Splitting Tensile	455
	91	Compressive	6770
	91	Splitting Tensile	505

Table B-3: Phase I Dolomitic Limestone Modulus of Elasticity Data

Mixture	Time (days)	Property	Strength (ksi)
No. 57 DL Blend 1	7	Modulus of Elasticity	5650
	28		6300
	91		7550
No. 57 DL Blend 2	7	Modulus of Elasticity	5875
	28		5875
	91		6975
No. 57 DL Blend 3	7	Modulus of Elasticity	4750
	28		5850
	91		6750
No. 57 DL Blend 4	7	Modulus of Elasticity	5000
	28		5500
	91		6300
No. 67 DL Blend 1	7	Modulus of Elasticity	4875
	28		6275
	91		7475
No. 67 DL Blend 2	7	Modulus of Elasticity	5275
	28		6575
	91		6750
No. 67 DL Blend 3	7	Modulus of Elasticity	5000
	28		6050
	91		7425
No. 67 DL Blend 4	7	Modulus of Elasticity	5425
	28		6050
	91		6875

Table B-4: Phase I River Gravel Compressive and Splitting Tensile Strength Data

Mixture	Time (days)	Property	Strength (psi)
No. 57 RG Blend 1	7	Compressive	4080
	7	Splitting Tensile	335
	28	Compressive	5130
	28	Splitting Tensile	375
	91	Compressive	6100
	91	Splitting Tensile	475
No. 57 RG Blend 2	7	Compressive	4460
	7	Splitting Tensile	350
	28	Compressive	5470
	28	Splitting Tensile	370
	91	Compressive	6850
	91	Splitting Tensile	560
No. 57 RG Blend 3	7	Compressive	4220
	7	Splitting Tensile	310
	28	Compressive	5290
	28	Splitting Tensile	365
	91	Compressive	6430
	91	Splitting Tensile	505
No. 57 RG Blend 4	7	Compressive	3890
	7	Splitting Tensile	345
	28	Compressive	4860
	28	Splitting Tensile	440
	91	Compressive	6220
	91	Splitting Tensile	490

Table B-5: Phase I River Gravel Compressive and Splitting Tensile Strength Data

Continued

Mixture	Time (days)	Property	Strength (psi)
No. 67 RG Blend 1	7	Compressive	4530
	7	Splitting Tensile	330
	28	Compressive	5580
	28	Splitting Tensile	390
	91	Compressive	6900
	91	Splitting Tensile	530
No. 67 RG Blend 2	7	Compressive	4330
	7	Splitting Tensile	-
	28	Compressive	5200
	28	Splitting Tensile	405
	91	Compressive	6440
	91	Splitting Tensile	535
No. 67 RG Blend 3	7	Compressive	4190
	7	Splitting Tensile	350
	28	Compressive	5240
	28	Splitting Tensile	405
	91	Compressive	6400
	91	Splitting Tensile	520
No. 67 RG Blend 4	7	Compressive	4160
	7	Splitting Tensile	330
	28	Compressive	5220
	28	Splitting Tensile	395
	91	Compressive	6360
	91	Splitting Tensile	495

Table B-6: Phase I River Gravel Modulus of Elasticity Data

Mixture	Time (days)	Property	Strength (ksi)
No. 57 RG Blend 1	7	Modulus of Elasticity	3850
	28		4250
	91		4550
No. 57 RG Blend 2	7	Modulus of Elasticity	4025
	28		4500
	91		4775
No. 57 RG Blend 3	7	Modulus of Elasticity	3900
	28		4575
	91		4725
No. 57 RG Blend 4	7	Modulus of Elasticity	4200
	28		4325
	91		5025
No. 67 RG Blend 1	7	Modulus of Elasticity	4900
	28		4825
	91		5025
No. 67 RG Blend 2	7	Modulus of Elasticity	4425
	28		4575
	91		5050
No. 67 RG Blend 3	7	Modulus of Elasticity	4550
	28		4600
	91		4925
No. 67 RG Blend 4	7	Modulus of Elasticity	4375
	28		4650
	91		4875

Table B-7: Phase II Dolomitic Limestone Compressive and Splitting Tensile Strength Data

Mixture	Time (days)	Property	Strength (psi)
No. 67 DL 0%	7	Compressive	4500
	7	Splitting Tensile	450
	28	Compressive	5810
	28	Splitting Tensile	505
	91	Compressive	7650
	91	Splitting Tensile	660
No. 67 DL 5%	7	Compressive	4670
	7	Splitting Tensile	-
	28	Compressive	6060
	28	Splitting Tensile	495
	91	Compressive	770
	91	Splitting Tensile	665
No. 67 DL 10%	7	Compressive	4650
	7	Splitting Tensile	365
	28	Compressive	5930
	28	Splitting Tensile	515
	91	Compressive	7470
	91	Splitting Tensile	670
No. 67 DL 15%	7	Compressive	4530
	7	Splitting Tensile	365
	28	Compressive	5650
	28	Splitting Tensile	530
	91	Compressive	7360
	91	Splitting Tensile	610
No. 67 DL 20%	7	Compressive	4460
	7	Splitting Tensile	380
	28	Compressive	5790
	28	Splitting Tensile	-
	91	Compressive	7130
	91	Splitting Tensile	490

Table B-8: Phase II River Gravel Compressive and Splitting Tensile Strength Data

Mixture	Time (days)	Property	Strength (psi)
No. 67 RG 0%	7	Compressive	4450
	7	Splitting Tensile	345
	28	Compressive	5460
	28	Splitting Tensile	410
	91	Compression	6770
	91	Splitting Tensile	545
No. 67 RG 5%	7	Compressive	4370
	7	Splitting Tensile	380
	28	Compressive	5810
	28	Splitting Tensile	450
	91	Compressive	7180
	91	Splitting Tensile	510
No. 67 RG 10%	7	Compressive	4280
	7	Splitting Tensile	360
	28	Compressive	5040
	28	Splitting Tensile	410
	91	Compressive	6420
	91	Splitting Tensile	570
No. 67 RG 15%	7	Compressive	4200
	7	Splitting Tensile	370
	28	Compressive	5560
	28	Splitting Tensile	425
	91	Compressive	6530
	91	Splitting Tensile	570
No. 67 RG 20%	7	Compressive	3890
	7	Splitting Tensile	360
	28	Compressive	4930
	28	Splitting Tensile	420
	91	Compressive	6370
	91	Splitting Tensile	510

Table B-9: Phase II Modulus of Elasticity Data

Mixture	Time (days)	Property	Strength (ksi)
No. 67 DL 0%	7	Modulus of Elasticity	5050
	28		6525
	91		7000
No. 67 DL 5%	7	Modulus of Elasticity	5400
	28		6775
	91		7350
No. 67 DL 10%	7	Modulus of Elasticity	5175
	28		5875
	91		6975
No. 67 DL 15%	7	Modulus of Elasticity	5125
	28		6400
	91		7100
No. 67 DL 20%	7	Modulus of Elasticity	5050
	28		6100
	91		7100
No. 67 RG 0%	7	Modulus of Elasticity	4050
	28		4700
	91		5050
No. 67 RG 5%	7	Modulus of Elasticity	4175
	28		4850
	91		5375
No. 67 RG 10%	7	Modulus of Elasticity	4000
	28		4450
	91		4950
No. 67 RG 15%	7	Modulus of Elasticity	4200
	28		4375
	91		5100
No. 67 RG 20%	7	Modulus of Elasticity	4050
	28		4675
	91		5375

Appendix C

DURABILITY RAW DATA

Table C-1: Phase I RCPT Data

Mixture	Property	Chloride Ion Penetration (Coulombs)
No. 57 DL Blend 1	Permeability	1486
No. 57 DL Blend 2	Permeability	1603.7
No. 57 DL Blend 3	Permeability	1582.3
No. 57 DL Blend 4	Permeability	1610
No. 67 DL Blend 1	Permeability	1273
No. 67 DL Blend 2	Permeability	1422.7
No. 67 DL Blend 3	Permeability	1395.7
No. 67 DL Blend 4	Permeability	1514.7
No. 57 RG Blend 1	Permeability	2883.3
No. 57 RG Blend 2	Permeability	2645
No. 57 RG Blend 3	Permeability	2028.3
No. 57 RG Blend 4	Permeability	1683.7
No. 67 RG Blend 1	Permeability	2146
No. 67 RG Blend 2	Permeability	2173
No. 67 RG Blend 3	Permeability	2104
No. 67 RG Blend 4	Permeability	1908.3

Table C-2: Phase I Dolomitic Limestone Drying Shrinkage Data

Mixture	Time (days)	Property	Measured Strain (in./in.)
No. 57 DL Blend 1	4	Drying Shrinkage	0.00019
	7	Drying Shrinkage	0.000243
	14	Drying Shrinkage	0.00038
	28	Drying Shrinkage	0.000417
	56	Drying Shrinkage	0.000553
	112	Drying Shrinkage	0.000577
	168	Drying Shrinkage	0.000597
No. 57 DL Blend 2	4	Drying Shrinkage	0.00017
	7	Drying Shrinkage	0.000203
	14	Drying Shrinkage	0.00034
	28	Drying Shrinkage	0.00041
	56	Drying Shrinkage	0.00047
	112	Drying Shrinkage	0.00055
	168	Drying Shrinkage	0.000583
No. 57 DL Blend 3	4	Drying Shrinkage	0.00022
	7	Drying Shrinkage	0.000283
	14	Drying Shrinkage	0.000383
	28	Drying Shrinkage	0.000477
	56	Drying Shrinkage	0.000617
	112	Drying Shrinkage	0.000647
	168	Drying Shrinkage	0.000663
No. 57 DL Blend 4	4	Drying Shrinkage	0.00016
	7	Drying Shrinkage	0.00026
	14	Drying Shrinkage	0.000347
	28	Drying Shrinkage	0.000463
	56	Drying Shrinkage	0.000567
	112	Drying Shrinkage	0.000613
	168	Drying Shrinkage	0.000633

Table C-3: Phase I Dolomitic Limestone Drying Shrinkage Data Continued

Mixture	Time (days)	Property	Measured Strain (in./in.)
No. 67 DL Blend 1	4	Drying Shrinkage	0.000137
	7	Drying Shrinkage	0.000197
	14	Drying Shrinkage	0.000337
	28	Drying Shrinkage	0.000383
	56	Drying Shrinkage	0.000487
	112	Drying Shrinkage	0.000557
	168	Drying Shrinkage	0.000557
No. 67 DL Blend 2	4	Drying Shrinkage	0.0001
	7	Drying Shrinkage	0.000203
	14	Drying Shrinkage	0.000277
	28	Drying Shrinkage	0.000317
	56	Drying Shrinkage	0.000347
	112	Drying Shrinkage	0.000437
	168	Drying Shrinkage	0.000443
No. 67 DL Blend 3	4	Drying Shrinkage	0.0002
	7	Drying Shrinkage	0.000247
	14	Drying Shrinkage	0.000307
	28	Drying Shrinkage	0.00049
	56	Drying Shrinkage	0.000503
	112	Drying Shrinkage	0.000547
	168	Drying Shrinkage	0.00056
No. 67 DL Blend 4	4	Drying Shrinkage	0.000153
	7	Drying Shrinkage	0.000237
	14	Drying Shrinkage	0.000263
	28	Drying Shrinkage	0.000433
	56	Drying Shrinkage	0.000463
	112	Drying Shrinkage	0.000507
	168	Drying Shrinkage	0.000507

Table C-4: Phase I River Gravel Drying Shrinkage Data

Mixture	Time (days)	Property	*Measured Strain (in./in.)
No. 57 RG Blend 1	4	Drying Shrinkage	0.00013
	7	Drying Shrinkage	0.000197
	14	Drying Shrinkage	0.000337
	28	Drying Shrinkage	0.000493
	56	Drying Shrinkage	0.00064
	112	Drying Shrinkage	
	168	Drying Shrinkage	
No. 57 RG Blend 2	4	Drying Shrinkage	0.000143
	7	Drying Shrinkage	0.000247
	14	Drying Shrinkage	0.00047
	28	Drying Shrinkage	0.00055
	56	Drying Shrinkage	0.000653
	112	Drying Shrinkage	
	168	Drying Shrinkage	
No. 57 RG Blend 3	4	Drying Shrinkage	0.000147
	7	Drying Shrinkage	0.000207
	14	Drying Shrinkage	0.000347
	28	Drying Shrinkage	0.000503
	56	Drying Shrinkage	0.00061
	112	Drying Shrinkage	
	168	Drying Shrinkage	
No. 57 RG Blend 4	4	Drying Shrinkage	0.00019
	7	Drying Shrinkage	0.000307
	14	Drying Shrinkage	0.000337
	28	Drying Shrinkage	.000447
	56	Drying Shrinkage	.000573
	112	Drying Shrinkage	
	168	Drying Shrinkage	

***Omitted data points due to inaccurate measurements**

Table C-6: Phase II RCPT Data

Mixture	Property	Chloride Ion Penetration (Coulombs)
No. 67 DL 0%	Permeability	1550.7
No. 67 DL 5%	Permeability	1391
No. 67 DL 10%	Permeability	1016.3
No. 67 DL 15%	Permeability	1314.7
No. 67 DL 20%	Permeability	1124
No. 67 RG 0%	Permeability	1474.3
No. 67 RG 5%	Permeability	1484.7
No. 67 RG 10%	Permeability	1200.7
No. 67 RG 15%	Permeability	1176.7
No. 67 RG 20%	Permeability	1228

Table C-7: Phase II Dolomitic Limestone Drying Shrinkage Data

Mixture	Time (days)	Property	*Measured Strain (in/in)
No. 67 DL 0%	4	Drying Shrinkage	0.000193
	7	Drying Shrinkage	0.00022
	14	Drying Shrinkage	0.00035
	28	Drying Shrinkage	0.000363
	56	Drying Shrinkage	0.00052
	112	Drying Shrinkage	0.000547
	168	Drying Shrinkage	
No. 67 DL 5%	4	Drying Shrinkage	0.000201
	7	Drying Shrinkage	0.000347
	14	Drying Shrinkage	0.000357
	28	Drying Shrinkage	0.000393
	56	Drying Shrinkage	0.000533
	112	Drying Shrinkage	0.00056
	168	Drying Shrinkage	
No. 67 DL 10%	4	Drying Shrinkage	0.000127
	7	Drying Shrinkage	0.000203
	14	Drying Shrinkage	0.00027
	28	Drying Shrinkage	0.000297
	56	Drying Shrinkage	0.000417
	112	Drying Shrinkage	0.000527
	168	Drying Shrinkage	
No. 67 DL 15%	4	Drying Shrinkage	0.00011
	7	Drying Shrinkage	0.00011
	14	Drying Shrinkage	0.000233
	28	Drying Shrinkage	0.00035
	56	Drying Shrinkage	0.000423
	112	Drying Shrinkage	0.00051
	168	Drying Shrinkage	
No. 67 DL 20%	4	Drying Shrinkage	0.0007
	7	Drying Shrinkage	0.000113
	14	Drying Shrinkage	0.000157
	28	Drying Shrinkage	0.000273
	56	Drying Shrinkage	0.00036
	112	Drying Shrinkage	0.000477
	168	Drying Shrinkage	

***Omitted data points due to inaccurate measurements**

Table C-8: Phase II River Gravel Drying Shrinkage Data

Mixture	Time (days)	Property	*Measured Strain (in/in)
No. 67 RG 0%	4	Drying Shrinkage	0.00019
	7	Drying Shrinkage	0.0003
	14	Drying Shrinkage	0.000417
	28	Drying Shrinkage	
	56	Drying Shrinkage	0.00054
	112	Drying Shrinkage	0.000643
	168	Drying Shrinkage	0.000603
No. 67 RG 5%	4	Drying Shrinkage	0.000207
	7	Drying Shrinkage	0.000303
	14	Drying Shrinkage	0.00041
	28	Drying Shrinkage	
	56	Drying Shrinkage	0.00046
	112	Drying Shrinkage	0.00049
	168	Drying Shrinkage	0.0005
No. 67 RG 10%	4	Drying Shrinkage	0.00017
	7	Drying Shrinkage	0.000213
	14	Drying Shrinkage	0.000383
	28	Drying Shrinkage	
	56	Drying Shrinkage	0.00039
	112	Drying Shrinkage	0.00043
	168	Drying Shrinkage	0.000447
No. 67 RG 15%	4	Drying Shrinkage	0.00015
	7	Drying Shrinkage	0.00023
	14	Drying Shrinkage	0.000357
	28	Drying Shrinkage	
	56	Drying Shrinkage	0.000593
	112	Drying Shrinkage	0.000627
	168	Drying Shrinkage	0.000547
No. 67 RG 20%	4	Drying Shrinkage	0.00016
	7	Drying Shrinkage	0.000233
	14	Drying Shrinkage	0.000317
	28	Drying Shrinkage	
	56	Drying Shrinkage	0.000473
	112	Drying Shrinkage	0.000427
	168	Drying Shrinkage	0.00046

***Omitted data points due to inaccurate measurements**

Table C-9: Phase II Abrasion Data

Mixture	Time (minutes)	Property	Depth of Wear (in.)
No. 67 DL 0%	5	Abrasion Resistance	0.017
	15	Abrasion Resistance	0.029
	30	Abrasion Resistance	0.045
	60	Abrasion Resistance	0.07
No. 67 DL 5%	5	Abrasion Resistance	0.019
	15	Abrasion Resistance	0.032
	30	Abrasion Resistance	0.046
	60	Abrasion Resistance	0.068
No. 67 DL 10%	5	Abrasion Resistance	0.012
	15	Abrasion Resistance	0.022
	30	Abrasion Resistance	0.035
	60	Abrasion Resistance	0.057
No. 67 DL 15%	5	Abrasion Resistance	0.019
	15	Abrasion Resistance	0.031
	30	Abrasion Resistance	0.044
	60	Abrasion Resistance	0.065
No. 67 DL 20%	5	Abrasion Resistance	0.015
	15	Abrasion Resistance	0.025
	30	Abrasion Resistance	0.039
	60	Abrasion Resistance	0.064

Appendix D

ABRASION TESTING PICTURES

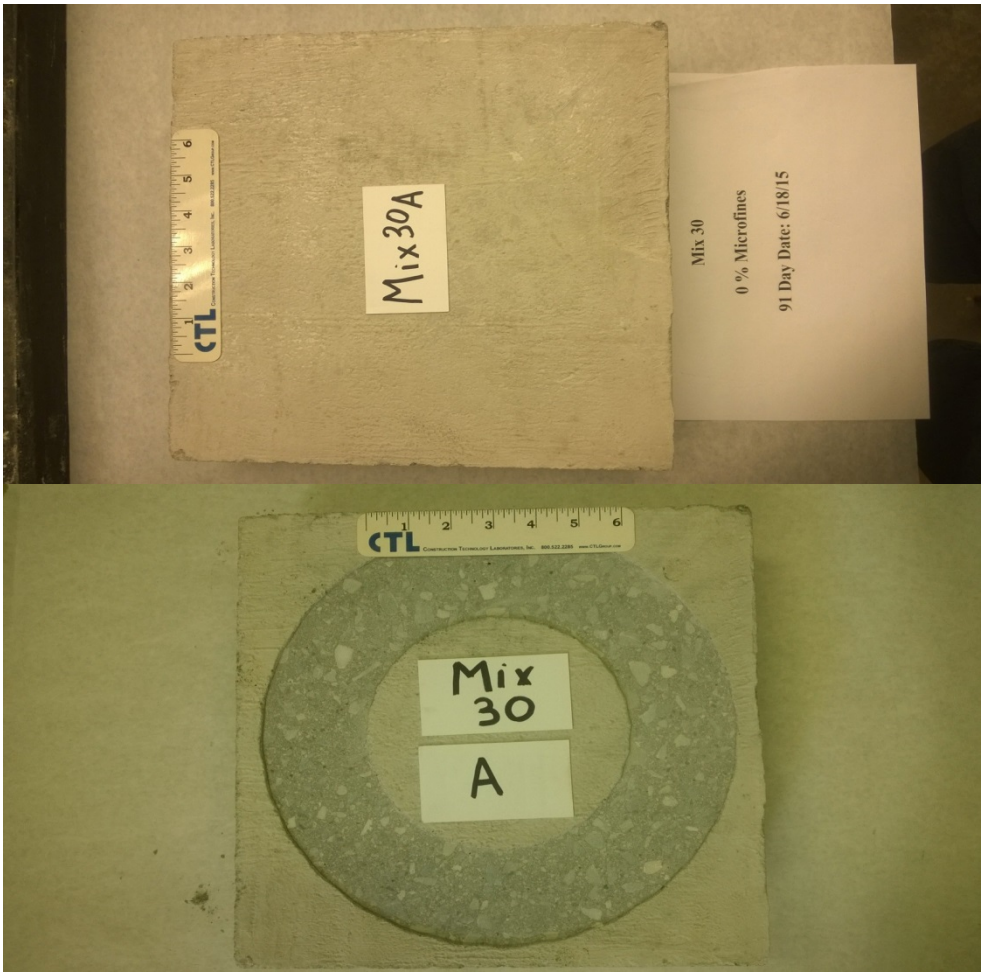

Figure D-1: Before (top) and after (bottom) pictures for dolomitic limestone 0% dust-of-fracture mineral filler

Figure D-2: Before (top) and after (bottom) pictures for dolomitic limestone 5% dust-of-fracture mineral filler

Figure D-3: Before (top) and after (bottom) pictures for dolomitic limestone 10% dust-of-fracture mineral filler

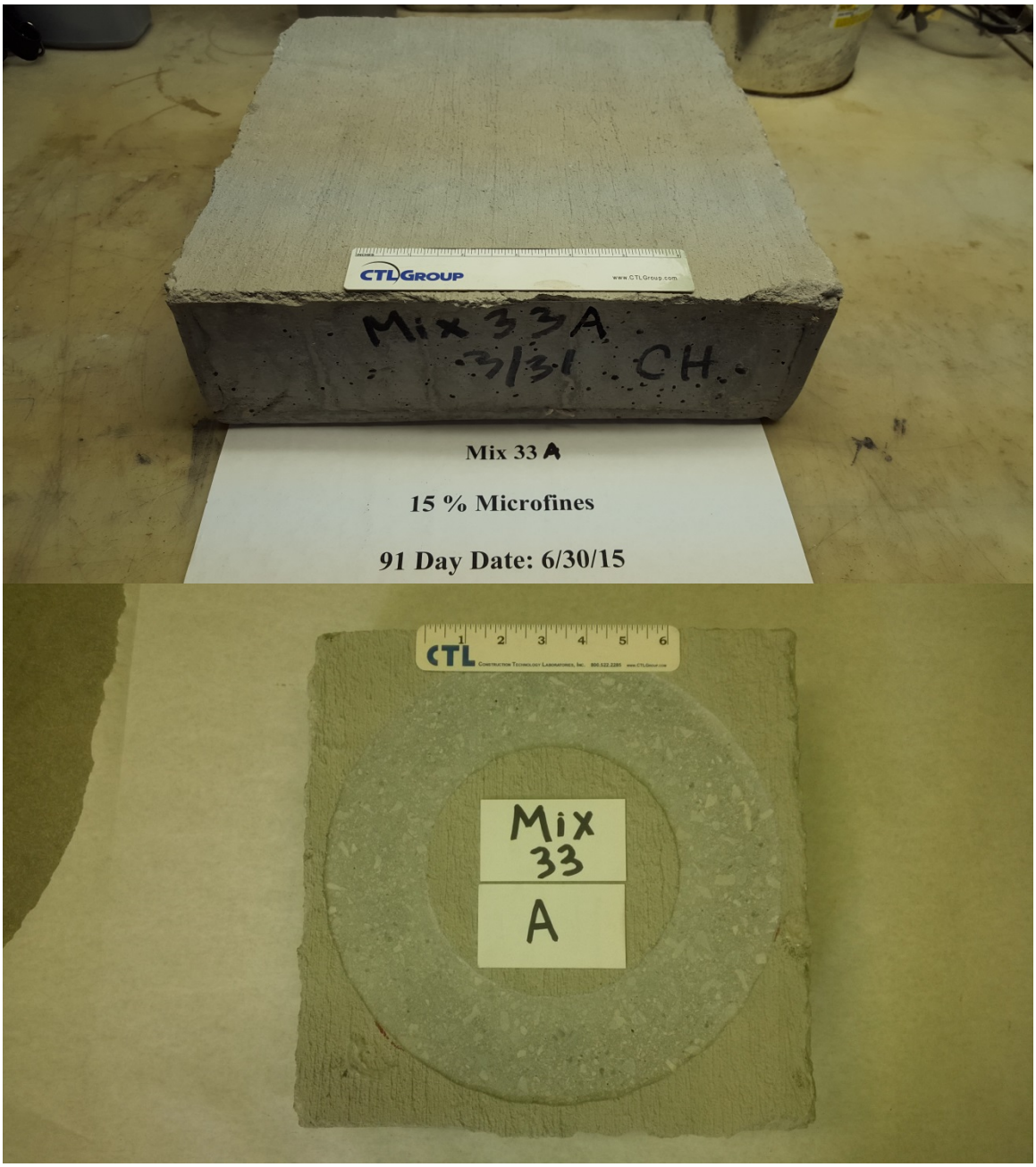

Figure D-4: Before (top) and after (bottom) pictures for dolomitic limestone 15% dust-of-fracture mineral filler

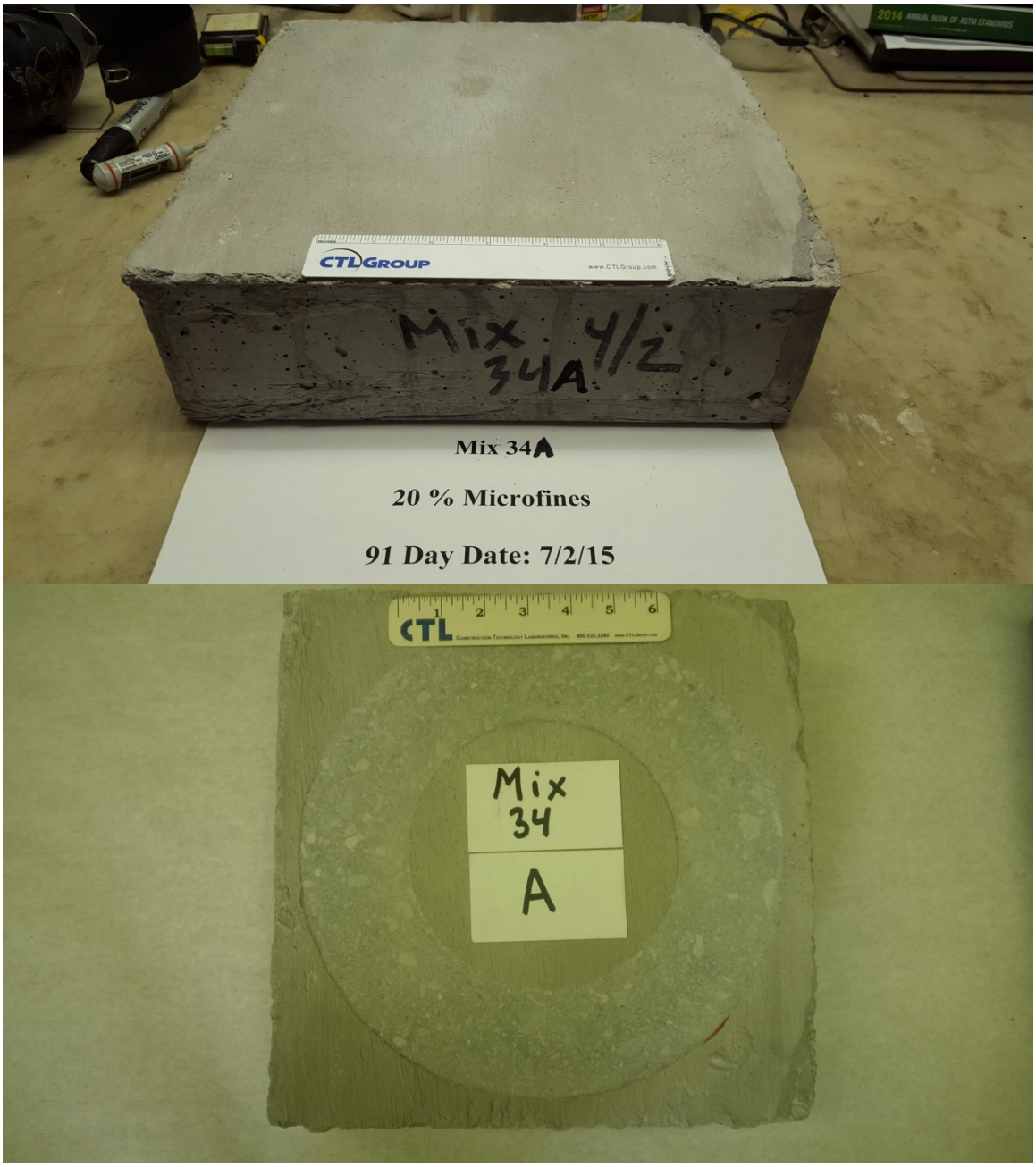

Figure D-5: Before (top) and after (bottom) pictures for dolomitic limestone 20% dust-of-fracture mineral filler